

REMOVAL OF IMIDACLOPRID FROM WASTEWATERS BY OZONATION  
AND PHOTO-OZONATION

A THESIS SUBMITTED TO  
THE GRADUATE SCHOOL OF NATURAL AND APPLIED SCIENCES  
OF  
MIDDLE EAST TECHNICAL UNIVERSITY



BY

BÜŞRA SÖNMEZ

IN PARTIAL FULFILLMENT OF THE REQUIREMENTS  
FOR  
THE DEGREE OF MASTER OF SCIENCE  
IN  
ENVIRONMENTAL ENGINEERING

JULY 2019



Approval of the thesis:

**REMOVAL OF IMIDACLOPRID FROM WASTEWATERS BY  
OZONATION AND PHOTO-OZONATION**

submitted by **BÜŞRA SÖNMEZ** in partial fulfillment of the requirements for the degree of **Master of Science in Environmental Engineering Department, Middle East Technical University** by,

Prof. Dr. Halil Kalıpçılar  
Dean, Graduate School of **Natural and Applied Sciences**

Prof. Dr. Bülent İçgen  
Head of Department, **Environmental Eng.**

Prof. Dr. Filiz Bengü Dilek  
Supervisor, **Environmental Eng., METU**

**Examining Committee Members:**

Prof. Dr. Ülkü Yetiş  
Environmental Eng., METU

Prof. Dr. Filiz Bengü Dilek  
Environmental Eng., METU

Prof. Dr. Bülent İçgen  
Environmental Eng., METU

Assoc. Prof. Dr. Tuba Hande Bayramoğlu  
Environmental Eng., METU

Assoc. Prof. Dr. Nuray Ateş  
Environmental Eng., Erciyes University

Date: 02.07.2019



**I hereby declare that all information in this document has been obtained and presented in accordance with academic rules and ethical conduct. I also declare that, as required by these rules and conduct, I have fully cited and referenced all material and results that are not original to this work.**

Name, Surname: Būşra Sönmez

Signature:

## ABSTRACT

### REMOVAL OF IMIDACLOPRID FROM WASTEWATERS BY OZONATION AND PHOTO-OZONATION

Sönmez, Büşra

Master of Science, Environmental Engineering

Supervisor: Prof. Dr. Filiz Bengü Dilek

July 2019, 185 pages

The widespread occurrence of micropollutants in the receiving water bodies apparently shows that conventional wastewater treatment plants (WWTP) are not capable to remove these compounds. Imidacloprid (IMI), which is a specific pollutant and an insecticide, exceeded Environmental Quality Standards (EQS) value (0.14 µg/L, annual average) in several receiving water bodies of WWTPs in Yeşilirmak basin. With the aim of examining advanced treatment methods to meet EQS value and to achieve good surface water quality in Yeşilirmak basin, the removal of IMI from water and wastewaters by ozonation and O<sub>3</sub>/UV was comparatively studied for the first time. To this end, kinetic study under different pH, ozone doses, ozone gas flowrates, initial IMI concentration and wastewater matrices was sought. The higher pH was effective for IMI ozonation. The water matrix effect on IMI removal was more pronounced during ozonation, than during O<sub>3</sub>/UV. For all wastewater matrices, O<sub>3</sub>/UV led to the best results in terms of both IMI and degradation by-products' elimination since production rate of OH• enhanced under UV irradiation. Within 10 min treatment, IMI removal efficiencies in Milli-Q water were 55% and 99.5% during ozonation and O<sub>3</sub>/UV, respectively. IMI degradation mechanism proved that it is an ozone-resistant pollutant and is mainly degraded by OH• via indirect mechanism. The second-order rate constants of IMI reacting with OH• calculated as  $2.23 \times 10^{11}$  and  $9.08 \times 10^{11} \text{ M}^{-1}\text{s}^{-1}$

during ozonation and O<sub>3</sub>/UV, respectively. The IMI degradation pathway showed that IMI lost NO<sub>2</sub> and HNO<sub>2</sub>. In addition, similar by-products were determined after IMI treatment by ozonation and O<sub>3</sub>/UV.

Keywords: Imidacloprid, Wastewater Treatment, Ozonation, Photo-ozonation, By-product



## ÖZ

### İMİDAKLOPRİD'İN ATIKSUDAN OZONLAMA VE FOTO-OZONLAMA İLE UZAKLAŞTIRILMASI

Sönmez, Büşra  
Yüksek Lisans, Çevre Mühendisliği  
Tez Danışmanı: Prof. Dr. Filiz Bengü Dilek

Temmuz 2019, 185 sayfa

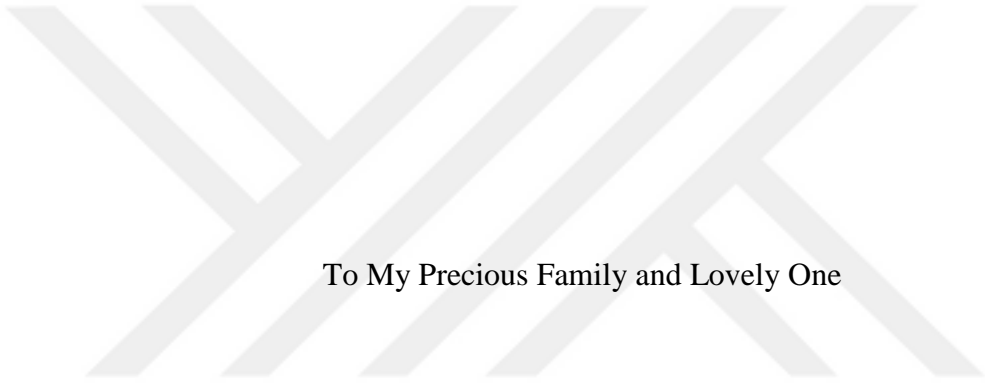
Mikrokirleticilerin alıcı ortamlarda yaygın olarak bulunması, konvansiyonel atıksu arıtma tesislerinin bu tür kirleticileri gideremediğini açıkça göstermektedir. Belirli kirletici ve insektisit olan İmidakloprid'in (IMI), Yeşilirmak havzasındaki çeşitli atıksu arıtma tesisinin alıcı ortamında Çevre Kalite Standartlarını (ÇKS) (0,14 µg/L, yıllık ortalama) aştığı gözlemlenmiştir. ÇKS değerinin sağlanması ve Yeşilirmak havzasında yüzey suyu kalitesine erişilmesi için ileri arıtma yöntemlerinin incelenmesi amaçlanarak ozonlama ve O<sub>3</sub>/UV prosesleriyle su ve atıksudan IMI giderimi karşılaştırılmalı olarak ilk kez çalışılmıştır. Bu amaçla, farklı pH, ozon dozu, ozon gazı debisi, başlangıç IMI konsantrasyonu ve atıksuların IMI giderim kinetiği üzerindeki etkileri araştırılmıştır. Yüksek pH'nın IMI ozonlamasında etkili olduğu görülmüştür. IMI gideriminde atıksu matrisinin etkisi ozonlama sırasında O<sub>3</sub>/UV'de gözlemlenenden daha belirgindir. Çalışılan bütün atıksu matrislerinde, UV ışınının OH• oluşumunu arttırmasından dolayı, IMI ve oluşan yan ürünlerin gideriminde O<sub>3</sub>/UV prosesi en iyi sonuçları vermiştir. 10 dakikalık arıtma süresince ozonlama ve O<sub>3</sub>/UV yöntemleri için IMI giderimi sırasıyla %55 ve %99,5'tir. IMI giderim mekanizması, IMI'in ozona karşı dirençli olduğunu ve indirekt mekanizma yoluyla esas olarak OH• tarafından giderildiğini kanıtlamıştır. IMI ile OH• arasındaki 2. derece hız sabitleri ozonlama ve O<sub>3</sub>/UV yöntemleri için sırasıyla 2,23×10<sup>11</sup> ve

$9,08 \times 10^{11} \text{ M}^{-1}\text{s}^{-1}$  olarak hesaplanmıştır. İMI giderim yolu İMI'in parçalanması sırasında  $\text{NO}_2$  ve  $\text{HNO}_2$  kaybettiğini göstermiştir. Ayrıca, İMI'in ozonlama ve  $\text{O}_3/\text{UV}$  prosesleriyle giderimi sonucunda benzer yan ürünlerin oluştuğu gözlemlenmiştir.

**Anahtar Kelimeler:** İmidaklopid, Atıksu Arıtımı, Ozonlama, Foto-ozonlama, Yan Ürün







To My Precious Family and Lovely One

## ACKNOWLEDGEMENTS

I would like to express my deepest respect and candid gratitude to my supervisor Prof. Dr. Filiz Bengü Dilek for her endless motivation, support, incredible guidance and immense knowledge. Her never-ending attention, patience and trust made me to proceed my research work in a stressless environment.

I greatly appreciate the financial support received from The Scientific and Technological Research Council of Turkey (TÜBİTAK) for the project with a title of “Management of Point and Non-Point Pollutant Sources in Yeşilırmak Basin”. I would also like to express my deepest appreciation to the project coordinator Prof. Dr. Ülkü Yetiş for her continual advices and helpful discussions.

I would like to thank to my dearest colleagues and friends Cansu, Dilan, Irmak, İrem, Selin, Umut, Elif and Dilara for providing me with unfailing support and continuous encouragement throughout my years of study, the process of researching and writing this thesis.

I would like to give my heartfelt thanks to my parents and my brother, whose endless love and support are with me in whatever I pursue. They always believe in me and encourage me to follow my dreams. Specials thanks to my fiancé, Mehmet for his eternal love, support, guidance and great joy. He has been by my side throughout this M.S. degree, and without whom, I would not have had the courage to embark on the journey towards my goals and dreams.

This work was supported by TÜBİTAK (Grant No: 115Y103) and partially supported by BAP METU (Grant No: YLT-311-2018-3495).

## TABLE OF CONTENTS

ABSTRACT .....	v
ÖZ .....	vii
ACKNOWLEDGEMENTS .....	x
TABLE OF CONTENTS .....	xi
LIST OF TABLES .....	xv
LIST OF FIGURES .....	xvi
LIST OF ABBREVIATIONS .....	xx
CHAPTERS	
1. INTRODUCTION .....	1
1.1. General .....	1
1.2. Relevant Legislation .....	3
1.3. Yeşilirmak Basin Case .....	4
1.4. Aim and Scope of the Study .....	8
2. THEORETHICAL BACKGROUND and LITERATURE REVIEW .....	11
2.1. Micropollutants .....	11
2.1.1. Occurrence .....	11
2.1.2. Adverse Effects .....	15
2.1.3. Treatment Options .....	17
2.2. Imidacloprid .....	24
2.2.1. Physicochemical Properties .....	26
2.2.2. Occurrence and Adverse Effect of IMI in Water .....	28
2.2.3. Fate of IMI in Water .....	29

2.3. Removal of IMI from Water .....	36
2.3.1. Biological Treatment .....	36
2.3.2. Physical Treatment .....	36
2.3.3. Chemical Treatment .....	39
2.4. Ozonation Process .....	43
2.4.1. Physicochemical properties of O <sub>3</sub> .....	44
2.4.2. The mechanism of O <sub>3</sub> action .....	46
2.4.3. Factors affecting the treatment efficiency of O <sub>3</sub> .....	51
2.4.4. Reaction Kinetics .....	56
2.5. Ozone/UV Process .....	57
3. MATERIALS AND METHODS .....	61
3.1. IMI Concentrations Studied .....	61
3.2. Water Samples and Sample Preparation .....	62
3.3. Experimental Set Up .....	64
3.3.1. Ozone Generator .....	64
3.3.2. Ozonation Reactor .....	65
3.3.3. Ozone/UV Reactor .....	67
3.4. Experimental Methods .....	68
3.4.1. Ozone Consumption in the Ozonation System .....	68
3.4.2. Ozonation of IMI .....	69
3.4.3. Photo-ozonation (O <sub>3</sub> /UV) of IMI .....	73
3.4.4. Hydroxyl Radical Analysis for Ozonation and O <sub>3</sub> /UV .....	75
3.5. Analytical Methods .....	77
3.5.1. IMI Measurement .....	77

3.5.2. HPLC Method Development .....	79
3.5.3. LOD and LOQ Determination .....	80
3.5.4. pCBA measurement.....	81
3.5.5. Ozone Measurement .....	82
3.5.6. By-Products' Determination .....	83
3.5.7. pH Measurement.....	84
3.5.8. UV Light Intensity Determination via KI/KIO <sub>3</sub> Actinometer .....	84
3.6. Chemicals Used .....	87
<b>4. RESULTS AND DISCUSSION .....</b>	<b>89</b>
4.1. Ozonation of IMI.....	89
4.1.1. Effect of Buffer .....	89
4.1.2. Effect of pH .....	93
4.1.3. Effect of Ozone Dose.....	96
4.1.4. Effect of Ozone Gas Flowrate .....	103
4.1.5. Effect of Initial IMI Concentration .....	107
4.1.6. Ozonation Mechanism of IMI Degradation.....	109
4.1.7. Effect of Water Matrix.....	112
4.1.8. Ozonation By-Products of IMI .....	115
4.2. Ozonation Reaction Kinetics .....	117
4.2.1. Effect of Buffer .....	119
4.2.2. Effect of pH .....	120
4.2.3. Effect of Ozone Dose.....	121
4.2.4. Effect of Ozone Gas Flowrate .....	122
4.2.5. Effect of Initial IMI Concentration.....	123

4.2.6. Ozonation Mechanism of IMI Degradation .....	125
4.2.7. Effect of Water Matrix .....	128
4.3. Photo-ozonation (O <sub>3</sub> /UV) of IMI.....	130
4.3.1. Effect of Water Matrix .....	130
4.3.2. Photo-ozonation Mechanism of IMI Degradation.....	134
4.3.3. Photo-ozonation By-Products of IMI.....	137
4.4. Photo-ozonation (O <sub>3</sub> /UV) Reaction Kinetics .....	139
4.4.1. Effect of Water Matrix .....	140
4.4.2. Photo-ozonation Mechanism of IMI Degradation.....	141
5. CONCLUSION .....	147
REFERENCES .....	153
APPENDICES .....	177
A. Ozone generator's performance curve .....	177
B. LC-MS/MS method information.....	178
C. LC-MS/MS Chromatograms.....	179

## LIST OF TABLES

### TABLES

Table 1. IMI levels at WWTPs of Yeşilırmak Basin .....	7
Table 2. Physicochemical properties of IMI [127,128] .....	27
Table 3. Imidacloprid levels in wastewater and surface water .....	29
Table 4. Oxidizing potential values for common oxidants [187] .....	45
Table 5. Physicochemical properties of O <sub>3</sub> [183,187] .....	45
Table 6. Examples for initiators, terminators and scavengers act during ozone decomposition [92].....	51
Table 7. Properties of IMI detection method in the HPLC .....	78
Table 8. HPLC gradient conditions for IMI.....	78
Table 9. HPLC method optimization for both IMI and by-products .....	80
Table 10. pCBA detection method in the HPLC .....	81
Table 11. Selected samples for analysis of possible by-products .....	84

## LIST OF FIGURES

### FIGURES

Figure 1. Map of the Yeşilırmak recharge basin in Turkey (a), Main cities and tributaries in Yeşilırmak basin (b) [16] .....	5
Figure 2. IMI exceeded EQS values in WWTPs in the Yeşilırmak basin .....	6
Figure 3. Micropollutant sources [31] .....	12
Figure 4. Significant neonicotinoid insecticides released to the market in chronological order [121] .....	25
Figure 5. Molecular Structure of IMI [127].....	26
Figure 6. The proposed mechanism for photo degradation of IMI [169].....	34
Figure 7. The proposed mechanism for hydrolysis of IMI [130] .....	35
Figure 8. Resonance structure of O <sub>3</sub> [186] .....	44
Figure 9. Ozone reactivity mechanism toward to pollutant, R [185] .....	46
Figure 10. Proposed reaction pathway for Criegee mechanism [191].....	47
Figure 11. Proposed reaction pathway of ozone and aromatic compound [185] .....	48
Figure 12. Overall mechanism for ozone decomposition [185] .....	49
Figure 13. Ozone generator .....	64
Figure 14. Experimental setup for ozonation .....	66
Figure 15. Experimental setup for O <sub>3</sub> /UV .....	67
Figure 16. Agilent HPLC.....	77
Figure 17. Calibration curve for IMI .....	79
Figure 18. HPLC Calibration curve for pCBA.....	82
Figure 19. Time course variation of absorbance of I <sub>3</sub> <sup>-</sup> at 352 nm.....	85
Figure 20. Variation of solution pH during the ozonation with and without buffer addition (Milli-Q water, O <sub>3</sub> dose= 2400 mg/h, O <sub>3</sub> flowrate= 100 L/h, C <sub>0</sub> = 500 ppb, T =24°C ±1°C.).....	90
Figure 21. Degradation of IMI with and without buffer addition. (Milli-Q water, O <sub>3</sub> dose= 2400 mg/h, O <sub>3</sub> flowrate= 100 L/h, C <sub>0</sub> = 500 ppb, T =24°C ±1°C.).....	90



Figure 22. Time course variation of (a) IMI concentration (b) Removal efficiencies at different pHs (Milli-Q water, $C_0= 500$ ppb, $O_3$ dose= 1200 mg/h, $O_3$ flowrate= 30 L/h $T=24^\circ C \pm 1^\circ C$ .).....	94
Figure 23. Time course variation of (a) IMI concentration (b) IMI removal efficiency at different ozone doses. (Milli-Q water, $C_0= 500$ ppb, $O_3$ flowrate= 30 L/h, $pH= 7.25 \pm 0.1$ , $T=24^\circ C \pm 1^\circ C$ .).....	97
Figure 24. Profile of IMI degradation as a function of applied ozone amount. (Milli-Q water, $C_0= 500$ ppb, $O_3$ flowrate= 30 L/h, $pH= 7.25 \pm 0.1$ , $T=24^\circ C \pm 1^\circ C$ .) .....	99
Figure 25. Time course variation of IMI and BP-1 at different ozone doses (Milli-Q water, $C_0= 500$ ppb, $O_3$ flowrate= 30 L/h, $pH= 7.25 \pm 0.1$ , $T=24^\circ C \pm 1^\circ C$ .) .....	101
Figure 26. Time course variation of IMI and BP-2 at different ozone doses (Milli-Q water, $C_0= 500$ ppb, $O_3$ flowrate= 30 L/h, $pH= 7.25 \pm 0.1$ , $T=24^\circ C \pm 1^\circ C$ .) .....	102
Figure 27. Time course variation of (a) IMI concentration (b) IMI removal efficiency at different ozone flowrates. (Milli-Q water, $C_0= 500$ ppb, $O_3$ dose= 1200 mg/h, $pH= 7.25 \pm 0.1$ , $T=24^\circ C \pm 1^\circ C$ .).....	104
Figure 28. Profile of IMI degradation as a function of applied ozone amount. (Milli-Q water, $C_0= 500$ ppb, $O_3$ dose= 1200 mg/h, $pH= 7.25 \pm 0.1$ , $T=24^\circ C \pm 1^\circ C$ .) .....	105
Figure 29. Time course variation of (a) IMI concentration (b) IMI removal efficiency at different initial IMI concentrations. (Milli-Q water, $O_3$ dose= 1200 mg/h, $O_3$ flowrate= 30 L/h, $pH= 7.25 \pm 0.1$ , $T=24^\circ C \pm 1^\circ C$ .) .....	108
Figure 30. Time course variation of (a) IMI concentration (b) IMI removal efficiency by $O_3$ and $O_3/OH^\bullet$ i.e. with and without TBA addition, respectively. (Milli-Q water, $C_{TBA}=100$ mM, $[IMI]_0= 1000$ ppb, $O_3$ dose= 1200 mg/h, $O_3$ flowrate= 30 L/h $pH= 7.25 \pm 0.1$ , $T=24^\circ C \pm 1^\circ C$ .).....	110
Figure 31. Time course variation of (a) IMI concentration (b) IMI removal efficiency in different water matrices. ( $[IMI]_0= 1000$ ppb for Milli-Q water and VRMBR WW, $[IMI]_0= 226$ ppb for Bio WW, $O_3$ dose= 1200 mg/h, $O_3$ flowrate= 30 L/h $pH= 7.25 \pm 0.1$ , $T=24^\circ C \pm 1^\circ C$ .).....	113
Figure 32. The proposed degradation pathway of IMI .....	116

Figure 33. Reaction kinetics of IMI with and without buffer addition. (Milli-Q water, O <sub>3</sub> dose= 2400 mg/h, O <sub>3</sub> flowrate= 100 L/h, C <sub>0</sub> = 500 ppb, T =24°C ±1°C.).....	119
Figure 34. Reaction kinetics of IMI at different pHs (Milli-Q water, C <sub>0</sub> = 500 ppb, O <sub>3</sub> dose= 1200 mg/h, O <sub>3</sub> flowrate= 30 L/h T=24°C ±1°C.) .....	120
Figure 35. Reaction kinetics of IMI at different ozone doses. (Milli-Q water, C <sub>0</sub> = 500 ppb, O <sub>3</sub> flowrate= 30 L/h, pH= 7.25 ± 0.1, T=24°C ±1°C.).....	121
Figure 36. Reaction kinetics of IMI at different ozone at different ozone gas flowrates. (Milli-Q water, C <sub>0</sub> = 500 ppb, O <sub>3</sub> dose= 1200 mg/h, pH= 7.25 ± 0.1, T=24°C ±1°C.) .....	123
Figure 37. Reaction kinetics of IMI at different initial IMI concentrations. (Milli-Q water, O <sub>3</sub> dose= 1200 mg/h, O <sub>3</sub> flowrate= 30 L/h, pH= 7.25 ± 0.1, T=24°C ±1°C.) .....	124
Figure 38. IMI degradation kinetics by O <sub>3</sub> and O <sub>3</sub> /OH• i.e. with and without TBA addition, respectively. (Milli-Q water, C <sub>TBA</sub> =100 mM, [IMI] <sub>0</sub> = 1000 ppb, O <sub>3</sub> dose= 1200 mg/h, O <sub>3</sub> flowrate= 30 L/h pH= 7.25 ± 0.1, T=24°C ±1°C.).....	125
Figure 39. Natural logarithm of the relative concentration of IMI vs pCBA (Milli-Q water, C <sub>pCBA</sub> =5 μM, [IMI] <sub>0</sub> = 1000 ppb, O <sub>3</sub> dose= 1200 mg/h, O <sub>3</sub> flowrate= 30 L/h pH= 7.25 ± 0.1, T=24°C ±1°C.) .....	128
Figure 40. Reaction kinetics of IMI in different water matrices. ([IMI] <sub>0</sub> = 1000 ppb for Milli-Q water and VRMBR WW, [IMI] <sub>0</sub> = 226 ppb for Bio WW, O <sub>3</sub> dose= 1200 mg/h, O <sub>3</sub> flowrate= 30 L/h pH= 7.25 ± 0.1, T=24°C ±1°C.).....	129
Figure 41. Time course variation of (a) IMI concentration (b) IMI removal efficiency in different water matrices. ([IMI] <sub>0</sub> = 1000 ppb for Milli-Q water and VRMBR WW, [IMI] <sub>0</sub> = 332 ppb for Bio WW, UV lamp= 10 W, O <sub>3</sub> dose= 1200 mg/h, O <sub>3</sub> flowrate= 30 L/h pH= 7.25 ± 0.1, T=24°C ±1°C.).....	131
Figure 42. Time course variation of (a) IMI concentration (b) IMI removal efficiency by O <sub>3</sub> and O <sub>3</sub> /OH• i.e. with and without TBA addition, respectively. (Milli-Q water, C <sub>TBA</sub> =200 mM, [IMI] <sub>0</sub> = 1000 ppb, UV lamp= 10 W, O <sub>3</sub> dose= 1200 mg/h, O <sub>3</sub> flowrate= 30 L/h pH= 7.25 ± 0.1, T=24°C ±1°C.) .....	136
Figure 43. Imidacloprid olefin desnitro ( <i>m/z</i> 208) [168] .....	138

Figure 44. Reaction kinetics of IMI in different water matrices. ([IMI]<sub>0</sub>= 1000 ppb for Milli-Q water and VRMBR WW, [IMI]<sub>0</sub>= 332 ppb for Bio WW, UV lamp= 10 W, O<sub>3</sub> dose= 1200 mg/h, O<sub>3</sub> flowrate= 30 L/h pH= 7.25 ± 0.1, T=24°C ±1°C.) .....140

Figure 45. IMI degradation kinetics by O<sub>3</sub> and O<sub>3</sub>/OH• i.e. with and without TBA addition, respectively during O<sub>3</sub>/UV. (Milli-Q water, C<sub>TBA</sub>=200 mM, [IMI]<sub>0</sub>= 1000 ppb, UV lamp= 10 W, O<sub>3</sub> dose= 1200 mg/h, O<sub>3</sub> flowrate= 30 L/h pH= 7.25 ± 0.1, T=24°C ±1°C.).....142

Figure 46. Natural logarithm of the relative concentration of IMI vs pCBA (Milli-Q water, C<sub>pCBA</sub>=5 μM, [IMI]<sub>0</sub>= 1000 ppb, O<sub>3</sub> dose= 1200 mg/h, O<sub>3</sub> flowrate= 30 L/h pH= 7.25 ± 0.1, T=24°C ±1° .....144

## LIST OF ABBREVIATIONS

ACN	Acetonitrile
AOP	Advanced Oxidation Processes
BP-1	By-product-1
BP-2	By-product-2
COD	Chemical Oxygen Demand
DO	Dissolved Ozone
EDC	Endocrine Disrupting Chemical
EQS	Environmental Quality Standard
GUS	Groundwater Ubiquity Score
HPLC	High Performance Liquid Chromatograph
IMI	Imidacloprid
O <sub>3</sub>	Ozone / Ozonation
O <sub>3</sub> /UV	Photo-ozonation
OH•	Hydroxyl radical
pCBA	P-chlorobenzoic acid
PPCP	Pharmaceuticals and Personal Care Product
SWQR	Surface Water Quality Regulation
TBA	Tert-butanol
TOC	Total Organic Carbon

WFD Water Framework Directive

WWTP Waste Water Treatment Plant





## CHAPTER 1

### INTRODUCTION

#### 1.1. General

In the recent years, micropollutants, also named as emerging contaminants, have become a major environmental concern. Micropollutants include pharmaceuticals and personal care products, (PPCPs), endocrine disrupting chemicals (EDCs), cosmetics, perfumes and pesticides. These pollutants have been ubiquitously detected at trace concentrations ranging from  $\mu\text{g/L}$  to  $\text{ng/L}$  in the receiving water bodies. Although the micropollutants are typically presented at very low concentrations, their adverse effects on the aquatic lives and humans are evident [1]. Indeed, the awareness of micropollutant occurrence in the water environment has been increased enormously due to the increased chance of cancer, extraordinary physiological processes and reproductive deterioration in humans, augmentation of antibiotic-resistant bacteria and potential raise of chemical mixture's toxicity [2]. There are several sources for the micropollutants as follows [3];

- Regular agricultural activities like pesticide treatment (up to  $10 \mu\text{g/L}$ )
- Water runoff from agricultural areas
- Rinsing the pesticide containers and spray equipment with water (10-100  $\text{mg/L}$ )
- Wastewater produced by agricultural industries during fruit and vegetable cleaning processes
- Wastewater produced by pesticide formulating and manufacturing plants
- Hospital discharges
- Domestic wastewater

The widespread occurrence of micropollutants in the water bodies apparently shows that conventional wastewater treatment plants (WWTPs) are not capable to remove these compounds, and hence the majority of micropollutants readily pass through treatment plants and are being continuously discharged into receiving water body. So, the treatment plants become major point sources for the micropollutants [4]. For this reason, implementation of advanced treatment processes is inevitable which aims to remove these micropollutants or to transform them into less harmful compounds.

In the literature studies, micropollutant removal has been widely performed by several advanced treatment processes. Physical treatment techniques such as adsorption [5] and membrane filtration [6] are frequently used but, these treatment processes have some operational and economic problems. One of the major disadvantages of the adsorption is adsorbent regeneration issues which make the adsorption process economically unfeasible. On the other hand, membrane filtration, besides being an energy intensive process, produces a concentrate which requires further treatment or disposal [7].

Advanced oxidation processes (AOPs), which is a chemical treatment method, have been found to be one of the most promising advanced treatment techniques to degrade vast range of micropollutants [8]. Ozonation, O<sub>3</sub>/UV, Fenton and photo-Fenton have been established as the most commonly used AOPs for micropollutant removal. However, some disadvantages of Fenton process are production of a sludge and the limitation of optimum operational pH range between 2.5 and 3.0 [7]. Although ozone has been widely applied for water and wastewater disinfection purposes for several decades, it has also been used in recent years to remove or degrade many micropollutants [9].



## 1.2. Relevant Legislation

In several countries, treatment and management of industrial wastewaters emerging from manufacturing of PPCPs, pesticide and other compounds has been suitably done in accordance with regulations [10]. European Union (EU) and United States Environmental Protection Agency (USEPA) have identified wide range of chemicals which are detected in the wastewater and surface waters and may pose a risk for aquatic environment. In 2000, as part of the EU, Water Framework Directive (WFD) 2000/60/EC identified an initial list of 33 “priority substances” in order to control these pollutants for the next 20 years [11]. In 2013, the WFD has reported Environmental Quality Standards (EQS) Directive (2013/39/EU) which defines EQS for priority substances in the surface waters [12]. Furthermore, “river basin specific pollutants” have been identified by Member States in the scope of WFD and the priority substances were increased to 45. The aim of this second list is to control the pollutants at the river basin scale since different river basins may have different substances. Therefore, during risk assessment of the aquatic environment, the EQS has to be used as classification of surface water status and discharge controlling within the context of WFD [13].

The WFD stipulates “good status” for all waters. “Surface water status” represents the poorer status of its chemical and ecological status. Chemical status regards level of the priority pollutants concentration in the concerned surface waters. Ecological status, on the other hand, represents the quality of structure and functioning of aquatic ecosystems. Moreover, ecological status considers the chemical, hydrological characteristic and the biological quality of the surface water by examining the level of specific pollutants [13]. The overall ecological status is determined by the assessment of the poorest condition. For instance, if chemical and physico-chemical properties of water body is in “Good Status” and biological assessment is classified as “Moderate Status” then the overall quality status of water body would be classified as “Moderate Status”. However, the WFD requires overall good surface water status which could be

possible by having at least “Good Ecological Status” and “Good Chemical Status” in that water body [13].

Turkey, as a candidate of EU, is also responsible for meeting environmental standards in WFD by 2025 [14]. In our country, Surface Water Quality Regulation (SWQR) was published by the former Ministry of Forestry and Water Affairs in order to maintain the water quality [15]. The water quality classes are specified as Class I, Class II, Class III and Class IV (in descending order of water quality). Furthermore, EQS values for 250 specific pollutants are given in SWQR (Appendix 2; Table 4 given in SWQR). Accordingly, these EQS values must be met on the receiving water body after the wastewater effluent was discharged. Thus, removal of IMI is of great importance to provide good surface water quality and in a way, to prevent possible the adverse effects on the receiving water body.

### **1.3. Yeşilırmak Basin Case**

Yeşilırmak basin is one of the 26 major basins in Turkey, located in the northern side of the country (Figure 1a). The coordinates of Yeşilırmak basin is 39°30' and 41°21' N, and 34°40' and 39°48' E [16]. The Yeşilırmak river flows 519 km and reaches to the Black Sea (near the city of Samsun) and generates large delta. Recharge basin area of Yeşilırmak is 38,730 km<sup>2</sup> which comprises of 5% of surface area of Turkey [17]. Some major cities in Yeşilırmak basin are Samsun, Amasya, Çorum, and Tokat (Figure 1b) [16].

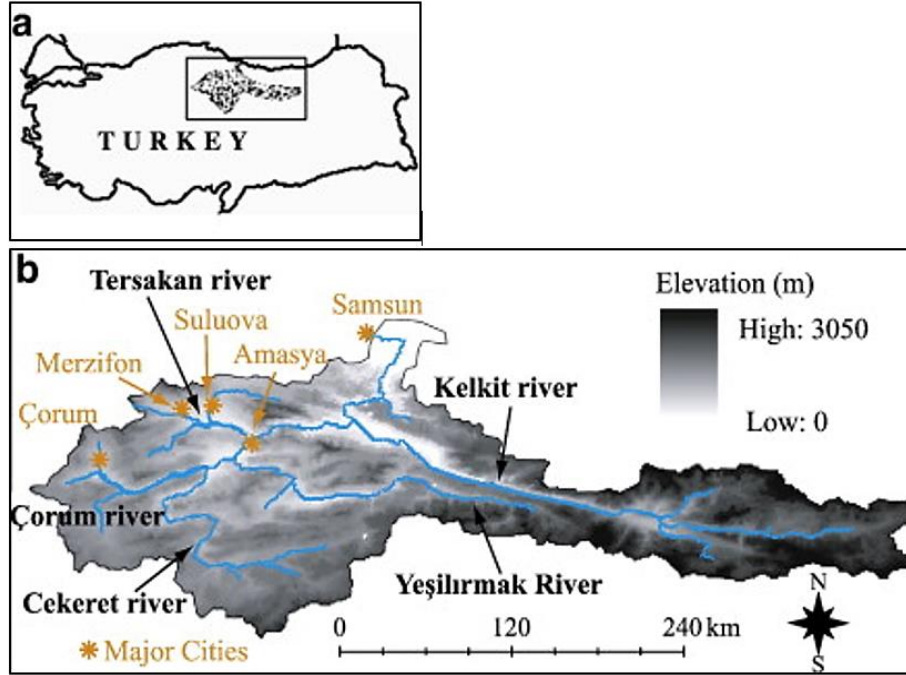


Figure 1. Map of the Yeşilirmak recharge basin in Turkey (a), Main cities and tributaries in Yeşilirmak basin (b) [16]

TUBITAK 1003 project with a title of “Management of Point and Non-Point Pollutant Sources in Yeşilirmak Basin” is being performed (Grant no: 115Y013) in our department.

The main goals of the project are;

- To develop a management strategy that will provide the management of point and non-point pollution sources causing water pollution with a holistic approach
- To ensure the water bodies in Yeşilirmak Basin to achieve the target of "good status" in accordance with the SWQR of Turkey.

Sub goals of the project are;

- Identification of the main point and non-point sources and the specific pollutants for the Yeşilırmak Basin
- Performing an inventory of pollutants indicating the spatial distribution of the pollutant sources, and pollution loads
- Evaluation of the processes and performances of existing treatment plants  
Determination of the most appropriate pollution control strategy for the provision of EQS for all point and non-point sources.

Within the scope of the project, monitoring studies were conducted in the Yeşilırmak basin area. Indeed, more than 100 stations including several municipal and industrial WWTPs were monitored during 8 monitoring periods between August 2016 and January 2018. In this monitoring studies, classical parameters, 45 priority and 250 specific pollutants were monitored. IMI is one of the most frequently observed pesticide in the Yeşilırmak river basin and in effluent of WWTPs. EQS values of IMI were specified in the SWQR of Turkey as  $0.14\mu\text{g/L}$  and  $1.4\mu\text{g/L}$  for annual average and maximum, respectively.



Figure 2. IMI exceeded EQS values in WWTPs in the Yeşilırmak basin

IMI exceeded the EQS several times in the WWTP's effluents (Table 1), indicating the possibility of exceedance of EQS in the receiving water bodies and hence not complying the SWQR in terms of the EQS set for IMI. Evidently, EQS for IMI was exceeded in the downstream of the Çorum WWTP (Table 1). The locations of these WWTPs are indicated in Figure 2.

Table 1. IMI levels at WWTPs of Yeşilirmak Basin

	<b>Çorum WWTP</b>	<b>Erbaa WWTP</b>	<b>Tokat WWTP</b>	<b>Dimes WWTP</b>
WWTP Type	Municipal	Municipal	Municipal	Industrial
Treatment Process	Biological treatment	Biological treatment	Advanced biological treatment	Biological treatment
Flowrate (m <sup>3</sup> /h)	2,350	395	123	17
IMI conc. (µg/L)	0.240	0.600	0.760	0.196
Exceeding level of EQS in WWTP's effluent	1.7 times	4.2 times	5.4 times	1.4 times
IMI conc. at Upstream Station	No data due to drought	< EQS	< EQS	< EQS
IMI conc. at Downstream Station	> 2.2 times	< EQS	< EQS	< EQS

As seen in Table 1, IMI exceeded EQS values in stated WWTPs' effluent at least 1.4 and at most 5.4 times indicating that IMI was detected in municipal and industrial WWTPs. Although IMI was observed above the EQS values at effluent discharge points, IMI was below the EQS value at the downstream stations of Erbaa, Tokat and Dimes WWTP. It should be pointed here that the downstream stations were not located very near to the discharge points, rather at a distance varying from 8 to 21.7 km. So, natural degradation or dilution effects were possibly in effect. On the other hand, IMI was observed above the EQS value at Çorum downstream station which could be due to not only effluents of WWTPs but also non-point sources such as agricultural

activities around this area. Near to downstream location of Çorum WWTP, it is known that wheat, grape, potato, tomato, apple, sugar beet and cherry are produced at this area. Although the exact IMI amount applied to these produces was not known, IMI is generally used for cultivation of aforementioned produces in the Yeşilirmak basin. Another point needs to be mentioned is related to the observation of IMI at Dimes WWTP owned by a fruit juice industry, which could be attributed to the pesticides used during the cultivation of the fruits processed at the Dimes Factory.

From the foregoing discussion, it is clear that the necessity for the IMI treatment at these WWTPs is apparent to achieve the EQS value stated in SWQR and to fulfill “Good Status” at receiving water body in the Yeşilirmak basin [15].

Regarding the literature studies on the removal of IMI from water or wastewaters, there are several studies in which various processes, such as adsorption [18], membrane filtration [6], photo-Fenton [19], photocatalysis [20], ozonation [21-23] and cavitation [24] were used. As mentioned above, there are some advantages and disadvantages of these processes. However, among these processes, ozonation, as one of the favorable AOPs [25], attracted our attention. Because, in addition to being used in very few studies for IMI removal, to the best of our knowledge, photo-ozonation, i.e. O<sub>3</sub>/UV has never been applied.

#### **1.4. Aim and Scope of the Study**

This thesis work aimed to fill the existing gap, which was put forward in above subsection, by providing comprehensive work on the removal of IMI from wastewaters by ozonation and photo-ozonation (O<sub>3</sub>/UV) processes in a comparative manner and by presenting the possible reaction pathway of degradation by-products, as well.

To this purpose, the following studies were conducted:

- Effects of operational parameters (pH buffer, solution pH, ozone dose, ozone gas flow rate, initial IMI concentration, water matrix) on the IMI removal by ozonation were investigated.
- IMI degradation mechanism during the ozonation was sought.
- Ozonation by-products were searched.
- Degradation kinetics study was performed for the ozonation experiments.
- Removal of IMI by photo-ozonation was investigated under the operational conditions leading to the highest IMI removal during the ozonation studies, for various water matrix conditions.
- IMI degradation mechanism during the photo-ozonation was sought.
- Photo-ozonation by-products were searched.
- Degradation kinetics study was performed for the photo-ozonation experiments.

To achieve the above-mentioned objectives, within the scope of the study, the followings were performed.

With regard to IMI ozonation, firstly, pH buffer effect was investigated by addition of phosphate buffer into the solution. Then, the effect of pH on the IMI removal was examined by working at different pH values, namely 6.20, 7.30 and 8.25. Secondly, the effects of other operational parameters such as ozone dose and ozone gas flowrate were investigated. IMI degradation by applying several ozone doses, namely 600, 1200 and 1800 mg/h were studied. Moreover, cases with different ozone gas flowrates of 15, 30 and 100 L/h were evaluated. The effect of initial IMI concentrations (i.e. 100 ppb, 500 ppb and 1000 ppb) on the IMI removal efficiency were also investigated. Further, the IMI degradation pathway was sought through the by-products formed via LC-MS/MS measurements. The IMI degradation mechanism if by direct (i.e. by O<sub>3</sub> itself) or indirect ozonation (i.e. by OH•) and indirect kinetic study were also sought

through addition of 100 mM tert-butanol (TBA) and 5  $\mu$ M p-chlorobenzoic acid (pCBA) into the reaction solution, respectively. Moreover, regarding the effect of water matrix on the IMI ozonation, ozonation experiments under the best conditions determined through the above-mentioned experiments were performed with Milli-Q water, VRMBR WW and Bio WW, as well.

During the experiments for photo-ozonation of IMI, 10-Watt UV lamp was coupled to ozonation to enhance production of  $\text{OH}\cdot$ , and hence to increase the IMI removal efficiency. In this respect, Milli-Q water, VRMBR WW and Bio WW were subjected to 1200 mg/h ozonation dose with 10-Watt UV irradiation in order to investigate the effect of water matrix. By-products which were formed during the photo-ozonation were analyzed with the help of LC-MS/MS. The IMI degradation mechanism and indirect reaction kinetic study during  $\text{O}_3/\text{UV}$  were determined by the addition of 200 mM tert-butanol (TBA) and 5  $\mu$ M p-chlorobenzoic acid (pCBA) into the photo-ozonation reaction solution, respectively.



## CHAPTER 2

### THEORETHICAL BACKGROUND AND LITERATURE REVIEW

#### 2.1. Micropollutants

Water is priceless resource for all living organisms and for several processes such as domestic and industrial usage and agricultural activities, as well. Nevertheless, several chemicals may contaminate water bodies. Micropollutants are one of the contaminant groups that are detected at the surface water, ground water and wastewaters. Micropollutants are present at trace amount ranging from  $\mu\text{g/L}$  to  $\text{ng/L}$  in the water bodies [26]. Micropollutants are consist of several materials including pesticides, pharmaceuticals and personal care products (PPCPs), endocrine disrupting chemicals (EDCs), cosmetics and perfumes [27]. Pharmaceutical products include variety types of human and veterinary antibiotics, drugs and some steroid hormones [2]. Personal care products consist of fragrance, cosmetics and disinfectants [28] that contains galaxolide and tonalide [2]. Moreover, household products that contain fragrance, surfactants, preservatives, plasticizers and biocides are also micropollutant sources [29]. It is well-known that only 0.1% of applied pesticides can reach to target pests, however, the majority of applied pesticide (99.9%) introduce into surrounding environment. Moreover, since conventional wastewater treatment plants are not designed for the removal of micropollutants, effluent discharge into aquatic environment may cause several adverse effects. For this reason, advanced treatment techniques are applied in WWTPs [4].

##### 2.1.1. Occurrence

Micropollutants may enter the water bodies via direct (i.e. point sources) or indirect pathways (i.e. nonpoint sources). Point source is diagnosable pollution source like

WWTPs. On the other hand, non-point source forms a diffuse pollution and the exact source cannot be easily identified. Common non-point sources may be rainfall runoff, agricultural and forestry land use [30].

The occurrence of micropollutants can manifest in several ways which include industrial wastewaters, runoff from agricultural sites, domestic and hospital discharges that may join into surface water and groundwater and eventually end up by drinking or wastewater treatment plants (Figure 3) [31].

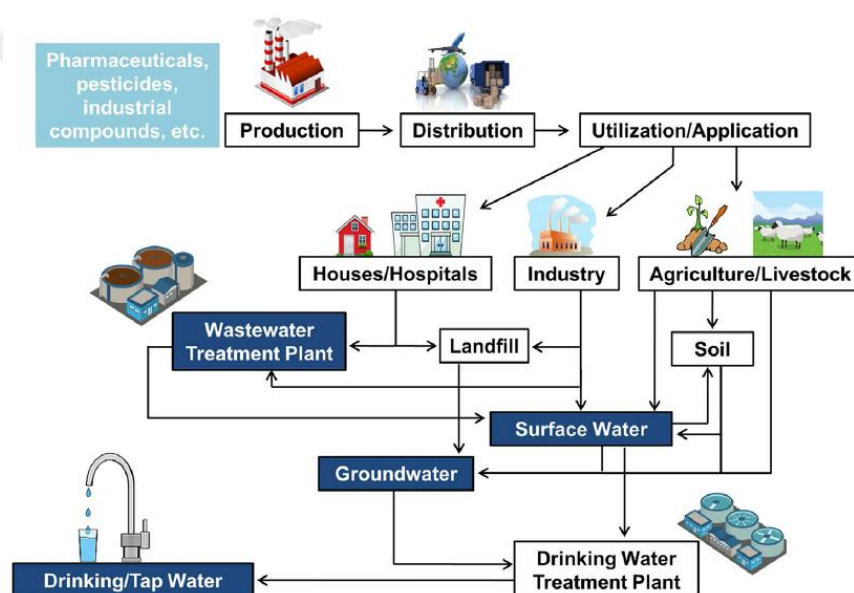


Figure 3. Micropollutant sources [31]

Although micropollutant sources in the environment are diverse, the main route for micropollutant entrance into environment is effluent wastewater discharges. For example, one of the major sources of PPCPs is domestic wastewater since the drugs used by both humans and animals can be discharged via wastewater [32]. Furthermore, dissolved but non-metabolized drugs can be excreted from the bodies via urine or feces which eventually present in wastewater [33]. Several countries such as USA [34],

United Kingdom [35], Finland [36], Japan [37], Spain [38], Italy [39] and Africa [40] reported occurrence of pharmaceuticals in concentration of ng/L to µg/L in WWTPs.

Pesticides are commonly used for protecting plants from various diseases, weed and insect harm. Pesticides are toxic to both vertebrate and non-vertebrate organisms which negatively affect the non-target organisms [41]. Pesticides are grouped based on their target pests such as insecticides, herbicides, fungicides, acaricides, nematicides, molluscicides and rodenticides [42]. Extensive usage of pesticides causes pollution in the surface water via water runoff, water flows through agricultural land to surface water and agricultural storm water discharges. During water runoff, pesticides are carried by water and eventually deposited into water bodies such as lakes, rivers and groundwater [43]. Pesticides which are polar and has high water solubility have been commonly observed in the surface waters at level of ng/L [44]. In rural areas, major pesticide water pollution sources are as follows [3];

- Water runoff from agricultural areas
- Regular agricultural activities like pesticide treatment (up to 10 µg/L)
- Rinsing the pesticide containers and spray equipment with water (10-100 mg/L)

On the other hand, in urban areas, effluent from WWTPs is the main source of pesticide in the surface water, coming out due to non-agricultural uses of pesticides [45]. These applications include grass management in parks, golf courses, industrial vegetation control such as industrial facilities and railroads, public health issues like mosquito control and rodent control [46]. In addition, wastewater produced by agricultural industries during fruit and vegetable cleaning processes or pesticide manufacturing plants may cause pesticide pollution in the receiving water body in the range of 10-100 mg/L. Indeed, the pesticide occurrence in the surface water could be as high as 1000 mg/L due to effluent produced by pesticide formulating and manufacturing plants [3].

Worldwide pesticide consumption has dramatically changed since 1960s. The sale of insecticides increased from 310 million US dollars in 1960 to 7,798 million US dollars in 2005. Similarly, herbicides' sale increased from 170 million US dollars to 14,971 million in 1960 and 2005, respectively [47]. According to US EPA, approximately 6 billion pounds (~ 2.7 million tons) pesticide was produced annually in the world in both 2011 and 2012. Moreover, between 2008 and 2012, nearly 50% of total produced pesticide was herbicides in all years and followed by fumigants, insecticides, and fungicides [48].

Nowadays, China is the largest consumer and producer of pesticides with an annual pesticide use of  $1.8 \times 10^9$  kg in 2011. The applied pesticide amount is 14 kg/ha in China whereas, this amount is 2.2 kg/ha in the USA, 2.9 kg/ha in France and 8.8 kg/ha in the Netherlands [49]. Therefore, great number of pollutants with concentration levels up to  $\mu\text{g/L}$  have been observed in seawaters in China. According to the study conducted by Zou et al. [50], 11 antibiotics which belong to groups of sulfonamides, fluoroquinolones, macrolides and tetracyclines were detected in Bohai Bay in China with a concentration range from 2.3 to 600 ng/L [50]. Xu et al. [51] revealed that triazine herbicides and its metabolites namely, atrazine, prometryn, propazine, ametryn and atrazine-desethyl (atrazine's metabolite) with a concentration range from 1.57 to 31.3 ng/L were detected in Laizhou Bay in China [51]. Xie et al. [52] reported that 7 pesticides and 6 antibiotics were detected around Bohai and Yellow Sea in China. Pesticides namely simazine, atrazine, triadimenol and acetochlor were detected in all samples and mean concentrations of them were 2.3, 23.3, 2.7 and 2.0 ng/L, respectively.

According to Xie et al. [52], the reason for occurrence of these pesticides in sea water is river input and wastewater effluent discharge into Bohai and Yellow Sea [52]. Papadakis et al. [53] conducted a monitoring study in the main river and lakes in Northern Greece. Twenty-four pesticides including 9 herbicides, 12 insecticides and acaricides, 1 fungicide and 2 pesticide metabolites were detected. Metolachlor, prometryn and alachlor which belong to herbicide group were the most frequently

observed pesticides. Moreover, the highest concentration of pesticides was detected during initial rain runoff right after pesticide application [53].

Köck-Schulmeyer et al. [54] conducted a study on the pesticide occurrence in influent and effluent of wastewater in 3 WWTPs in Catalonia. The most widespread pesticides were diazinon and diuron and these were detected in more than 80% of 48 influent wastewater samples. Furthermore, in the effluent samples, the most frequently detected pesticides were diazinon, diuron, atrazine and tertbutylazine [54].

Aforementioned studies clearly show that micropollutants including pharmaceuticals, personal care products, pesticides, endocrine disrupting chemicals are ubiquitous in the surface waters. Therefore, not only presence of these pollutants but also their adverse effects on human health and aquatic life should be taken into consideration, and it is crucial to observe long-term trends of micropollutant (esp. pesticide) concentration in the surface waters to understand about their adverse effects [55].

### **2.1.2. Adverse Effects**

It is well-known that micropollutants have been introduced into the water environment for many years. Therefore, over the past decades, there has been growing concerns about unintentional existence of micropollutants in aquatic environments such as water, sediment and biota [56]. Micropollutants can be very harmful to both human health and aquatic life since they may enter in the food chain via reuse of wastewater, effluent discharges into water bodies and sludge applications as fertilizer during the agricultural activities. The awareness of micropollutant presence in the water environment has been increased enormously due to the increased chance of cancer, extraordinary physiological processes and reproductive deterioration in humans, augmentation of antibiotic-resistant bacteria and potential raise of chemical mixture's toxicity [2].

Pharmaceuticals which are continuously being released into the environment can cause serious undesired adverse effects on aquatic lives and humans via consumption of contaminated water [1]. For instance, endocrine hormone pharmaceuticals are biologically reactive even at very low concentrations such as ng/L or µg/L and endocrine disrupting chemicals (EDCs) alter endocrine system by mimicking, blocking or hinder hormone functions [57]. Therefore, EDCs can lead to several reproductive and sexual abnormalities in both humans and aquatic organisms that live at downstream of WWTP effluent [58]. According to Purdom et al. [57], presence of vitellogenin which is an indicator protein for estrogenic stimulation in female fish liver was observed in male fish liver living near WWTP effluent downstream [57].

Although pesticides have several benefits on crop protection and efficiency, they may cause numerous adverse effects on not only aquatic life, but also animals [59]. For instance, malathion and chlorpyrifos which are organophosphate pesticides can lead to neurobehavioral injuries in the salmon olfactory system [60]. Moreover, organochlorine pesticides (e.g. DDT) can cause to either estrogenic or androgenic contamination effect on birds, mammals and aquatic life forms [61]. In addition to organophosphate and organochlorine pesticides, other pesticides groups such as carbamates, thiocarbamates, pyrethroids, triazoles, and triazines are extremely responsible for chronic toxicity and thyroid disruption in birds, fish and amphibians [62].

Pesticides may unintentionally intoxicate not only aquatic life and animals but also humans due to improper and excessive usage of pesticides [59]. People can be exposed to pesticides via direct routes (e.g. inhalation, oral, dermal) and indirect routes (e.g. food consumption and agricultural application) [63]. As stated by Jones et al. [59] healthy children were suffered from gastrointestinal symptoms due to organophosphate or carbamate residues in crops [59]. Cao et al. [64] studied effect of dermal exposure and inhalation of imidacloprid (IMI) on humans during backpack spraying treatment in cotton fields in China. They claimed that pesticide usage way and spraying techniques highly affects the exposure pattern. For example, while total

exposure was 188 mg/kg of applied IMI during backward walking, it increased to 2059 mg/kg of applied IMI during forward walking [64]. Besides agricultural workers, residents near to agricultural lands were also negatively affected by the pesticide applications due to pesticide loss via volatilization or drift. Larsen et al. [65] observed more than 500,000 birth from 1997 to 2011 in San Joaquin Valley, California where is agriculturally dominated area. Their study showed that pesticide exposure during pregnancy can adversely affect the birth weight and the duration of pregnancy as well as it may cause birth abnormalities. They observed 5 to 9% increase in the adverse birth outcome in this agriculturally dominated area [65].

Neonicotinoid systemic pesticides (IMI, nitenpyam, acetamiprid, thiamethoxam, thiacloprid, clothianidin and dinotefuran) are known as that they cause severe acute consequences on bees [66]. Henry et al. [67] tested indirect sublethal effect of thiamethoxam on rise of honey bees' death rate. Thiamethoxam was found in nectar and pollen while right after the initial visits of honey bees. They revealed that thiamethoxam lead to intoxication and disrupt homing ability which consequently causes high mortality of honey bees [67]. In other study, Stanley et al. [68] revealed that 10 ppb of thiamethoxam exposure to bumble bee colonies caused to lessen visitation rates that eventually led to decrease of pollen collection from the apple trees. As pollination decreases, apples were produced with 36% less seeds which adversely affects crop yields [68].

### **2.1.3. Treatment Options**

In recent decades, water bodies contaminated with micropollutants has received rising both scientific and public awareness [69]. Since current treatment plants' prior aim is removing organic matter and nutrients [70] and they are not especially designed for the removal of micropollutants at low concentrations [71], the majority of micropollutants readily pass through treatment plant and are discharged into receiving

water body [4]. Hence, the treatment plants become major point sources for the micropollutants [4].

Conventional WWTPs generally consist of primary and secondary treatment processes [2]. Tertiary treatment can be also applied if higher quality water is desired. Primary treatment comprises of grit chamber and sedimentation tank which aim to remove suspended solids [72]. The micropollutants might be removed during primary treatment [72], or their concentration might increase, as well [73]. Literature studies have proved that primary and secondary treatment are not capable to degrade and eliminate micropollutants. Carballa et al. [72], studied removal of micropollutants including cosmetic ingredients, pharmaceuticals and hormones through municipal WWTP in Galicia, NW Spain. During primary treatment process, around 40% of fragrances and 20% of hormone (i.e.  $17\beta$ -estradiol) were removed. On the other hand, pharmaceuticals such as ibuprofen and naproxen were not significantly removed and remained stable. These results showed that the main removal mechanism during primary treatment was adsorption of these pollutants onto the solid particles [72]. Nie et al. [73], investigated removal of EDCs including estrone,  $17\beta$ -estradiol,  $17\alpha$ -ethinylestradiol, estriol, bisphenol A and 4-nonylphenol in municipal WWTP in Beijing, China. They concluded that after aerated grit chamber, concentration of bisphenol A and 4-nonylphenol increased due to detachment of these compounds from grits. Moreover, remaining micropollutants were almost remained stable [73].

In the secondary treatment, micropollutants may be subjected to biodegradation, physical or chemical transformation and sorption [74]. However, removal during secondary treatment highly depends on micropollutant chemical properties and characteristic of biodegradation [75]. For instance, although pharmaceuticals belong in same therapeutical group, they may reveal different biodegradation results. Salgado et al. [76] investigated that ketoprofen or ibuprofen exhibited higher degradation (75%), yet diclofenac showed low biodegradation (25%). Moreover, many polar drugs and biocides were partially degraded or absorbed onto sludge and some antiepileptic drug such as carbamazepine nearly remained stable [77]. Köck-Schulmeyer et al. [44]



investigated removal of 22 pesticides in three different domestic WWTPs in Spain. These WWTPs were those each having only biological, biological plus tertiary and biological plus P and N removal units. Concentration of 22 pesticides in both influent and effluent were measured. All three WWTPs demonstrated almost no removal for all pesticides studied [44]. Stamatis et al. [78] investigated removal of widely used fungicides (cyproconazole, penconazole, pyrimethanil, tebuconazole, triadimefon) from municipal WWTP in Greece. This WWTP receives both sewage and runoff water near to agricultural land. The WWTP consisted of pre-treatment (grit chamber), secondary treatment (conventional biological treatment) and tertiary treatment (sand filtration and chlorination) units. After primary and secondary treatment, removal of cyproconazole, penconazole, pyrimethanil, tebuconazole, triadimefon were 40, 49, 31, 39 and 65%, respectively. Stamatis et al. proved that primary and secondary treatments were not adequate to remove the studied fungicides and tertiary treatment was needed [78].

Although conventional WWTPs are not specifically designed for elimination of micropollutants, biodegradable, hydrophobic and volatile micropollutants can be removed. On the contrary, refractory and hydrophilic compounds were still existed in the treated wastewater [79]. For this reason, implementation of advanced treatment processes is more and more kept in sight by WWTP managers and decision makers [80]. The improvement of the treatment processes for effluent of conventional treatment plants may curtail the amount of micropollutants that discharged into receiving water bodies. Furthermore, these implementations can even mineralize or convert micropollutants into less harmful compounds [81].

In the literature studies, micropollutant abatement have been performed by numerous advanced treatment processes such as adsorption (activated carbon [5,82], biochar [18,83,84], carbon nanotube [85]), AOPs (ozonation [86-94], ozone/H<sub>2</sub>O<sub>2</sub> [95], ozone/H<sub>2</sub>O<sub>2</sub>/UV [96], ozone/UV [97], photocatalytic ozonation [98], photocatalysis [99], Fenton [100], photo-Fenton [101]), UV radiation, electroperoxone [97],

chlorination [78], membrane filtration (microfiltration, reverse osmosis [102]). Some of these studies are summarized below:

### **Adsorption**

Margot et al. [82] investigated removal of micropollutants in municipal WWTP in Lausanne, Switzerland. They designed a powered activated carbon treatment pilot plant which receives influent bearing 70 dissolved organic micropollutants such as pharmaceuticals, biocides, pesticides and EDCs. While the biological treatment was able to remove only 50 of these micropollutants on average by less than 50%, advanced treatment with a dose of 13 mg/L activated carbon was able to remove an average more than 70% of the remaining micropollutants [82].

In the adsorption process, biochar is one of the low-cost adsorbents that have recently being used in water treatment. Mandal and Singh [18] investigated the removal efficiency of atrazine and Imidacloprid from water by both normal (RSBC) and phosphoric acid treated (T-RSBC) rice straw biochars. They implemented single, two and three-stage adsorber plant model in order to come up with the most economical removal method. In the single-stage adsorber plant (volume: 1000L) 2.47, 3.05, 3.90, 5.36, and 8.84 kg of RSBC was used to remove, 75, 80, 85, 90, and 95% of 10 ppm atrazine, respectively. For the same degree of atrazine removal, 1.65, 1.95, 2.38, 3.05, and 4.47 kg of T-RSBC were needed, respectively. In two-stage adsorber plant system, 95% of atrazine was removed by using approximately 68% less adsorbent amount than single-stage system. In fact, this result showed that, when the two-stage was performed, much less adsorbent was adequate to achieve the same degree of atrazine removal. In the three-stage system, same percent of atrazine removal required lower amount of adsorbent, as expected. However, application of the three-stage system will require greater system and maintenance cost since it is immensely complex system. Considering the cost analysis, the two-stage system was found more feasible than the three-stage. Biochars have been widely applied as an adsorbent to eliminate not only

pesticides but also pharmaceuticals [83] and veterinary medicines [84] from water. Jung et al. [83] reported the abatement efficiency of the acetaminophen and naproxen by 94.1% and 97.7%, respectively. Huang et al. [84] obtained the sulfamethazine, a common veterinary medicine, sorption capacity of 10.95  $\mu\text{mol/g}$  for biochar and 23.42  $\mu\text{mol/g}$  for graphene oxide-coated biochar.

Dehghani et al. [85] studied the diazinon removal from water by carbon nanotube (CNT) adsorption at lab-scale. Diazinon is widely applied organophosphorus insecticide in agricultural and farm animal activities in order to control insects. The results showed that 100% removal of diazinon with an initial concentration of 0.3 ppm was achieved within 15 min contact time and with 0.1 g/L adsorbent dose. They concluded that adsorption process via CNT application has high capability to obviate organophosphorus pesticides from water [85]. Furthermore, several pharmaceuticals such as amoxicillin [103], ciprofloxacin [104], norfloxacin [105] and ibuprofen [106] were eliminated by 90% to 100% via the application of CNT as an adsorbent during water treatment.

### **Advanced Oxidation Processes (AOPs)**

Advanced oxidation processes (AOPs) have been found to be one of the most promising advanced treatment techniques to degrade wide range of micropollutants [8]. The AOPs are mainly based on production of hydroxyl radicals ( $\text{OH}\cdot$ ) which are highly reactive [107], non-selective and have powerful oxidizing ability [108]. Various AOPs, specifically ozonation and UV radiation have been well settled and operated at full-scale WWTPs for many years [109]. Ozonation process for the micropollutant abatement has been described as an effective treatment method [93]. Evaluation of real wastewater treatment plant consist of primary treatment, conventional biological treatment and sand filtration in Dübendorf, Switzerland was carried out by Bourgin et al [93]. The ozonation and biological post-treatment units were established in order to eliminate 43 frequently detected micropollutants after

secondary treatment. They examined the efficiency of ozonation processes for degradation of micropollutants. When the specific ozone dose of 0.35 g O<sub>3</sub>/g DOC was applied, 20 out of 43 micropollutants were removed by 80% since these compounds have high ozone reactivity. After specific ozone dose was increased to 0.97 g O<sub>3</sub>/g DOC, these compounds were removed up to 93% (<LOD). On the other hand, compounds with low ozone affinity were removed by less than 30% and 71% at 0.35 g O<sub>3</sub>/g DOC and 0.97 g O<sub>3</sub>/g DOC specific ozone doses, respectively. They concluded that ozonation as a tertiary treatment has significantly reduced the micropollutant concentration in the effluent [93]. Almomani et al. [94] investigated the removal of various pharmaceuticals including estrogens, antibiotics, acidic and neutral from surface water, synthetic and effluent of wastewater treatment plant. The average specific ozone dose and optimum ozone input dose for estrogens, antibiotics and neutral pharmaceuticals was found as, 1.11, 2.05 and 1.30 O<sub>3</sub>/DOC and 222.3, 188.1 and 222.4 mg/h, respectively [94].

Moreover, O<sub>3</sub> can be combined with H<sub>2</sub>O<sub>2</sub> or UV so as to enhance reaction rate and increase removal efficiency of pollutants [97]. These ozone-based AOPs are successful for degradation of various micropollutants [110]. Yao et al. [97] evaluated the removal of several micropollutants including diclofenac naproxen, gemfibrozil, bezafibrate, clofibriz acid, ibuprofen and chloramphenicol by ozonation, O<sub>3</sub>/UV and electroperoxone (E-peroxone) processes in the pilot scale WWTP. Three different water matrices (surface water, groundwater and secondary effluent wastewater) were evaluated. Some of the micropollutants (diclofenac, naproxen, gemfibrozil, and bezafibrate) were removed by more than 90% by ozonation for all water matrices. On the other hand, others that have low affinity toward to ozone (ibuprofen, clofibriz acid, and chloramphenicol) were degraded by 68-91%, 32-68% and 73-90% for surface water, groundwater and secondary effluent wastewater during ozonation, respectively. To enhance the abatement of ozone-resistant micropollutants, O<sub>3</sub>/UV and E-peroxone processes were applied and significant advancement for all water matrices was observed [97]. Moreover, the addition of H<sub>2</sub>O<sub>2</sub> to ozonation process also improves

removal of not only micropollutants but also TOC [111]. Catalkaya and Kargi [111] investigated the degradation and mineralization of simazine by peroxone ( $O_3/H_2O_2$ ) process. Simazine with an initial concentration of 2.0 mg/L disappeared by 95% within 5 min treatment when 75 mg/L  $H_2O_2$  was applied. Nevertheless, even after 60 min of peroxone application, mineralization was not completely achieved due to formation of some intermediate compounds. Moreover, they reported that the maximum removal of pesticide (94%) and TOC (82%) was obtained at 75, 11 and 0.5 mg/L of  $H_2O_2$ , pH, simazine concentrations, respectively [111]. Lekkerkerker-Teunissen et al. [96] investigated the application of sequential  $O_3/H_2O_2$  and UV process in order to remove 14 micropollutants including pharmaceuticals, pesticides and EDCs from pre-treated surface water in a pilot plant WWTP in Netherlands. They reported that more than 70% and 90% of atrazine and isoproturon were degraded, respectively, by  $O_3/H_2O_2/UV$  process. They concluded that 8 out of 14 micropollutants were degraded by more than 90% through the application of 1.5 mg/L ozone and 6 ppm  $H_2O_2$  concentration [96].

Regarding the use of Fenton's process to remove the micropollutants from water, several researches were performed using both Fenton ( $H_2O_2/Fe^{2+}$ ) and photo-Fenton ( $H_2O_2/Fe^{2+}/UV$ ) processes [100,110,112,113]. For instance, Sanchis et al. [100] investigated the degradation of herbicides namely, alachlor, atrazine and diuron and TOC removal by Fenton process. They reported that complete conversion of alachlor, atrazine and diuron with an initial concentration of 180, 27 and 27 mg/L, respectively, was achieved within 30 min treatment when  $Fe^{2+}/H_2O_2$  molar ratio was kept at 1/10. Moreover, reduction of TOC and COD hardly reached by 50–55% and 60–65%, respectively, at most within 180 min treatment [100]. De la Cruz et al. [113] investigated abatement of 32 micropollutants including pharmaceuticals, pesticides, and corrosion inhibitors by photo-Fenton process ( $H_2O_2/Fe^{2+}/UV$ ) from the secondary treatment effluent of the pilot scale treatment plant. The highest removal (97%) was obtained within 5 min, at 50 and 5 mg/L concentrations of  $H_2O_2$  and  $Fe^{2+}$ , respectively.

## **Chlorination**

Stamatis et al. [78] examined the removal of fungicides (cyproconazole, penconazole, pyrimethanil, tebuconazole, triadimefon) in a WWTP having tertiary treatment units (sand filtration and chlorination). The overall removal of cyproconazole, penconazole, pyrimethanil, tebuconazole and triadimefon attained in the secondary level increased from 40, 49, 31, 39, 65% to 55, 68, 46, 57, 93%, respectively, with the application of tertiary treatment.

As understood from all these literature studies, conventional biological treatment was not adequate to remove micropollutants from water and wastewater [72-79]. Therefore, treatment plants have been compelled to be improved by implementation of several advanced treatment processes [80-113].

## **2.2. Imidacloprid**

Neonicotinoid insecticides are systemic, selective insecticides and impact as agonists of the postsynaptic nicotinic acetylcholine receptors (nAChRs) in the central nervous system of the insects [66]. The term “neonicotinoid” was formerly suggested for imidacloprid and similar insecticidal compounds that have resemblance to insecticidal alkaloid (S)-nicotine with an analogue mode of action [114]. Before the invention of the neonicotinoids, organophosphates, pyrethroids and carbamates were widely used in the agrochemical market which caused to the pest resistance and cumulative exposure concerns of these chemicals. As a partial reaction to these concerns, neonicotinoids were invented [115].

One of the significant benefits of the use of neonicotinoids instead of traditional and long-established organophosphates, pyrethroids and carbamates is that there is no cross-resistance between the neonicotinoids and the above-mentioned chemical classes since neonicotinoids have different mode of action than them [66]. Another benefit of neonicotinoid insecticide is being immensely toxic to insects, yet they have

lower toxicity to mammals than its replacements [116]. For that reason, conventional insecticides such as chlorinated hydrocarbons, carbamates, pyrethroids and organophosphorus pesticides have been being replaced by neonicotinoids [117].

Neonicotinoid insecticides are very active and efficient against insects since they are effective for broad spectrum of insecticides, are powerful at low doses, make long-term control possible, have high potency of crop safety and are systemic [66]. Since neonicotinoid insecticides are absorbed by the leaves or roots and transported into all tissues of the plant, they are classified as systemic insecticides [118]. Moreover, neonicotinoid insecticides can be applied in several ways such as seed dressing, foliar spray, drench and tree injection [119].

In 1991, the first neonicotinoid insecticide, IMI, was launched by Bayer Crop Science and has become the most selling insecticide for many years [120]. As seen in Figure 4, subsequent to launch of the IMI, other neonicotinoids named as nitenpyam, acetamiprid, thiamethoxam, thiacloprid, clothianidin and dinotefuran released into the market in 1995, 1995, 1998, 2000, 2001 and 2002, respectively [121].

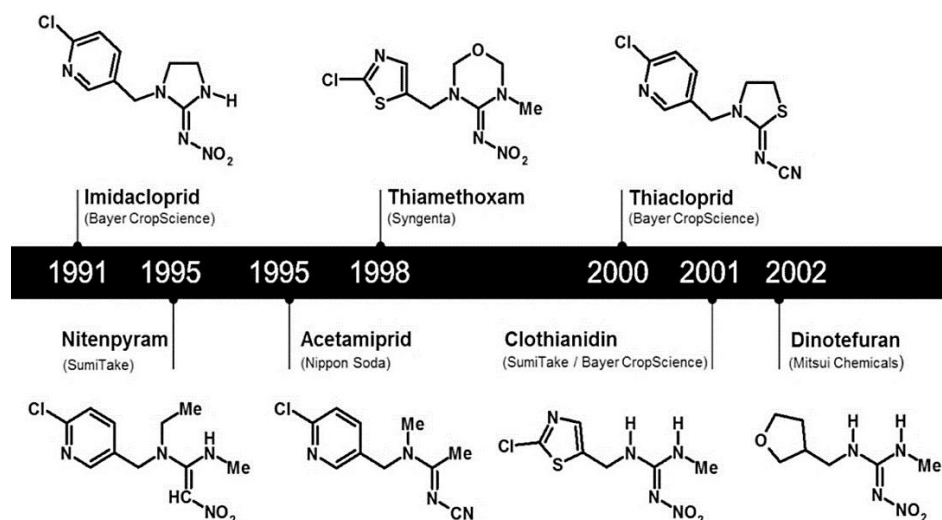


Figure 4. Significant neonicotinoid insecticides released to the market in chronological order [121]

These neonicotinoids can be categorized into 2 groups; the nitro group containing chemicals such as IMI, nitenpyram, thiamethoxam, clothianidin and dinotefuran and the cyano group containing chemicals such as acetamiprid and thiacloprid [122,123]. In a commercial market, IMI can be found as Admire, Gaucho, Confidor and Provado [124]. While the Admire and Gaucho are used for soil application and seed treatment, Confidor and Provado are used for foliar application [66]. IMI is used for oilseed rape, sunflower, maize and cotton [125]. By 2008, neonicotinoids have been registered in more than 120 countries for use on more than 140 different crops [126] and they have 25% market sale in 2014 [121]. However, IMI have shown adverse effect on non-target organisms especially on honeybees [67]. For that reason, in 2013, European Union introduced a temporary ban on the IMI [117].

### 2.2.1. Physicochemical Properties

IMI (CAS No:138261-41-3 and IUPAC name: 1-(6-chloro-3-pyridylmethyl)-N-nitroimidazolidin-2-ylideneamine) is chloronicotinyl nitroguanidine containing systemic insecticide with the chemical formula of  $C_9H_{10}ClN_5O_2$ . Figure 5 shows the chemical structure of IMI [127]. IMI molecule consists of chloro-pyridine and imidazolidine rings.

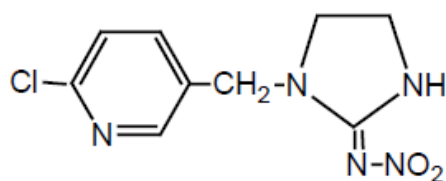


Figure 5. Molecular Structure of IMI [127]

IMI is stable, hydrophilic, non-volatile and colorless crystal with a weak characteristic smell [128]. Solubility of neonicotinoids highly depends on the pH of the solution,



temperature and the pesticide's physical state [129]. IMI has solubility of 610 mg/L (at 20°C) in water which shows that it is highly soluble in the water [128]. The pesticide's water solubility must be known since the solubility determines possible degradation pathways. For example, highly soluble pesticides like IMI will stay in the water and it has low tendency to be adsorbed in the soil. It is fairly stable to hydrolysis at acidic and neutral pHs in the aqueous solution, but hydrolysis of IMI accelerated at basic conditions [130]. Moreover, it shows rapid photolytic degradation which lasts less than 2 hours [127]. It has vapor pressure of  $1 \times 10^{-7}$  mmHg (at 20°C) and Henry's constant of  $6.5 \times 10^{-11}$  atm.m<sup>3</sup>/mole which indicates that it has low volatility and low vapor pressure [128]. IMI's octanol-water partitioning coefficient (log K<sub>ow</sub>) is 0.57 (at 21°C) [128] and soil adsorption coefficients K<sub>d</sub> and K<sub>oc</sub> ranges are 0.956-4.18 and 132-310, respectively. Since IMI has high water solubility and low adsorption coefficient K<sub>d</sub> value, it is not likely to adsorb into soil [127]. Physicochemical properties of IMI are tabulated and given in Table 2.

Table 2. Physicochemical properties of IMI [127,128]

Physicochemical Property	Value
CAS Number	138261-41-3
IUPAC Name	1-(6-chloro-3-pyridylmethyl)-N-nitroimidazolidin-2-ylideneamine)
Form	Colorless Crystal
Mode of Action	Systemic insecticide which binds to nicotinic acetylcholine receptors of the insect [66]
Molecular Formula	C <sub>9</sub> H <sub>10</sub> ClN <sub>5</sub> O <sub>2</sub>
Molecular Weight	255.7 g/mole
Water Solubility	610 mg/L (at 20°C)
Melting Point	143 °C
Vapor Pressure	$1 \times 10^{-7}$ mmHg (at 20°C)
Hydrolysis Half-life	> 30 days (at 25°C and pH 7)

<b>Physicochemical Property</b>	<b>Value</b>
Aqueous Photolysis Half-life	< 2 hours (at 24°C and pH 7)
Henry's Constant	$6.5 \times 10^{-11}$ atm m <sup>3</sup> /mole
Octanol-water Coefficient ( $K_{ow}$ )	0.57
Soil Adsorption Coefficient ( $K_d$ )	0.956-4.18
Soil Adsorption Coefficient ( $K_{oc}$ )	132-310

### **2.2.2. Occurrence and Adverse Effect of IMI in Water**

IMI is amenable for in broad range of agricultural activities such as production of corn, soybean, canola and tomato production in several countries as United States, Canada [131], Netherlands, Sweden and Vietnam [132] due to its properties like being highly water soluble [128] and systemic insecticide [66].

There are several different ways of IMI access into water bodies. Since the solubility of IMI is high and partitioning ( $\log K_{ow}$ ) and soil adsorption ( $\log K_{oc}$ ) coefficients are low (Table 2), IMI migration through surface and subsurface runoff is promoted. In other words, IMI can effortlessly reach into the water bodies [133]. The environmental conditions such as pH, light, temperature and turbidity or the formulation of pesticide can alter the persistence of IMI in the water bodies such as that increasing the pH and turbidity cause to strengthen the persistence [134].

IMI may leach into the groundwater and it consequently appears in the surface water. Moreover, treated seeds decay in the water and application of pesticide by spray nozzle are other ways of water contamination [125]. On the other hand, according to Hladik et al. [135], rainfall run-off causes larger part of the water body contamination. Table 3 shows IMI occurrence in several WWTPs and surface waters.

Table 3. Imidacloprid levels in wastewater and surface water

Occurrence Area	Sample Type	Concentration	Reference
Bucharest WWTP, Romania	WWTP influent	60.8-80.2 ng/L	[136]
	WWTP effluent	53.6 ng/L	
USA	WWTP influent	60.5 ng/L	[137]
	WWTP effluent	55.8 ng/L	
Ebro River, Spain	Surface water	14.96 ng/L (max.) 1.66 ng/L (mean)	[138]
Guadalquivir River, Spain	Surface water	19.2 ng/L (max.) 2.2 ng/L (mean)	[139]
Turia River, Spain	Surface water	207 ng/L (max.) 23 ng/L (mean)	[140]
Llobregat River, Spain	Surface water	67 ng/L (max.) 25 ng/L (mean)	[141]
Old Mans Creek, USA	Surface water	42.7 ng/L (max.) <2 ng/L (mean)	[135]
South Fork Iowa River, USA	Surface water	9.2 ng/L (max.) <2 ng/L (mean)	[135]
Little Sioux River, USA	Surface water	24.9 ng/L (max.) <2 ng/L (mean)	[135]
Nishnabotna River, USA	Surface water	27.9 ng/L (max.) <2 ng/L (mean)	[135]
Missouri River, USA	Surface water	17.1 ng/L (max.) <2 ng/L (mean)	[135]

### 2.2.3. Fate of IMI in Water

Several physical processes such as adsorption, biodegradation, volatilization and sedimentation control the distribution of pesticides in the environment. After distribution, chemical and biological processes cause to degradation of the pesticides. Chemical reactions such as oxidation, reduction, hydrolysis and photolysis mainly take place in the water or the atmosphere. Biological degradation of pesticides occurs via utilization of oxidation, reduction, hydrolysis and conjugation processes in soil by the living organisms. Therefore, aforementioned physical processes control the pesticide distribution and the degradation is controlled by the environmental media like soil, water or air [142].

## **Adsorption**

The environmental fate of the pesticides is primarily determined by their behavior in soil since the numerous physicochemical and biological processes regulate their movement, transport and dissipation towards other environmental media such as water, air and soil [143]. These physicochemical properties involve soil texture, organic matter content, pH, moisture and electrical conductance [127]. Sorption process, which means the migration of chemical solute from the aqueous phase to the solid adsorbent's surface, primarily plays a crucial role for the pesticide retention time in the soil [144].

Desorption is conversely related to sorption and when the sorption is great then the desorption is small or vice versa [145]. Sorption-desorption processes are important for the pesticide availability for the living organisms, target species and plants and pesticide's attitude in surface and groundwater pollution [146,147].

Bajeer et al. [148] investigated the IMI's adsorption and leaching potential through the alluvial soil in both column and field study. In contrast to Cox et al. [149], Oi et al [150], and Zheng and Liu [130], Bajeer et al. conducted a study in sodic and alkaline soils. They used the soil that has high percent of sandy loam, high pH and low in organic matter. In these experiments both high purity and commercial IMI was applied. They concluded that since these soils have low organic matter and high pH, IMI had great potential to leach and they found that IMI leached up to 60 cm soil depth. In other words, in basic and low organic matter containing soils tend to have a high leaching of IMI and is of potential danger for environment [148]. According to Liu et al. [151], the most affecting factor for soil sorption is soil organic matter. For instance, the more organic carbon soil has, the more IMI sorption occurs [151]. Therefore, half-life of IMI in soil changes related to organic matter. For instance, half-lives for IMI were found as 455-518 days, 233-366 days, 34-45 days and 36-46 days in sandy loam, silt clay loam, alluvial and coastal alkaline soils, respectively [152].

Furthermore, as the temperature increases, sorption rate also increases for different soil types [153].

IMI has been classified as 'persistent' with a 'high leaching' potential by Pest Management Regulatory Agency of Canada (PMRA). According to European Food Safety Authority, soil surface spraying of IMI results in higher persistence in soil than seed treatment [154]. For instance, Selim et al. [155] found that leaching of IMI was around 27-69% and 97% in contrasted textures and sand column, respectively [155]. For these reasons, IMI may cause groundwater contamination. Indeed, Groundwater Ubiquity Score (GUS) leaching potential index of IMI was found as 3.76, which also indicates the high leachability [156].

### **Biodegradation**

Bacterial biodegradation may be performed either biodegradation by microbial consortia or by pure bacterial cultures. Moreover, bacterial biodegradation can be divided into two categories: catabolic and cometabolic. In the former, organic matter serves as a sole source of carbon or nitrogen for growth, whereas the latter stands for additional carbon or nitrogen sources provided for growth [157].

Biodegradation of IMI has been investigated by several researches. In one of these studies, IMI was successfully degraded at most by 78% within 7 days at 30 °C by isolated bacterium *Klebsiella pneumoniae* strain BCH1 in agricultural soils [158]. Furthermore, biodegradation of IMI yielded to formations of nitrosoguanidine, imidacloprid guanidine and 6-chloronicotinic acid [158] which is mainly found as soil metabolite of IMI [159]. The biodegradation of IMI by an isolated microorganism was also conducted by Anhalt et al [160]. The IMI was degraded by *Leifsonia* sp. strain PC-21. Degradation of IMI with an initial concentration of 25 mg/L was in the range of 37-58% within 3 weeks [160].

The IMI degradation and characterization and isolation of bacteria from vegetable farms in Malaysia was investigated by Sabourmoghaddam et al. [161]. They revealed that among 50 soil bacterial isolates, only 5 of them (*Bacillus* sp., *Brevibacterium* sp., *Pseudomonas putida* F1, *Bacillus subtilis* and *Rhizobium* sp.) were able to degrade IMI with an initial concentration of 25 mg/L within 25 days. They also concluded that these bacterial strains might be promising for bioremediation [161]. In addition to these isolated bacterial strains, *Bacillus aerophilus* [162], *Brevundimonas* sp. [163], *Burkholderia cepacia* strain CH9 [164] and *Mycobacterium* sp. strain MK6 [165] were responsible for IMI degradation in sugarcane, cotton and agricultural field soils, respectively.

As seen, these biodegradation studies belong to the degradation of IMI in soil, but not in the water environment.

### **Photolysis**

For the photolysis of IMI, there are several studies conducted. Moza et al. [166] examined the photolysis of the IMI in the aqueous solution under the 290 nm irradiation and concluded that 90% of the IMI degraded in 4 hours. The degradation followed the first-order kinetics and the half-life was determined as 1.2 hours. These results pointed out that degradation of IMI was fairly rapid under the UV light. The same IMI solution was kept in the dark as a control and it was observed that the IMI concentration did not decrease. The proposed photodegradation pathway was determined and degradation compounds were identified by GC-MS. Photodegradation of IMI resulted in formation of eight photoproducts. The main photoproducts were 6-Chloro-nicotinaldehyde, N-methylnicotinamide, 1-(6-chloronicotiny)imidazolidone and 6-chloro-3-pyridyl-methylethylendiamine [166].

Wamhoff and Schneider [167] also investigated the photodegradation of IMI. They found that under the wavelength greater than 280 nm, half-lives of the IMI in HPLC grade water, in tap water and in tap water with TiO<sub>2</sub> were 43, 126 and 144 minutes,

respectively. The photodegradation followed the first-order kinetics. The degradation pathway was proposed, and eight photoproducts were identified. Among these eight products, 1-[(6-chloro-3-pyridinyl)methyl]-2-imidazolidone (IMI urea) were the most abundant one [167].

In other study, Liu et al. [151] examined the sorption, hydrolysis and photodegradation of IMI. During the photodegradation experiments mercury lamps with 254 nm were used. IMI photodegradation followed the pseudo-first order kinetics. The rate constant depends on the initial IMI concentration which may be due to limited photons. Moreover, as the temperature was increased, photodegradation rate of the IMI also increased. The degradation mechanism for photodegradation of IMI was determined and various intermediate compounds were observed. Similar to Moza et al [166] and Wamhoff and Schneider [167], Liu et al. [151] also determined imidacloprid-urea as the main photoproduct. The proposed pathway of IMI photoproducts formation can be depicted in Figure 6.

Ding et al. [168] have conducted the most recent study for the photodegradation of IMI. They observed that 95% of the initial IMI solution ( $2 \times 10^{-4}$  M) was decomposed in 40 hours under the 280 nm UV light. The degradation followed first-order kinetics and the degradation half-life was determined as 10.2 hours. Ding et al. [168] explained the reason for having longer half-life time than Moza et al.'s study as photon flux and stirring rate were not same. Similar to other researches, Ding et al. [168] also identified several photoproducts including the IMI urea, IMI olefin, and IMI desnitro [168].

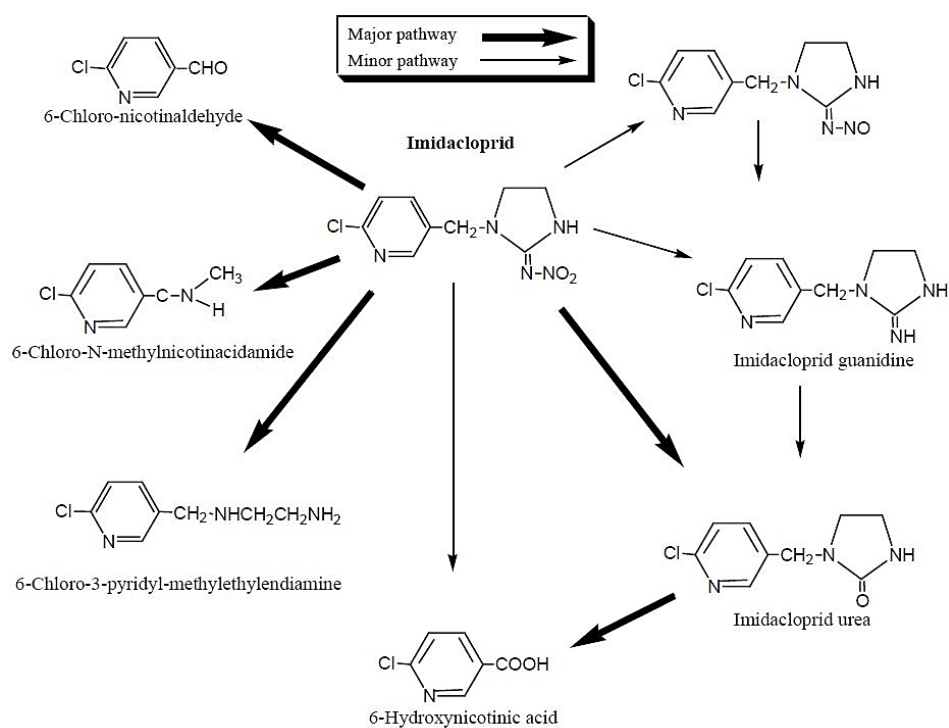


Figure 6. The proposed mechanism for photo degradation of IMI [169]

### Hydrolysis

According to Zheng and Liu [130], IMI hydrolysis greatly depends on the pH of the solution. In order to examine the pH effect on the IMI hydrolysis, they worked with the pH values of 3, 5, 7 and 8. IMI exhibited minor hydrolysis in acidic and neutral conditions. At pH 7, the hydrolyzed portion of IMI was only 1.5% after three months. On the other hand, at pH 9, the hydrolysis became faster and the 20% of the IMI disappeared after three months. Moreover, the temperatures of 10 °C, 20 °C, 30 °C, 40 °C, 50 °C and 60 °C were studied and they reported that the temperature increase also caused hydrolysis to rise significantly.



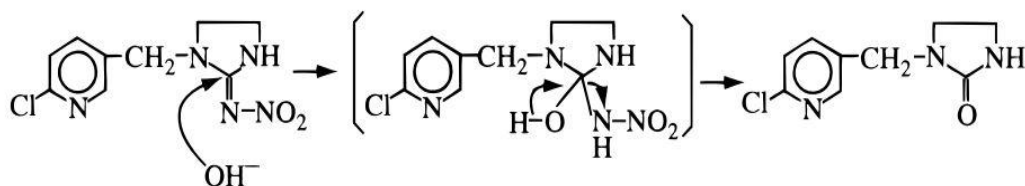


Figure 7. The proposed mechanism for hydrolysis of IMI [130]

The proposed mechanism for hydrolysis of IMI is given in Figure 7 and there was only one main product, namely 1-[(6-chloro-3-pyridinyl)methyl]-2-imidazolidone (IMI urea), after the hydrolysis. IMI urea was observed at basic conditions and remained stable [130].

Sarkar et al. [170] investigated the hydrolysis of IMI in water, based on formulation types of the pesticide. Commercial IMI pesticides namely Confidor 200 SL and Gaucho 70 WS were used. The hydrolysis followed the first-order kinetic rate. Apart from the other researches, Sarkar et al. pointed out that the powder formulation has longer hydrolysis half-life than the liquid formulation indicating that the powder formulation is more persistent in the environment compared to the liquid formulation [170]. Another study which was conducted by Malato et al. [171] revealed that IMI was stable in aqueous solution. In the dark conditions and at pH values of 2.7, 5 and 8, IMI was chemically stable and did not undergo hydrolysis in 36 hours [171].

### **Volatilization**

Since IMI has low volatility ( $1 \times 10^{-7}$  mmHg) [127], it is not commonly present in the air for a long time. During spray application, IMI can be observed as aerosols in the air, but then it is quickly photodegraded [127]. Another possibility of IMI presence in the air can be due to dust and dispersion which may occur during seed sowing machines planting the treated seeds [156].

### **2.3. Removal of IMI from Water**

The removal methods for IMI from water can be classified into three categories as biological, physical and chemical treatment. For the IMI removal from real wastewaters, biological treatment such as activated sludge, physical removal methods such as activated carbon adsorption, membrane filtration and chemical treatment such as AOPs are evaluated in this section.

#### **2.3.1. Biological Treatment**

Biological treatment at WWTPs are usually performed by means of activated sludge process. Removal of IMI via biological treatment was investigated by Sadaria et al. [137]. They examined removal efficiency in both constructed wetland and WWTP. IMI influent and effluent concentrations at WWTP were 54.7 and 48.6 ng/L, respectively. Conducted mass balance over the WWTP proved almost no IMI removal. Moreover, influent and downstream concentrations of IMI at constructed wetland were 54.4 and 49.9 ng/L, respectively. Similar to WWTP, constructed wetland also showed almost no IMI degradation. These results indicated that IMI could be identified as recalcitrant wastewater constituent [137]. Furthermore, the treatment of IMI during Bucharest WWTP was evaluated by Iancu et al. [136]. They observed a slight IMI removal since IMI concentration measured in the influent and effluent were 60.8-80.2 ng/L and 53.3 ng/L, respectively.

#### **2.3.2. Physical Treatment**

Physical treatment processes include adsorption and membrane filtration [6,18,172-175]. For the removal of IMI, adsorption has been widely applied by implementation of various adsorbents such as rice straw biochar, coconut shell, natural sepiolite, powdered and granular activated carbon [18,172-175]. Among these adsorbents, generally, powdered and granular activated carbon are used for pollutants removal in

WWTPs [5]. Zahoor and Mahramanlioglu [5] investigated the IMI removal from water by using adsorbents of powdered (PAC) and magnetic activated carbon (MAC), in a comparative way under different pH values and initial IMI concentrations. The XRD measurements showed that PAC had higher surface area and micropore volume than MAC. The IMI removal data fitted Langmuir adsorption isotherm with curve types of H and L for PAC and MAC, respectively. Although increase in the initial IMI concentration resulted in higher equilibrium time for both adsorbents, significant removal was achieved for both 25 and 50 mg/L initial IMI concentrations. Since the pH of solution also highly affects the adsorption processes, thereby pollutant removal efficiency, different pHs (1-8) were investigated for both adsorbents. The acidic pHs caused to iron oxide production and loss of magnetization for MAC. Moreover, changing pH from 4.8 to 8 did not result in notable IMI removal for both PAC and MAC [5]. Similar findings were also reported by Daneshvar et al. [175] for IMI abatement by granular activated carbon (GAC) at pH 4 and 7. They also investigated the IMI removal at different temperatures ranging from 25 to 55 °C. The IMI with 25 ppm initial concentration was removed at least by 80% within 90 min for all temperatures. The removal kinetics fitted to second-order model [175]. Although activated carbon is one of the most widely used adsorbent in WWTPs, due to its high cleanup cost, more economical, and environmentally friendly adsorbents are being used in recent years [18,172-174]. These adsorbents include agricultural waste biochars such as corn cob (CCBC), bamboo chips (BCBC), eucalyptus bark (EBBC), rice husk (RHBC), rice straw (RSBC) and acid treated RSBC (T-RSBC) [172]. Mandal et al. [172] investigated IMI removal from water through these biochars. Firstly, they pyrolyzed these feedstocks under similar conditions. However, due to their different natures, biochar characteristics, in turn their adsorption capacity altered. For instance, the most efficient IMI removal was achieved by RSBC (up to 77.7%), but CCBC exhibited the least removal ability (up to 20.1%). Furthermore, phosphoric treatment of the most effective biochar (RSBC) improved the IMI removal from 77.7% to 89.5%. The IMI sorption data fitted well to the Freundlich isotherm with a Freundlich coefficient of 1706 for RSBC.

Further study was conducted by Mandal and Singh [18] and they investigated the removal efficiency of atrazine and IMI from water by both normal (RSBC) and phosphoric acid treated (T-RSBC) rice straw biochars. They implemented single-stage, two-staged and three-stage adsorber plant model in order to evaluate the most economical removal method. In the single-stage adsorber plant (volume: 1000L) 1.38, 1.65, 2.03, 2.64, and 3.97 kg of RSBC was used to remove, 75, 80, 85, 90, and 95% of 10 ppm IMI. For the same degree of IMI removal, 1.66, 1.94, 2.31, 2.87, and 3.98 kg of T-RSBC were needed, respectively. In two-stage adsorber plant system, 95% of IMI was removed by using 69% less RSBC amount than single-stage system. In fact, this result showed that, when the two-stage was performed, much less adsorbent was adequate to achieve same degree of IMI removal. At the three-stage system, same percent of IMI removal requires lower amount of adsorbent, as expected. However, application of the three-stage system will require greater system and maintenance costs since it is immensely complex system. Considering the cost analysis, two-stage system has been found to be more feasible than the three-stage [18]. Furthermore, activated carbon obtained from coconut shell was also used as adsorbent to remove IMI from water [173]. Kouakou et al. [173] compared the IMI removal from wastewater by both laboratory-made coconut shell activated carbon (CAS) and industry-made activated carbon (NORIT) which had similar surface area ( $721 \text{ m}^2/\text{g}$ ). The isotherm test results showed that for both adsorbents, Langmuir and Freundlich models were followed and IMI adsorbed quite better onto NORIT than CAS. Similar to previous studies, Kouakou et al. [173] also observed that the pH of solution did not significantly affect the IMI removal by NORIT activated carbon. On the other hand, CAS was highly efficient for IMI adsorption at pH 3.84 and these results proved the pH of solution affect the adsorption process [173]. Apart from agricultural feedstocks and its biochars, inexpensive natural geological stones such as sepiolite was applied as an adsorbent during IMI removal [174]. Gonzalez-Pradas et al. [174] conducted column experiments in order to examine IMI removal from synthetic wastewater by using the natural sepiolite which is a magnesium silicate clay with a fibrous structure. The IMI removal data well fitted the Langmuir isotherm model. The equilibrium was

reached within 50 min and 99.9% of IMI ( $20 \times 10^{-4} \text{ cmol/dm}^3$  initial concentration) was removed from water [174].

Apart from adsorption processes, membrane filtration techniques (nanofiltration, reverse osmosis and membrane bioreactor) were also applied to remove micropollutants [6,102,176]. In this respect, Genc et al. [6] investigated IMI removal by reverse osmosis by using three different membranes (BW30, LFC-3, CPA-3) with a polyamide basis. Apart from IMI removal, they also examined TOC and TDS removal, as well. They reported that IMI, TOC and TDS removal were by 97.8%, 98% and 97.5%, respectively, with BW30 at pH 11. Furthermore, they examined permeate flux which is an important membrane operation parameter. They observed more cake layer and membrane fouling with the membranes BW30 and LFC-3. Despite the fouling observed, for all membrane types, more than 95% IMI rejection was achieved with the main rejection mechanism of size exclusion [6]. Literature studies showed that physical treatment of IMI mainly depends on adsorption techniques.

### 2.3.3. Chemical Treatment

Chemical removal techniques include AOPs such as ozonation,  $\text{O}_3/\text{UV}$ ,  $\text{O}_3/\text{H}_2\text{O}_2$ , Fenton and photo-Fenton processes [81]. Several AOPs have been established as the most commonly used techniques for IMI removal including photochemical degradation processes such as photo-Fenton [19] and photocatalysis [20,177,178], catalytic ozonation [21], cavitation [24,179] and ozonation [22,23].

Furthermore, hybrid processes were also applied to promote IMI degradation. These processes aim to decompose organic pollutants to less complex form and to mineralize them [81]. Photo-Fenton ( $\text{H}_2\text{O}_2/\text{Fe}^{2+}/\text{UV}$ ) process is known to be effective for not only pesticide degradation but also TOC removal [19].

Segura et al. [19] investigated IMI degradation and TOC reduction by photo-Fenton process. The effect of  $\text{Fe}^{2+}$  concentration on the IMI removal was apparent since the

increase of  $\text{Fe}^{2+}$  concentration resulted in less time for 80% IMI degradation. At 35 mg/L  $\text{Fe}^{2+}$  and 150 mg/L  $\text{H}_2\text{O}_2$  initial concentrations, 50% of IMI was degraded in only 1 min and then reaction was slowed down until the IMI was fully degraded. On the other hand,  $\text{H}_2\text{O}_2$  concentration played an important role in TOC reduction. The maximum TOC removal (77%) was achieved at 23 mg/L  $\text{Fe}^{2+}$  and 393 mg/L  $\text{H}_2\text{O}_2$  initial concentrations. Moreover, acute toxicity to *Daphnia magna* and genotoxicity to *Bacillus subtilis* was presented in both raw IMI and degraded IMI due to produced by-products. However, after reasonable mineralization occurred by photo-Fenton, both acute toxicity and genotoxicity were significantly decreased and disappeared eventually [19].

In addition to photo-Fenton process, heterogeneous photocatalysis has gained growing interest in recent years. Malato et al. [20] examined removal of four pesticides including IMI by photo-Fenton and heterogeneous photocatalysis (solar energy) with  $\text{TiO}_2$  at pilot-scale treatment plant. The initial concentration of IMI,  $\text{TiO}_2$  and Fe were 50 mg/L, 100 mg/L and 0.05 mM, respectively. While the IMI was fully degraded within 120 min by  $\text{TiO}_2$ , it lasted only 20 min with photo-Fenton process. Furthermore, not only degradation of IMI but also TOC removal was enhanced by the application of photo-Fenton. The 90% TOC removal was achieved in more than 400 min and 200 min for  $\text{TiO}_2$  and photo-Fenton, respectively. These findings clearly showed that photo-Fenton was more successful in mineralization of both IMI and degradation by-products [20]. Another research conducted by Zabar et al. [177] also obtained similar results with the previous study. They conducted pesticide degradation including IMI by immobilized- $\text{TiO}_2$  photocatalysis. The results showed that fully IMI disappearance was lasted 120 min. Nevertheless, 120 min degradation was not adequate to complete mineralization indicating a need for more treatment [177]. Similarly, Kitsiou et al. [178] also investigated homogeneous and heterogeneous photocatalytic treatment for IMI degradation. Unlike for previous researches, Kitsiou et al. [178] applied UV-A and visible illumination combined with  $\text{TiO}_2$  and Fenton. The removal of IMI by  $\text{TiO}_2$ /UV-A was quite slow and required more than 240 min

of treatment. On the other hand, when the  $\text{TiO}_2$  was coupled with  $\text{Fe}^{3+}$  and  $\text{H}_2\text{O}_2$  removal efficiency was significantly enhanced due to synergistic effect [178]. Although removal efficiency of  $\text{TiO}_2$  (photocatalysis) is generally comparable with photo-Fenton process,  $\text{TiO}_2$  can be coupled with ozone such as  $\text{O}_3/\text{TiO}_2/\text{UV}$  process to enhance production of  $\text{OH}\cdot$ , in turn to improve IMI degradation. Cernigoj et al. [21] examined neonicotinoid insecticides (IMI and thiacloprid) removal by  $\text{O}_3/\text{TiO}_2/\text{UV}$  as well as the effect of pH and ozone dose in the  $\text{TiO}_2$  photocatalysis. They found that half-life of IMI at pH 10 was 1.5 months indicating that the IMI was easily affected by hydroxide anions at alkaline pH. The degradation of IMI was quite slow by  $\text{O}_2/\text{UV}$  at 300 nm UV-A light emission. Since the IMI has maximum adsorption at 270 nm, during the UV radiation photons were efficiently absorbed by IMI. Moreover, for further degradation by  $\text{O}_3/\text{TiO}_2/\text{UV}$ , thiacloprid was investigated since it has higher stability than IMI [21].

Other than photocatalysis processes, several AOPs have been applied to enhance  $\text{OH}\cdot$  production, which, in turn, is directly related to the increased removal efficiency of IMI [24]. Cavitation process which can be hydrodynamic [24] or ultrasound-based treatment system can be also regarded as oxidation process since it enhances the generation of  $\text{OH}\cdot$  in the solution [180]. The cavitation leads to bubble formation, growth and consequent collapse of formed bubbles. Indeed, hydrodynamic cavitation is promoted by liquid flow through basic mechanical constriction like venture and orifice [181]. Raut-Jadhav et al. [24] investigated the IMI degradation by hydrodynamic cavitation (HC) and its hybrid processes with several AOPs such as HC/Fenton, HC/photo-Fenton, HC/UV and HC/UV/ $\text{Nb}_2\text{O}_5$  processes. The initial concentration of IMI was 25 ppm, and the pressure was set at 15 ppm. At this condition, nearly 26% IMI degradation was achieved by HC application. Effect of pH on the IMI removal was evident and the removal sharply decreased when the pH increases from 3 to 4. The maximum IMI removal (26%) was observed at pH 2. To promote  $\text{OH}\cdot$  production and to enhance IMI removal, hybrid processes were applied. The percentage of IMI degradations were 97.77% and 99.23% within 15 min of the

applications of HC/Fenton and HC/photo-Fenton, respectively. While the synergistic effect was apparent for both HC/Fenton and HC/photo-Fenton processes, HC/UV did not show any synergistic effect since the reaction rate constant of the combined HC/UV process was lower than the one obtained in HC and UV processes. Within 120 min treatment time, while the IMI removal efficiency was 45.56% for HC/UV application, it slightly increased to 55.18% with addition of niobium pentoxide as a photocatalyst (HC/UV/Nb<sub>2</sub>O<sub>5</sub>) [24].

When the cavitation is promoted by ultrasound rather than liquid flow, it is called as ultrasound-based cavitation which is induced by high frequency sound waves in the range from 16 kHz to 1 MHz. The liquid molecules are pulled apart to create cavities while the ultrasound passing through liquid media [179]. The IMI degradation by ultrasound-based cavitation was investigated by Patil et al [179]. Experimental results clearly showed that degradation of IMI by ultrasonic horn (US) was strongly affected by pH and H<sub>2</sub>O<sub>2</sub>. When the pH decreased from 11 to 3, IMI degradation increased from ~35% to 70% since the cavitation is favored at acidic pHs. Similarly, increase of H<sub>2</sub>O<sub>2</sub> from 15 to 80 ppm, cause the IMI removal to enhance since H<sub>2</sub>O<sub>2</sub> provides OH• which has further degradation ability. Moreover, combination of US and H<sub>2</sub>O<sub>2</sub>/UV was examined to achieve complete degradation of IMI and higher TOC removal. It was mentioned that 84% IMI and 79% TOC removal were achieved upon 35 ppm H<sub>2</sub>O<sub>2</sub> addition within 120 min. In all degradation methods studied in this research apparently demonstrated that combination of US/H<sub>2</sub>O<sub>2</sub>/UV resulted in the best TOC removal, in turn, complete mineralization of IMI [179].

Ozonation is one of the most typical AOPs to degrade micropollutants [81]. Although ozone has been widely applied for water and wastewater disinfection purposes for several decades [9], it has also been used in recent years to remove or degrade many micropollutants including IMI. Bourgin et al. [22] examined the removal of IMI from synthetic wastewater by injecting standard and seed loading solutions in semi-batch reactor. Furthermore, occurrence and degradation of by-products were also investigated. Degradation of IMI yielded to production of 13 degradation by-products.



The IMI degradation pathway which would enlighten the production of these by-products was proposed. They applied different ozone concentrations such as 25, 50 and 100 g/m<sup>3</sup> in order to examine the IMI removal and degradation kinetics. As expected, an increase in the ozone concentration resulted in higher IMI degradation within a shorter time. The degradation yields of IMI within 90 min were 96.5, 99.9 and 99.8% for ozone concentrations of 25, 50 and 100 g/m<sup>3</sup>, respectively. In turn, the higher ozone concentration lead to the faster IMI degradation. The reaction kinetic was found to follow a pseudo-first order reaction with rates constants between 0.129–0.147 min<sup>-1</sup> [22].

Another IMI ozonation study which was conducted in batch reactor also showed that the degradation of IMI followed pseudo-first order reaction kinetics with a rate constant of 0.121 min<sup>-1</sup> at pH 7.0 [23]. Furthermore, in this study, Chen et al. [23] also examined the effects of pH on the IMI degradation. The findings showed that as the pH increased from 6.02 to 8.66, the degradation rate constant improved more than four-fold. On the other hand, degradation of IMI was negatively affected by the alkalinity increase from 0 to 250 mg/L as CaCO<sub>3</sub>. The reason could be a decrease of available OH• in the solution for IMI degradation due to the reaction of CO<sub>3</sub><sup>-</sup> with OH•. Therefore, they also concluded that the OH• plays a significant role during IMI removal [23].

#### **2.4. Ozonation Process**

AOPs are widely applied to remove organic pollutants such as pesticides from wastewater treatment plants. AOPs include implementation of O<sub>3</sub>, UV, H<sub>2</sub>O<sub>2</sub>, Fenton process, photocatalysis [81]. Among these processes ozonation is one of the most typical and promising treatment method [25], and it has been applied for wastewater treatment due to high oxidation efficiency for several decades [9].

### 2.4.1. Physicochemical properties of O<sub>3</sub>

Ozone was firstly discovered by the German scientist C. F Schönbein in 1840. The O<sub>3</sub> name originated from Greek word “ozein” which means “to smell” due to its very distinctive odor. In 1856, Thomas Andrews discovered that ozone was formed by only oxygen atoms. In 1863, it was shown that three volumes of oxygen are equal to two volumes of O<sub>3</sub> [182]. Formation of ozone is endothermic process and the O<sub>3</sub> is thermodynamically unstable which means it spontaneously comes back into oxygen atom. Since O<sub>3</sub> is an unstable gas, it should be generated “in-situ” [183].

O<sub>3</sub> is a pale blue gas with a higher density than air. O<sub>3</sub> is an allotrope of oxygen [184] and the chemical properties are subjected to molecule structure of O<sub>3</sub> [185]. The resonance structure of O<sub>3</sub> is illustrated in Figure 8 [186]. Molecular O<sub>3</sub> may react as a dipole, an electrophilic or nucleophilic agent due to its resonance structure. Hence, O<sub>3</sub> is highly unstable and reactive [183].

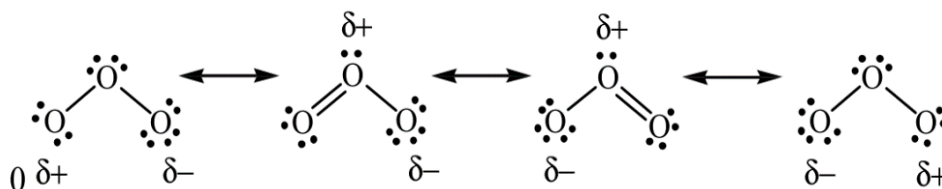


Figure 8. Resonance structure of O<sub>3</sub> [186]

Furthermore, half-life of O<sub>3</sub> may differ from a few seconds to few minutes depending on several properties such as pH, temperature, organic and inorganic compounds' concentration [185].

Table 4. Oxidizing potential values for common oxidants [187]

Oxidizing Species	Oxidation Potential (E <sub>0</sub> )
Fluorine	3.03 V
Hydroxyl radical (OH•)	2.80 V
Ozone (O <sub>3</sub> )	2.07 V
Persulfate anion (S <sub>2</sub> O <sub>8</sub> <sup>2-</sup> )	2.10 V
Hydrogen peroxide (H <sub>2</sub> O <sub>2</sub> )	1.78 V
Permanganate ion (MnO <sub>4</sub> <sup>-</sup> )	1.68 V
Peroxymonosulfate anion (HSO <sub>5</sub> <sup>-</sup> )	1.40 V
Chlorine	1.36 V
Oxygen	0.40 V

The chemistry of O<sub>3</sub> is generally carried out by its strongly electrophilic nature. Table 4 shows oxidation potential of several oxidizing species. Ozone is highly reactive with an oxidation power of 2.07 V [183]. It has more oxidation potential than both chlorine (1.36 V) and oxygen (0.40 V). Since it is unstable and very reactive, it cannot be stored or transported. Therefore, it has to be produced in-situ. Furthermore, it is very explosive even at low concentrations. It also shows toxicity to humans, but due to distinctive smell, it can be detected before it comes dangerous level. Furthermore, solubility of O<sub>3</sub> in water is ten times higher than the oxygen [188]. Further physicochemical properties of O<sub>3</sub> is given in Table 5.

Table 5. Physicochemical properties of O<sub>3</sub> [183,187]

Property	Value
Form	Pale blue gas
Molecular weight	48 g/mole
Density (gas) (at 0 °C)	2.144 km/m <sup>3</sup>
Melting point	-192.7 °C
Boiling point	-110.5 °C
Solubility in water (at 0 °C)	2.2×10 <sup>-2</sup> M

Property	Value
Solubility in water (at 20 °C)	$1.19 \times 10^{-2}$ M
Henry's constant (at 0 °C)	35 atm/M
Henry's constant (at 20 °C)	100 atm/M
Explosion threshold	10% ozone

#### 2.4.2. The mechanism of O<sub>3</sub> action

As mentioned previous section, both O<sub>3</sub> and hydroxyl radicals (OH•) are one of the strongest oxidants after fluorine (Table 4). Chemical oxidation during ozonation can occur by two ways, direct reaction or indirect reaction [189]. While the former one represents that the degradation of compound is occurred by only O<sub>3</sub>, the latter represents various radical species, which are formed as a result of O<sub>3</sub> decomposition, also play a role in addition to O<sub>3</sub> [189]. Therefore, indirect reaction is also named as radical-type reaction.

Radical species such as OH•, superoxide radicals (O<sub>2</sub><sup>-•</sup>), hydroperoxyl radicals (HO<sub>2</sub>•) attracted the most attention in AOPs due to their highly reactive and powerful oxidizing ability. Indeed, these radical species are strong enough to initiate AOPs and oxidize pollutants in the water [108].

Moreover, ozone action towards to micropollutants strongly depends on nature of organic pollutant and pH of the solution [188], which is further discussed in the following sections. These two degradation pathways are illustrated in Figure 9.

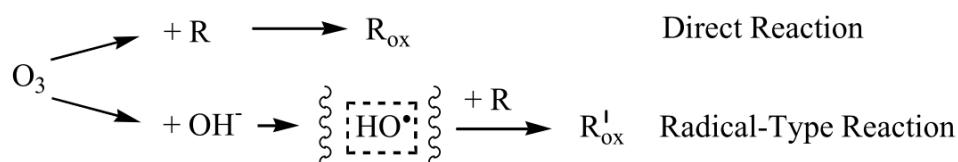


Figure 9. Ozone reactivity mechanism toward to pollutant, R [185]

## Direct Reaction

Direct oxidation of pollutants by ozone is an extremely selective reaction with a typical kinetic reaction rate between 1 to  $10^6 \text{ M}^{-1}\text{s}^{-1}$  [190]. Due to dipolar structure of ozone, ozone molecule attacks to unsaturated bonds of pollutant compound and it leads to bond splitting. This process is called as Criegee mechanism and proposed reaction pathway is illustrated in Figure 10 [191].

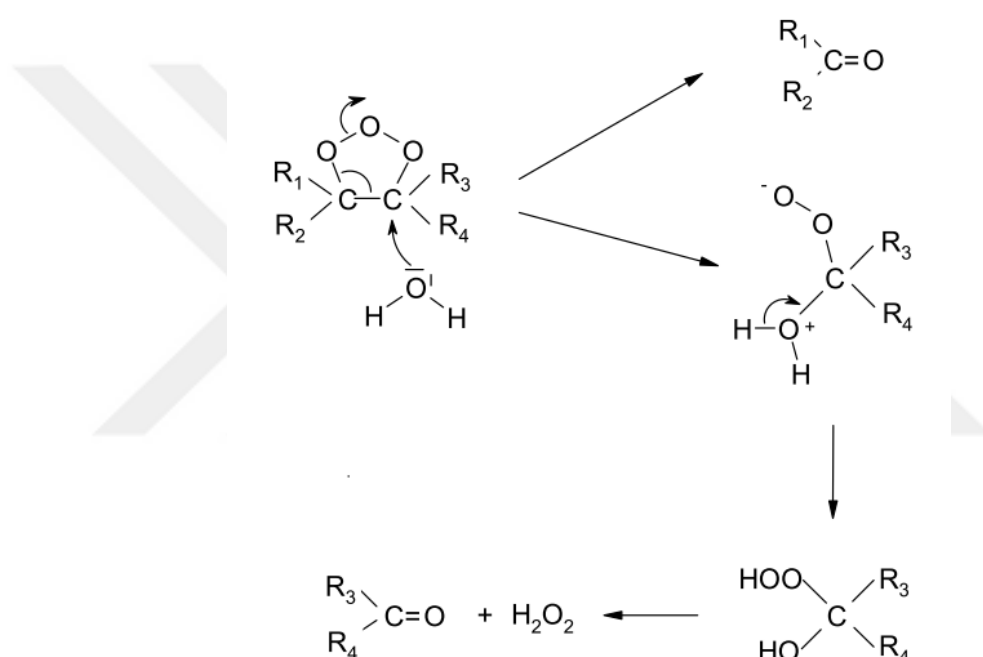


Figure 10. Proposed reaction pathway for Criegee mechanism [191]

$O_3$  is strong electrophile and reacts quickly with organic and inorganic compounds. The electrophilic reaction is limited to certain aromatic compounds and sites that have strong electronic density. For instance, electron donor groups ( $OH$ ,  $NH_2$  etc.) are strongly reactive with  $O_3$  due to their high electronic densities.

As illustrated in Figure 11, O<sub>3</sub> quickly reacts with electron donor group (shown as D) of aromatic compound [183]. Other than aromatic compounds, O<sub>3</sub> has selective reactivity towards double bonds, secondary and tertiary amines (non-protonated) and sulfur species [192]. On the other hand, electron withdrawing groups (-COOH, -NO<sub>2</sub> etc.) are less O<sub>3</sub> reactive [9]. In this case, O<sub>3</sub> acts as a nucleophile depending the nucleophilicity degree of compound [185]. Moreover, pH affects the reaction mechanism since the decomposition of O<sub>3</sub> highly depends on the pH [88]. Indeed, direct mechanism is favored at acidic pH (i.e. pH<7), since the concentration of OH<sup>-</sup> and in turn, decomposition of O<sub>3</sub> is less [189].

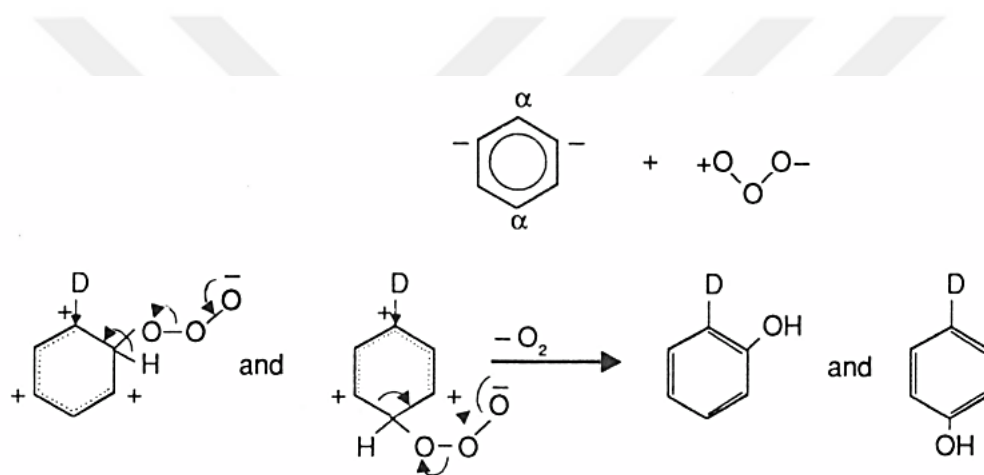


Figure 11. Proposed reaction pathway of ozone and aromatic compound [185]

### Indirect Reaction

The second degradation pathway is indirect reactions. It is also named as radical-type reaction since decomposition of O<sub>3</sub> forms several radicals. The radicals have unpaired electron which make them highly unstable. The unpaired is generally represented by “•”. Moreover, the reaction rates of the most radicals are generally high since they prone to undergo reaction with a pollutant immediately. While the direct reaction is dominant at acidic pHs (i.e. pH<7), indirect mechanism is favored at basic pHs (i.e.

pH>7) [88]. Therefore, at basic pHs, decomposition of O<sub>3</sub> increases due to highly available amount of OH<sup>-</sup> [189].

The O<sub>3</sub> decomposition occurs with chain reactions including initiation, propagation and termination steps [189]. The overall ozone degradation pathway is illustrated in Figure 12 and these steps and reactions are further discussed in this section.

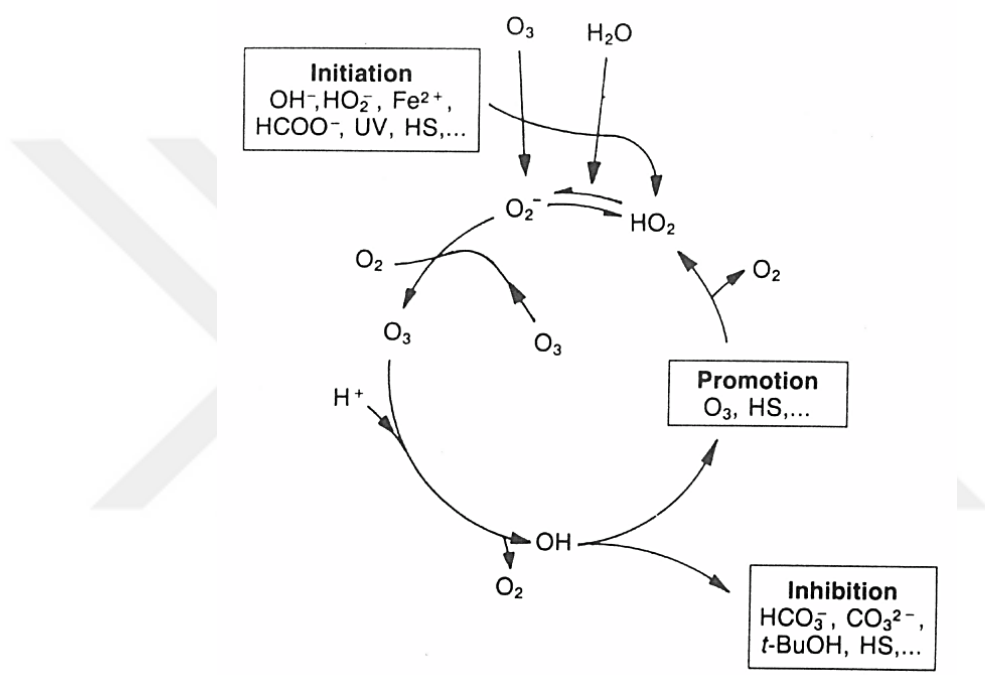
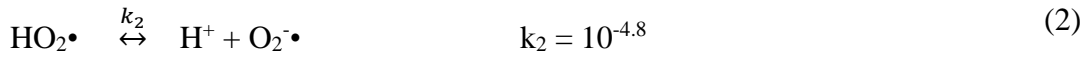
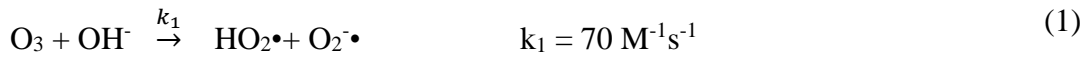


Figure 12. Overall mechanism for ozone decomposition [185]

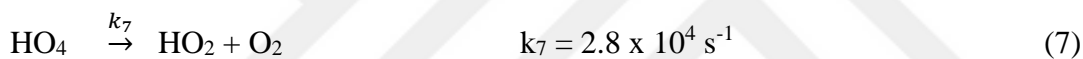
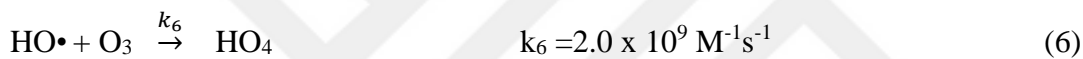
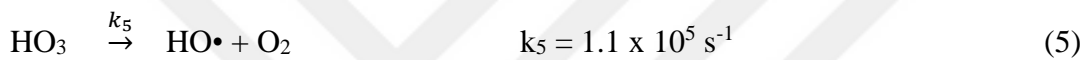
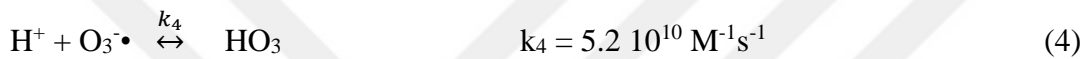
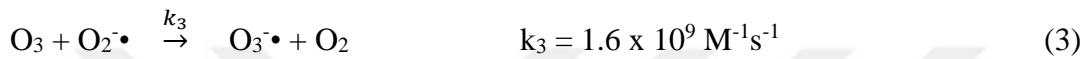
*Initiation step:*

Ozone decomposition starts with attack of OH<sup>-</sup> to ozone and this rate-determining step leads to formation of one superoxide radical ion (O<sub>2</sub><sup>-•</sup>) and one hydroperoxyl radical HO<sub>2</sub><sup>•</sup> (Eq. (1)) The second equation represents the regeneration of O<sub>2</sub><sup>-•</sup> since HO<sub>2</sub><sup>•</sup> is in acid-base equilibrium with O<sub>2</sub><sup>-•</sup> [189].



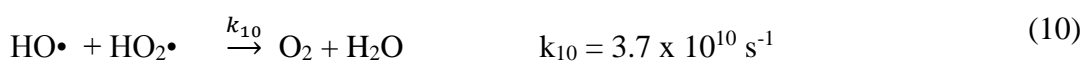
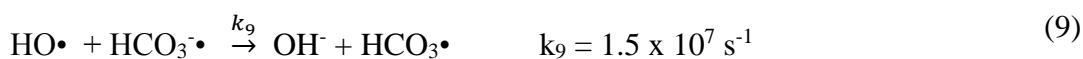
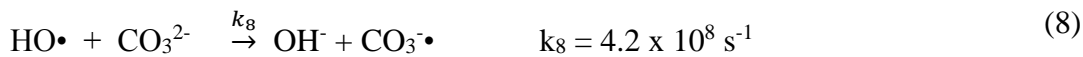
*Propagation step:*

This step includes ozonide anion ( $\text{O}_3^{\bullet-}$ ) production by attack of ozone to  $\text{O}_2^{\bullet-}$ . Further reactions constitute  $\text{OH}\bullet$  [189].



*Termination step:*

Several organic and inorganic compounds react with  $\text{OH}\bullet$  to form secondary radicals which not further form superoxide radicals such as  $\text{HO}_2\bullet$  and  $\text{O}_2^{\bullet-}$  (Eq. (8) and Eq. (9)) [189]. These compounds are generally named as scavengers or inhibitors since they inhibit ozone decay and in turn, radical production. Another possibility for scavenging radicals can be reaction of two radicals (Eq. (10)).





There are several compounds that may act as an initiator, a terminator or a scavenger. Some of the examples of these substances are given in Table 6. As seen from Table 6, humic acid may act as either promoter or scavenger.

Table 6. Examples for initiators, terminators and scavengers act during ozone decomposition [92]

<b>Initiator</b>	<b>Promoter</b>	<b>Scavenger</b>
OH <sup>-</sup>	Humic acid	Tert-butyl alcohol (TBA)
H <sub>2</sub> O <sub>2</sub> / HO <sub>2</sub> <sup>-</sup>	Aryl-R	HCO <sub>3</sub> <sup>-</sup> / CO <sub>3</sub> <sup>2-</sup>
Fe <sup>2+</sup>	Primary and secondary alcohols	PO <sub>3</sub> <sup>4-</sup>
		NO <sub>3</sub> <sup>-</sup> , NO <sub>2</sub>
		Cl <sup>-</sup> , Br <sup>-</sup>
		Humic acid

The presence of scavengers in the wastewater may cause consumption of the radical species. These scavengers may consume OH• or compete with micropollutants for indirect degradation reactions. Scavengers may include organic matters like humic or fulvic acids, proteins and amino acids, or inorganic matter such as sulfide, carbonate, bicarbonate, bromide and nitrate [92]. The scavenging effect should be taken into consideration while applying ozonation treatment in WWTPs.

### 2.4.3. Factors affecting the treatment efficiency of O<sub>3</sub>

The operational parameters, such as ozone dose, pH, water matrix have an impact on both ozone decomposition and pollutant degradation [193,194]. Hence, their effects are discussed further in the following sections.

## Effect of Ozone Dose

Ozonation is an energy intensive treatment process. Therefore, it is highly crucial to maintain micropollutant removal by using optimum amount of ozone in WWTPs. Indeed, based on lab-scale experiments ozone dose is determined and it gives essential concept of ozone application at WWTPs, since ozone dose is key parameter for estimation of operational costs [192]. Moreover, different pollutants may need different amount of ozone during ozonation process [91]. Antoniou et al. [91] investigated ozonation of 6 different secondary effluent wastewaters which were spiked with 42 micropollutants including PPCPs. They performed several ozone doses between 0.5 to 12.0 mg/L in lab-scale experiments. They concluded that each micropollutant has different ozone consumption during treatment. For example, for all wastewaters, degradation of Carbamazepine and Naproxen showed an increase with the increase of applied ozone dose. According to this study, required ozone dose should be specified based on target pollutant compound [91]. Tetracycline hydrochloride which is well-known antibiotic group was treated from water by lab-scale semi-batch ozonation treatment [194]. In this study, 3 different ozone doses (i.e. 0.53, 0.86 and 1.13 mmol/L) were applied to remove tetracycline with an initial concentration of 2.08 mmol/L. The obtained results showed that as the ozone dose increases, removal of tetracycline also increases due to raise of ozone equilibrium concentration in the liquid phase.

Bourgin et al. [22] investigated the IMI removal by ozonation and formation of degradation by-products. They applied 3 different doses (i.e. 25, 50 and 100 g/m<sup>3</sup>) during 90 min ozonation. The results showed that as the ozone dose increases, IMI degradation rate increases. Indeed, 96.5% and 99.9% IMI removal were achieved within 90 min ozonation for ozone doses of 25 and 50 g/m<sup>3</sup>. On the other hand, just within 45 min 99.8% of IMI was degraded with 100 g/m<sup>3</sup> ozone dose [22]. Orhon et al. [90] applied 5 different ozone doses (i.e. 5, 10, 15, 24 and 70 mg/L) during ozonation of triclosan which is a well-known antimicrobial compound and belongs in personal care products. The findings showed that application of 24 and 70 mg/L ozone

resulted in almost complete degradation just in 2 min ozonation. Contrarily, longer time was needed to complete triclosan degradation at low ozone doses. For example, 98% triclosan removal was achieved in 1 and 10 min with the application of 70 and 5 mg/L ozone doses, respectively [90]. Hansen et al. [89] evaluated the effect of pH on the pharmaceutical removal from hospital wastewater by ozonation. They investigated the impact of ozone dose on the removal of several pharmaceuticals such as mefenamic acid, diclofenac, naproxen, gemfibrozil ketoprofen, ibuprofen, triclosan and clofibrac acid from wastewater. At ozone dose of 2.9 mg/L, removal efficiencies range from 25% to 85% at pH 5.00. On the other hand, increase of ozone dose from 2.9 to 18 mg/L resulted in almost complete degradation of all studied pharmaceuticals at the same pH [89].

### **Effect of pH**

Besides ozone dose, efficiency of micropollutant removal highly depends on characteristic of wastewater, such as pH [88]. Significant changes of pH will affect the ozone half-life, treatment efficiency and in turn, required ozonation tank size in WWTPs [89].

For these reasons, pH effect on the micropollutant removal was investigated by several studies. For instance, degradation efficiency of triclosan by ozonation was evaluated under 4 different pHs (i.e. 6, 7.3, 8 and 10) [90]. According to Orhon et al. [90], more than 96% triclosan removal was achieved at all pHs. Although increase of pH up to 8 resulted in increase of degradation efficiency, when the OH• are abundant in the solution at pH 10, the degradation efficiency decreased. Ozonation process may lead to produce some degradation by-products. In this case, Orhon et al. [90] concluded that acidic ozonation by-products may be the reason behind degradation efficiency decrease [90]. Furthermore, pharmaceutical removal from hospital wastewater by ozonation showed dependency on pH [89]. Hansen et al. [89] evaluated the effect of different initial pHs, such as 5.00 and 6.25 on the degradation efficiency at same ozone

dose. While the pH increase from 5.00 to 6.25 resulted in slightly higher removal efficiencies for ketoprofen, ibuprofen, triclosan and clofibric acid, removal efficiency decrease was observed for mefenamic acid, diclofenac, naproxen and gemfibrozil at ozone dose of 2.9 mg/L [89]. In another study, gemfibrozil, clofibric acid and methicillin showed almost no change of removal rate at pH range of 5-10. In addition, triclosan and fenoterol removal rate was increased with pH increase from 5 to 8, but the rate remained constant with further pH increase to 10. Some other micropollutants like equilenin, butylated hydroxyanisole, 17 $\alpha$ -ethinylestradiol and phenol demonstrated an increasing trend with the increase of pH [195].

Changes in pH may affect not only the target micropollutant removal but also COD and TOC in wastewater. Jung et al. [196] investigated effect of initial pH on the removal of ampicillin, COD and TOC. Ampicillin is widely used penicillin-type bacteriostatic antibiotics in human and veterinary applications. Performed kinetic study under different pHs (5.0, 7.2 and 9.0) showed that as the pH increased, reaction rate for ampicillin degradation also increased. The rate constants  $2.2 \times 10^5$ ,  $4.1 \times 10^5$  and  $5.4 \times 10^5 \text{ M}^{-1}\text{s}^{-1}$  were obtained at pH 5.0, 7.2 and 9.0, respectively. It was clearly seen that pH increase from 5.0 to 7.2 almost doubled the reaction rate. Moreover, COD removal also showed dependency on pH since COD removal rates were 60%, 70% and 80% at pH 5.0, 7.2 and 9.0, respectively. However, TOC removal did not show any significant differences between the studied pHs and the removal trends were almost same. After 90 min of ozonation, TOC removal range was between 35-42% which suggested that there were still oxidation by-products remained in the aqueous solution [196].

### **Effect of Water Matrix**

Although treatment of micropollutants and obtaining reaction kinetic constants using ultrapure water spiked with the pollutant can be used as a primary approach for establishing full-scale treatment units, treatment studies involving real wastewater

effluents must be investigated at lab-scale and pilot-scale before verifying the removal efficiencies at full-scale treatment plants [92]. Moreover, as mentioned before, ozone leads to production of several radical species which have non-selective oxidation ability. However, some organic and inorganic compounds such as  $\text{HCO}_3^-$ ,  $\text{CO}_3^{2-}$ ,  $\text{NO}_3^-$ ,  $\text{NO}_2^-$ ,  $\text{Cl}^-$  and  $\text{Br}^-$  in wastewater cause scavenging of these radicals [92]. In addition to scavenging effect, chemical properties of the micropollutants also alter the ozone requirement of the system. For instance, if the treatment objective is to remove most of the pollutants rather than ozone reactive ones, then required ozone amount and hence the energy demand of the ozonation process should be determined by ozone resistant ones in the water matrix [97]. For these reasons, several ozonation studies involve real wastewater effluents or compare removal efficiency of micropollutants using different water matrices.

Some studies showed that the degradation rate of pharmaceutical compounds decreased or residence time for the same abatement percentage increased during ozonation of real wastewater effluent with respect to ultrapure water matrix [90,197]. Orhon et al. [90] performed water matrix effect on triclosan removal by using 2 different water matrices (Milli-Q water and surface water). For 90% removal of triclosan with an initial concentration of 3 mg/L, 3 and 6 min was required in Milli-Q water and surface water, respectively. They also investigated the initial triclosan concentrations 1 and 5 mg/L and noted that triclosan degradation after 5 min of ozonation was nearly same in both water matrices [90]. In fact, during ozonation, even different wastewater effluents exhibit different pollutant degradation efficiency due to various properties of wastewater such as COD and alkalinity [91]. Antoniou et al. [91] investigated removal of 42 micropollutants in 6 different wastewater matrices. Effluent 1 and 3 have less COD values (29 and 30 mg/L, respectively) with respect to others. Therefore, competition for  $\text{O}_3$  and  $\text{OH}\cdot$  between micropollutants and organic matter in the wastewater was also low. This turned out the highest removal efficiencies (50-100%) at lowest ozone dose (0.5-0.6 mg/L  $\text{O}_3$ ) among the all wastewater effluents. On the other hand, at the low  $\text{O}_3$  dose, effluent 5 was the most recalcitrant to ozonation

due to high COD (90 mg/L) and alkalinity values (250 mg HCO<sub>3</sub><sup>-</sup>/L). All micropollutants exhibited less than 50% abatement. Although O<sub>3</sub> dose was increased to 8.9 mg/L, up to 90% removal for only 18 out of 42 micropollutant was achieved, whereas the same removal was achieved for 36 and 39 out of 42 micropollutant for effluent 1 and 3, respectively [91].

In addition, comparison of several types of water matrices were conducted by researchers. Benitez et al. [198] examined the impact of different water matrices on degradation of four pharmaceuticals (metoprolol, naproxen, amoxicillin, and phenacetin) by ozonation process. They performed ozonation in groundwater (PZ), reservoir water (PA), and 3 different wastewater effluents obtained by municipal treatment plants of Alcala (AL), Badajoz (BA) and Mostoles (MO) in Spain. For instance, residual phenacetin concentration (initial concentration=1 μM) for water matrices PZ, PA, AL, BA and MO were 0.0, 0.58, 0.71, 0.80 and 0.90 μM, respectively at 1 mg/L ozone dose. When 3 mg/L ozone dose was applied, removal of phenacetin increased, and the remaining phenacetin concentrations were 0.0, 0.0, 0.52, 0.56 and 0.57 μM for the corresponding water matrices. The water matrix effect on phenacetin degradation was apparent during both applied ozone doses. For instance, groundwater had lower DOM content regarding other water matrices, lowest ozone decomposition and the highest removal were observed in groundwater. The least removal percentages were observed in all 3 wastewaters. Indeed, the lowest removal was observed for the wastewaters having highest COD and TOC values [198].

#### 2.4.4. Reaction Kinetics

As mentioned at the previous part, ozonation may take place either direct or indirect reaction [199]. The direct ozonation of IMI was exhibited pseudo first-order kinetics, as following;

$$-\frac{d [IMI]}{dt} = k_{o_3} [IMI] \quad (11)$$

where;

[IMI]: Concentration of IMI

$k_{O_3}$ : Pseudo first-order rate constant at excess  $O_3$  supply

Bourgin et al. [22] stated that the degradation of IMI showed pseudo-first order kinetics since increase of ozone concentration resulted in degradation kinetics at excess amount of IMI (39 mg/L). Moreover,  $\ln(C/C_0)$  versus time graph showed linearity which also confirms the pseudo-first order kinetics. Therefore, they stated the rate law of IMI removal as;

$$r = k_{IMI} * C_{Ozone} * C_{IMI} \quad (12)$$

where;

$k_{IMI}$ : Reaction rate constant

$C_{Ozone}$ : Ozone concentration

$C_{IMI}$ : IMI concentration

## 2.5. Ozone/UV Process

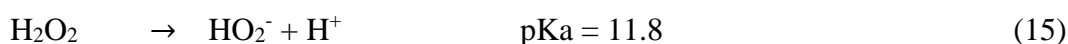
Although ozonation is highly effective treatment process, several AOPs can be combined in order to increase treatment efficiency by enhancing radical production. Indeed, combination of ozone with  $H_2O_2$ , iron salts with  $H_2O_2$  and  $TiO_2$  with UV irradiation yields  $OH\cdot$  production [179].

Combination of  $O_3$  and UV is one of the AOPs and it has many benefits on improving micropollutant degradation in aqueous media. In addition to removal of micropollutant by ozone, this AOP provides 3 more degradation ways by [183];

- H<sub>2</sub>O<sub>2</sub>
- UV
- OH•

Therefore, the overall evaluation of AOP should be performed by considering all these removal ways. Apart from degradation by O<sub>3</sub> and UV, OH• and H<sub>2</sub>O<sub>2</sub> production and their oxidizing abilities should be further investigated.

For instance, H<sub>2</sub>O<sub>2</sub> is produced by UV irradiation of O<sub>3</sub> (Eq. (13)). Furthermore, generated H<sub>2</sub>O<sub>2</sub> enhances the production of OH• (Eq. (14)) which has the highest oxidation potential (2.80 V) after fluorine (3.03 V) [189]. However, generation of OH• is quite slow since the k<sub>14</sub> is much lower than k<sub>13</sub> at 254 nm UV irradiation [200]. Some fraction of H<sub>2</sub>O<sub>2</sub> is dissociated into HO<sub>2</sub><sup>-</sup> with pKa value of 11.8 (Eq. (15)) [201]. After that, produced HO<sub>2</sub><sup>-</sup> reacts with soluble O<sub>3</sub> and produce some radicals such as HO<sub>2</sub>• and O<sub>3</sub><sup>-</sup>• (Eq. (16)) [202].



In the literature, several studies investigated removal of micropollutants by O<sub>3</sub>/UV and the studies even compared the degradation efficiencies of O<sub>3</sub> and O<sub>3</sub>/UV. Irmak et al. [203] investigated abatement of endocrine disrupters such as 17β-estradiol (E<sub>2</sub>) and bisphenol A (BPA) by O<sub>3</sub> and O<sub>3</sub>/UV processes. Experiments were conducted at semi-batch mode for ozonation and O<sub>3</sub>/UV processes. Complete degradation of E<sub>2</sub> with 0.1 mmol initial concentration was achieved within 55, 75 and 90 min of ozonation with corresponding ozone doses of 15.78×10<sup>-3</sup>, 12.25×10<sup>-3</sup> and 9.78×10<sup>-3</sup> mmol/min. In the case of O<sub>3</sub>/UV process, applying same ozone doses provided complete degradation within 45, 55 and 67 min, respectively. For removal of BPA,



three different ozone doses (i.e.  $18.67 \times 10^{-3}$ ,  $15.78 \times 10^{-3}$  and  $10.33 \times 10^{-3}$  mmol/min) were applied for 0.1 mmol initial BPA concentration. Although BPA degradation was not improved by UV addition as much as E<sub>2</sub> did, reaction rates of BPA obtained during O<sub>3</sub>/UV process became faster than rates of BPA for ozonation process. The results showed that reaction between ozone and BPA was slower than the one with E<sub>2</sub> during ozonation. Indeed, O<sub>3</sub>/UV process decreased the consumed O<sub>3</sub> amount during treatment and 1 mole of BPA and E<sub>2</sub> reacted with 21.1 and 18.9 moles of O<sub>3</sub>. Therefore, O<sub>3</sub>/UV process was more effective at removing E<sub>2</sub> and BPA than only O<sub>3</sub> process.

Accordingly, Chen et al. [204] observed synergistic effect of O<sub>3</sub>/UV process during removal of N-Nitrosopyrrolidine (NPYR) which is a nitrogen containing micropollutant. In 300 seconds of treatment by UV, O<sub>3</sub> and O<sub>3</sub>/UV processes showed degradation efficiencies of 60%, 65% and 100%, respectively. The effect of pH was also studied. The obtained results at pH 4 showed that while single ozonation did not achieve any removal of NPYR, more than 80% removal was achieved by O<sub>3</sub>/UV process. On the other hand, with the increase of pH to 7 and 8, NPYR degradation was enhanced significantly. For instance, for O<sub>3</sub> and O<sub>3</sub>/UV processes, degradation efficiency at pH 7 were 70% and 60% and at pH 8 were 65% and 100% in 300 seconds, respectively. In addition, NO<sub>2</sub><sup>-</sup>, the well-known by-product of NPYR, was formed less in the O<sub>3</sub>/UV than ozonation alone [204]. Cernigoj et al. [21] investigated Thiachloprid degradation by O<sub>3</sub> and O<sub>3</sub>/UV. The results showed an apparent difference between these treatment processes due to photo degradation of O<sub>3</sub>. Thiachloprid with an initial concentration  $2 \times 10^{-4}$  M was treated around 80% and 93% in 30 min of O<sub>3</sub> and O<sub>3</sub>/UV treatment, respectively [21]. Lau et al. [205] examined removal of carbofuran by UV (254 nm), O<sub>3</sub> and O<sub>3</sub>/UV processes. Carbofuran, which is a carbamate insecticide and known as potential EDC, is widely found in surface water and wastewater. Degradation efficiency of carbofuran with an initial concentration 0.2 mM was 35, 82 and 100% in 30 min by UV, O<sub>3</sub> and O<sub>3</sub>/UV application, respectively. Furthermore, effect of pH was investigated within the pH range between 3 and 11. Degradation rate

of carbofuran by UV application was  $0.02 \text{ min}^{-1}$  and remained same from pH changes from 3 to 9. During ozonation, the degradation rate was around  $0.05 \text{ min}^{-1}$  up to pH 7 and then increased up to  $0.10 \text{ min}^{-1}$  at pH 9. On the other hand,  $\text{O}_3/\text{UV}$  application showed higher degradation rates for all pH range. The kinetic rate constant accelerated with respect to pH increase during  $\text{O}_3/\text{UV}$  process, especially the pH ranges that ozonation kinetic rate constant remained same. Therefore,  $\text{O}_3/\text{UV}$  provided high removal efficiencies compared to single ozonation and UV for all pH ranges [205].

Various studies proved that ozonation process coupled with UV becomes more effective AOP technique than merely ozonation process since it leads to generation of radical species that have further oxidation capability.

## CHAPTER 3

### MATERIALS AND METHODS

#### 3.1. IMI Concentrations Studied

IMI is an insecticide that belongs to neonicotinoid pesticide group. It is widely used during production of sugar beet, grape, apple, pear and tomato. IMI is colorless crystals that is highly soluble in the water (0.61 g/L) and has low octanol-water coefficient ( $\log K_{ow}$ ) 0.52 at 21 °C and at pH 7 (further physicochemical properties are given in Sec. 2.2.1). Therefore, IMI can easily reach to water bodies [126]. For example, the IMI concentration in Yeşilirmak river basin range from 0.0143 to 0.3193  $\mu\text{g/L}$  [206]. Indeed, evidently, IMI was detected in the municipal and industrial WWTPs in the basin, namely, Çorum, Erbaa, Tokat (municipal) and Dimes (industrial), as also stated in Sec 1.3. Although IMI was observed above the EQS values at these effluent discharge points, IMI was below the EQS value at upstream and downstream stations for Erbaa, Tokat and Dimes WWTP cases, possibly due to natural degradation or dilution effects. On the other hand, IMI was observed above the EQS value at Çorum downstream station possibly due to non-point sources such as agricultural activities around this area. Despite these differences in cases, so far, IMI did appear in the WWTPs within the range between 0.0255 to 0.7570  $\mu\text{g/L}$  (Table 1 and [206]).

On the other hand, during the measurement of IMI at HPLC, LOD was found as 5 ppb ( $\mu\text{g/L}$ ) which is much higher than the concentrations observed in Yeşilirmak basin (Table 1). So, in order to be able to observe the concentration of IMI after the treatment it was deemed necessary to work with some higher initial concentrations as such possibly to give 5 ppb final concentration with at least 95% removal. In this way, it would be also possible to follow the degradation kinetics, as well as the by-product

formation. Additionally, occurrence levels of IMI in secondary effluents (Table 3) and possible higher IMI concentration in industrial wastewaters originating from the IMI formulating and manufacturing plants was also taken into consideration while determining the initial IMI concentration to study. Therefore, in this thesis study, IMI concentrations between 100 and 1000 ppb were studied.

### **3.2. Water Samples and Sample Preparation**

In the ozonation and O<sub>3</sub>/UV experiments three types of water samples, namely, Milli-Q water and two different secondary level treated wastewaters, were used. The former is the ultra-pure water obtained from Milli-Q water system (Millipore) with a specific resistance of 18.2 MΩ•cm. Milli-Q water was used as a control to figure out ozone decomposition factors by eliminating the matrix effect of wastewater and perform a parametric study. This Milli-Q water was spiked with the desired IMI amounts prior to experimentations.

The latter two were belonging to different wastewater matrices used in order to understand matrix effect on the degradation of IMI by ozonation and O<sub>3</sub>/UV processes. One of these secondary level treated wastewaters was collected from full-scale Vacuum Rotating Membrane Bioreactor plant (VRMBR) which is in operation at METU Campus, Ankara. The plant composed of two tanks while the first tank is for biological sludge aeration, the second one is for vacuum rotating membrane unit. Before and after membrane bioreactor treatment, COD (i.e. influent) and COD (i.e. effluent) were 426 mg/L and 19 mg/L, respectively. The high COD removal efficiency could be due to absence of IMI. The treated wastewater sample was collected in 30-liter bottle and transferred to the laboratory urgently. Before sampling, the bottle was washed with Alconox which is concentrated, anionic powder detergent. Later the bottle was rinsed firstly with tap water, then with pure water and finally rinsed thoroughly with Milli-Q water. The treated wastewater was filtered through a 0.45 μm Millipore membrane filters via vacuum filtration unit within 24 hours after sampling.

The filtration was applied in order to remove impurities which may cause to clogging of HPLC column and avert inaccurate measurements during the analysis of samples. After filtration, treated wastewater was poured into 2.5-liter amber glass bottles that were primarily washed with Alconox and rinsed thoroughly with tap water, pure water and Milli-Q water, respectively. These 2.5-L amber glass bottles were stored in refrigerator at +4 °C in the dark. This real wastewater sample was spiked with IMI at desired concentrations prior to ozonation experimentations.

The second water matrix was biologically treated wastewater (Bio WW) which was obtained from the operation of laboratory scale instantaneous fed-batch reactor (FBR) receiving IMI (as spiked) in its influent. The purpose of applying ozone and O<sub>3</sub>/UV to Bio WW is to mimic real wastewater treatment plant that consist of secondary and tertiary treatment. This Bio WW was produced during the study by Kocaman [207] as also part of the TÜBİTAK project mentioned earlier. Kocaman [207] operated lab-scale FBR seeded with activated sludge taken from Tatlar WWTP (Ankara, Turkey) and acclimated to IMI. After acclimation, various concentrations of IMI were spiked to the reactor and treated biologically up to certain levels. Before and after biological treatment, COD (i.e. influent) and COD (i.e. effluent) were 500 mg/L and 247 mg/L, respectively. Since FBR was initially injected by IMI, which creates inhibition, the removal efficiency of COD in the Bio WW was lower than the one obtained by VRMBR WW.

The treated Bio WW, provided by Kocaman [207], was filtered through a 0.45 µm Millipore membrane filters via vacuum filtration unit within 24 hours after sampling. The filtration was applied in order not to clog HPLC column due to impurities. After filtration, treated wastewater was poured into 0.5-liter plastic bottles and stored in the refrigerator at +4 °C in the dark. After biological treatment, remaining IMI was treated with ozone and O<sub>3</sub>/UV.

### 3.3. Experimental Set Up

#### 3.3.1. Ozone Generator

The laboratory scale ozonation experiments was carried out in semi-batch mode and consisted of an ozone generator, ozonation reactor and gas washing bottle. All ozonation experiments were done in Unit Operations Laboratory in the Department of Environmental Engineering at METU. Ozone gas was produced on-site by WEDECO (OSC-Modular 4HC-AirSep AS 12) ozone generator (Figure 13).

The ozone generator feed-gas is air. The ozone generator has maximum ozone production of 4 g/h with an operation pressure of 0.5 bar. The ozone generator, which is shown in Figure 13, has dimensions as 600 mm length, 210 mm width and 600 mm height. Concentration and flowrate of the output ozone gas can be adjusted between 0 to 200 mg/L and 10 L/h to 140 L/h, respectively.



Figure 13. Ozone generator

In order to achieve preferred ozone doses to be sparged through the reactor, potentiometer and gas flow buttons were manually adapted as stated in generator's performance curve (given in Appendix A) and concentration and flowrate of ozone gas was kept constant during the ozonation experiments. The desired ozone dose was calculated by the multiplication of ozone concentration and ozone flowrate as showed in following equation.

$$m_{\text{Ozone}} = C_{\text{Ozone}} * Q_{\text{Ozone}} \quad (17)$$

where,

**m<sub>Ozone</sub>**: Ozone dose (mg/h)

**C<sub>Ozone</sub>**: Ozone concentration (mg/L)

**Q<sub>Ozone</sub>**: Gas flowrate (m<sup>3</sup>/h)

During determination of potentiometer setting, once the desired ozone concentration and flowrate were known potentiometer number was selected by using generator's performance curve (given in Appendix A). In that graph, a parallel line to x-axis was drawn from the ozone concentration point which was selected from the y-axis. The line was intersected with selected flowrate curve. Then a parallel line to y-axis was drawn from the intersection point to determine potentiometer number.

### 3.3.2. Ozonation Reactor

The ozonation experiments were conducted in a 1000 ml borosilicate glass reactor at semi-batch conditions in which ozone was continuously purged and the water was stable. The cylindrical glass reactor has dimensions as 6 cm diameter and 35 cm length. The flowrate of sparged ozone gas to the reactor was altered via button and the

concentration was adjusted by potentiometer on the generator panel. The reactor was connected to an ozone generator by a PTFE pipe.

The ozonation experimental system is shown in Figure 14. The ozone that is produced by ozone generator was entered from top of the reactor then, it reached to bottom of the reactor via cylindrical glass rod that has a spherical glass frit end. Therefore, the ozone continuously bubbled through that fritted spherical glass diffuser from the bottom of the reactor in order to increase ozone solubility in the water. The reactor was covered with aluminum foil to avoid IMI degradation due to photolysis.



Figure 14. Experimental setup for ozonation

As seen in Figure 14, while the inlet of the reactor was connected to an ozone generator, the outlet of the reactor was connected to gas washing bottle which contains 500 ml of 2% KI solution and 2N  $\text{H}_2\text{SO}_4$ . The escaping ozone was quantified by the iodometric titration method [199]. The amount of escaped ozone is significant to determine ozone consumption by IMI in the reactor.



### 3.3.3. Ozone/UV Reactor

Similar to ozonation experiments, O<sub>3</sub>/UV process was also carried out via semi-batch process. The experimental system of O<sub>3</sub>/UV process is shown in Figure 15.



Figure 15. Experimental setup for O<sub>3</sub>/UV

The jacketed reactor is made of borosilicate glass with the dimensions of diameter and height of 13.5 and 25 cm, respectively. The working volume of the reactor was 1 L for all water matrices. The temperature of the water matrices was maintained at 24°C ±0.1°C by circulating water through the cooling jacket of the reactor via Julabo F12 cooling water circulator. The reactor was magnetically stirred by Isolab magnetic stirrer during the experiments. The UV lamp, has a power of 10 Watt and produced a monochromatic emission at wavelength of 254 nm, was firstly placed into a quartz tube and the tube was immersed vertically at the center of the reactor. The quartz tube which is heat-resistant was used in order to prohibit water contact with UV lamp. The reactor was covered with aluminum foil to avoid adverse effects of UV irradiation. In like manner to ozonation experiments, ozone inlet and outlet kept as same and gas

washing bottle which contains 500 ml of 2% KI solution 2N H<sub>2</sub>SO<sub>4</sub> was placed to determine escaped ozone amount from the reactor.

### **3.4. Experimental Methods**

#### **3.4.1. Ozone Consumption in the Ozonation System**

Better treatment assessment of the ozonation for water treatment could be determined by evaluating the specific ozone consumption of pollutants. Therefore, in this thesis study, amount of ozone consumption by IMI was comprehensively investigated. The ozone mass balance was applied to the reactor which was chosen as control volume. Prior to determination of ozone consumption by IMI, other constituents in Eq. (18) must be established. The influent ozone was adjusted via control panel of the ozone generator, kept constant during the experiment and continuously monitored. The unreacted and escaped ozone entered into the gas washing bottle. The escaped ozone reacted with the potassium iodide (KI) in the gas washing bottle which contains 500 ml 2% of KI and 5 ml 2N H<sub>2</sub>SO<sub>4</sub>. Titration of liberated iodine with 0.025 M Na<sub>2</sub>S<sub>2</sub>O<sub>3</sub> and the amount of titrant was calculated to determine escaped ozone amount.

The unused ozone was determined by using N,N-diethyl-p-phenylenediamine (DPD) reagent via Hach pocket colorimeter. The ozone consumption by the system was calculated by ozonation of Milli-Q water without addition of IMI. Since the water matrix was Milli-Q water and IMI was not added,  $X_{\text{organic}}$  and  $X_{\text{IMI}}$  were eliminated in Eq. (18). Therefore, ozone consumption by the system was calculated by subtracting unused ozone and escaped ozone amounts from influent ozone. When the water matrix was wastewater, organics in the water also consumed ozone. Therefore, ozonation was applied to wastewater without addition of IMI.

In order to find ozone consumption by the organics, unused ozone, escaped ozone amounts and system ozone consumption, which were calculated as aforesaid, were subtracted from influent ozone amount. After calculation of each constituent in the

Eq. (18), amount of ozone consumed by IMI was calculated by conducting experiments with an addition of IMI.

$$X_{\text{inflow}} = X_{\text{organic}} + X_{\text{system}} + X_{\text{unused}} + X_{\text{escaped}} + X_{\text{IMI}} \quad (18)$$

where;

$X_{\text{inflow}}$  : Ozone inflow to system (mg)

$X_{\text{organics}}$ : Ozone consumption by organics in wastewater (mg)

$X_{\text{system}}$  : Self-decomposition (mg)

$X_{\text{unused}}$  : Dissolved and unused ozone in solution (mg)

$X_{\text{escaped}}$  : Unreacted and escaped ozone from the reactor (mg)

$X_{\text{IMI}}$  : Ozone consumption by IMI (mg)

### 3.4.2. Ozonation of IMI

All ozonation experiments were done at room temperature ( $24^{\circ}\text{C} \pm 1^{\circ}\text{C}$ ) with a working volume of 1 L. In order to eliminate possible experimental errors, all the experiments were conducted in duplicate, the average of these results were calculated, and error bars are shown in the figures. Unless otherwise stated, water matrices were buffered by using 0.1 M phosphate buffer and the pH was adjusted at  $7.25 \pm 0.1$ . Throughout the ozonation experiments, samples were withdrawn at 0, 1, 5, 10, 20, 30, 40, 50, 60, 70, 80, 90, 100, 110, 120, 150 and 180 min, if not defined otherwise. Sampling times were purposely selected to observe not only IMI degradation, but also production and removal of degradation by-products, if any. At each sampling times, 15 ml of sample was withdrawn from the reactor for measurement of dissolved ozone (DO), pH, IMI and degradation by-products. While the DPD reagent was immediately added into 5 ml of the sample for the DO measurement, the rest of the sample's pH

was recorded firstly. Then it was urgently quenched with N<sub>2</sub> gas for 5 min to stop the further reaction between IMI and ozone, before the HPLC analysis. This quenching step is crucial to remove any residual ozone and hydroxyl radicals to get more accurate result. After quenching the sample, 0.5 ml of the samples was withdrawn with automatic pipette and was analyzed by HPLC equipped with UV detector in triplicate for quantification of IMI and determination of by-products. For the by-product analysis, selected experiments' samples were stored at most for 14 days in refrigerator at +4 °C in the dark until analysis was performed. The selected experiments are Milli-Q water and VRMBR WW with an initial IMI concentration of 1000 ppb ozonation. Prior to VRMBR WW ozonation experiments, unspiked wastewater samples were withdrawn and analyzed in order to determine IMI concentration and there was not greater IMI concentration than LOD value. Gas washing bottle which has 500 ml of 2% KI solution and 2N H<sub>2</sub>SO<sub>4</sub> was placed next to the reactor to be able to determine escaped ozone amount [208]. At each of aforementioned sampling times, 10 ml of sample was withdrawn from the gas washing bottle and put into Erlenmeyer flasks for iodometric titration.

Before and after each ozonation experiments, the reactor, gas washing bottle, Erlenmeyer flasks, volumetric flasks, graduated glass pipettes and burette were washed with Alconox that was prepared with warm water and were rinsed firstly with tap water, then with pure water and finally rinsed thoroughly with Milli-Q water. At the beginning of each experiment for Milli-Q water and VRMBR WW, desired amount of IMI was spiked from stock solution. The aqueous IMI stock solution with 100 mg/L concentration was prepared by dissolving an accurate quantity of IMI in acetonitrile in 250-ml borosilicate glass volumetric flask. Once the IMI stock solution was added into the reactor, in order to get homogeneous solution, firstly the top of the reactor was closed with parafilm and then the reactor was shaken upside down for several times.

### **Effect of Buffer**

For the investigation of phosphate buffer effects on the ozonation, experiments were conducted with and without buffer. Ozonation experiments were performed at constant ozone dose of 2400 mg/h and ozone concentration of 24 mg/L in 1 L of Milli-Q water that was spiked with 500 ppb IMI. While the unbuffered experiment was maintained without adding any buffer solution, buffered experiments were conducted with 0.1 M phosphate buffer addition and the pH was adjusted at  $7.25 \pm 0.1$ . The pH of the solution was also measured during the experiment. The further experiments were conducted at buffered conditions.

### **Effect of pH**

The effect of pH on the IMI degradation was performed at three different pHs of 6.20, 7.30 and 8.25 in 1 L of Milli-Q water. The constant ozone dose of 1200 mg/h that correspond to 40 mg/L ozone concentration and constant 500 ppb IMI concentration were applied in these experiments. The desired pHs were attained by using 0.1 M phosphate buffer solution and pH was measured at each sampling times during the experiments.

### **Effect of Ozone Dose**

Throughout determination of optimum ozone dose, ozonation of IMI was conducted at three different ozone doses in Milli-Q water. Ozone doses of 600, 1200 and 1800 mg/h were applied for 180 min at constant flowrate of 30 L/h with corresponding ozone concentrations of 20, 40 and 60 mg/L, respectively. In these experiments the initial IMI concentration was kept same (500 ppb) and it was achieved with the spike of IMI into 1 L of Milli-Q water. During the 180 min ozonation of water, not only IMI degradation, but also production and removal of degradation by-products were observed. The further experiments were performed at ozone dose of 1200 mg/h.

### **Effect of Ozone Gas Flowrate**

Prior to ozonation experiments, the optimum flowrate was determined. The aim was to figure out effect of ozone flowrate on the degradation of IMI and solubility of ozone in the water. By keeping the ozone dose constant (1200 mg/h), three different ozone gas flow rates as 15 L/h, 30 L/h and 100 L/h were conducted in 1 L of Milli-Q water that was spiked with 500 ppb IMI. To get desired amount of ozone dose, while the flowrate button was adjusted to 15 L/h, 30 L/h and 100 L/h, the potentiometer was set to 4.1, 3.4 and 2.5, respectively. These ozone flowrates were selected according to gas flowrates indicated at ozone generator's performance curve (Appendix A). The further experiments were conducted at optimum flowrate determined by this experiment.

### **Effect of Initial IMI Concentration**

Another ozonation experiments were carried out to understand the effect of initial IMI concentration on the degradation. In this respect, by keeping the ozone dose constant at 1200 mg/h, three different initial IMI concentrations, which were 100 ppb, 500 ppb and 1000 ppb, were investigated. The desired initial IMI concentrations were attained with a spike from IMI stock solution into 1 L of Milli-Q water. For the by-product analysis, samples of 1000 ppb IMI at the sampling times of 5, 70, and 180 min were further analyzed by the LC-MS/MS.

### **Effect of Water Matrix**

Subsequently, in addition to Milli-Q water, two wastewater matrices (i.e. VRMBR and Bio WW) were ozonated separately in order to comprehend effect of wastewater matrix on the IMI and by-product removal. The ozonation of VRMBR WW was performed in duplicate at ozone dose of 1200 mg/h at  $\text{pH } 7.25 \pm 0.1$ . Higher IMI concentration (i.e. 1000 ppb) than previous experiments (i.e. 500 ppb) was spiked into the reactor to detect not only IMI but also ozonation by-products, if any by LC-

MS/MS. Before the experiment, the wastewater was filtered through 0.45  $\mu\text{m}$  filter and sampling was done as aforesaid sampling times. For the by-product analyses, samples that were taken at 5, 90, and 180 min were further analyzed by the LC-MS/MS. Secondly, biologically treated wastewater was ozonated at ozone dose of 1200 mg/h without any IMI addition and further filtration.

### **3.4.3. Photo-ozonation ( $\text{O}_3/\text{UV}$ ) of IMI**

After determination of optimum ozone dose, ozone gas flowrate and pH at ozonation experiments,  $\text{O}_3/\text{UV}$  experiments were conducted in order to increase degradation efficiency of IMI and by-products, if any. All  $\text{O}_3/\text{UV}$  experiments were done at ozone dose of 1200 mg/h and ozone gas flowrate of 30 L/h with 1000 ppb initial IMI concentration and at constant temperature ( $24^\circ\text{C} \pm 0.1^\circ\text{C}$ ) with a working volume of 1 L. In order to get homogeneous solution throughout the experiments, the reactor was continuously stirred by magnetic stirrer at 600 rpm. Unless otherwise stated, water matrices were buffered by using 0.1 M phosphate buffer and the pH was adjusted at  $7.25 \pm 0.1$ . In order to eliminate possible experimental errors, all the experiments were conducted in duplicate, the average of these results were calculated, and error bars were shown in the figures. During the  $\text{O}_3/\text{UV}$  experiments, samples were withdrawn at 0, 1, 3, 5, 10, 20, 30, 40, 50 and 60 min, if not defined otherwise. Sampling times were purposely selected to observe not only IMI degradation, but also production and removal of degradation by-products, if any. As stated in the ozonation experiments, sampling for dissolved ozone (DO), pH, IMI and degradation by-products measurement, was performed in the same manner with the ozonation experiments. At each sampling times, 15 ml of sample was withdrawn from the reactor for measurement of DO, pH, IMI and degradation by-products.

While the DPD reagent was immediately added into 5 ml of the sample for the DO measurement, the rest of the sample's pH was recorded firstly. Then it was urgently quenched with  $\text{N}_2$  gas for 5 min to stop the further reaction between IMI and ozone,

before the HPLC analysis. This quenching step is crucial to remove any residual ozone and hydroxyl radicals to get more accurate result. After quenching the sample, 0.5 ml of the samples was withdrawn with automatic pipette and was analyzed by HPLC equipped with UV detector in triplicate for quantification of IMI and determination of by-products. For the by-product analysis, selected experiments' samples were stored at most for 14 days in refrigerator at +4 °C in the dark until analysis was performed. The selected experiments are Milli-Q water and VRMBR WW with an initial IMI concentration of 1000 ppb O<sub>3</sub>/UV experiments. Prior to VRMBR WW O<sub>3</sub>/UV experiments, unspiked wastewater samples were withdrawn and analyzed in order to determine IMI. Gas washing bottle which has 500 ml of 2% KI solution and 2N H<sub>2</sub>SO<sub>4</sub> was placed next to the reactor to be able to determine escaped ozone amount [208]. At each of aforementioned sampling times, 10 ml of sample was withdrawn from the gas washing bottle and put into Erlenmeyer flasks for iodometric titration with 0.025 M Na<sub>2</sub>S<sub>2</sub>O<sub>3</sub>.

Before and after each O<sub>3</sub>/UV experiment, the reactor and all other used glassware was washed and rinsed as stated in the ozonation experiments. At the beginning of each experiment for Milli-Q water and VRMBR WW, desired amount of IMI was spiked from stock solution to get 1000 ppb initial IMI concentration. The same aqueous IMI stock solution (100 mg/L), this is previously stated in the ozonation experiments, was used. Once the IMI stock solution was added into the reactor, in order to get homogeneous solution, the solution was magnetically stirred for 10 min at 600 rpm. For the Bio WW, additional IMI was not spiked, and existing IMI was subjected to degradation.

### **Effect of Wastewater Matrix**

For the O<sub>3</sub>/UV experiments, firstly Milli-Q water with 1000 ppb IMI initial concentration was used in order to eliminate any matrix effect. After that, O<sub>3</sub>/UV applied to the two wastewater matrices (i.e. VRMBR WW and Bio WW) in order to



understand matrix effect on the removal of both IMI and by-products. The purpose of conducting experiments with 1000 ppb initial IMI concentration is to get enough by-product amount to further analysis with LC-MS/MS. The O<sub>3</sub>/UV application to VRMBR WW was performed in duplicate at ozone dose of 1200 mg/h and 1000 ppb initial IMI concentration. Before the experiment, the wastewater was filtered through 0.45 µm filter and sampling was done as aforesaid sampling times. For the by-product analysis, both Milli-Q water and VRMBR WW samples that were taken at 5, 10 and 60 min were further analyzed by the LC-MS/MS. These sampling times are intentionally selected to observe IMI degradation and by-products' both production and degradation. Secondly, O<sub>3</sub>/UV was applied to biologically treated wastewater was at ozone dose of 1200 mg/h without any IMI addition and further filtration. All experiments were done at pH 7.25 ± 0.1 by stabilizing the pH by phosphate buffer.

#### **3.4.4. Hydroxyl Radical Analysis for Ozonation and O<sub>3</sub>/UV**

##### **Tert-butanol (TBA) Addition**

In order to establish the influence of radical pathway on the ozonation and O<sub>3</sub>/UV experiments, tert-butanol (TBA) was presented in 1L of Milli-Q water. TBA is a well-known OH• scavenger which quickly reacts with OH• but reacts slowly with O<sub>3</sub> (k= 0.001 M<sup>-1</sup>s<sup>-1</sup>) [209]. Therefore, TBA is mainly degraded by O<sub>3</sub> instead of OH•.

In the ozonation experiments, at ozone dose of 1200 mg/h, which correspond to 40 mg/L ozone concentration, and constant 500 ppb IMI concentration, was conducted with and without TBA addition. At pH 7.25 ± 0.1 and temperature 24°C ± 1°C, 100 mM TBA was spiked into the Milli-Q water to inhibit OH• reactions. Sampling was done at 0, 1, 5, 10, 20, 30, 40, 50, 60, 70, 80, 90, 100, 110, 120, 150 and 180 min. IMI was analyzed by HPLC equipped with UV detector in triplicate for quantification. In order to eliminate possible experimental errors, all the experiments were conducted in

duplicate, the average of these results were calculated, and error bars are shown in the relevant figures.

In the O<sub>3</sub>/UV experiments, UV light was applied in addition to 1200 mg/h ozone dose and 500 ppb IMI concentration. Since UV irradiation enhances OH• production, in order to inhibit OH• adequately, more TBA than as the case with ozonation experiments were added. The 200 mM of TBA was introduced into Milli-Q water at pH 7.25 ± 0.1 and temperature 24°C ± 0.1°C to investigate OH• effect on IMI degradation. Samples were withdrawn at 0, 1, 5, 7, 10, 20, 30, 40, 50 and 60 min.

### **P-chlorobenzoic Acid (pCBA) Addition**

In order to measure OH• concentration pCBA was used as a probe compound. The reaction rate of pCBA with ozone is very low ( $k < 0.15 \text{ M}^{-1}\text{s}^{-1}$ ), whereas its reaction rate with OH• is significantly high ( $k = 5.2 \times 10^9 \text{ M}^{-1}\text{s}^{-1}$ ) [210]. Indeed, consumption of OH• by pCBA gives significant understanding about the indirect degradation process.

Therefore, consumption of OH• during ozonation and O<sub>3</sub>/UV experiments were investigated in order to evaluate indirect reaction kinetics of IMI with OH•. For both ozonation and O<sub>3</sub>/UV experiments, 5 μM pCBA was spiked into the Milli-Q water to monitor OH• reactions at pH 7.25 ± 0.1 and temperature 24°C ± 1°C. The ozone dose of 1200 mg/h, which correspond to 40 mg/L ozone concentration was applied. Sampling was performed at 0, 1, 5, 10, 20, 30, 40, 50 and 60 min. In order to eliminate possible experimental errors, all the experiments were conducted in duplicate, the average of these results were calculated, and error bars are shown in the relevant figures. pCBA was analyzed by HPLC equipped with UV detector in triplicate for quantification.

### 3.5. Analytical Methods

#### 3.5.1. IMI Measurement

Analysis of IMI and degradation by-products were performed via Agilent 1200 high-performance liquid chromatograph (HPLC). HPLC is equipped with (from top to bottom) a 1200 Series vacuum degasser (4-channel vacuum container), a 1200 Series high-pressure binary pump, a 1200 Series autosampler (6-port injection valve unit), a 1260 Infinity II thermostatted column compartment and a 1260 Infinity II variable wavelength UV detector (Figure 16). Data acquisition and processing were performed with the Chemstation software.



Figure 16. Agilent HPLC

HPLC method properties are given in Table 7. The elution was performed under the gradient conditions, where A is acetonitrile (ACN) and B is Milli-Q water (Table 8).

Table 7. Properties of IMI detection method in the HPLC

<b>HPLC Brand</b>	Agilent 1200 Series
<b>Column Properties</b>	ZORBAX Rapid Resolution Eclipse Plus C18 column (4.6 × 100 mm, 3.5-μm particle size)
<b>Detector Type</b>	UV Detector
<b>Wavelength</b>	270 nm
<b>Injection Volume</b>	20 μL
<b>Column Oven Temperature</b>	30 °C
<b>Mobile Phase</b>	ACN and Milli-Q water
<b>Flowrate</b>	0.5 ml/min
<b>Retention Time of IMI</b>	~6.30 min

Table 8. HPLC gradient conditions for IMI

<b>Time (min)</b>	<b>A (ACN)</b>	<b>B (Milli-Q Water)</b>	<b>Flow rate (ml/min)</b>
0.0	20	80	0.5
0.1	20	80	0.5
4.0	50	50	0.5
7.0	20	80	0.5
10.0	20	80	0.5

The aqueous stock solution of IMI (100 mg/L) was prepared by dissolving an accurate quantity of IMI in acetonitrile (ACN) in 250-ml borosilicate glass volumetric flask, protected from light and stored at +4 °C in the dark. Different standard solutions of IMI with concentration range from 5 to 1000 μg/L were prepared by dilution of IMI stock solution (100 mg/L) with Milli-Q water. Ten-point calibration curve was generated by injecting standard solutions with concentrations of 1000, 800, 600, 500, 400, 200, 100, 50, 10 and 5 μg/L. As seen in Figure 17, calibration curve with a coefficient of determination value of 0.9998 was obtained. The  $R^2 > 0.99$  was considered satisfactory and hence high linearity was observed.

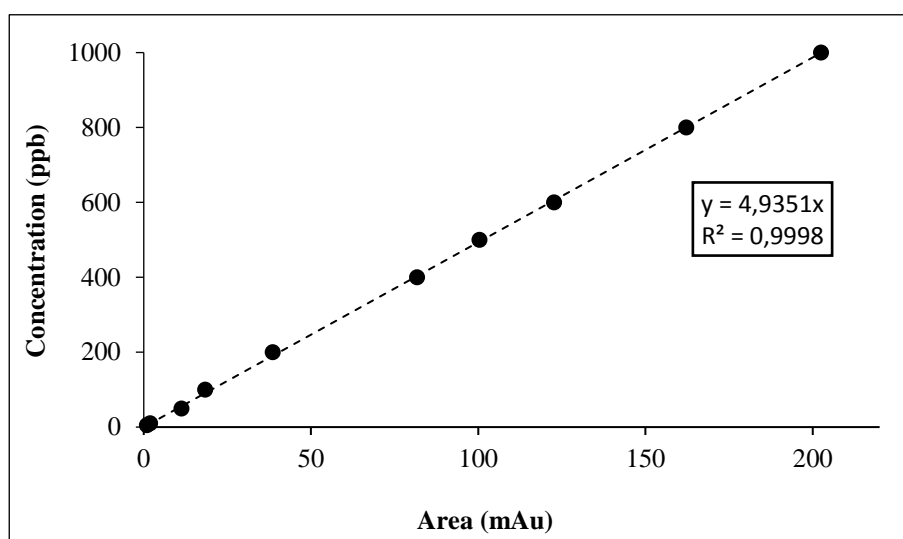


Figure 17. Calibration curve for IMI

### 3.5.2. HPLC Method Development

While the development of HPLC method, not only IMI but also by-products were taken into consideration. Therefore, the HPLC method was developed to get high efficiency and excellent peak shapes for both IMI and by-products and good separation between them. For that purpose, several HPLC methods were tested with various flowrates, column temperatures, injection volumes and gradient ratios. In all tried HPLC methods, wavelength chosen as 270 nm, the column oven was kept at 30 °C and the injection volume was 20  $\mu$ L. For the all elution methods, A and B represent ACN and Milli-Q water, respectively. Performed HPLC methods are summarized in Table 9.

Table 9. HPLC method optimization for both IMI and by-products

<b>Injection Volume</b>	<b>Oven Temp.</b>	<b>Elution condition</b>	<b>Flow rate (ml/min)</b>	<b>A-B % (v,v)</b>	<b>Separation Performance</b>
20 $\mu$ L	30 $^{\circ}$ C	Isocratic	0.75	50:50	Good for IMI Poor for by-products
20 $\mu$ L	30 $^{\circ}$ C	Isocratic	0.50	50:50	Poor for both IMI and by-products
20 $\mu$ L	30 $^{\circ}$ C	Gradient	0.40	t=0 min, A-B (30:70); t=4.0 min, A-B (50:50)	Good for IMI Poor for by-products
20 $\mu$ L	30 $^{\circ}$ C	Gradient	t=0 min, 0.5 ml/min; t=2.5 min, 0.75 ml/min	t=0 min, A-B (30:70); t=2.5 min, A-B (50:50)	Poor for both IMI and by-products
20 $\mu$ L	30 $^{\circ}$ C	Gradient	0.50	t=0 min, A-B (20:80); t=0.1 min, A-B (20:80); t=4 min, A-B (50:50); t=7 min, A-B (20:80); t=10 min, A-B (20:80).	Excellent for both IMI and by-products

### 3.5.3. LOD and LOQ Determination

The aim of the analytical methods is to supply accurate, reliable and consistent data. Therefore, external impacts and method limitations must be determined. For this reason, “validation” plays significant role in providing proper results. Validation includes several parameters like statistical, operating and economical [211]. Limit of Detection (LOD) and Limit of Quantification (LOQ) are two fundamental validation terms in analytical measurements [212].

LOD is the minimum concentration that can be trustworthily distinguished from background noise signal, with a 5% significance level. If the analyte concentration is <LOD, then it would create uncertainty. Hence, it must be mentioned as “concentration is less than LOD” instead of “concentration is zero”. The LOQ is the minimum concentration that can be quantitatively determined with an acceptable accuracy and precision [211].

In this study, during LOD and LOQ determination, ANOVA statistical method was applied with the help of ten-point calibration curve. LOD and LOQ were calculated and found as 5 and 16.9 µg/L, respectively.

#### 3.5.4. pCBA measurement

pCBA analysis were performed via Agilent 1200 HPLC with a reverse phase C18 column (ZORBAX Rapid Resolution Eclipse Plus; 4.6 × 100 mm, 3.5 µm) and a UV wavelength detector. Further properties for HPLC method are given in Table 10.

Table 10. pCBA detection method in the HPLC

<b>HPLC Brand</b>	Agilent 1200 Series
<b>Column Properties</b>	ZORBAX Rapid Resolution Eclipse Plus C18 column (4.6 × 100 mm, 3.5-µm particle size)
<b>Detector Type</b>	UV Detector
<b>Wavelength</b>	240 nm
<b>Injection Volume</b>	100 µL
<b>Column Oven Temperature</b>	30 °C
<b>Mobile Phase</b>	60% Methanol; 40% Milli-Q water (10 mM phosphoric acid)
<b>Flowrate</b>	1 ml/min

The aqueous stock solution of pCBA (100 mg/L) was prepared by dissolving an accurate quantity of pCBA in methanol in 100-ml borosilicate glass volumetric flask,

protected from light and stored at +4 °C in the dark. Quantification was performed using eight-point, linear calibration curve for each solution in the concentration range of 5-1000 µg/L. As seen in Figure 18, the calibration curve with a coefficient of determination value of 0.9918 was obtained. The  $R^2 > 0.99$  was considered satisfactory and high linearity was observed.

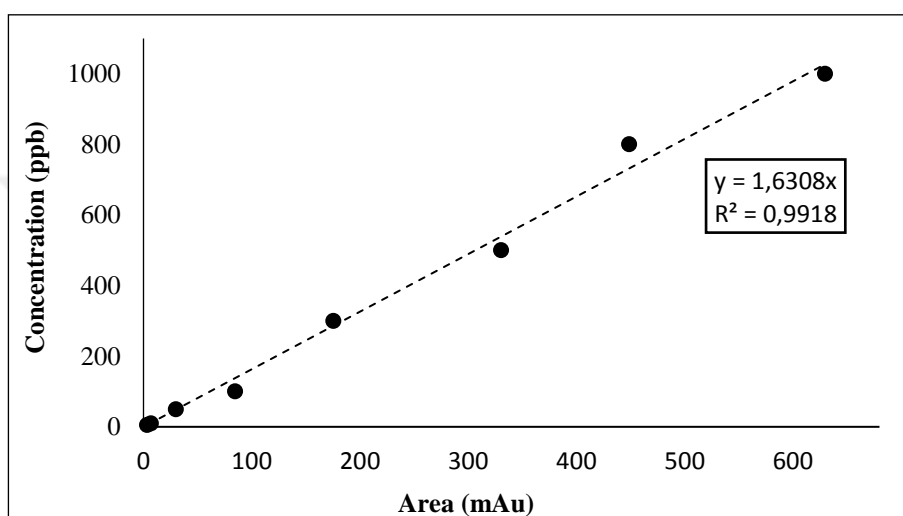


Figure 18. HPLC Calibration curve for pCBA

### 3.5.5. Ozone Measurement

Ozone that comes from generator passes through the reactor. Ozone in the reactor is either dissolved in the water and used by the IMI and by-products or dissolved in the water but are not consumed by the pollutants. The former one is named as ozone consumption by IMI, the latter one is named as unused ozone. Unused ozone represents the portion of ozone that was dissolved but not used by the IMI. The amount of unused ozone in water medium was determined with addition of N,N-diethyl- p-phenylenediamine (DPD) Free Chlorine Reagent Powder Pillows into the 5 ml of sample. Oxidizer in the water sample gives reaction with the DPD and the color changes from clear to pink. The more oxidizer presents in the water; the darker pink



color appears. The dissolved ozone concentration was measured spectrophotometrically via Hach pocket colorimeter by using method 10069. Although DPD colorimetric method is a well-known method to determine chlorine, any oxidant in the water can be measured by that method. This method can be applied by using test kits and it is fast and straight forward [213-215]. Some portion of ozone escaped from the reactor and comes in gas washing bottle that contains 500 ml of 2% KI and 5 ml of 2N H<sub>2</sub>SO<sub>4</sub>. 10 ml of samples were withdrawn at aforesaid sampling times from the gas washing bottle and put into the Erlenmeyer flasks. In order to measure the escaped ozone amount, the liberated iodine in the sample was titrated with 0.025 M Na<sub>2</sub>S<sub>2</sub>O<sub>3</sub> using a starch indicator [208]. The volume of titrant was used to calculate escaped ozone amount.

### **3.5.6. By-Products' Determination**

The LC-MS/MS analyses of possible by-products produced during ozonation and O<sub>3</sub>/UV processes were conducted by METU Central Laboratory, Molecular Biology and Biotechnology Research and Development Center, Mass Spectroscopy Laboratory (Ankara, Turkey). These possible by-products were analyzed by AGILENT 6460 Triple Quadrupole System (ESI+Agilent Jet Stream) coupled with AGILENT 1200 Series HPLC. Further information and operating parameters of LC-MS/MS are given Appendix B. The selection of fragmentation of ions for LC-MS/MS analyses were coordinately conducted. Prior to LC-MS/MS analyses, IMI and by-products screened at both positive and negative ESI modes. Since the IMI and by-products were better observed at the positive mode than the negative mode, further analyses conducted at ESI positive mode. The 3 different samples for each treatment processes for both Milli-Q and VRMBR WW were analyzed by LC-MS/MS. The details of the selected samples were given in Table 11.

Indeed, the first sampling time represents the beginning of the treatment processes and includes IMI with some possible by-products. The second sampling time depicts the

treated IMI (i.e. <LOD) and possible by-products. The last sampling time shows the end of the treatment processes.

Table 11. Selected samples for analysis of possible by-products

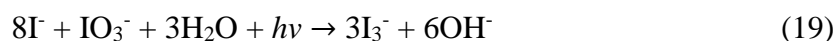
	Sampling Times (min)					
	Milli-Q Water			VRMBR WW		
<b>O<sub>3</sub></b>	5	70	180	5	90	180
<b>O<sub>3</sub>/UV</b>	5	10	60	5	10	60

### 3.5.7. pH Measurement

The pH was measured via Hach HQ40D portable multimeter (Hach, USA) during both ozonation and O<sub>3</sub>/UV experiments.

### 3.5.8. UV Light Intensity Determination via KI/KIO<sub>3</sub> Actinometer

Prior to the O<sub>3</sub>/UV experiments, in order to determine UV light intensity and quantum yield ( $\phi_{tri}$ ), iodide-iodate (KI/KIO<sub>3</sub>) actinometer was applied. The KI/KIO<sub>3</sub> actinometer is reliable and timesaving method since it takes less than 2 hours to complete [216]. The following photochemical reaction takes place during the KI/KIO<sub>3</sub> actinometer [217];



Triiodide complex (3I<sub>3</sub><sup>-</sup>), photoproduct of the above equation, can be easily analyzed at 352 nm due to its maximum spectral absorption. Another advantage of this actinometer method is easily applicable at room light since it is unimpressionable that

UV irradiation range (i.e.  $\lambda > 320$  nm). The molar absorptivity ( $\epsilon$ ) of  $I_3^-$  is given as  $2.76 \times 10^4$  L/mole.cm at 352 nm [218].

In the actinometry experiment, 99.6 g KI, 21.4 g  $KIO_3$  and 2.0122 g  $Na_2B_4O_7$  were put into the same 1 L of Milli-Q water to get 0.6 M KI, 0.1 M  $KIO_3$  and 0.01 M  $Na_2B_4O_7$  solution. The same reactor which was also performed during  $O_3/UV$  experiments was used since the geometry of the reactor affects UV light intensity. UV lamp with 10-Watt power was placed into the center of the reactor. In order to obtain homogeneous solution, the reactor was continuously stirred by magnetic stirrer at 600 rpm during the experiments. The samples were withdrawn at 0, 60, 120, 180, 240, 300, 360, 420, 480 and 540 seconds.

The absorbance values of the samples obtained from spectrophotometer (Hach 3900) were multiplied with molar absorptivity ( $\epsilon$ ) and they were plotted against time (Figure 19). Thus, the slope of the graph (i.e. 1.2422) shown in Figure 19 gives concentration of  $I_3^-$  ( $\mu M$ ) per unit time (i.e.  $C_{tri}/t$ ).

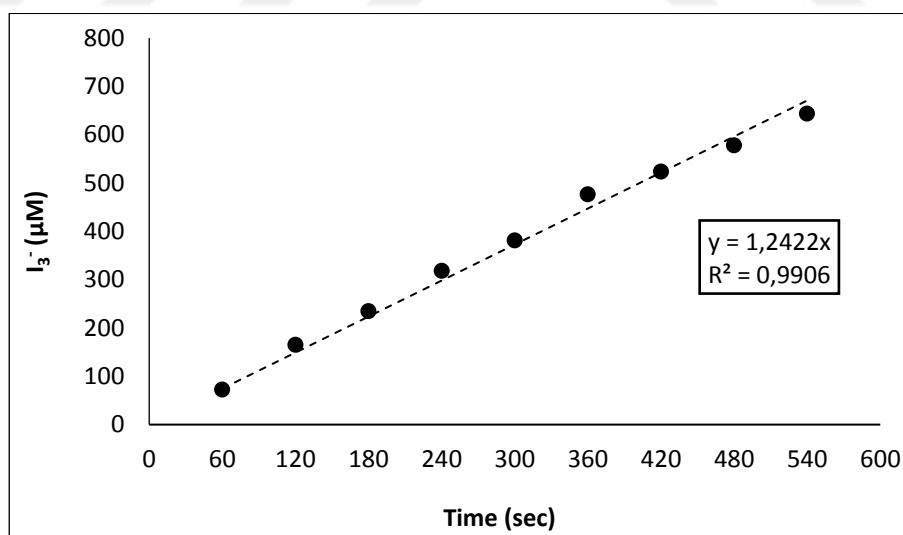


Figure 19. Time course variation of absorbance of  $I_3^-$  at 352 nm

Quantum yield of  $I_3^-$  ( $\Phi_{tri}$ ) for KI/KIO<sub>3</sub> actinometer (at 253.7 nm, 20°C) was calculated according to below equation [216].

$$\Phi_{tri} = (0.71 \pm 0.02) + (0.0099 \pm 0.0004) * (t - 24) \quad (20)$$

In the Eq. (20), t is the solution temperature with a unit of °C. Since the experiment performed at 24 °C,  $\Phi_{tri}$  was found as 0.71. Then, photon flux,  $I_0$ , was calculated according to below equation [219].

$$I_0 = C_{tri} * V * \frac{1}{\Phi_{tri}} * \frac{1}{t} \quad (21)$$

where;

$I_0$ : Photon flux ( $\mu$ Einstein/s)

$C_{tri}$ : Concentration of  $I_3^-$

V: Volume (L)

$\Phi_{tri}$ : Quantum yield of  $I_3^-$

t: time

As mentioned before,  $C_{tri}/t$  was obtained from slope of the  $I_3^-$  vs. time graph (Figure 19).  $\Phi_{tri}$  was also found as 0.71. Thus,  $I_0$  was obtained as 1.7496  $\mu$ Einstein/s.

$$\text{Avg. Intensity} = \frac{I_0}{\pi * r^2} \quad (22)$$

Average UV light intensity per unit area was calculated by above equation. The average UV light intensity was obtained as  $12.2 \times 10^{-3}$   $\mu$ Einstein/cm<sup>2</sup>.s.

### 3.6. Chemicals Used

Analytical grade standard of IMI (99.9%) was purchased from Dr. Ehrenstorfer GmbH (Augsburg, Germany). DPD free chlorine reagent powder pillows (for 25 ml sample) were obtained from Hach. Potassium iodide ( $\geq 99\%$  purity), potassium iodate ( $\geq 99.7\%$  purity), sodium thiosulphate pentahydrate ( $\geq 99.5\%$  purity), starch (iso reagent), tert-butanol ( $\geq 99.5\%$  purity), sulfuric acid (95-98% purity), potassium dihydrogen phosphate ( $\geq 99.5\%$  purity), dipotassium hydrogen phosphate ( $\geq 98\%$  purity), acetonitrile (gradient grade for liquid chromatography,  $\geq 99.9\%$  purity) were purchased from Merck (Darmstadt, Germany). P-chlorobenzoic acid (pCBA,  $\geq 99\%$  purity) was obtained from Sigma-Aldrich (Germany). Milli-Q (Type 1) water and pure water (Type 3) were prepared using Merck Millipore Milli-Q A10 ultra-pure water purification system (Darmstadt, Germany) and RiOs Essential 16 water purification system (Darmstadt, Germany), respectively.



## CHAPTER 4

### RESULTS AND DISCUSSION

#### 4.1. Ozonation of IMI

In this chapter, the results obtained from the experiments conducted are provided and discussed in the light of similar literature studies in order to have a deeper understanding about the ozonation of IMI. To this purpose, effect of buffer, pH, ozone dose, ozone gas flowrate, initial IMI concentration and water matrix, reaction kinetics and possible production pathway of by-products are presented and discussed explicitly in the following sections.

##### 4.1.1. Effect of Buffer

In several studies conducted with ozonation process, pH decrease during ozonation were observed due to ozone degradation mechanism [21,220,221]. In the light of these studies, the ozone decomposition rate highly depends on solution pH and it eventually affects micropollutant degradation. For that reason, effect of buffer was studied primarily. The pH of the solution in the reactor was continuously measured throughout the ozonation experiments in order to understand whether a buffering is needed or not. To this purpose, when an unbuffered Milli-Q water solution spiked with IMI was ozonated, it was observed that its initial pH of 7.7 decreased continuously and reached to 4.4 at the end of 180 min. Similarly, the pH of Milli-Q water without IMI also decreased from 7.4 to 6.3 during 180 min of ozonation as can be seen from Figure 20. For the investigation of phosphate buffer effects on the IMI degradation, experiments were presented with or without buffer and results are shown in Figure 21.

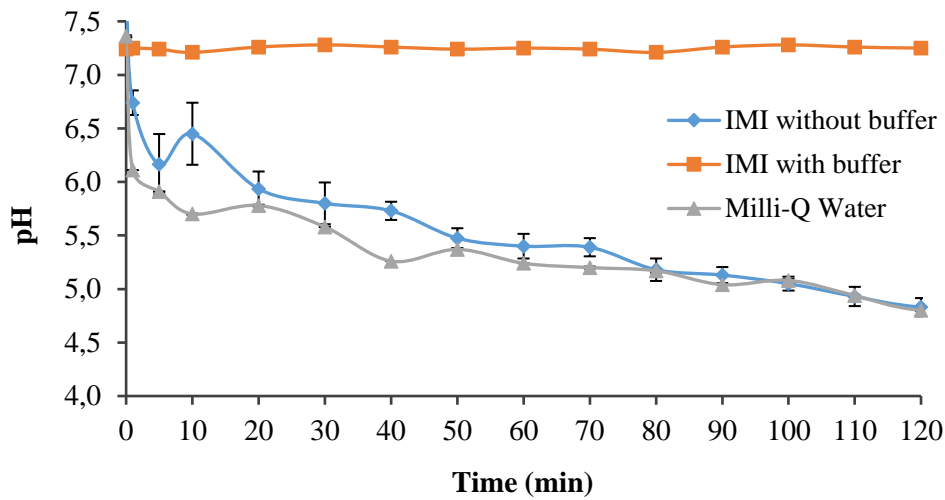


Figure 20. Variation of solution pH during the ozonation with and without buffer addition (Milli-Q water, O<sub>3</sub> dose= 2400 mg/h, O<sub>3</sub> flowrate= 100 L/h, C<sub>0</sub>= 500 ppb, T =24°C ±1°C.)

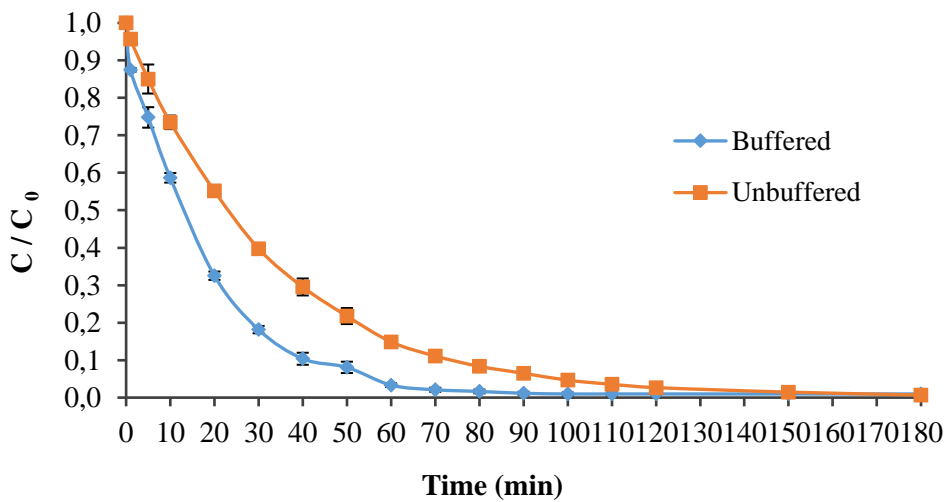


Figure 21. Degradation of IMI with and without buffer addition. (Milli-Q water, O<sub>3</sub> dose= 2400 mg/h, O<sub>3</sub> flowrate= 100 L/h, C<sub>0</sub>= 500 ppb, T =24°C ±1°C.)



As seen in Figure 20, not only Milli-Q water with IMI but also the one without IMI experienced a decrease in pH with time. Therefore, the consumption of  $\text{OH}^-$  was evident even when there is no IMI in the medium. Indeed, one should expect this to observe as  $\text{OH}^-$  will be consumed during the initiation reaction of ozonation as indicated in Eq. (1). Accordingly, pH of the solution will decrease due to the concentration of  $\text{OH}^-$  lessened.

The ozone decomposition boosts at basic condition since  $\text{OH}^-$  will be more readily available, and ozone and  $\text{OH}^-$  reacts in order to initiate the generation of  $\text{OH}^\bullet$  [222]. Throughout the experiments, since there was relatively higher  $\text{OH}^-$  concentration in the buffered solution (at  $\text{pH } 7.25 \pm 0.1$ ) as compared to the unbuffered solution, both direct and indirect ozonation reactions occurred in buffered solution. On the other hand, at acidic conditions due to low  $\text{OH}^\bullet$  concentration, direct ozonation mechanism dominates [199]. In other words, the relative lack of  $\text{OH}^\bullet$  indicates that IMI and possible by-products are mainly attacked by ozone at acidic conditions.

When Figure 20 and Figure 21 are examined together, the effect of buffer is evident. As it can be seen in Figure 21, the disappearance of IMI for both buffered and unbuffered solutions were similar at first 5 min of ozonation since the pH difference between buffered and unbuffered solutions was not yet remarkable (Figure 20). This indicates that the ozonation reactions and removal mechanisms reactions were similar for both buffered and unbuffered cases within this time interval. After 5 min, the pH of unbuffered solution decreased dramatically, which led to the decrease of  $\text{OH}^\bullet$  production rate and resulted in the slower degradation of IMI. At the end of 20 min, 67.5% and 44.9% of IMI was degraded in buffered and unbuffered solutions, respectively. Moreover, 40 min of ozonation was enough to remove 90% of IMI in buffered solution, whereas, at least 80 min was required to achieve almost the same percentage of IMI disappearance in unbuffered solution. Based on these findings, it is clear that IMI degradation is a highly pH dependent process and to get a proper understanding of IMI degradation, pH has to be controlled by a buffer solution.

These observations were in accordance with the relevant literature studies. For example, similar results were obtained in case of removal of Thiocloprid, which belongs in the same chemical group with IMI, by ozonation [21]. These results reported by Cernigoj et al. [21] showed that the pH of unbuffered solution declined from 6.2 to 3.2 during 100 min of ozonation due to organic and inorganic acid production. Because of pH decrease, decomposition rate of ozone and in turn, production rate of OH• was lowered. Therefore, the removal efficiency of Thiocloprid was decreased and they did use a pH buffer in their subsequent experiments. In agreement with the foregoing, Restivo et al. [220] observed that during ozonation of Metolachlor, the pH value decreased from 6.7 to 3.9 for semi-batch mode and to 5.0 for continuous mode at the end of the experiments. Because of the ozone decomposition and OH• production rates declined, the degradation of by-products was also slowed down. In a similar study, Lucas et al. [221] performed the treatment of winery wastewater by ozone-based AOPs (O<sub>3</sub>, O<sub>3</sub>/UV and O<sub>3</sub>/UV/H<sub>2</sub>O<sub>2</sub>). The wastewater with three different initial pHs (i.e. pH 4, 7 and 10) were investigated during 300 min of O<sub>3</sub>/UV application. Initial pH of 4 exhibited a negligible decrease so that the final pH was 3.8. On the other hand, in the experiments with the initial pH of 7 and 10, the pH of the solutions decreased sharply to 3.8 and 4.0, respectively. The decrease of the solution pH was attributed to the production of dicarboxylic acids, CO<sub>2</sub> and carbonic acids as a result of the mineralization of organic matter. In our study, although Milli-Q water was used instead of wastewater, decrease of pH from 7.7 to 4.4 was observed which is very similar to results obtained by Lucas et al [221].

The results obtained by Cernigoj et al. [21], Restivo et al. [220] and Lucas et al. [221] revealed that pH decrease may also be due to the formation of acidic intermediates. Accordingly, in our case, the reason of pH decrease might also be due to acidic intermediates formed during the ozonation of IMI. According to Bourgin et al. [22] 6-chloronicotinic acid (C<sub>6</sub>H<sub>4</sub>ClNO<sub>2</sub>), a type of carboxylic acid, was formed during the ozonation of IMI. Although they did not mention whether the pH changed or not, 6-

chloronicotinic acid may be the factor for the pH decrease that was observed during our experiments.

Thus, our results were in agreement with the aforementioned literatures in terms of both observing a pH decrease due to formation of acidic compounds and slowing down the removal of target chemical compound. Cernigoj et al. [21], Restivo et al. [220] and Lucas et al. [221] clearly indicated that the pH of the solution, ozone decomposition and hydroxyl radical production rates are very important parameters, which in turn determine the processes efficiency. Taking into account that ozonation mechanism and degradation efficiency are highly affected by the pH, subsequent experiments were conducted at the presence of pH buffer with a constant initial pH  $7.25 \pm 0.1$ .

#### **4.1.2. Effect of pH**

It is well known that the pH is highly significant during ozone decomposition and production of hydroxyl radicals. As the pH rises, hydroxyl ions trigger the ozone decomposition and the hydroxyl radicals in the solution become higher (Eq. (1)) [189]. Hence, the degradation of IMI is boosted by the increase of hydroxyl radicals in water. At acidic pHs, ozone-based degradation is dominant, on the contrary, at basic pHs hydroxyl radicals contributes to IMI degradation as well. In order to determine the effect of pH on the IMI degradation, 500 ppb IMI spiked into Milli-Q water and 1200 mg/h ozone dose was applied at pHs of 6.20, 7.30 and 8.25. The desired pHs were attained with the use of phosphate buffer solution. The samples were taken at 1, 5, 10, 20, 30, 40, 50, 60, 70, 80 and 90 min, and each sample was analyzed by HPLC for three times in order to observe IMI degradation. During pH 8.25 experiments in addition to aforementioned sampling times, samples at 7 and 15 min were also taken to investigate IMI degradation more precisely. The results obtained are shown in Figure 22.

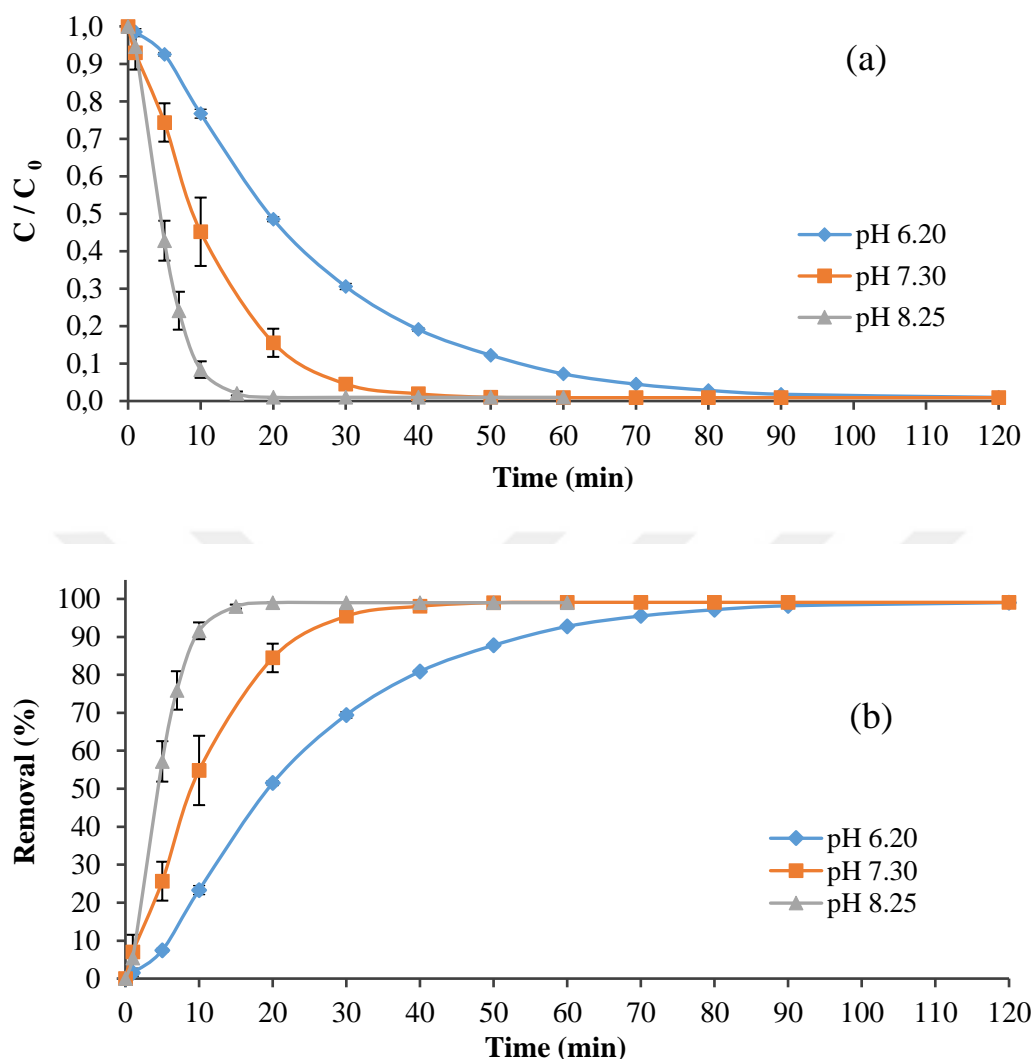


Figure 22. Time course variation of (a) IMI concentration (b) Removal efficiencies at different pHs (Milli-Q water,  $C_0= 500$  ppb,  $O_3$  dose= 1200 mg/h,  $O_3$  flowrate= 30 L/h  $T=24^\circ\text{C} \pm 1^\circ\text{C}$ .)

When these pHs are compared, it can be clearly seen from Figure 22, the highest removal efficiency was achieved at the pH 8.25, whereas the pH 6.20 showed the least removal efficiency. To explain more, during the first 30 min of the ozonation, IMI removal efficiencies were 69%, 95% and 99% at pHs 6.20, 7.30 and 8.25, respectively. Furthermore, 60 min and 20 min were enough to 99% (<LOD) disappearance of IMI

at pHs 7.30 and 8.25, respectively, on the other hand, at least 120 min were required for the same amount of IMI degradation at pH 6.20. The reason might be that  $\text{OH}^-$  has a significant role initiation reaction (Eq. (1)) and chain reaction which produces radicals stated by Staehelin and Hoigne [189]. As concentration of  $\text{OH}^-$  gets higher in alkaline solution, more radicals which also have oxidizing capacity are produced. Therefore, as the pH gets higher (i.e. pH 8.25), IMI removal efficiency increases due to degradation by both ozone and radicals. On the other hand, at low pH value (i.e. pH 6.20), the rate of ozone decomposition and radical formation are very slow. So, degradation of IMI was mainly due to ozone. Cernigoj et al. [21] reported similar results in the case of Thiacloprid removal by ozonation [21]. Thiacloprid is one of the pesticides belongs to neonicotinoid chemical group like IMI. In that study, disappearance rate constant of Thiacloprid was given at different pHs such as 2.75, 5.50, 8.25 and 11.0. Although increase of pH from 2.75 and 5.50 was hardly affect the disappearance rate, after increasing pH from 5.50 to 11.0, the disappearance rate increased almost 8 times.

Another ozonation study conducted to degrade two pesticides (i.e. Bromoxynil and Trifluralin) by Chelme-Ayala et al. [223] also obtained similar results with our study. For example, at pH 2, 98% of Bromoxynil and 50% of Trifluralin were degraded within 2 and 5 min of ozonation, respectively. This low degradation efficiency also showed that Trifluralin is highly robust to ozone attack since direct reaction dominates at acidic pHs. Trifluralin has high electronegativity since it contains 3 fluorine which eventually results in resistance toward ozone during ozonation process. Moreover, IMI showed similarity to Trifluralin in terms of electronegativity since the IMI has chloropyridine ring which is known as highly electronegative moiety. Therefore, it can be said that at acidic pHs, removal of ozone-resistant chemicals is less efficient since the degradation mainly depends on direct reaction mechanism. On the other hand, at pH 7, although degradation rate of both Bromoxynil and Trifluralin increased, degradation rate differences were more noticeable for Trifluralin [223]. Indeed, the disappearance of IMI also showed significant improvement even at one-unit change

in the pH scale. Therefore, ozone-resistant chemicals are generally found to be highly removable at alkaline conditions with respect to acidic conditions.

Regarding the results of our study and referenced studies, the pH is a significant parameter that effects micropollutant removal efficiency in ozonation. Therefore, the pH of wastewater at the entrance of ozonation unit in the treatment plant should be taken into consideration when implementing the ozonation in the WWTP. Ozonation unit generally placed after biological treatment and secondary effluent of municipal wastewaters generally have pH between 6-9 [224]. On the basis of our findings, wastewaters containing IMI with neutral to basic pH would be treated in relatively shorter time with consuming less ozone amount. Therefore, the treatment of municipal wastewater containing IMI could be notably treatable, especially for higher pH, when implementing the ozonation in the WWTP.

#### **4.1.3. Effect of Ozone Dose**

In this part, it was aimed to investigate how different ozone doses affect the disappearance of IMI and the ozonation by-products and to decide about the required ozone dose for the IMI disappearance. For this purpose, Milli-Q water with 500 ppb of initial IMI concentration was subjected to several ozone doses under buffering conditions. Applying the ozone doses of 600, 1200 and 1800 mg/h, which correspond to 20, 40, 60 mg/L of ozone concentration at a constant ozone flowrate of 30 L/h, results obtained are provided in Figure 23.

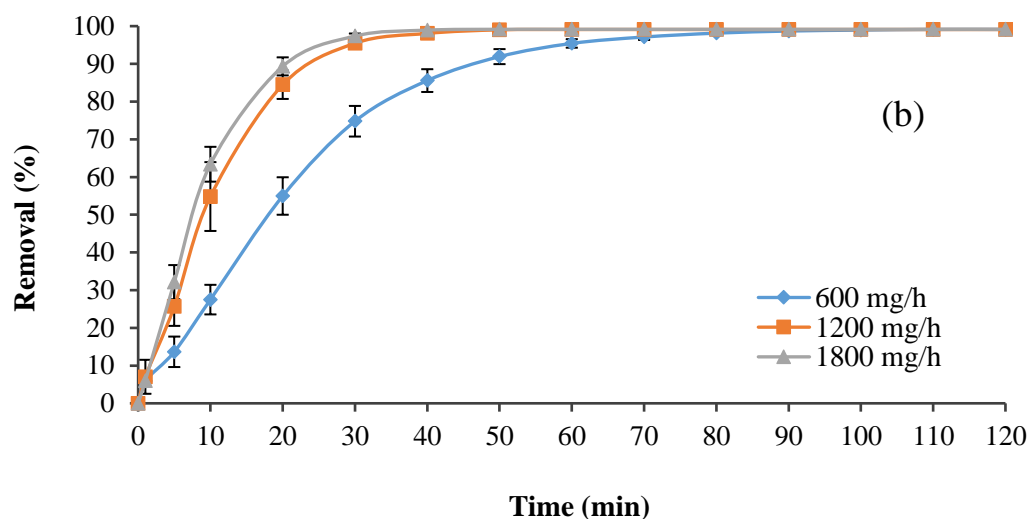
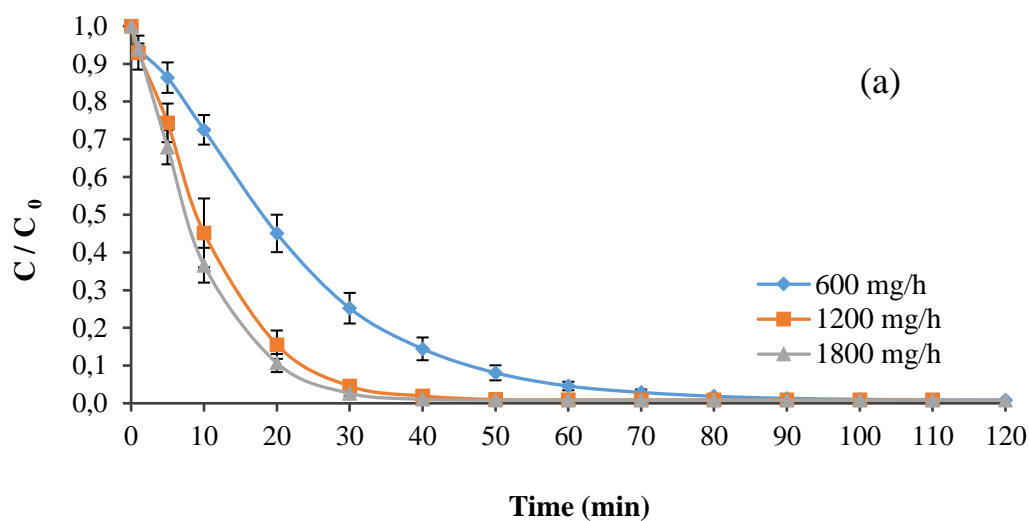


Figure 23. Time course variation of (a) IMI concentration (b) IMI removal efficiency at different ozone doses. (Milli-Q water,  $C_0 = 500$  ppb,  $O_3$  flowrate = 30 L/h,  $pH = 7.25 \pm 0.1$ ,  $T = 24^\circ C \pm 1^\circ C$ .)

In all ozone doses, degradation of IMI was instantly started as the ozone was introduced into the system. As can be seen from the Figure 23, for all ozone doses studies, there occurs two phases of IMI disappearance; a rapid decrease in IMI (at first 10 min), then followed by a gradual decline. The highest initial disappearance rate

(during the first 10 min) was observed at 1800 mg/h, whereas, gradual decline phase took longest time at 600 mg/h of ozone dose. As it can also be depicted from Figure 23, the disappearance of IMI with time was very similar in cases of 1200 and 1800 mg/h, however, the behavior was quite distinct in the case of 600 mg/h. Hence, it can be stated that 1200 mg/h of ozone dose provided a saturation level of ozone and/or hydroxyl radicals, at a flowrate 30 L/h. In accordance, it can be depicted from Figure 23 that 90% of IMI can be degraded within 50, 25 and 20 min, which correspond to 500, 500 and 600 mg of applied ozone amount at 600, 1200 and 1800 mg/h ozone doses, respectively. To clarify, IMI disappearance by at least 90% can be achieved in 25 min for the ozone doses of 1200 and 1800 mg/h, however, 50 min is required to achieve the same removal efficiency for 600 mg/h of ozone dose. Furthermore, 95% of IMI degradation requires 60, 30, 25 min, which correspond to 600, 600 and 750 mg applied ozone amount for 600, 1200 and 1800 mg/h ozone doses, respectively. In other words, different ozone doses necessitated different treatment time.

However, after 95% of IMI degraded, the further degradation process became more difficult and it took almost half of the whole removal time period to achieve >99% disappearance (i.e. <LOD). Initial IMI concentration of 500 ppb was decreased down to below LOD value within 120, 60 and 50 min by applying 600, 1200 and 1800 mg/h ozone doses corresponding to 1200, 1200 and 1500 mg ozone, respectively. On the other hand, half of these process times i.e. 60, 30 and 25 min were necessary additionally to increase the removal efficiency from 95% to 99%, respectively. This observation could be explained due to ozonation of degradation by-products. It is worthy to mention that while the amount of IMI decreases, production of by-products increases. Indeed, the available dissolved ozone was used for both IMI and its by-products ozonation after some treatment time. The consumption of ozone by transformation by-products during ozonation has been also reported by several studies [225,226].



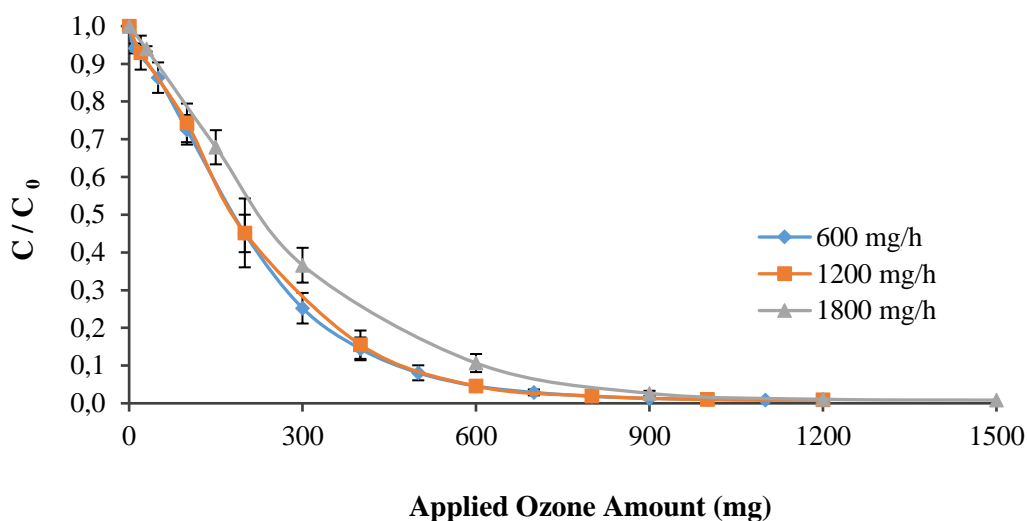


Figure 24. Profile of IMI degradation as a function of applied ozone amount. (Milli-Q water,  $C_0 = 500$  ppb,  $O_3$  flowrate = 30 L/h,  $pH = 7.25 \pm 0.1$ ,  $T = 24^\circ C \pm 1^\circ C$ .)

Figure 24 shows the variation of IMI disappearance as a function of ozone amount applied. It is clearly seen from this figure that removal of IMI highly depends on the applied ozone amount. In order to remove almost all of IMI from the solution, required ozone amount was observed to be 1200, 1200 and 1500 mg when the ozone was applied at 600, 1200 and 1800 mg/h, respectively. As previously mentioned, same amount of ozone was applied to remove same degree of IMI removal in both 600 and 1200 mg/h ozone dose application. Nevertheless, 600 mg/h ozone dose required two times higher degradation time than 1200 mg/h ozone dose application. Moreover, consumed ozone during 600 and 1200 mg/h ozone doses were calculated as 9.3 and 10.1 mg ozone/mg IMI. It clearly showed that almost same amount of ozone was used to degrade 1 mg IMI. Although almost same ozone amount was consumed by 1 mg IMI for 600 and 1200 mg/h ozone doses, when the required times are considered (90 min vs. 30 min, for 600 and 1200 mg/h, respectively; Figure 23), 1200 mg/h ozone dose seems to be more appropriate to apply in practice.

The results presented in Figure 23 indicates that 99% IMI removal was achieved in a shorter time for 1800 mg/h ozone dose application than for the other doses, as expected. This can be explained as, for the same time interval an increase in the ozone dose provides faster removal of IMI since applied ozone amount was higher. However, when 1200 and 1800 mg/h ozone doses were compared, 1200 mg/h ozone dose required only 10 more minutes to remove almost all of IMI. Although removing 99% of IMI by 1200 mg/h ozone dose takes a little bit more time, the applied ozone amount (i.e. 1200 mg) was lower than the one (i.e. 1500 mg) for 1800 mg/h ozone dose. Hence, this proves that after some point, increasing the ozone dose did not affect the removal efficiency dramatically.

The reason for this observation may lie behind the values of reaction rate constants during the production of OH•. Kinetic constant for the initiation reaction between O<sub>3</sub> and OH<sup>-</sup> (Eq. (1)) was determined as 70 M<sup>-1</sup>s<sup>-1</sup> by Staehelin and Hoigne [189]. On the contrary, subsequent radical propagation reactions rate constants are at least five orders of magnitude larger than for Eq. (1). As aforementioned, OH• has very high impact on the removal of IMI. Although ozone dose was increased from 1200 to 1800 mg/h, the OH• formation was not increased proportionally since the initiation reaction (i.e. Eq. (1)) is the rate-limiting step. Therefore, the removal percentage of IMI did not enhance proportionally as ozone dose increase from 1200 mg/h to 1800 mg/h. For that reason, the following experiments were conducted at 1200 mg/h which was chosen as an optimum ozone dose.

It is well known that while the ozonation removes compounds, they are not completely mineralized and are transformed into oxidation products which can be called as by-products [227]. Effect of ozone dose on two by-products detected by HPLC is assessed below. These two by-products were named as By-product-1 (BP-1) and By-product-2 (BP-2) since the exact chemical structures were not known. Profiles of BP-1 and BP-2 with respect to different ozone doses (i.e. 600, 1200 and 1800 mg/h) are presented in Figure 25 and Figure 26, respectively. Although IMI was immediately degraded from first minute of ozonation, by-products did not appear simultaneously.

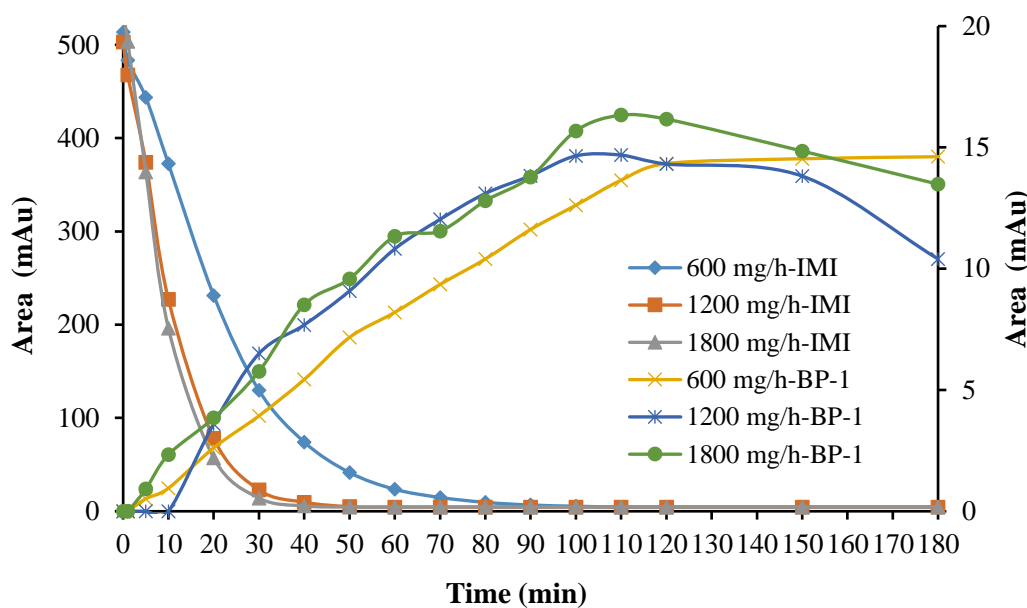


Figure 25. Time course variation of IMI and BP-1 at different ozone doses (Milli-Q water,  $C_0 = 500$  ppb,  $O_3$  flowrate= 30 L/h,  $pH = 7.25 \pm 0.1$ ,  $T = 24^\circ C \pm 1^\circ C$ .)

As seen in Figure 25, in all ozone doses, BP-1 was observed starting from 5<sup>th</sup> min. It reached to its maximum area around 110 min for both 1200 and 1800 mg/h ozone doses whereas; the plateau was not apparently reached within 180 min for 600 mg/h ozone dose. To add more, during ozonation of BP-1, areas obtained in 1200 and 1800 mg/h ozone dose experiments were similar and it may indicate that the increase of ozone dose did not significantly affect the amount formation of BP-1. On the contrary, area of BP-1 at 600 mg/h ozone dose application was relatively smaller than the other ozone doses. To add more, IMI was degraded below LOD value (i.e. 99% disappearance) within 110, 60 and 50 min, for 600, 1200 and 1800 mg/h ozone doses, BP-1 still continued to present during 180 min of ozonation for the same ozone doses.

Similar to BP-1, BP-2 was also presented starting with the 5<sup>th</sup> min (Figure 26). On the other hand, BP-2 reached to its maximum area sooner but having lower area than the BP-1. The data in Figure 26 apparently indicates that as the ozone doses were increased, BP-2 reached to its maximum area faster and started to lessen proportional

to ozone doses. BP-2 was almost not detected after 150 min of ozonation for 1200 and 1800 mg/h ozone doses; on the other hand, 180 min was not enough to remove almost all of BP-2 for 600 mg/h ozone dose.

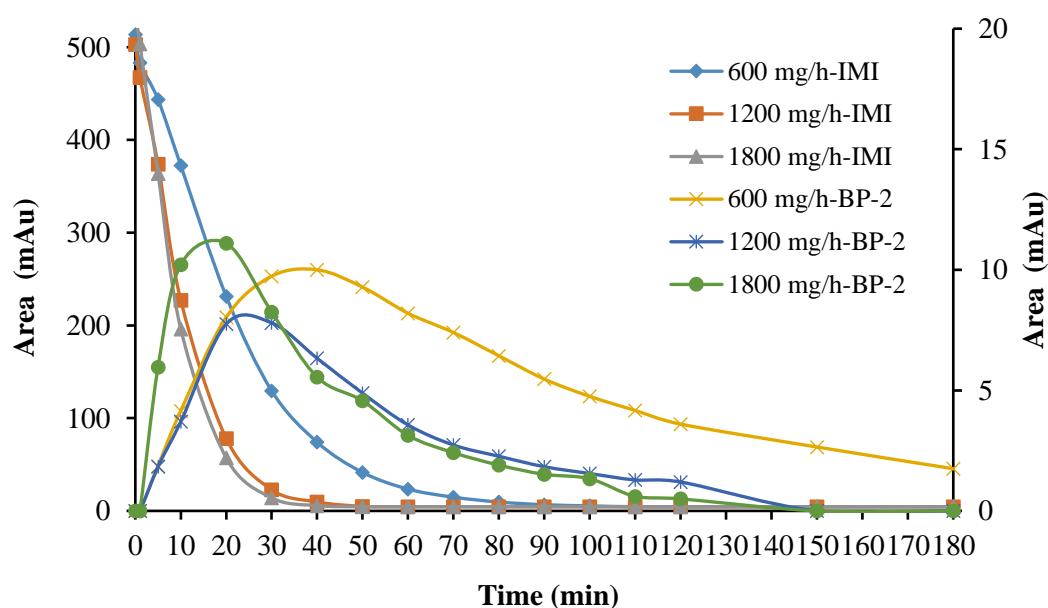


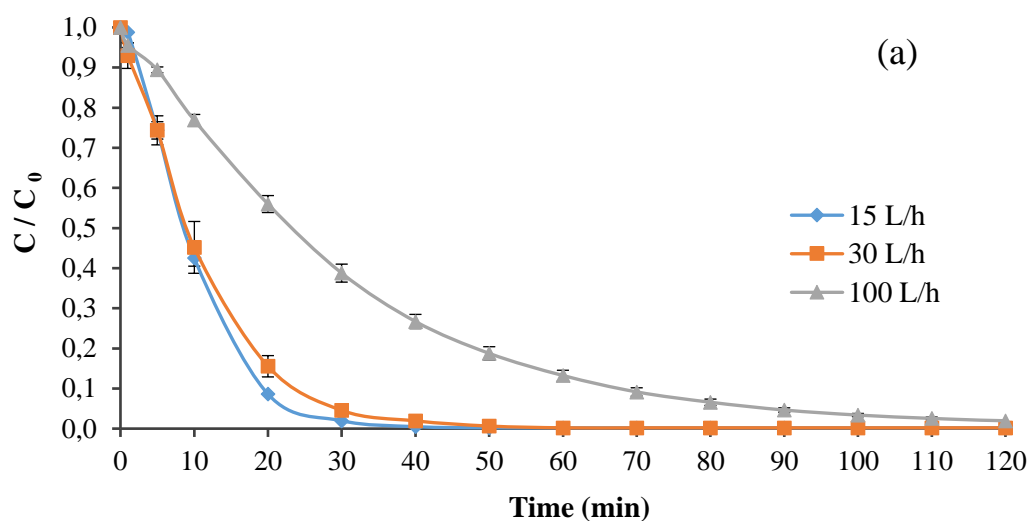
Figure 26. Time course variation of IMI and BP-2 at different ozone doses (Milli-Q water,  $C_0 = 500$  ppb,  $O_3$  flowrate = 30 L/h,  $pH = 7.25 \pm 0.1$ ,  $T = 24^\circ C \pm 1^\circ C$ .)

It can be interpreted from Figure 23a and Figure 26 that while 110, 60 and 50 min required to degrade 99% of IMI for 600, 1200 and 1800 mg/h ozone doses, respectively, more than 180 min was required in order to disappear BP-1 and BP-2. Moreover, the highest concern regarding the incomplete degradation of by-products is due to the effect of these by-products on the aquatic environment. Unfortunately, oxidation by-products might be more toxic than the parent compound [228]. Therefore, toxicity of the treated solution should also be taken into consideration and it should be further investigated.

It should be pointed here that there may be other by-products which are not detectable by HPLC. Indeed, accordingly, a study concerning on these other possible by-products were conducted using LC-MS/MS at a constant ozone dose and the relevant results are provided in Sec 4.1.8.

#### 4.1.4. Effect of Ozone Gas Flowrate

In this part, effect of ozone gas flowrate on the IMI degradation is evaluated. Ozonation of 1 L Milli-Q water containing 500 ppb IMI was conducted at constant ozone dose (i.e. 1200 mg/h) applied with different ozone flowrates, namely 15, 30 and 100 L/h. Corresponding ozone concentrations applied were 80, 40 and 12 mg/L, respectively. The disappearance profiles of IMI with time are presented in Figure 27.



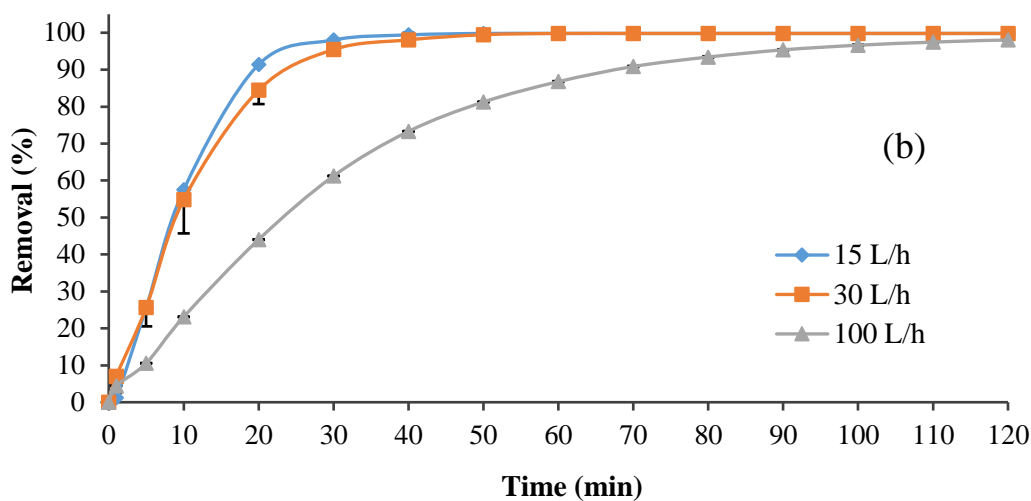


Figure 27. Time course variation of (a) IMI concentration (b) IMI removal efficiency at different ozone flowrates. (Milli-Q water,  $C_0= 500$  ppb,  $O_3$  dose=  $1200$  mg/h, pH=  $7.25 \pm 0.1$ ,  $T=24^\circ\text{C} \pm 1^\circ\text{C}$ .)

As can be seen from Figure 27, as the applied ozone gas flowrate was decreased, the disappearance of IMI was faster. At the constant ozone dose of  $1200$  mg/h, 90% of IMI degradation did occur in 20, 25 and 70 min at the ozone flowrate of 15, 30, 100 L/h, respectively. To increase IMI removal from 90% to 95%, while 5 min was enough for 15 and 30 L/h ozone flowrate, 20 min was required at 100 L/h flowrate. To enhance the removal further from 95% to 99.8%, almost half of the entire degradation time period was necessary. To clarify, at 15 L/h ozone flowrate, while 99.8% disappearance of IMI (i.e. <LOD) was obtained within 50 min, the half of it (i.e. 25 min) was for to increase the removal from 95% to 99.8%. Similarly, at 30 L/h ozone flowrate, 60 min were sufficient to get almost complete disappearance (<LOD) of IMI and half of it was spent to achieve 95% disappearance. On the other hand, more than 180 min of ozonation was necessary to get 99.8% disappearance of IMI at 100 L/h ozone flowrate. Therefore, the operation time strongly depends on the target removal percentage. In other words, if 95% is enough for achieving EQS value, then the ozonation time will be selected accordingly.

As mentioned before, the ozone dose was kept same at all flowrates studied. In other words, the cumulative applied ozone amount (mg) was constant in every hour and also in every minute for all flowrates. For example, within the first 5 min, 100 mg ozone was applied at all flowrates (Figure 28). However due to the flowrate differences, ozone concentration applied to the reactor also differs as stated previously. Therefore, the IMI disappearances were different at each flowrate during the entire experimental duration, although the applied ozone amount was same.

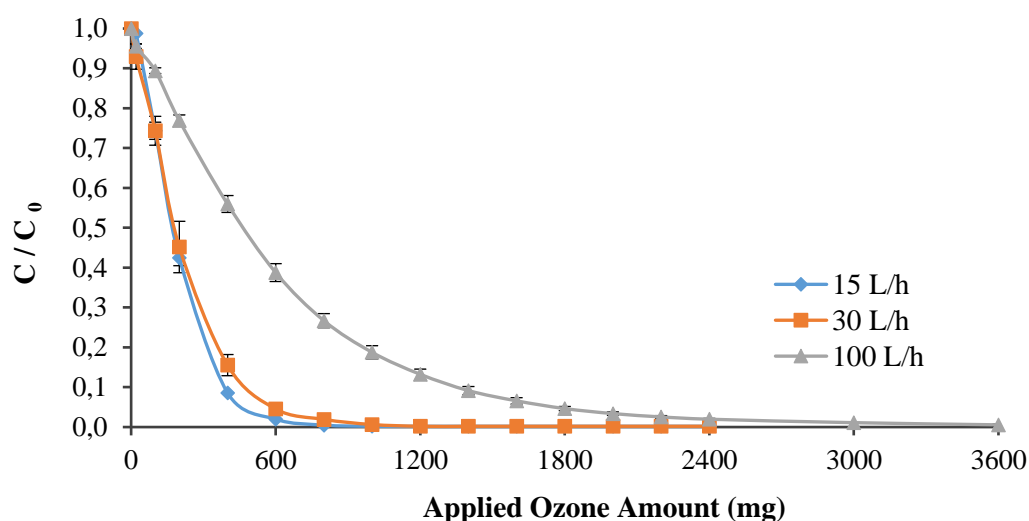


Figure 28. Profile of IMI degradation as a function of applied ozone amount. (Milli-Q water,  $C_0 = 500$  ppb,  $O_3$  dose = 1200 mg/h,  $pH = 7.25 \pm 0.1$ ,  $T = 24^\circ C \pm 1^\circ C$ .)

As can be depicted from Figure 28, 400 mg, 500 mg and 1000 mg ozone was enough to degrade the IMI by 90%, 95% and 99%, respectively, at the flowrate of 15 L/h, whereas at the ozone flowrate of 30 L/h, 500 mg, 600 mg and 1200 mg ozone, respectively, was required to achieve the same respective removal efficiencies. It can be stated that, although the ozone flowrate was doubled, applied ozone dose for the same removal efficiencies were not increased dramatically. On the other hand, at the 100 L/h ozone flowrate, 1400 mg, 1800 mg and more than 3600 mg ozone amount

was consumed in order to achieve 90%, 95% and 99% IMI disappearance, respectively. It is here worthy to mention that these applied ozone amounts were at least three times of the ones applied at 15 and 30 L/h.

While comparing all ozone gas flowrates, it is clearly seen that as the ozone flowrate increases, the disappearance of IMI decreases within the same ozonation time interval. The reason could be the rate of ozone escape from the reactor increases as ozone gas flowrate increased from 15 to 100 mg/h. So, the reaction of ozone with IMI was lowered.

Similar results were obtained at the study conducted by Prasetyaningrum et al. [229] They applied different ozone gas flowrates range from 2 to 5 L/min. The dissolved ozone concentration increased with the increase of the gas flowrate up to 4 L/min. On the other hand, further increase of gas flowrate caused decrease of the dissolved ozone concentration since the residence of ozone gas in the reactor becomes shorter as the flowrate increases [229]. Similarly, Wu and Masten [230] modeled ozone decomposition in deionized distilled water with respect to different ozone gas flowrates (100, 200 and 400 mL/min). Their findings confirm the shorter residence time at higher ozone gas flowrates. The residence times were 20, 10 and 5 min for applied gas flowrates of 100, 200 and 400 mL/min, respectively [230].

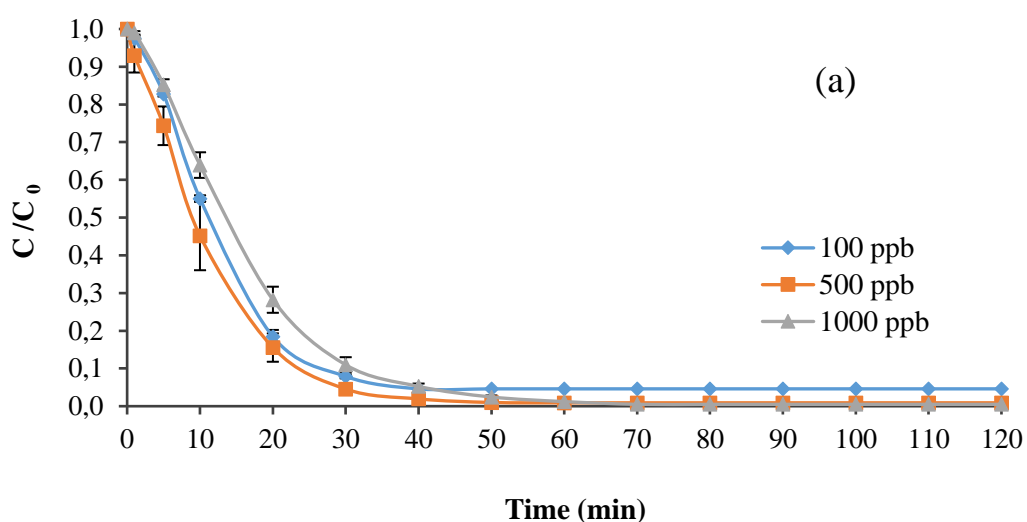
Based on our findings and referenced studies, the impact of ozone flowrate on the IMI degradation during the semi-batch ozonation process is apparent. For overall comparison, 100 L/h of ozone gas flowrate was the least efficient one, since it resulted in the lowest IMI removal at the same amount of applied ozone. When the 15 and 30 L/h ozone flowrates are compared, both of them achieved nearly 90%, 95% and 99% degradation efficiency in less than 25, 30 and 60 min, respectively. Moreover, for the same removal percentages, the applied ozone amount at 30 L/h was at most 200 mg higher than at 15 L/h. Although 15 L/h gas flowrate showed the most effective IMI removal with shorter time, setting the flowrate at 15 L/h at ozone generator panel was difficult since it could not be kept constant during ozonation. Because the flowrate of



15 L/h was very close to the minimum point (10 L/h), flow was fluctuating between 10 and 15 L/h. Therefore, considering this stability issue, 30 L/h was selected as an optimum ozone flowrate for the further experiments.

#### 4.1.5. Effect of Initial IMI Concentration

In order to understand effect of initial IMI concentration on the degradation, 3 different initial IMI concentrations (i.e. 100 ppb, 500 ppb and 1000 ppb) were studied. The constant ozone dose (i.e. 1200 mg/h) at 30 L/h ozone flowrate applied in these experiments and Milli-Q water was spiked with different IMI concentrations.



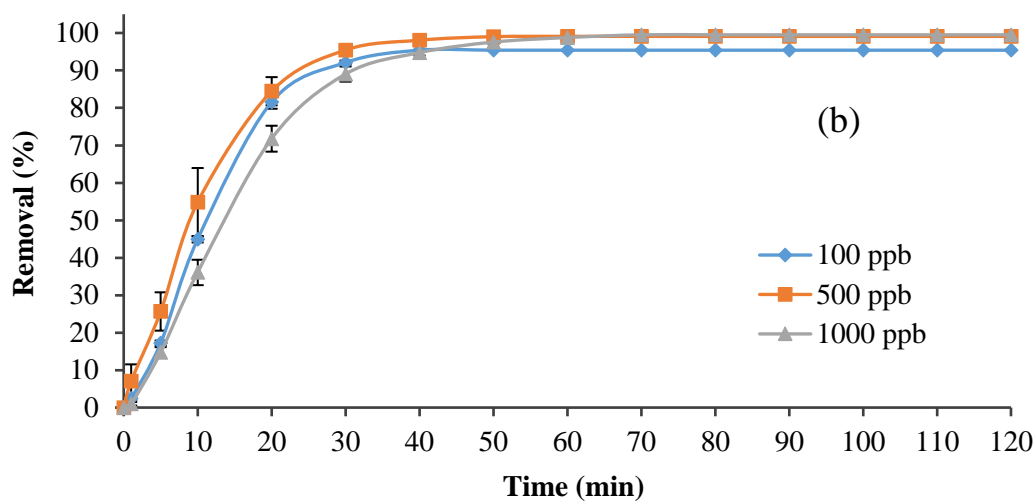


Figure 29. Time course variation of (a) IMI concentration (b) IMI removal efficiency at different initial IMI concentrations. (Milli-Q water, O<sub>3</sub> dose= 1200 mg/h, O<sub>3</sub> flowrate= 30 L/h, pH= 7.25 ± 0.1, T=24°C ±1°C.)

In all IMI concentrations, degradation immediately started as the ozone was introduced into the system. As seen in Figure 29b, IMI removal efficiencies slightly differed for different initial IMI concentrations. For 40 min ozonation, nearly 95%, 98% and 95% of IMI disappearance was observed for 100, 500 and 1000 ppb initial IMI concentrations, respectively. Moreover, IMI was degraded below LOD value (5 ppb) within 40, 50 and 70 min corresponding 95.4%, 99% and 99.5% IMI disappearance for 100, 500 and 1000 ppb initial IMI concentrations, respectively.

Given that only the IMI concentration was monitored in these experiments, it is possible that IMI by-products also consumed ozone during ozonation. Indeed, the greater the initial IMI concentration, the greater the by-product produced. Therefore, the lowest IMI disappearance was observed for 1000 ppb.

#### 4.1.6. Ozonation Mechanism of IMI Degradation

As aforementioned, the IMI was oxidized by ozone and OH• during ozonation. When the degradation is ozone-based, direct mechanism dominates. On the other hand, if the radicals are responsible for the degradation, indirect mechanism is favored. In order to find out the IMI degradation mechanism, whether it is dominated by direct or indirect mechanisms, TBA was added during ozonation of IMI. The results are given in this section.

##### O<sub>3</sub>-Only Removal Mechanism (TBA Addition)

As mentioned before, degradation is achieved with both direct and indirect ozonation. While the former one represents degradation by only ozone, the latter is for degradation by both ozone and radicals [199]. Ozone decomposition in the aqueous solution produces OH• which has further oxidizing ability and cause indirect degradation [189].

Tert-butanol (TBA) is a well-known OH• scavenger and widely applied to understand ozone degradation mechanisms as indicated in the literature [86,98,204,231,232]. Furthermore, TBA was chosen since the reaction rate of TBA with ozone is very slow ( $k_{O_3-TBA} = 1 \times 10^3 \text{ M}^{-1}\text{s}^{-1}$ ) but it quickly reacts with OH•.

For the investigation of OH• contribution on the IMI disappearance during ozonation, experiments were presented with and without TBA. Ozone dose of 1200 mg/h was applied to Milli-Q water with a spike of IMI at the pH  $7.25 \pm 0.1$ . While results obtained by TBA addition refers to O<sub>3</sub>-only removal mechanism, IMI degradation without presence of TBA corresponds to O<sub>3</sub>/OH• removal (Figure 30). As stated in the literature studies, applied TBA amount range differ from 20 to 100 mM [231,233,234]. Since our working volume (i.e. 1L) is more than referenced studies, 100 mM of TBA was introduced into the ozonation reactor.

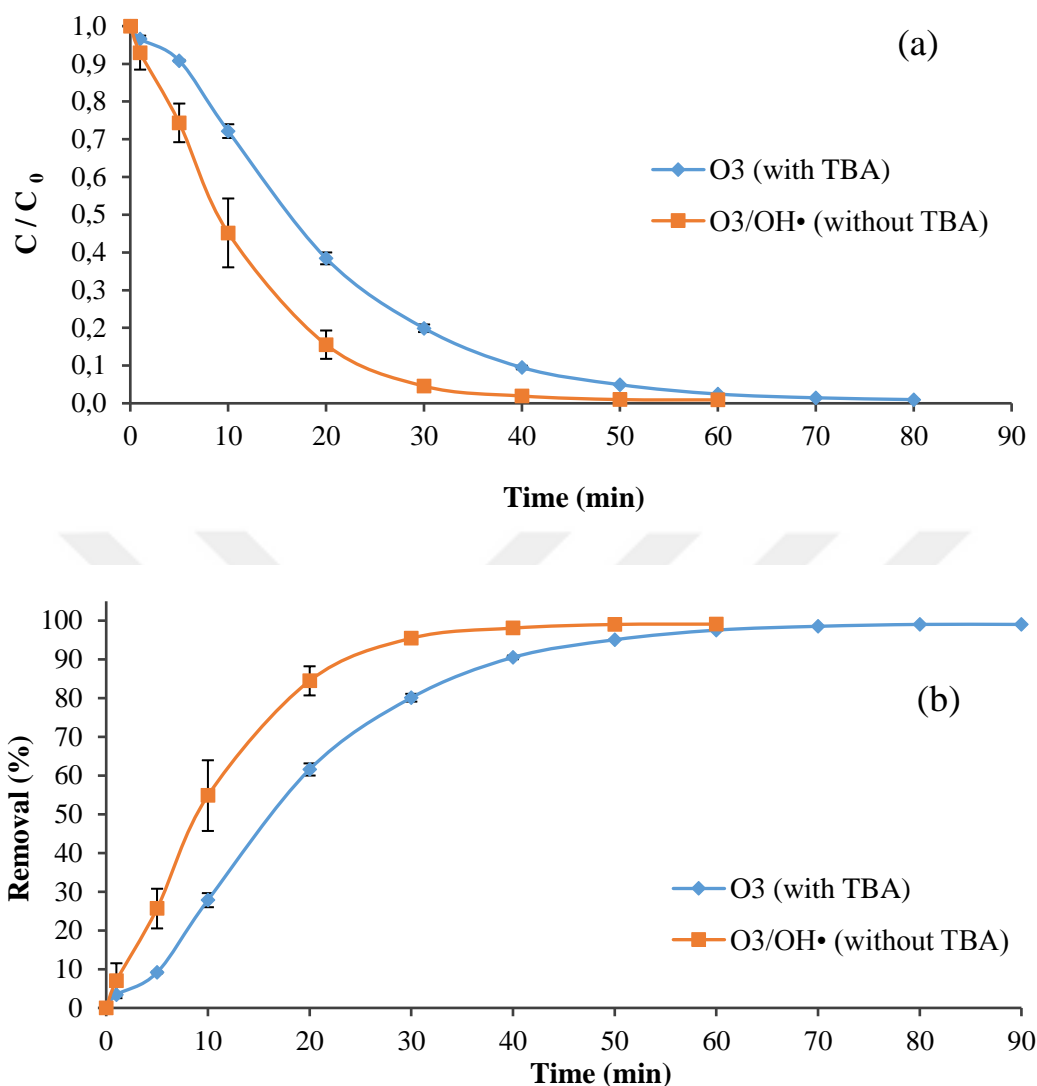


Figure 30. Time course variation of (a) IMI concentration (b) IMI removal efficiency by O<sub>3</sub> and O<sub>3</sub>/OH• i.e. with and without TBA addition, respectively. (Milli-Q water, C<sub>TBA</sub>=100 mM, [IMI]<sub>0</sub>= 1000 ppb, O<sub>3</sub> dose= 1200 mg/h, O<sub>3</sub> flowrate= 30 L/h pH= 7.25 ± 0.1, T=24°C ±1°C.)

As depicted Figure 30, at all sampling times, the removal efficiency of O<sub>3</sub>/OH• mechanism was higher than O<sub>3</sub> mechanism. Indeed, the difference was observed from at the very beginning of the ozonation even at the 1<sup>st</sup> min. This can be explained by

the fact that  $\text{OH}^\bullet$  simultaneously formed as the ozone dissolved in the aqueous solution and IMI was readily undergone reaction with  $\text{OH}^\bullet$ . In addition, 90% disappearance of IMI was achieved at 25 and 40 min and 95% degradation of IMI was observed at 30 and 50 min by  $\text{O}_3/\text{OH}^\bullet$  and  $\text{O}_3$ , respectively. IMI was measured below LOD value (5 ppb) within nearly 50 and 90 min of ozonation for  $\text{O}_3/\text{OH}^\bullet$  and  $\text{O}_3$ , respectively. The contribution of  $\text{OH}^\bullet$  on the disappearance of IMI was obvious. These results indicated that  $\text{OH}^\bullet$  was the major oxidizing species to degrade IMI and indirect mechanism was highly effective during ozonation.

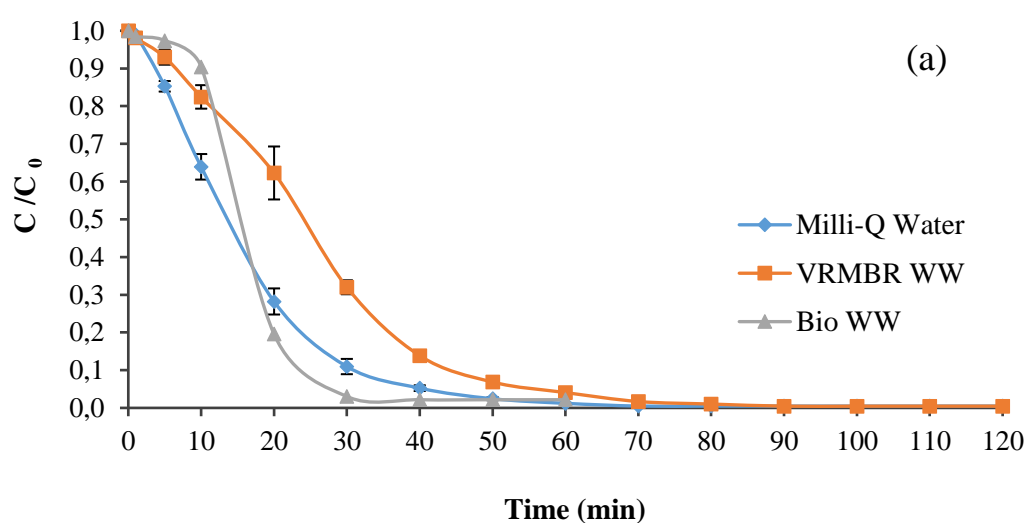
Another reason for low degradation efficiency with TBA addition (i.e.  $\text{O}_3$ -only mechanism) can be due to chemical structure of IMI. As given IMI chemical structure previously (Figure 5), it has two primary moieties including a chloro-pyridine ring and an imidazolidine ring. The chloro-pyridine ring contains nitrogen and chlorine atoms with high electronegativity [23]. So, the chloro-pyridine ring is not easily oxidized by electrophilic ozone. This finding is well in accordance with the previous study conducted during IMI ozonation [23]. Chen et al. [23] showed that degradation of IMI by ozonation highly depends on the concentration of  $\text{OH}^\bullet$ . They introduced 50 mM TBA into the reactor at pHs of 6.02, 6.97, 7.92 and 8.64. The IMI degradation rate constant by  $\text{OH}^\bullet$  was determined as  $3.79 \times 10^9 \text{ M}^{-1}\text{s}^{-1}$  at pH 7.92 which is greater than rate constant of ozone (i.e.  $10.92 \text{ M}^{-1}\text{s}^{-1}$ ).

Moreover, a pesticide namely Acetamiprid (ACMP), which belongs in the same chemical class (i.e. neonicotinoid) with the IMI, was removed by ozonation [86]. In that study, Cruz-Alcalde et al. [86] investigated degradation mechanism of ACMP. They introduced 25 mM of TBA into the reactor and adjusted pH at 7 by adding 1 mM phosphate buffer. Their results clearly showed that TBA addition almost blocked the degradation of ACMP, since its reaction rate with ozone has extremely low [86]. Indeed, the common feature of IMI and ACMP is containing chloro-pyridine ring in their chemical structure. So, these findings confirm that when a pollutant contains high electronegative moiety, it is mainly degraded by  $\text{OH}^\bullet$  instead of ozone during

ozonation. Therefore, our results are in accordance with the literature studies and  $\text{OH}\cdot$  played a significant role in IMI degradation.

#### 4.1.7. Effect of Water Matrix

As known, the effectiveness of the oxidation processes depends on both micropollutant reaction with ozone and ozone consumption by water matrix [235]. Indeed, the water matrix strongly affects removal efficiency of micropollutants, especially  $\text{O}_3$  resistant ones [236]. As previously stated, since IMI is ozone resistant and the degradation mainly depends on the  $\text{OH}\cdot$ , the water matrix seems to play a crucial role in IMI degradation. Therefore, the effect of water matrix was investigated, and results are given in this part. For this purpose, in addition to Milli-Q water, both VRMBR WW and Bio WW were subjected to 1200 mg/h ozonation dose with 30 L/h ozone flowrate. All the experiments were conducted at constant pH at  $7.25 \pm 0.1$  by using phosphate buffer. Prior to VRMBR WW ozonation experiments, 1000 ppb IMI was spiked into the reactor. On the other hand, untreated IMI after biological treatment was subjected to ozonation without further IMI addition into Bio WW. The results obtained are showed in Figure 31 for Milli-Q water, VRMBR WW and Bio WW.



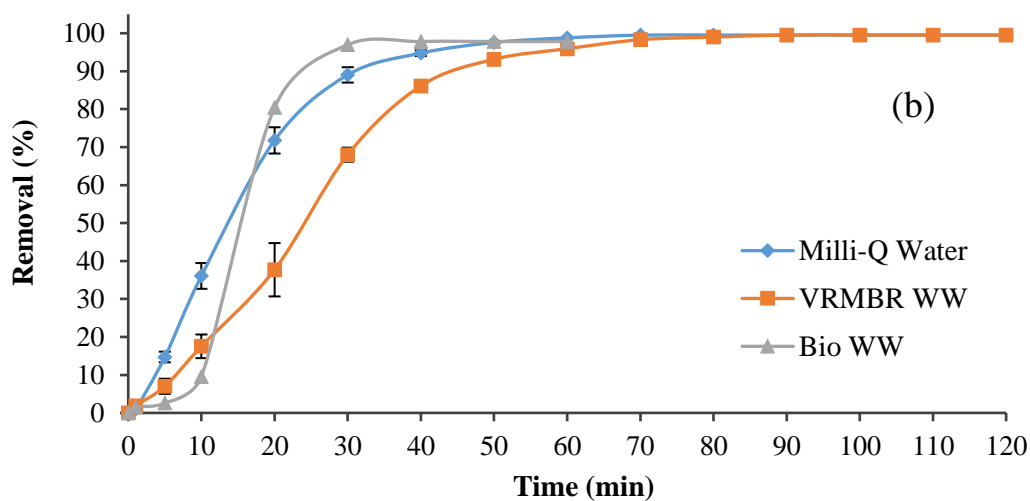


Figure 31. Time course variation of (a) IMI concentration (b) IMI removal efficiency in different water matrices. ( $[IMI]_0 = 1000$  ppb for Milli-Q water and VRMBR WW,  $[IMI]_0 = 226$  ppb for Bio WW,  $O_3$  dose= 1200 mg/h,  $O_3$  flowrate= 30 L/h pH=  $7.25 \pm 0.1$ ,  $T = 24^\circ C \pm 1^\circ C$ .)

As seen in Figure 31, the disappearance of IMI in Milli-Q water started even at the very beginning of ozonation. In addition, among these water matrices, the fastest IMI disappearance was observed in Milli-Q water, as expected. On the other hand, the remarkable difference between Milli-Q water and real wastewaters was delay of degradation of IMI in real wastewaters. Wastewaters contains organic constituents such as proteins, carbohydrates and humic acids and inorganic matters like carbonate and bicarbonate ions [81]. These constituents are known as major oxidant consumers since they consume dissolved  $O_3$  [237]. Moreover, presence of these matters causes radical scavenger since they also deplete the available  $OH^\bullet$  [81]. Therefore, at the very beginning of ozonation, wastewaters consume available ozone and radicals which eventually caused delay in IMI disappearance with respect to Milli-Q water as seen in Figure 31.

During first 10 min of ozonation, nearly 36%, 18% and 10% of IMI was degraded for Milli-Q water, VRMBR WW and Bio WW, respectively. It clearly showed that organics in the Bio WW were greater than VRMBR WW and consume dissolved ozone [238]. Indeed, COD of Bio WW effluent (i.e. 247 mg/L) was higher than COD of VRMBR WW effluent (i.e. 19 mg/L). Therefore, VRMBR WW may be more amenable to IMI ozonation than Bio WW.

Since Bio WW has the least IMI concentration, 97.8% IMI disappearance (i.e. <LOD) was observed within almost 30 min. On the other hand, at least 70 and 90 min were required 99.5% disappearance (i.e.<LOD) for Milli-Q water and VRMBR WW, respectively. Although these duration times are approximate, the removal difference between Milli-Q water and VRMBR WW matrices were apparent from the very beginning to 50<sup>th</sup> min ozonation. As previously proved in our study, the impact of OH• on IMI disappearance is discernable. Indeed, the reason for disappearance differences might be due to presence of organics and inorganics in the wastewaters that act as a radical scavenger [239]. When the radicals in the solution decreases, IMI disappearance also decreases.

To the best of our knowledge, there is no literature study that investigated IMI removal in different water matrices. Yet, water matrix effect on micropollutant degradation has been widely investigated for pharmaceuticals and other pesticides. Benitez et al. [198] investigated several pharmaceuticals (metoprolol, naproxen, amoxicillin, and phenacetin) removal in different water matrices such as groundwater (PZ), reservoir water (PA), and 3 different wastewater effluents obtained by municipal treatment plants of Alcala (AL), Badajoz (BA) and Mostoles (MO) in Spain. Almost complete disappearance of phenacetin, for example, was observed at groundwater and reservoir water at 3 mg/L ozone dose. On the other hand, at most 50% phenacetin removal was observed in all wastewaters at the same ozone dose. Moreover, they also noted that as the COD and TOC of wastewaters increases, the removal efficiency decreases. In accordance, Antoniou et al. [91] investigated removal of 42 pharmaceuticals in 6 different wastewater matrices. All the micropollutants in the wastewater which has



high COD (90 mg/L) and alkalinity values (250 mg HCO<sub>3</sub><sup>-</sup>/L) were removed up to 50%. Besides, higher removal rates (50-100%) were observed in the wastewaters that have relatively lower COD values such as 30 mg/L.

Although elimination of micropollutants is somewhat decreases in real wastewater matrix with respect to Milli-Q or surface water, ozonation is a promising advanced treatment technique especially for inadequately treated secondary effluents [7]. For instance, MBR with post-ozonation processes are widely applied treatment technique in order to degrade micropollutants in the WWTPs. Kovalova et al. [240] investigated removal of 56 micropollutants by the ozonation as a post-treatment process, treating an effluent of an MBR fed with raw hospital wastewater. MBR treatment process only achieved 22% of removal efficiency. Addition of ozonation unit greatly improved overall micropollutant elimination and 62% removal was achieved. Indeed, ozonation boosted the elimination of pharmaceuticals and industrial chemicals since their removal increased to 99% and 100%, respectively. Moreover, removal of recalcitrant micropollutants such as iodinated X-ray contrast media increased from 1% to 51% which shows that ozonation is one of the most promising post-treatment processes [240].

#### **4.1.8. Ozonation By-Products of IMI**

Ozonation may result in incomplete degradation of pesticide molecules and this may cause to undesirable degradation by-products formation [227]. Therefore, the possible IMI degradation pathway and the potential ozonation by-products of IMI was investigated and the results are given in this section. The LC-MS/MS chromatograms of IMI ozonation in Milli-Q water and VRMBR WW are given in Figure C.2 and Figure C.3 (Appendix C), respectively.

As seen in Figure C.4 (Appendix C), *m/z* 99 and 195 ions were detected in all samples due to presence of phosphate buffer in the Milli-Q water. Another ion, *m/z* 239, was detected in all samples with an almost constant concentration may show that this ion

could be occurred due to impurities in the samples. For that reason, these ions were neglected during evaluation of IMI degradation pathway and produced by-products.

IMI ( $m/z$  256) significantly decreased after 70 min ozonation. After 180 min of ozonation, IMI slightly occurred which could correspond to below LOD value in the HPLC, as mentioned previously. As the IMI ( $m/z$  256) degraded,  $m/z$  188,  $m/z$  209,  $m/z$  253,  $m/z$  275 and  $m/z$  314 increased in 70 min ozonation, but then they decreased to some degree. Indeed, 180 min of ozonation was not enough to remove these by-products. Moreover,  $m/z$  270 was generated within the first 5 min of treatment, it gradually decreased and eventually disappeared after 180 min of ozonation. The IMI degradation pathway was proposed by fragmentation of  $m/z$  256 in the LC-MS/MS. As depicted in Figure 32, IMI lost  $\text{HNO}_2$  and the fragment ion  $m/z$  209 formed. The other way represents that IMI consecutively lost  $\text{NO}_2$  and  $\text{Cl}$  and the fragment ions  $m/z$  210 and  $m/z$  175 formed, respectively.

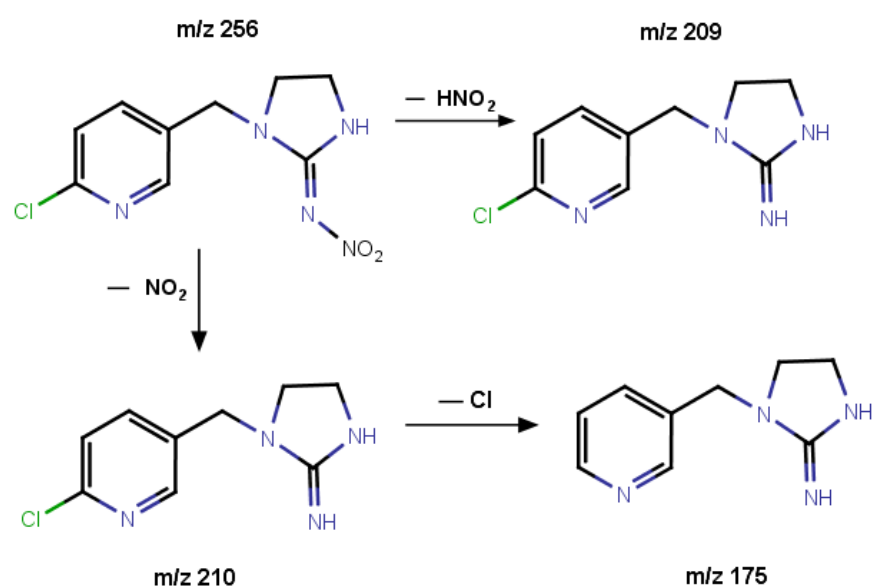


Figure 32. The proposed degradation pathway of IMI

Similar to Bourgin et al. [22], the opening of the imidazoline ring produced a by-product which was detected the ion at  $m/z$  230 ozonation in Milli-Q water. Indeed, IMI lost  $C_2H_2$  during formation of  $m/z$  230. Fragmentation of  $m/z$  230 yielded to  $m/z$  186 and  $m/z$  148. The fragment ion at  $m/z$  186 was obtained by loss of  $N_2O$ , whereas the fragment ion at  $m/z$  148 was observed by the consecutive loss of  $N_2O$  and HCl similar to the referenced literature.

IMI ( $m/z$  256) ozonation yielded to  $m/z$  270. Carbonylated forms of IMI could be resulted in detection of  $m/z$  270 ion which was also mentioned by Bourgin et al. [22]. On the other hand, different from the referenced study, fragmentation of  $m/z$  270 yielded to  $m/z$  253 ion by the loss of  $NH_3$  in our study. Moreover, dehydroxylated form of IMI, which was also supposed by the referenced study, gives the fragment ion at  $m/z$  288. Bourgin et al. [22] stated that before the carbonylated and dehydroxylated forms of IMI were produced, monohydroxylation of IMI was detected with an ion at  $m/z$  272. Nevertheless, in our study  $m/z$  272 ion was not detected. The reason could be that the  $m/z$  272 might have quickly transformed into  $m/z$  270 and  $m/z$  288 ions.

As can be seen from the above-mentioned  $m/z$  values, during ozonation, in total 11 by-products with fragmented ions were detected by LC-MS/MS. However, after treatment, only  $m/z$  270 ion was completely disappeared. By-products mentioned in Sec 4.1.3, namely BP-1 and BP-2, were those detectable by HPLC. Unfortunately, it was not possible to match BP-1 and BP-2 with those detected by LC-MS/MS due to differences in both equipments and methods used. Nevertheless, it is for sure that any two of 11 by-products were corresponding to BP-1 and BP-2.

## 4.2. Ozonation Reaction Kinetics

The ozonation reaction kinetics is second-order since both  $O_3$  and  $OH\cdot$  oxidize the IMI. The overall reaction kinetics can be described as follows;

$$-\frac{d [IMI]}{dt} = k_{OH\cdot-IMI}[IMI][OH\cdot] + k_{O_3-IMI}[IMI][O_3] \quad (23)$$

where,

[IMI]: Concentration of IMI

[OH•]: Concentration of OH•

[O<sub>3</sub>]: Concentration of O<sub>3</sub>

k<sub>OH•-IMI</sub>: The second-order rate constant of OH• with IMI

k<sub>O<sub>3</sub>-IMI</sub>: The second-order rate constant of O<sub>3</sub> with IMI

During ozonation experiments, ozone was excessively supplied into the system with respect to IMI concentration. So, the reaction rate of ozonation mainly depended on the concentration of IMI. The ozonation reactions followed pseudo first-order kinetics which was also supported by the linear plot with a high R<sup>2</sup> value obtained by plotting the -ln(C/C<sub>0</sub>) against the time (min) graph.

The direct ozonation of IMI was exhibited pseudo first-order reaction, as following;

$$-\frac{d [IMI]}{dt} = k_{app} [IMI] \quad (24)$$

where;

[IMI]: Concentration of IMI

k<sub>app</sub>: The apparent pseudo first-order rate constant (k<sub>app</sub>= k<sub>OH•-IMI</sub> + k<sub>O<sub>3</sub>-IMI</sub>)

The effect of different operating parameters such as buffer addition, pH, ozone dose, ozone gas flowrate and initial IMI concentration and water matrix on the IMI degradation kinetic rate was investigated. The obtained results were given in the following sections.

#### 4.2.1. Effect of Buffer

The degradation kinetics of IMI was performed using the semi-batch ozonation system with and without phosphate buffer addition. It was found that the degradation of IMI in buffered solution (i.e. at  $\text{pH } 7.25 \pm 0.1$ ) was much faster compared to unbuffered solution. The  $R^2$  values which are greater than 0.99 suggests that a quite good linear correlation was achieved.

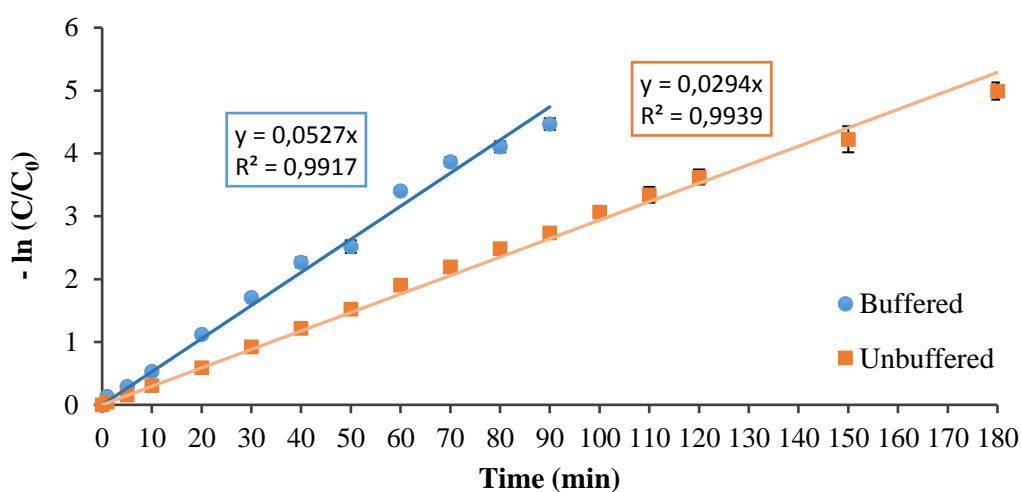


Figure 33. Reaction kinetics of IMI with and without buffer addition. (Milli-Q water,  $\text{O}_3$  dose= 2400 mg/h,  $\text{O}_3$  flowrate= 100 L/h,  $C_0$ = 500 ppb,  $T = 24^\circ\text{C} \pm 1^\circ\text{C}$ .)

As shown in Figure 33, the calculated slope of the fitted linear line presenting the buffered system is  $0.0527 \text{ min}^{-1}$ , which is almost 2 times higher than in the case of unbuffered system ( $0.0294 \text{ min}^{-1}$ ). Indeed, the improvement of reaction rate was pronounced even in the very first minutes.

A comparison of the buffered and unbuffered reaction rate constants corroborated the effects observed in the IMI disappearance profiles and helped to determine the operating condition for further ozonation experiments.

#### 4.2.2. Effect of pH

The effect of the different pH on the IMI degradation kinetics was investigated. The kinetic analysis showed that the IMI removal follows the pseudo-first order. The high  $R^2$  values (0.9825-0.9950) suggested a quite good linear correlation (Figure 34). The apparent rate constant for pH 6.20, 7.30 and 8.25 were calculated as 0.0436, 0.0956 and 0.2374  $\text{min}^{-1}$ , respectively. Degradation of IMI was much slower at pH 6.20 compared other pHs. Indeed, it was found that the increase of the solution pH from 6.20 to 7.30 caused a 2.2 times increase in the IMI disappearance rate. When pH was 8.25, it was also obtained that the kinetic rate constant was more than doubled at even one-unit increase in the pH scale.

In general, the rate of degradation of IMI was faster with higher pH. Figure 34 indicates that IMI disappearance kinetic rate at basic pH is almost 5.4 times faster than the one at acidic pH.

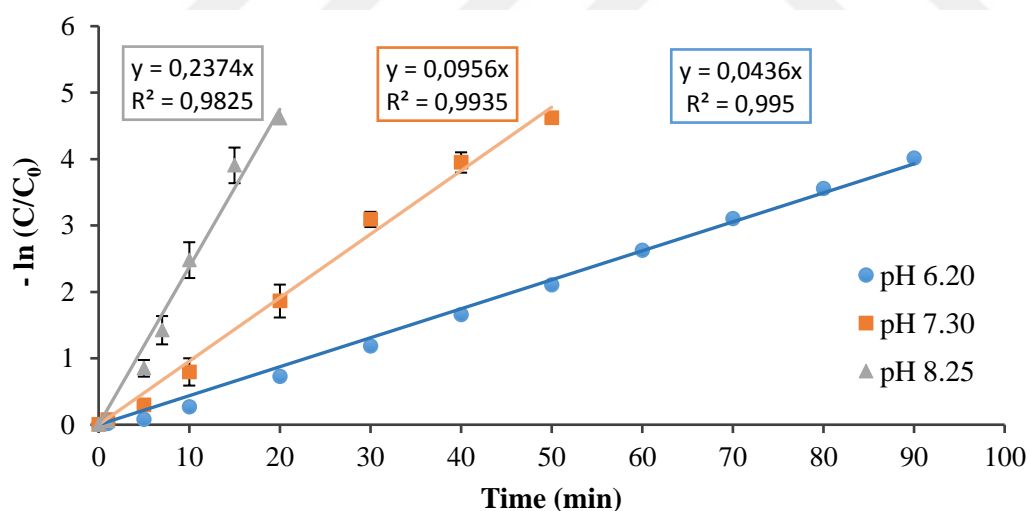


Figure 34. Reaction kinetics of IMI at different pHs (Milli-Q water,  $C_0 = 500$  ppb,  $O_3$  dose = 1200 mg/h,  $O_3$  flowrate = 30 L/h  $T = 24^\circ\text{C} \pm 1^\circ\text{C}$ .)

Similar results have been reported by Chen et al. [23]. Although they applied different pHs than our study, their results showed that the least IMI ozonation kinetic rate was observed at pH 6.02 (i.e. acidic pH) which is similar to our results. Moreover, the increase of pH from 6.02 to 8.66 showed that the kinetic rate was almost 4.1 times increased.

Therefore, basic conditions (pH 8.25) resulted to be the most convenient pH for IMI removal by ozonation. This was likely due to formation of  $\text{OH}\cdot$  through the ozone decomposition at these conditions.

### 4.2.3. Effect of Ozone Dose

Besides pH, the ozone dose strongly affects the kinetic rate constants. The reaction kinetics was investigated in the ozone dose range 600-1800 mg/h. The ozonation kinetics of IMI followed pseudo-first order kinetics. The rate constants were determined by calculating the slope of the lines given in Figure 35.

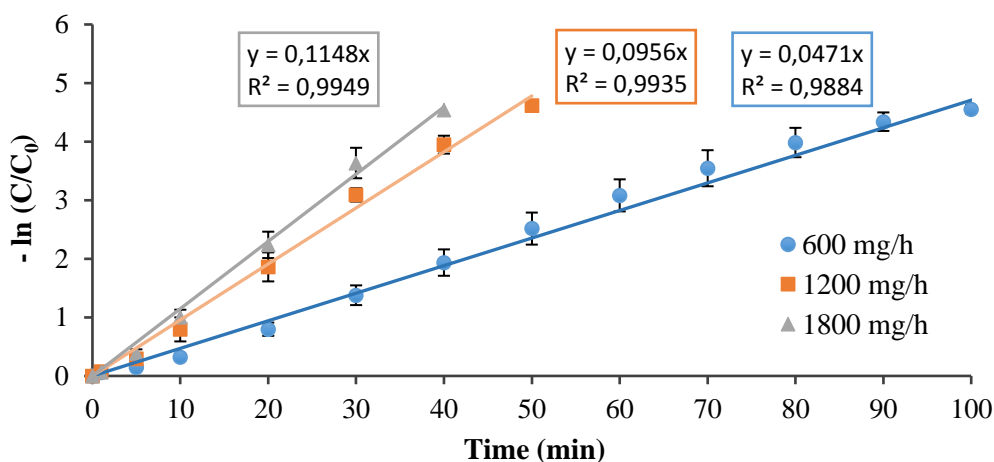


Figure 35. Reaction kinetics of IMI at different ozone doses. (Milli-Q water,  $C_0=500$  ppb,  $\text{O}_3$  flowrate= 30 L/h, pH=  $7.25 \pm 0.1$ ,  $T=24^\circ\text{C} \pm 1^\circ\text{C}$ .)

As seen in Figure 35, it was found that the IMI disappearance rate increased with the increase of ozone dose. It was observed that an increase of the ozone dose from 600 to 1200 mg/h provided a pronounced increase in the reaction rate constant, even from the very beginning of ozonation. As the ozone dose was doubled (i.e. increased from 600 mg/h to 1200 mg/h), the reaction rate also doubled from 0.0471 to 0.0956 min<sup>-1</sup>.

This confirms previous results reported by Bourgin et al. [22] where an increase in rate constants with increasing ozone dose was found. The kinetic rate constants were calculated as 0.036, 0.071 and 0.129 min<sup>-1</sup> when the applied ozone concentrations were 25, 50 and 100 g/m<sup>3</sup>, respectively.

On the other hand, increase of ozone dose from 1200 mg/h to 1800 mg/h did not significantly affect the reaction rate since it increased from 0.0956 to 0.1148 min<sup>-1</sup> (Figure 35). It is interesting to mention here that these results could be an indication of a rate-limiting step of the initiation reaction (i.e. Eq. (1)). Since IMI disappearance mainly depends on the OH• formation, rate-limiting step may have caused to less OH• production and hence less increase in rate kinetics when ozone dose increased from 1200 to 1800 mg/h as compared to ozone dose increased from 600 to 1200 mg/h.

So, the obtained kinetic rates showed that increase of the ozone dose caused overall enhancement of reaction rate. Although the reaction rate was proportionally increased up to 1200 mg/h ozone dose, after that point it was not followed same correlation.

#### **4.2.4. Effect of Ozone Gas Flowrate**

The effect of the ozone gas flowrate on the reaction kinetics was depicted in the flowrate range 15 to 100 L/h. The high correlation coefficients R<sup>2</sup> ranged from 0.9863 to 0.9986 proved that the apparent pseudo-first-order kinetics could fit the experimental results well.

The apparent rate constants for ozone gas flowrate 15, 30 and 100 L/h were calculated as 0.0335, 0.1011 and 0.1288 min<sup>-1</sup>, respectively. As shown in Figure 36, the ozone



dose of 15 L/h presented the highest disappearance rate and higher flowrate slowed down the reaction efficiency. Indeed, since the increase of ozone gas flowrate leads to enhance of ozone escape from the reactor, soluble ozone decreases and hence the IMI disappearance rate also lessen. For instance, when the ozone flowrate increased to 100 L/h, the reaction rate almost 4 times decreased.

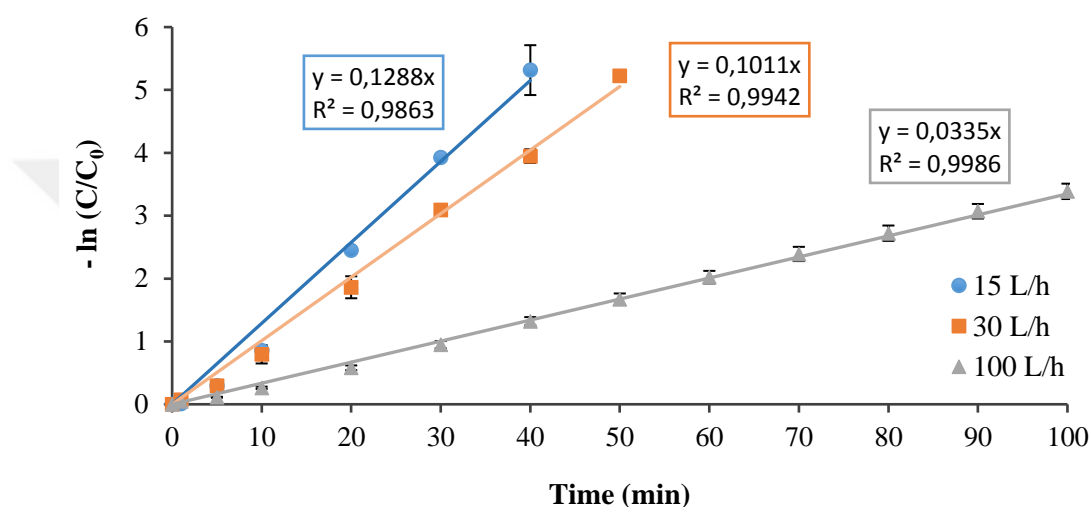


Figure 36. Reaction kinetics of IMI at different ozone at different ozone gas flowrates. (Milli-Q water,  $C_0 = 500$  ppb,  $O_3$  dose= 1200 mg/h,  $pH = 7.25 \pm 0.1$ ,  $T = 24^\circ C \pm 1^\circ C$ .)

#### 4.2.5. Effect of Initial IMI Concentration

The effect of the initial IMI concentrations on the reaction kinetics was examined. The apparent rate constants were evaluated with respect to initial IMI concentration ranging from 100 ppb to 1000 ppb. The high  $R^2$  value (0.9797-0.9935) suggests a quite good linear correlation was achieved. The IMI degradation was followed pseudo-first order kinetics. The calculated apparent kinetic rates were 0.0820, 0.0956 and 0.0729  $\text{min}^{-1}$  at initial IMI concentration 100, 500 and 1000 ppb, respectively.

As shown in Figure 37, the solution with an initial 500 ppb IMI concentration presented the highest kinetic rate, a lower or higher IMI concentration slows down the reaction efficiency. The apparent rate constant of 500 ppb is  $0.0956 \text{ min}^{-1}$ , which is only 1.1 and 1.3 times than those of 100 and 1000 ppb, respectively.

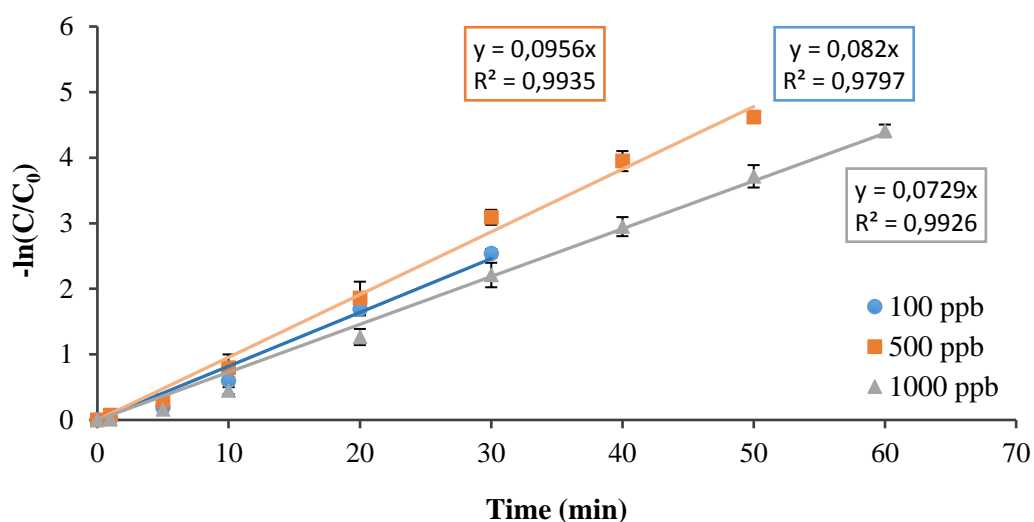


Figure 37. Reaction kinetics of IMI at different initial IMI concentrations. (Milli-Q water,  $\text{O}_3$  dose= 1200 mg/h,  $\text{O}_3$  flowrate= 30 L/h,  $\text{pH} = 7.25 \pm 0.1$ ,  $T = 24^\circ\text{C} \pm 1^\circ\text{C}$ .)

While examining the rate constants, it should be noted that as the initial concentration of IMI increases, the concentration of degradation by-products also increases. It is well-known that besides micropollutants, degradation by-products may consume available ozone, as well. For that reason, available ozone was used for both IMI and its by-products degradation. So, during ozonation experiments of 1000 ppb IMI, there was a pronounced decrease in the rate constant with respect to other concentrations.

#### 4.2.6. Ozonation Mechanism of IMI Degradation

The kinetic study of IMI degradation mechanism was investigated to determine whether it is dominated by direct or indirect mechanisms. In this respect, TBA was added during ozonation of IMI. Moreover, the indirect reaction rate constant of ozonation was investigated by reference compound namely pCBA. The results are given in this section.

##### O<sub>3</sub>-Only Removal Mechanism (TBA Addition)

In order to investigate the effect of OH• on the IMI removal, TBA was introduced into the reactor during IMI ozonation. Indeed, the differences between with and without TBA addition apparently showed impact of OH• on IMI degradation. The high R<sup>2</sup> values (>0.99) suggested a quite good linear correlation (Figure 38). The IMI ozonation kinetics was followed pseudo-first order kinetics.

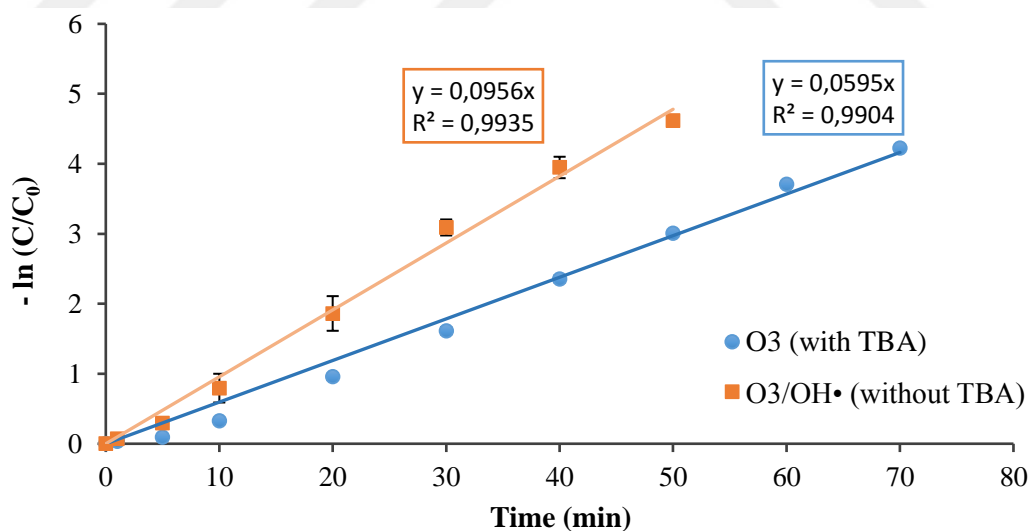


Figure 38. IMI degradation kinetics by O<sub>3</sub> and O<sub>3</sub>/OH• i.e. with and without TBA addition, respectively. (Milli-Q water, C<sub>TBA</sub>=100 mM, [IMI]<sub>0</sub>= 1000 ppb, O<sub>3</sub> dose= 1200 mg/h, O<sub>3</sub> flowrate= 30 L/h pH= 7.25 ± 0.1, T=24°C ±1°C.)

As seen in Figure 38, the rate constants of IMI degradation by O<sub>3</sub>-only and O<sub>3</sub>/OH• were calculated as 0.0595 and 0.0956 min<sup>-1</sup>, respectively. Since OH• in the solution was scavenged by TBA, the kinetic constant was significantly affected, and almost decreased to half of the one without TBA addition. On the other hand, without TBA addition, both O<sub>3</sub> and OH• took place during IMI degradation. These findings are clear evidence that almost half of the IMI degradation was due to OH•.

Indeed, Cruz-Alcalde et al. [86] reported that, Acetamiprid degradation by ozonation was almost completely blocked with TBA addition (i.e. O<sub>3</sub>-only removal). Considering that Acetamiprid belongs to the neonicotinoid group like IMI, the removal rate mainly depends on OH• during ozonation.

#### **OH• Removal Mechanism (pCBA as a Reference Compound)**

Since the OH• cannot be measured directly during ozonation process, competition kinetics method was used to determine the second-order rate constants for the reactions of IMI with OH•. pCBA which is a well-known reference compound is widely applied to indirectly measure OH•. In addition, measurement of probe compound, pCBA, is rather easy since it can be easily detected by HPLC. The pCBA reacts only OH• ( $k_{\text{OH}\cdot\text{-pCBA}} = 5 \times 10^9 \text{ M}^{-1}\text{s}^{-1}$ ) and not considerably reacts with other radicals or O<sub>3</sub> ( $k_{\text{O}_3\text{-pCBA}} = 0.15 \text{ M}^{-1}\text{s}^{-1}$ ) [210]. For that purpose, 5 μM pCBA was introduced into Milli-Q water at pH 7.25 ± 0.1 in ozonation. The results are given in this section.

The kinetics of IMI degradation by OH• can be described as follows;

$$-\frac{d [IMI]}{dt} = k_{\text{OH}\cdot\text{-IMI}}[IMI][\text{OH}\cdot] \quad (25)$$

where,

$k_{\text{OH}\cdot\text{-IMI}}$ : The second-order rate constant of OH• with IMI

[IMI]: Concentration of IMI

[OH•]: Concentration of OH•

The degradation kinetics of pCBA by OH• can be described as;

$$-\frac{d [pCBA]}{dt} = k_{OH\cdot-pCBA}[pCBA][OH \cdot] \quad (26)$$

where,

$k_{OH\cdot-pCBA}$ : The second-order rate constant of OH• with pCBA

[pCBA]: Concentration of pCBA

[OH•]: Concentration of OH•

The ratio of integration of Eq. (25) and Eq. (26) yields to below equation;

$$\ln \frac{[IMI]_t}{[IMI]_0} / \ln \frac{[pCBA]_t}{[pCBA]_0} = k_{OH\cdot-IMI} / k_{OH\cdot-pCBA} \quad (27)$$

The left-hand side of Eq. (27) was calculated by the slope of the line (Figure 39). Since the reaction rate of OH• with pCBA is  $5 \times 10^9 \text{ M}^{-1}\text{s}^{-1}$  [210] and the slope of the lines were calculated,  $k_{OH\cdot-IMI}$  could be easily obtained. During the ozonation, the ratio of  $k_{OH\cdot-IMI} / k_{OH\cdot-pCBA}$  was  $4.4657 \text{ M}^{-1}\text{s}^{-1}$  and hence, the second-order rate constant of IMI by OH• ( $k_{OH\cdot-IMI}$ ) was calculated as  $2.23 \times 10^{11} \text{ M}^{-1}\text{s}^{-1}$ .

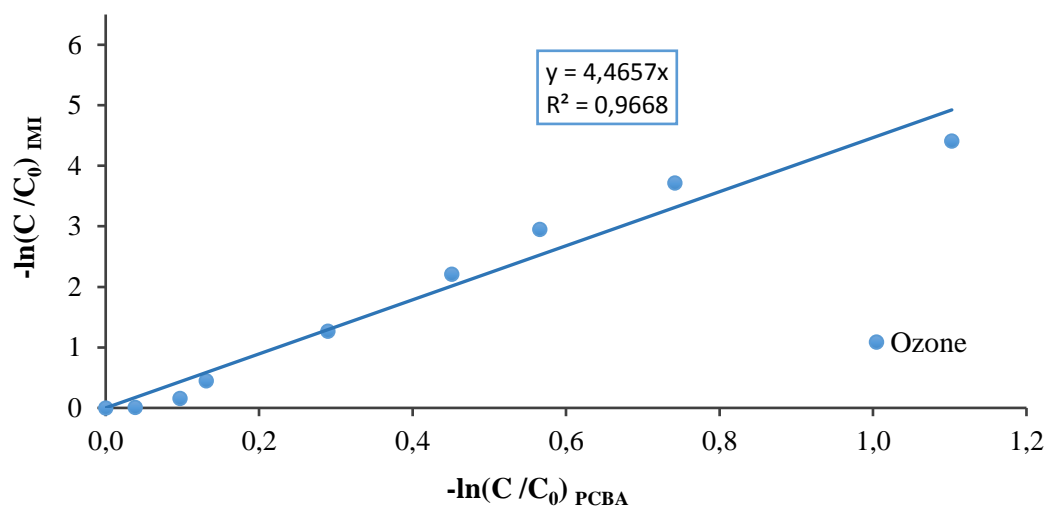


Figure 39. Natural logarithm of the relative concentration of IMI vs pCBA (Milli-Q water,  $C_{PCBA}=5 \mu M$ ,  $[IMI]_0= 1000$  ppb,  $O_3$  dose= 1200 mg/h,  $O_3$  flowrate= 30 L/h pH=  $7.25 \pm 0.1$ ,  $T=24^\circ C \pm 1^\circ C$ .)

Indeed, Chen et al. [23] found the second-order rate for  $OH^\bullet$   $2.92 \times 10^9 M^{-1}s^{-1}$  during ozonation of IMI at pH 6.97. The difference between the reaction rates found during our study and the referenced study could be due to different experimental conditions. Chen et al. [23] investigated batch ozonation of IMI and applied different pH value than our study. Since the ozone was continuously supplied in this thesis study, the  $OH^\bullet$  could be much higher than the referenced study. Furthermore, the effect of pH was pronounced, and it highly affected the production of  $OH^\bullet$ . Since the pH in this thesis study, i.e.  $7.25 \pm 0.1$ , was higher than the one in the referenced study, i.e. 6.97, the production of  $OH^\bullet$  could be higher in our study.

#### 4.2.7. Effect of Water Matrix

Besides aforementioned operational parameters, the water matrix strongly affects the kinetic rate constants. So, the effect of the different water matrices on the IMI

degradation kinetics was investigated. The degradation kinetics of IMI followed pseudo-first order kinetics. The rate constants were determined by calculating the slope of the lines given in Figure 40.

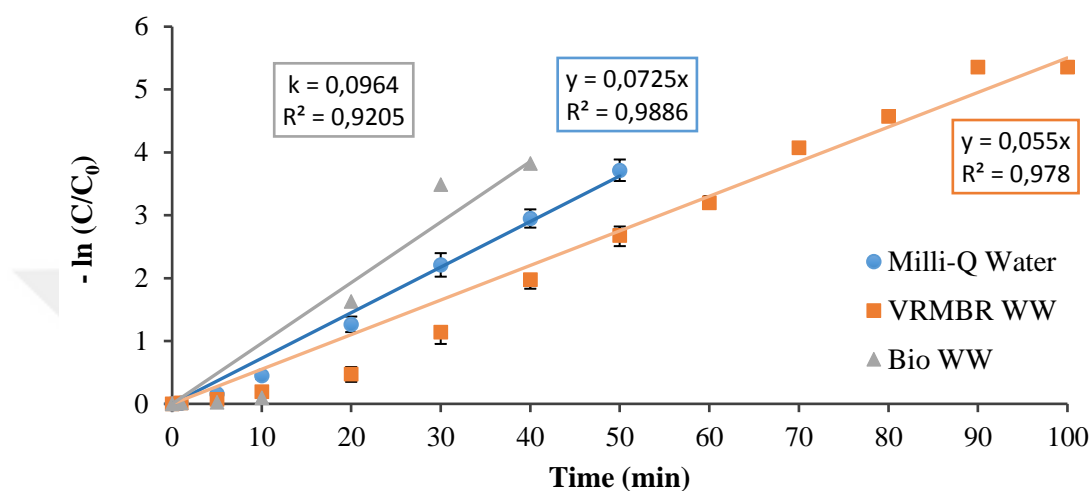


Figure 40. Reaction kinetics of IMI in different water matrices. ( $[IMI]_0 = 1000$  ppb for Milli-Q water and VRMBR WW,  $[IMI]_0 = 226$  ppb for Bio WW,  $O_3$  dose = 1200 mg/h,  $O_3$  flowrate = 30 L/h pH =  $7.25 \pm 0.1$ ,  $T = 24^\circ C \pm 1^\circ C$ .)

As shown in Figure 40, the apparent rate constant for water matrices Milli-Q, VRMBR WW and Bio WW were calculated as 0.0725, 0.055 and 0.0964  $\text{min}^{-1}$ , respectively. It should be noted that the initial IMI concentration of Bio WW (i.e. 226 ppb) is less than the others' concentration (i.e. 1000 ppb). As aforementioned previous sections, 1000 ppb initial IMI concentration depicted the least reaction rate constant with respect to others. Indeed, even the Bio WW has scavenging potential, due to initial IMI concentration differences, the reaction rate was much higher than the other water matrices. While comparing the Milli-Q and VRMBR WW, the water matrix effect is pronounced and even the reaction rate of VRMBR WW nearly decreased to half of the one in Milli-Q. Since direct reaction of IMI with  $O_3$  is very slow and IMI is mainly

degraded by  $\text{OH}\cdot$ , the observed decrease can consequently be attributed to radical scavenging capacity of wastewaters.

### **4.3. Photo-ozonation ( $\text{O}_3/\text{UV}$ ) of IMI**

Since single ozonation process required long treatment time for IMI degradation, it was considered necessary to apply UV irradiation in order to enhance IMI removal. The improvement of treatment efficiencies by coupling ozone with UV irradiation was proved for micropollutant removal [21] and wastewater treatment (e.g. COD removal) studies, as well [241].

In this part, the results obtained from the  $\text{O}_3/\text{UV}$  experiments are provided and discussed in the light of similar literature studies in order to have a deeper understanding about the photo-ozonation of IMI. On this target, effect of wastewater matrix on IMI degradation during  $\text{O}_3/\text{UV}$  process and reaction kinetics were given comparatively with ozonation process. To add, possible by-products' production pathway was also demonstrated and discussed explicitly in the following sections.

#### **4.3.1. Effect of Water Matrix**

The UV irradiation effect on ozonation is a complex matter affecting several key processes in reactions, the ozone decomposition as well as the radical production as discussed in previous section 2.5. Indeed, it is well-known that wastewater matrix highly affects degradation of pollutants [91]. For this reason, removal of IMI and possible degradation by-products by  $\text{O}_3/\text{UV}$  process were investigated.

In this sense, Milli-Q water, VRMBR WW and Bio WW were subjected to 1200 mg/h ozonation dose with 10-Watt UV irradiation at  $\text{pH } 7.25 \pm 1$  and at temperature of  $24^\circ\text{C} \pm 1^\circ\text{C}$ . Prior to Milli-Q water and VRMBR WW  $\text{O}_3/\text{UV}$  application, the synthetic and real WW was prepared by spiking of 1000 ppb IMI into the reactor. On the other hand, IMI was not added into Bio WW and remained IMI in that wastewater was subjected



to ozonation. The results obtained are showed in Figure 41 for Milli-Q water, VRMBR WW and Bio WW.

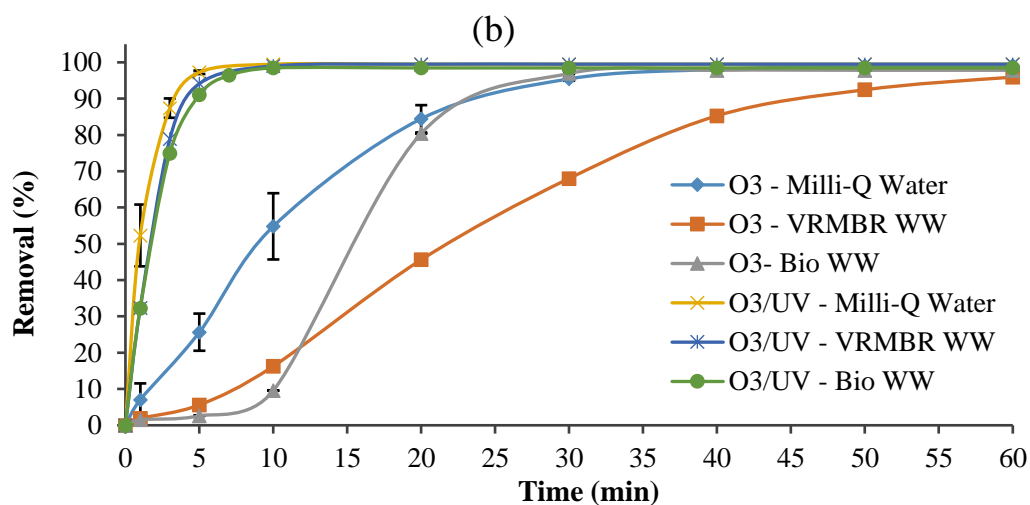
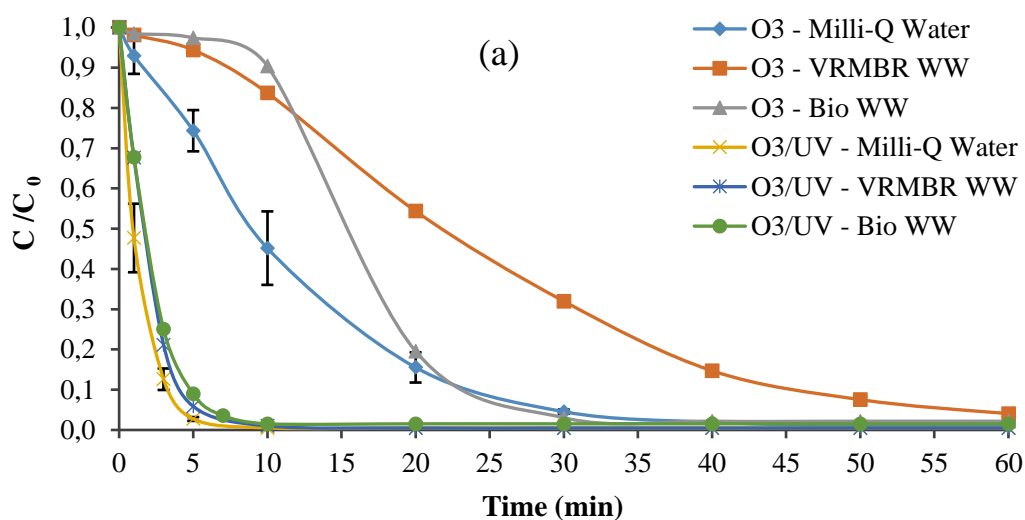


Figure 41. Time course variation of (a) IMI concentration (b) IMI removal efficiency in different water matrices. ( $[IMI]_0 = 1000$  ppb for Milli-Q water and VRMBR WW,  $[IMI]_0 = 332$  ppb for Bio WW, UV lamp= 10 W,  $O_3$  dose= 1200 mg/h,  $O_3$  flowrate= 30 L/h pH=  $7.25 \pm 0.1$ ,  $T = 24^\circ C \pm 1^\circ C$ .)

Figure 41, shows the time-dependent IMI degradation by the O<sub>3</sub>/UV process, compared with ozonation, in different water matrices. As expected, the removal of IMI from all studied water matrices was greatly improved when UV was coupled with ozonation. Indeed, the improvement was clearly seen from the very beginning of O<sub>3</sub>/UV process. For instance, within the first 3 min of treatment, 87.4%, 78.9% and 75.0% of IMI were degraded in Milli-Q water, VRMBR WW and Bio WW, respectively. After 10 min process, the removal increased to 99.5% (<LOD), 99.0% and 96.4%, respectively. By that time, the fastest IMI disappearance was observed for Milli-Q water, as expected, and VRMBR WW showed slightly better removal than Bio WW.

At the end of 20 min of O<sub>3</sub>/UV application, IMI disappearance (i.e. <LOD) was observed for all wastewater matrices. Indeed, it was clearly seen that the wastewater matrices may not significantly affect IMI removal since the removal rates were very near throughout the process. Hence, it can be said that IMI removal was enhanced by addition of UV irradiation regardless of the water matrix. Our findings are in accordance with the results obtained by Yao et al [97]. They showed that micropollutants removal from different matrices (surface water, groundwater and secondary effluent wastewater) were improved regardless of the water matrices by O<sub>3</sub>/UV application compared to single ozonation [97]. The reason behind this incident could be that, the ozone decomposition rate, in turn production rate of OH• and other radicals was quite enhanced under UV irradiation although wastewaters have OH• scavenging capacity [189]. Therefore, scavengers may not affect OH• concentration, since OH• was being greatly produced during O<sub>3</sub>/UV.

On the other hand, for the same treatment time (i.e. 20 min), single ozonation resulted in only 80.4% and 45.6% IMI removal in VRMBR WW and Bio WW, respectively. It was also clearly obtained from Figure 41 that degradation of IMI in VRMBR WW and Bio WW matrices were delayed at the beginning of the treatment. Moreover, since Bio WW has higher COD value (i.e. 247 mg/L) than VRMBR WW (i.e. 19 mg/L), the delay time was more pronounced for Bio WW. The reasons could be ozone

consumption by organic and inorganic constituents in the wastewater [235] and/or radical scavenging ability of these constituents [189]. Contrarily, IMI degradation was instantly started in Milli-Q water by application of O<sub>3</sub>/UV. On the basis of these results, the matrix of the real wastewaters could be more important during ozonation since its effect was more apparent than O<sub>3</sub>/UV application. Accordingly, Chen et al. [204] showed the degradation of N-Nitrosopyrrolidine (NPYR) in treated drinking water sample by ozone and O<sub>3</sub>/UV. Within just 1 min treatment, 15% and 80% of NPYR removal was observed by ozone and O<sub>3</sub>/UV treatment, respectively [204]. The sharp increase of micropollutant degradation at the very beginning of the O<sub>3</sub>/UV treatment was in agreement with our study.

More importantly, the overall IMI removal efficiency was remarkably improved by notable production of OH• during O<sub>3</sub>/UV, which is not surprising regarding that IMI is known as somewhat ozone-resistant due to containing electronegative moiety [23]. TBA results presented in this thesis study (given in Section 4.2.6) supported yet another confirmation. Additionally, the research study presented by Yao et al. [97] further confirms this idea. Their results demonstrated that ozone-resistant micropollutants (ibuprofen, clofibric acid, p-CBA and chloramphenicol) were more effectively abated by O<sub>3</sub>/UV compared to single ozonation for all studied water matrices. For instance, removal of aforementioned micropollutants from groundwater respectively increased from nearly 70, 55, 50 and 35% by ozonation to 85, 90, 85 and 75% by O<sub>3</sub>/UV. They concluded that O<sub>3</sub>/UV considerably enhanced O<sub>3</sub> decomposition to OH• under similar conditions of ozone reactor during the treatment of all water matrices [97].

Similar results considering improvement of micropollutant degradation performance have been reported in the case of thiacloprid removal from deionized water by O<sub>3</sub> and O<sub>3</sub>/UV [21]. Thiacloprid is one of the neonicotinoid insecticides which belongs to same chemical group with IMI. Although Cernigoj et al. [21] applied UVA irradiation ( $\lambda < 355$  nm), part of it ( $300 < \lambda < 320$ ) caused to decomposition of ozone and yielded radicals' production. Thiacloprid removal significantly increased when UV was added

to ozonation process. Indeed, thiacloprid with an initial concentration of 50 mg/L was degraded to nearly 15 and 7.5 mg/L within 30 min of ozonation and O<sub>3</sub>/UV application, respectively [21].

In the light of these studies and our results, O<sub>3</sub>/UV process for IMI degradation was proven to be efficient process, especially for removal of ozone-resistant micropollutants. Furthermore, the combination of biological treatment processes and AOPs has traditionally been applied for the treatment of effluents containing bio-resistant and biodegradable fractions [242]. When O<sub>3</sub>/UV process was applied to Bio WW, the combination of biological treatment and AOPs obviously showed enhanced IMI removal efficiency. Indeed, insufficient removal of IMI in the biologically treated wastewater was improved and the complete disappearance of IMI was achieved by applying O<sub>3</sub>/UV processes as an advanced treatment technique.

However, some limitations may occur for the application of O<sub>3</sub>/UV process in the real WWTPs. Since the secondary level treated effluent may have a dark color, the transmittance of the UV light will possibly decrease. Moreover, the total suspended solids in the effluent may cause UV light scattering. Although it is known that effluent of membrane bioreactor systems, which was used in this study (i.e. VRMBR WW), has lower turbidity than that of conventional WWTP, highly turbid effluents would need pre-treatment before O<sub>3</sub>/UV process. Indeed, these drawbacks are of concern, if O<sub>3</sub>/UV would be used. On the other hand, for the ozonation process, that limitation would not be a critical issue since there is no UV application.

#### **4.3.2. Photo-ozonation Mechanism of IMI Degradation**

The overall IMI disappearance should be investigated by considering several removal ways that are aforementioned in Section 2.5. Therefore, in addition to O<sub>3</sub> and oxidizing radicals, the disappearance of IMI could be achieved by H<sub>2</sub>O<sub>2</sub> and UV irradiation, as well. As stated in Eq. (13), UV radiation causes formation of H<sub>2</sub>O<sub>2</sub> by decomposition of O<sub>3</sub>. As mentioned previously, H<sub>2</sub>O<sub>2</sub> has oxidizing potential of 1.78 V (Table 4).

Guittonneau et al. [243] proved that under 253.7 nm UV irradiation, 1 mole of O<sub>3</sub> decomposition yields to 1 mole of H<sub>2</sub>O<sub>2</sub> production at pH less than 1.8. For higher pH values than 1.8, the H<sub>2</sub>O<sub>2</sub> yield ratio decreases as the pH increases. More importantly, under the conditions of room temperature and pH between 5 and 10, oxidation potential of H<sub>2</sub>O<sub>2</sub> is generally neglected [183]. Therefore, it can be clearly concluded that H<sub>2</sub>O<sub>2</sub> showed almost no oxidizing capability in this study since IMI ozonation was conducted at pH 7.25.

Furthermore, as stated in Section 2.5, UV irradiation can degrade micropollutants by itself. Ding et al. [168] investigated IMI degradation under 269 nm and its by-product formation. They used  $2 \times 10^{-4}$  M (~51 ppm) initial IMI concentration which was 50 times more than the concentration that was used in this thesis study (i.e. 1 ppm). They revealed that 95% of IMI was degraded within 40 hours. Furthermore, Moza et al. [166] showed that IMI with an initial concentration of 2 ppm was degraded nearly to 90% within 2 hours under 290 nm. Since the initial IMI concentrations, UV irradiation wavelengths and photon fluxes of referenced studies were different from our study, it is hard to compare their results with ours and evaluate the portion of IMI removal was achieved by UV. In spite of all, there is an overt evidence that UV irradiation also provides very slightly IMI removal in the aqueous solution. Therefore, IMI degradation by only UV was neglected.

In this thesis study, it was proved that the IMI disappearance strongly depends on the radical formation. For that reason, TBA was added during IMI ozonation in order to investigate direct and indirect mechanism during the IMI degradation.

### **O<sub>3</sub>-Only Removal Mechanism (TBA Addition)**

TBA was introduced into the reactor during IMI ozonation, in order to examine the effect of OH• on the IMI removal. The time-dependent degradation of IMI was further examined with and without the presence of TBA and the results were given in Figure 42.

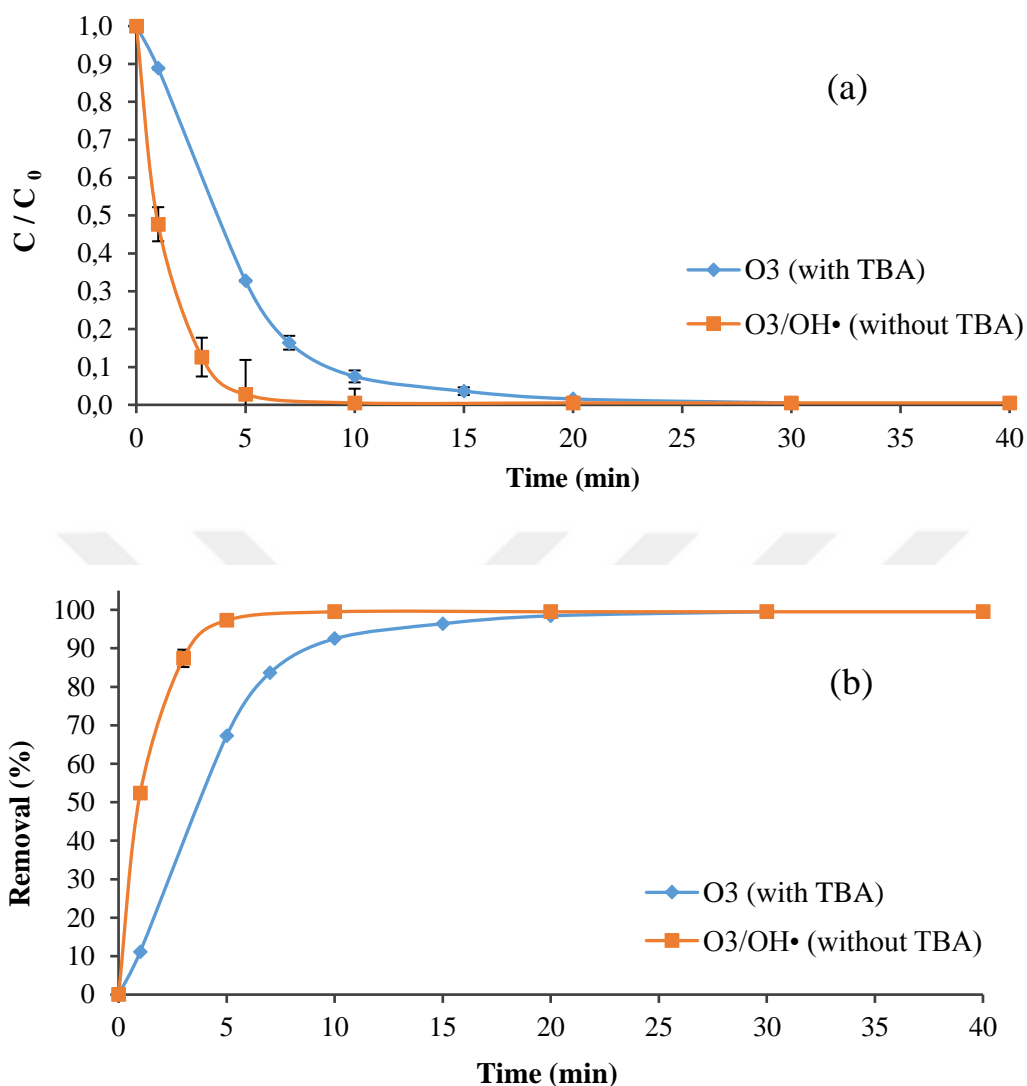


Figure 42. Time course variation of (a) IMI concentration (b) IMI removal efficiency by O<sub>3</sub> and O<sub>3</sub>/OH• i.e. with and without TBA addition, respectively. (Milli-Q water, C<sub>TBA</sub>=200 mM, [IMI]<sub>0</sub>= 1000 ppb, UV lamp= 10 W, O<sub>3</sub> dose= 1200 mg/h, O<sub>3</sub> flowrate= 30 L/h pH= 7.25 ± 0.1, T=24°C ±1°C.)

As seen in Figure 42, when TBA was added into the system, the available OH• should have been scavenged by TBA since the removal differences between O<sub>3</sub> and O<sub>3</sub>/OH• was pronounced. From the first minute of O<sub>3</sub>/UV, it was highly apparent that O<sub>3</sub>-only

mechanism did not remove IMI as much as the  $O_3/OH^\bullet$  mechanism did. While the 67% of IMI was removed by  $O_3$ -only (i.e. with TBA), 97% of IMI was degraded by  $O_3/OH^\bullet$  (i.e. without TBA) for the first 5 min of treatment process. In addition, disappearance of IMI under LOD concentration was achieved in 30 min and 10 min by  $O_3$ -only and  $O_3/OH^\bullet$  mechanisms, respectively.

Therefore, the high IMI removal rates during  $O_3/UV$  could be associated with the production of radicals especially  $OH^\bullet$ . As mentioned before, due to low reactivity of IMI with  $O_3$ , IMI abated almost exclusively by  $OH^\bullet$ . So, indirect mechanism was highly effective during  $O_3/UV$ . Chen et al. [204] obtained similar results during removal of NPYR, which is known as ozone-resistant micropollutant, by  $O_3/UV$  at pH 7. They conducted the experiments with and without TBA addition. After 300 seconds of degradation, nearly 58% and more than 95% NPYR was removed with and without TBA addition (i.e. by  $O_3$ -only and  $O_3/OH^\bullet$  mechanisms), respectively [204]. Likewise, the results obtained in this thesis study highlighted the significant role of  $OH^\bullet$  for ozone-resistant micropollutant removal, as well.

#### **4.3.3. Photo-ozonation By-Products of IMI**

The possible IMI degradation pathway and the potential  $O_3/UV$  by-products of IMI was investigated, and the results are given in this section. First of all, unlike for ozonation case, no-byproduct was detected by HPLC at the end of photo-ozonation experiment. On the other hand, there were still present by-products detected by LC-MS/MS, though smaller in number than in ozonation case. However, some by-products were common in both cases. Comparative presentation of the by-products is provided in Appendix C (Table C.1). Observing smaller number of by-products in photo-ozonation can be considered as another indication of better performance of photo-ozonation as compared ozonation.

The LC-MS/MS chromatograms of IMI photo-ozonation in Milli-Q water and VRMBR WW are given in Figure C.5 and Figure C.6 (Appendix C), respectively.

In both Milli-Q water and VRMBR WW, IMI ( $m/z$  256) was not detected, which shows that  $O_3/UV$  is successful treatment application for IMI removal. Moreover, the  $m/z$  209 ion, which was also detected during IMI fragmentation in ozonation case, was detected during  $O_3/UV$ , but it disappeared after 60 min of treatment. It could be either generated by subtracting  $HNO_2$  from IMI [22] or protonated form of IMI olefin desnitro [168]. Although Ding et al. [168] studied by-products of IMI photolysis, they observed protonated form of IMI olefin desnitro. In addition to  $m/z$  209 ion,  $m/z$  206 ion was also detected at almost same level with  $m/z$  209 ion. However, since the  $m/z$  206 ion was detected in the phosphate buffer solution, this ion was not taken into account while evaluating the IMI degradation pathway and produced by-products.

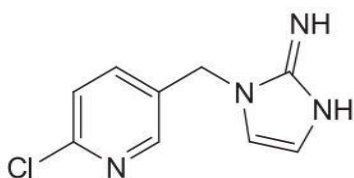


Figure 43. Imidacloprid olefin desnitro ( $m/z$  208) [168]

The  $m/z$  253 ion, which was also detected during IMI fragmentation in ozonation case, was detected during  $O_3/UV$  in both Milli-Q water and VRMBR WW. After 60 min of treatment, the  $m/z$  253 ion decreased to some degree, but it was not completely removed.

The ion at  $m/z$  186 was observed in only Milli-Q water analyzes (Figure C.5). During  $O_3/UV$ ,  $m/z$  186 ion was appeared from the very beginning (i.e. 5 min of treatment), then decreased and eventually disappeared. The presence of  $m/z$  186 could be via fragmentation of  $m/z$  230 which was mentioned as the way of  $m/z$  186 production during ozonation. However,  $m/z$  230 was not detected during  $O_3/UV$ . Indeed, this could show that it might be transformed into  $m/z$  186 within the first 5 min of treatment. Moreover, the ion at  $m/z$  270, which was also detected during ozonation,



decreased continuously during O<sub>3</sub>/UV in the VRMBR WW and disappeared to signal noise level (<1×10<sup>4</sup> area) after 60 min of treatment (Figure C.6). Hence, these studies showed that only 4 by-products were observed and just one of them (*m/z* 253) remained during O<sub>3</sub>/UV.

6-chloronicotinic acid has been reported by Moza et al. [166], Warmhoff and Schneider [167] and Ding et al. [168] as a major degradation product of IMI. Unlike referenced studies, 6-chloronicotinic acid was not detected in this study. One of the reasons could be that the initial concentration of IMI was not enough to yield detectable by-product in LC-MS/MS. Another reason, which was stated by Ding et al. [168], 6-chloronicotinic acid is far more sensitive to negative ion ESI mode whereas, our results were obtained in the positive ion ESI mode.

#### 4.4. Photo-ozonation (O<sub>3</sub>/UV) Reaction Kinetics

In order to investigate the treatment efficiency of UV coupled with ozone, kinetic study was conducted, and the results are given in this section. Indeed, water matrix effect on the kinetic rate was examined by comparing with the results obtained by ozonation. Furthermore, the results obtained from kinetic study of IMI degradation mechanism was also given.

Similar to ozonation experiments, ozone was excessively supplied into the system with respect to IMI concentration. Therefore, the degradation kinetic reactions of O<sub>3</sub>/UV process followed pseudo first-order kinetics which was also supported by the linear plot with a high R<sup>2</sup> value obtained by plotting the -ln(C/C<sub>0</sub>) against the time (min) graph.

The O<sub>3</sub>/UV degradation of IMI was exhibited pseudo first-order reaction, as following;

$$-\frac{d [IMI]}{dt} = k_{app} [IMI] \quad (28)$$

where;

[IMI]: Concentration of IMI

$k_{app}$ : The apparent pseudo first-order rate constant

#### 4.4.1. Effect of Water Matrix

The kinetic study of IMI degradation by the  $O_3/UV$  process, compared with ozonation, in different water matrices was investigated. The degradation kinetics of IMI followed pseudo-first order kinetics. The rate constants were determined by calculating the slope of the lines given in Figure 44.

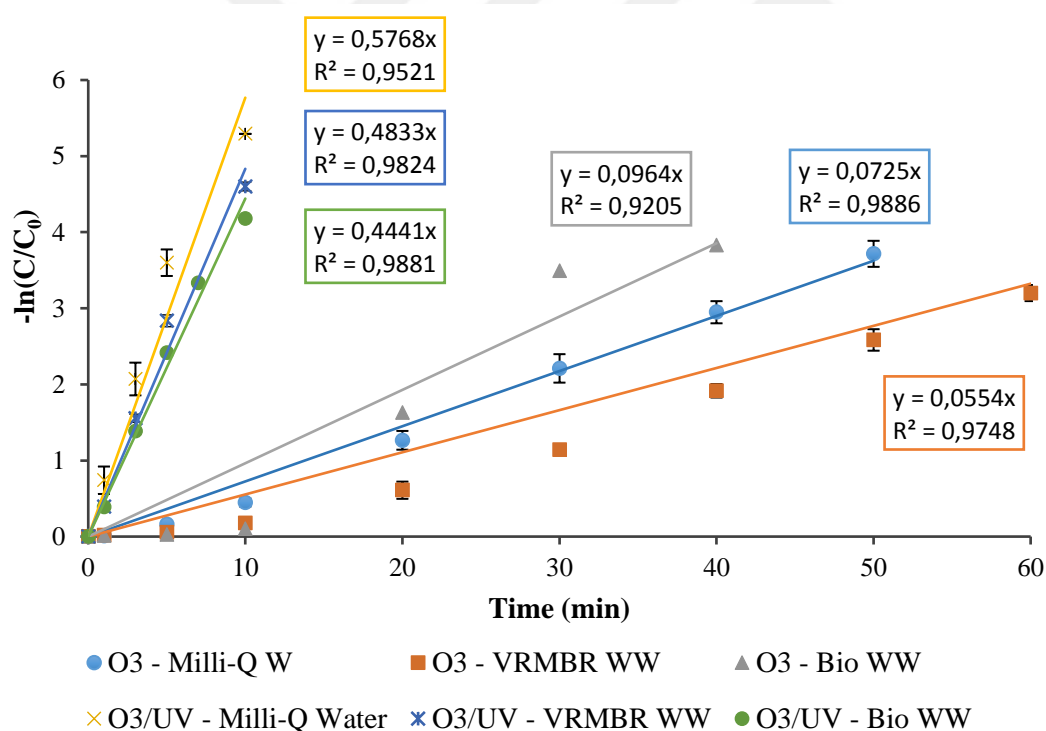


Figure 44. Reaction kinetics of IMI in different water matrices. ( $[IMI]_0 = 1000$  ppb for Milli-Q water and VRMBR WW,  $[IMI]_0 = 332$  ppb for Bio WW, UV lamp= 10 W,  $O_3$  dose= 1200 mg/h,  $O_3$  flowrate= 30 L/h pH=  $7.25 \pm 0.1$ ,  $T=24^\circ C \pm 1^\circ C$ .)

During O<sub>3</sub>/UV process, the apparent rate constants for water matrices Milli-Q, VRMBR WW and Bio WW were calculated as 0.5768, 0.4833 and 0.4441 min<sup>-1</sup>, respectively. During O<sub>3</sub>/UV process, the rate constant obtained in Milli-Q water was slightly higher than those gained in wastewaters, as expected.

On the other hand, compared to rate kinetics obtained during ozonation, O<sub>3</sub>/UV process apparently increased the reaction rate constants regardless of water matrices. Indeed, the reaction rate constants of O<sub>3</sub>/UV process were 8.0, 8.7 and 4.6 times higher than those obtained during ozonation in Milli-Q, VRMBR WW and Bio WW, respectively. The reason behind this remarkable improvement at rate constants is most likely due to the OH• and other radicals' production which were quite enhanced under UV irradiation [189]. These findings confirmed that IMI degradation kinetics strongly depend on OH• in the solution. Furthermore, the idea that O<sub>3</sub>/UV process highly enhanced degradation of ozone-resistant ones micropollutants was also proved in our study [204].

#### **4.4.2. Photo-ozonation Mechanism of IMI Degradation**

The kinetic study of IMI degradation mechanism was conducted in order to determine dominated mechanism. In this respect, TBA was added during photo-ozonation of IMI. Moreover, the indirect reaction rate constant of photo-ozonation was investigated by reference compound namely pCBA. In this section, the obtained kinetic rate constants are given, and the results are discussed by comparison with ozonation.

##### **O<sub>3</sub>-Only Removal Mechanism (TBA Addition)**

A kinetic study was established to delineate the contribution of OH• on the IMI degradation by introducing TBA was into the reactor during O<sub>3</sub>/UV of IMI in the Milli-Q water. Indeed, the obtained results showed that the scavenging effect of TBA was pronounced even from the very first minutes (Figure 45). The high correlation

coefficients  $R^2$  ranged from 0.9521 to 0.9808 proved that the apparent pseudo-first-order kinetics could fit the experimental results well.

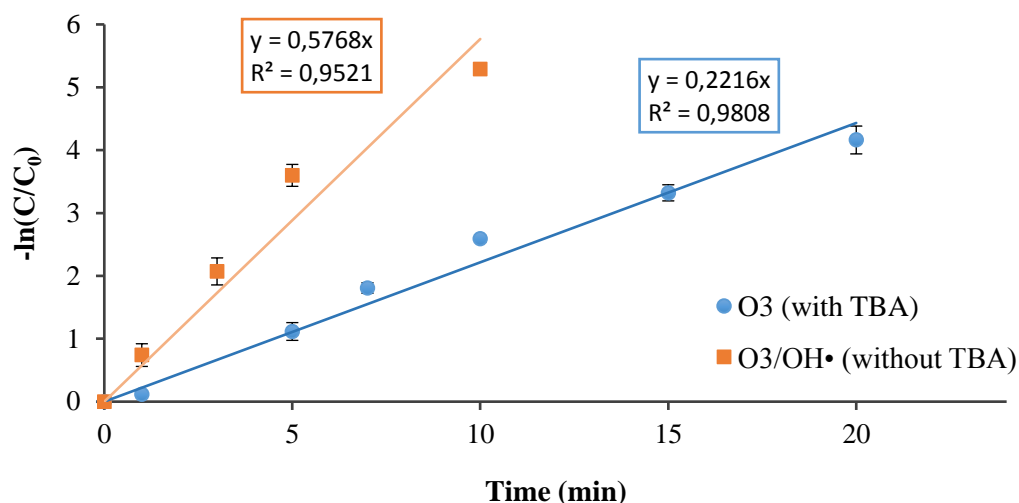


Figure 45. IMI degradation kinetics by  $O_3$  and  $O_3/OH^\bullet$  i.e. with and without TBA addition, respectively during  $O_3/UV$ . (Milli-Q water,  $C_{TBA}=200$  mM,  $[IMI]_0= 1000$  ppb, UV lamp= 10 W,  $O_3$  dose= 1200 mg/h,  $O_3$  flowrate= 30 L/h pH=  $7.25 \pm 0.1$ ,  $T=24^\circ C \pm 1^\circ C$ .)

When the  $OH^\bullet$  was scavenged by TBA, the removal rate constant of IMI by  $O_3$ -only mechanism was much less than the  $O_3/OH^\bullet$  mechanism. Indeed, the calculated slope of the fitted linear line presenting the  $O_3/OH^\bullet$  system (without TBA addition) is  $0.5768 \text{ min}^{-1}$ , which is 2.6 times higher than in the case of  $O_3$ -only removal (with TBA addition) mechanism (i.e.  $0.2216 \text{ min}^{-1}$ ). It clearly showed that the high IMI disappearance rates can be associated with the high production of  $OH^\bullet$ .

### **OH• Removal Mechanism (pCBA as a Reference Compound)**

Since the OH• cannot be measured directly during ozonation and O<sub>3</sub>/UV processes, competition kinetics method was used to determine the second-order rate constants for the reactions of IMI with OH•. pCBA which is a well-known reference compound is widely applied to indirectly measure OH•. In addition, measurement of probe compound, pCBA, is rather easy since it can be easily detected by HPLC. The pCBA reacts only OH• ( $k_{\text{OH}\cdot\text{-pCBA}} = 5 \times 10^9 \text{ M}^{-1}\text{s}^{-1}$ ) and not considerably reacts with other radicals or O<sub>3</sub> ( $k_{\text{O}_3\text{-pCBA}} = 0.15 \text{ M}^{-1}\text{s}^{-1}$ ) [210]. For that purpose, 5 μM pCBA was introduced into Milli-Q water at pH  $7.25 \pm 0.1$  in ozonation and O<sub>3</sub>/UV processes. The results are given comparatively in this section.

The kinetics of IMI degradation by OH• can be described as follows;

$$-\frac{d [\text{IMI}]}{dt} = k_{\text{OH}\cdot\text{-IMI}}[\text{IMI}][\text{OH}\cdot] \quad (29)$$

where,

$k_{\text{OH}\cdot\text{-IMI}}$ : The second-order rate constant of OH• with IMI

[IMI]: Concentration of IMI

[OH•]: Concentration of OH•

The degradation kinetics of pCBA by OH• can be described as;

$$-\frac{d [\text{pCBA}]}{dt} = k_{\text{OH}\cdot\text{-pCBA}}[\text{pCBA}][\text{OH}\cdot] \quad (30)$$

where,

$k_{\text{OH}\cdot\text{-pCBA}}$ : The second-order rate constant of OH• with pCBA

[pCBA]: Concentration of pCBA

[OH•]: Concentration of OH•

The ratio of integration of Eq. (29) and Eq. (30) yields to below equation;

$$\ln \frac{[IMI]_t}{[IMI]_0} / \ln \frac{[pCBA]_t}{[pCBA]_0} = k_{OH\cdot-IMI} / k_{OH\cdot-pCBA} \quad (31)$$

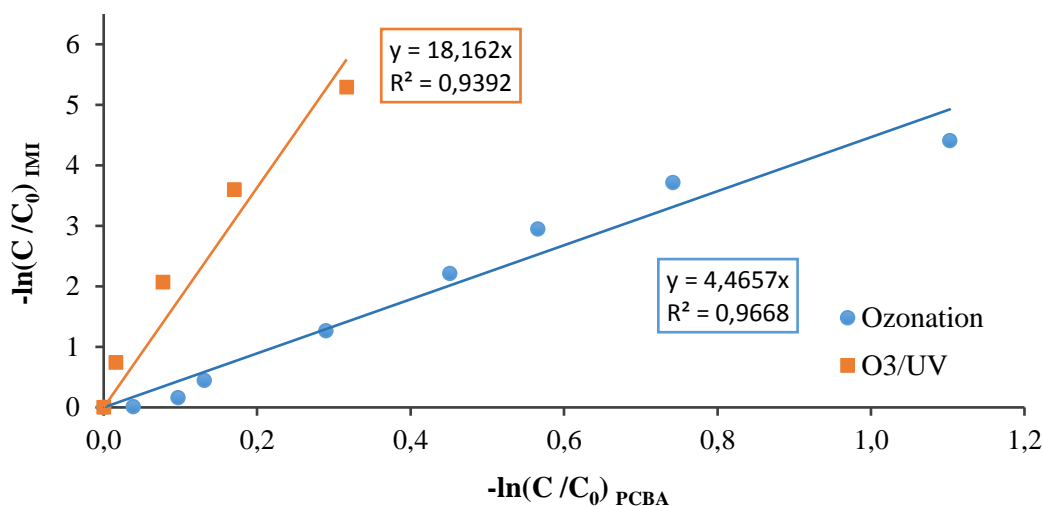


Figure 46. Natural logarithm of the relative concentration of IMI vs pCBA (Milli-Q water,  $C_{pCBA}=5 \mu\text{M}$ ,  $[IMI]_0=1000 \text{ ppb}$ ,  $O_3 \text{ dose}=1200 \text{ mg/h}$ ,  $O_3 \text{ flowrate}=30 \text{ L/h}$ ,  $\text{pH}=7.25 \pm 0.1$ ,  $T=24^\circ\text{C} \pm 1^\circ$ )

The left-hand side of Eq. (31) was calculated by the slope of the line (Figure 46). Since the reaction rate of  $\text{OH}\cdot$  with pCBA is  $5 \times 10^9 \text{ M}^{-1}\text{s}^{-1}$  [206] and the slope of the lines were calculated,  $k_{\text{OH}\cdot-IMI}$  could be easily obtained. During  $O_3/\text{UV}$ , the ratio of  $k_{\text{OH}\cdot-IMI} / k_{\text{OH}\cdot-pCBA}$  was  $18.162 \text{ M}^{-1}\text{s}^{-1}$  and hence, the second-order rate constant of IMI by  $\text{OH}\cdot$  ( $k_{\text{OH}\cdot-IMI}$ ) was calculated as  $9.08 \times 10^{11} \text{ M}^{-1}\text{s}^{-1}$ . On the other hand, during ozonation, the ratio of  $k_{\text{OH}\cdot-IMI} / k_{\text{OH}\cdot-pCBA}$  and  $k_{\text{OH}\cdot-IMI}$  were obtained as  $4.4657 \text{ M}^{-1}\text{s}^{-1}$  and  $2.23 \times 10^{11} \text{ M}^{-1}\text{s}^{-1}$ , respectively. This showed that  $k_{\text{OH}\cdot-IMI}$  was much higher in  $O_3/\text{UV}$  than ozonation. Furthermore, this could be another evidence for that IMI is

highly reactive toward to OH• since the production of OH• was boosted during the O<sub>3</sub>/UV process.

The study conducted by Chen et al. [201] showed that the second-order reaction rate of NPYR with OH• is  $1.38 \times 10^9 \text{ M}^{-1} \text{ s}^{-1}$  at pH 7 and at ozone concentration of 1 mg/L during O<sub>3</sub>/UV. They applied much less ozone than our study which could be the reason for that they obtained much less reaction rate than the one we calculated in this thesis study.







## CHAPTER 5

### CONCLUSION

Within the scope of this thesis study, removal of IMI from wastewater by ozonation and O<sub>3</sub>/UV was investigated in a comparative way. Main conclusions obtained from this study are summarized below:

- IMI could be removed by 96% - >99% from water by ozonation, depending on the operational conditions, such as pH buffering, solution pH, ozone dose, ozone concentration, initial IMI concentration. The IMI removal rates were also highly depending on these conditions with pseudo-first order rate constants varying between 0.0335 and 0.1288 min<sup>-1</sup>. The time required to reach to >99% removal was variable between 20 min and 180 min, accordingly. In this respect:
  - The effect of pH buffer on the IMI removal was highly evident. The IMI degradation reaction rate constant in buffered solution was found to be nearly 2-fold of the one obtained in unbuffered solution.
  - The pH of the solution strongly affected the IMI removal efficiency. Higher pH resulted in the higher IMI removal rates since the OH• generation was enhanced with the increase of pH. At pHs 7.30 and 8.25, 60 min and 20 min were enough, respectively, to remove IMI by >99%, whereas at least 120 min was required for the same IMI disappearance at pH 6.20 (ozone dose: 1200 mg/h).

- Ozone dose was found to be an important operational parameter as such that IMI disappearance by >99% was achieved within 120, 60 and 50 min when applying 600, 1200 and 1800 mg/h ozone doses, respectively.
- Ozone gas flowrate was found to affect the IMI removal rates remarkably as such that 99.8% of IMI disappearance occurred in 50, 60 and >180 min at the ozone flowrate of 15, 30, 100 L/h, respectively.
- IMI was degraded below LOD value within 40, 50 and 70 min corresponding 95.4%, 99% and 99.5% IMI disappearance for 100, 500 and 1000 ppb initial IMI concentrations (ozone dose: 1200 mg/h), respectively.
- Indirect mechanism (i.e. by OH•) dominated the IMI disappearance. The rate constants of IMI degradation by O<sub>3</sub>/OH• and O<sub>3</sub>-only were calculated as 0.0956 and 0.0595 min<sup>-1</sup>, respectively.
- Two by-products (BP-1 and BP-2) were detected by HPLC. BP-1 was not completely removed at the end of 180 min of ozonation for all the ozone doses applied. BP-2, on the other hand, disappeared within the same time interval when ozone dose was applied at 1200 and 1800 mg/h, but not at 600 mg/h.
- Radical scavenging capacity of wastewaters caused decrease in IMI disappearance. The apparent rate constant for water matrices of Milli-Q (spiked with IMI), secondary level treated real wastewater and secondary

level treated synthetic wastewater spiked with IMI was calculated as 0.0725, 0.0550 and 0.0964 min<sup>-1</sup>, respectively.

- The ozonation process coupled with 10-Watt UV improved IMI removal remarkably as compared to ozonation regardless of wastewater matrix. IMI disappearance by >99% became possible within only 10 min of process operation. Although wastewaters have OH• scavenging capacity, production rate of OH• and other radicals quite enhanced under UV irradiation. So, the overall IMI removal efficiency was remarkably improved compared to ozonation.
- The IMI degradation by O<sub>3</sub>/UV followed pseudo-first order kinetics, like for the ozonation case. However, the apparent rate constants (between 0.4441 - 0.5768 min<sup>-1</sup> depending on the water matrix) were remarkably different from those attained for ozonation. The kinetic study proved that the IMI degradation rate during O<sub>3</sub>/UV was 4.6 - 8.7 times higher than those obtained during ozonation, depending on operational conditions and water matrices.
- The water matrix effect on IMI removal was more pronounced during ozonation than during O<sub>3</sub>/UV.
- Like for the ozonation cases, IMI degradation by photo-ozonation is based on indirect mechanism.
- During treatment processes, total of 11 and 4 by-products were detected using LC-MS/MS in case of ozonation and photo-ozonation, respectively. Four of them were common in both cases. After ozonation and photo-ozonation treatments, 6 and 1 by-products remained, respectively. Smaller

number of by-products detected in case of photo-ozonation indicated that the performance of photo-ozonation is better than the ozonation to treat the IMI containing wastewaters. Based on the by-products detected, the IMI degradation pathway was proposed as same for both ozonation and photo-ozonation.

All in all, this thesis study showed that IMI is an ozone-resistant compound and its complete disappearance is mainly achieved by virtue of  $\text{OH}\cdot$ . As expected, IMI removal by ozonation and  $\text{O}_3/\text{UV}$  leads to the production of some by-products. Indeed,  $\text{O}_3/\text{UV}$  is more successful for the removal of these by-products than ozonation. To this end, photo-ozonation seems as a more promising advanced treatment technique as compared to ozonation.

## CHAPTER 6

### RECOMMENDATION

The following studies can be recommended for future researches:

- To ensure that human or aquatic health will not be impacted by IMI or its by-products, complete removal of IMI must be achieved. Indeed, in this thesis study, this has been followed via the measurements of both IMI and its by-products. However, as it was not possible to remove all of the by-products even with photo-ozonation, one cannot state that the toxicity of IMI has been totally removed. So, toxicity of untreated and treated samples would be investigated and correlated to the data obtained in this thesis regarding the appearance and disappearance of the by-products. In a way, the possible adverse effects of by-products would be clearly understood.
- As indicated in this thesis, water matrix plays an important role. So, to clarify this effect further, investigation of IMI treatment in the presence of different Natural Organic Matter content is recommended.



## REFERENCES

- [1] J. Jean, Y. Perrodin, C. Pivot, D. Trepo, M. Perraud, J. Droguet, F. Tissot-Guerraz and F. Locher, "Identification and prioritization of bioaccumulable pharmaceutical substances discharged in hospital effluents," *Journal of Environmental Management*, vol. 103, pp. 113-121, 2012.
- [2] A. Gogoi, P. Mazumder, V. K. Tyagi, T. Chaminda, A. K. An and M. Kumar, "Occurrence and fate of emerging contaminants in water environment: A review," *Groundwater for Sustainable Development*, vol. 6, pp. 169-180, 2018.
- [3] S. Chiron, A. R. Fernandez-Alba and A. Rodriguez, "Pesticide chemical oxidation processes: an analytical approach," *TrAC Trends in Analytical Chemistry*, vol. 16, no. 9, pp. 518-527, 1997.
- [4] N. Bolong, A. Ismail, M. Salim and T. Matsuura, "A review of the effects of emerging contaminants in wastewater and options for their removal.," *Desalination*, vol. 239, no. 1-3, pp. 229-246, 2009.
- [5] M. Zahoor and M. Mahramanlioglu, "Adsorption of Imidacloprid on Powdered Activated Carbon and Magnetic Activated Carbon," *Chem. Biochem. Eng.*, vol. 25, no. 1, pp. 55-63, 2011.
- [6] N. Genç, E. Doğan, A. Narıcı and E. Bican, "Multi-Response Optimization of Process Parameters for Imidacloprid Removal by Reverse Osmosis Using Taguchi Design," *Water Environ Res*, vol. 89, no. 5, pp. 440-450, 2017.
- [7] M. O. Barbosa, N. F. F. Moreira, A. R. Ribeiro, M. Pereira and A. Silva, "Occurrence and removal of organic micropollutants: An overview of the watch list of EU Decision 2015/495," *Water Research*, vol. 94, pp. 257-279, 2016.
- [8] D. Kanakaraju, B. Glass and M. Oelgemöller, "Advanced oxidation process-mediated removal of pharmaceuticals from," *Journal of Environmental Management*, vol. 219, pp. 189-207, 2018.
- [9] U. von Gunten, "Ozonation of drinkingwater: Part II. Disinfection and by-product formation in presence of bromide, iodide or chlorine," *Water Research*, vol. 37, p. 1469–1487, 2003.
- [10] J. Birkett and J. Lester, *Endocrine Disrupters in Wastewater and Sludge Treatment Processes*, Florida: CRC Press LLC, 2003.

- [11] European Commission (EC)., "Commission Directive 2009/90/EC of 31 July 2009 laying down, pursuant to Directive 2000/60/EC of the European Parliament and of the Council, technical specifications for chemical analysis and monitoring of water status," *Official Journal of the European Union*, vol. L 201/36, 1 August 2009.
- [12] European Commission, "Directive 2013/39/EU of the European Parliament and of the Council of 12 August 2013," *Official Journal of the European Union*, vol. L 226/1, 2013.
- [13] European Commission, "Introduction to the EU Water Framework Directive," 25 March 2019. [Online]. Available: [http://ec.europa.eu/environment/water/water-framework/info/intro\\_en.htm](http://ec.europa.eu/environment/water/water-framework/info/intro_en.htm). [Accessed 29 April 2019].
- [14] M. Moroglu and M. Yazgan, "Implementation of EU water framework directive in Turkey," *Desalination*, vol. 226, pp. 271-278, 2008.
- [15] Orman ve Su İşleri Bakanlığı, "YERÜSTÜ SU KALİTESİ YÖNETMELİĞİNDE DEĞİŞİKLİK YAPILMASINA DAİR YÖNETMELİK," *Resmi Gazete*, no. 29797, 10 August 2016.
- [16] M. Hadjikakou, P. G. Whitehead, L. Jin, M. Futter, P. Hadjinicolaou and M. Shahgedanova, "Modelling nitrogen in the Yeşilirmak River catchment in Northern Turkey: Impacts of future climate and environmental change and implications for nutrient management," *Science of The Total Environment*, vol. 409, no. 12, pp. 2404-2418, 2011.
- [17] A. Kurunc, K. Yurekli and F. Ozturk, "Effect of discharge fluctuation on water quality variables from the Yeşilirmak River," *Tarım Bilimleri Dergisi*, vol. 11, pp. 189-195, 2005.
- [18] A. Mandal and N. Singh, "Optimization of atrazine and imidacloprid removal from water using biochars: Designing single or multi-staged batch adsorption systems," *International Journal of Hygiene and Environmental Health*, vol. 220, no. 3, pp. 637-645, 2017.
- [19] C. Segura, C. Zaror, H. Mansilla and M. Mondaca, "Imidacloprid oxidation by photo-Fenton reaction," *Journal of Hazardous Materials*, vol. 150, pp. 679-686, 2008.
- [20] S. Malato, J. Blanco, J. Cacered, A. Fernandez-Alba, A. Agüera and A. Rodriguez, "Photocatalytic treatment of water-soluble pesticides by photo-



- Fenton and TiO<sub>2</sub> using solar energy," *Catalysis Today*, vol. 76, no. 2-4, pp. 209-220, 2002.
- [21] U. Cernigoj, U. L. Stangar and P. Trebse, "Degradation of neonicotinoid insecticides by different advanced oxidation processes and studying the effect of ozone on TiO<sub>2</sub> photocatalysis," *Applied Catalysis B: Environmental* 75, vol. 75, p. 229–238, 2007.
- [22] M. Bourgin, F. Violleau, L. Debrauwer and J. Albet, "Ozonation of imidacloprid in aqueous solutions: Reaction monitoring and identification of degradation products," *Journal of Hazardous Materials*, vol. 190, pp. 60-68, 2011.
- [23] S. Chen, J. Deng, Y. Deng and N. Gao, "Influencing factors and kinetic studies of imidacloprid degradation by ozonation," *Environmental Technology*, pp. 1-8, 2018.
- [24] S. Raut-Jadhav, V. Saharan, D. Pinjari, D. Saini, S. Sonawane and A. Pandit, "Intensification of degradation of imidacloprid in aqueous solutions by combination of hydrodynamic cavitation with various advanced oxidation processes (AOPs)," *Journal of Environmental Chemical Engineering*, vol. 1, pp. 850-857, 2013.
- [25] G. Reynolds, N. Graham, R. Perry and R. Rice, "Aqueous Ozonation of Pesticides-A Review," *Ozone Sci. Eng.*, vol. 11, no. 4, p. 339–382, 1989.
- [26] M. Clara, B. Strenn, E. Martinez, N. Kreuzinger and H. Kroiss, "Removal of selected pharmaceuticals, fragrances and endocrine disrupting compounds in a membrane bioreactor and conventional wastewater treatment plants," *Water Research*, vol. 39, p. 4797–4807, 2005.
- [27] C. Grandclement, I. Seyssiecq, A. Piram, P. Wong-Wah-Chung, G. Vanot, N. Tiliacos, N. Roche and P. Doumenq, "From the conventional biological wastewater treatment to hybrid processes, the evaluation of organic micropollutant removal: A review," *Water Research*, vol. 111, pp. 297-317, 2017.
- [28] S. Papoutsakis, *Enhancing the photo-Fenton treatment of contaminated water by use of ultrasound and iron-complexing agents*, 2015.
- [29] L. Hernandez Leal, N. Vieno, H. Temmink, G. Zeeman and C. Buisman, "Occurrence of xenobiotics in gray water and removal in three biological treatment systems," *Environ. Sci. Technol.*, vol. 44, pp. 6835-6842, 2010.

- [30] E. P. A. Victoria, "Point and nonpoint sources of water pollution," 31 August 2018. [Online]. Available: <https://www.epa.vic.gov.au/your-environment/water/protecting-victorias-waters/point-and-nonpoint-sources-of-water-pollution>. [Accessed 28 March 2019].
- [31] S. Mompelat, B. Bot and O. Thomas, "Occurrence and fate of pharmaceuticals products and by-products, from resource to drinking water," *Environ. Int.*, vol. 35, no. 5, pp. 803-814, 2009.
- [32] C. Daughton and T. A. Ternes, "Pharmaceuticals and personal care products in the environment: agents of subtle change?," *Environ Health Perspect.*, vol. 107, no. 6, pp. 907-938, 1999.
- [33] K.-R. Kim, G. Owens, S.-I. Kwon, K.-H. So, D.-B. Lee and Y. S. Ok, "Occurrence and Environmental Fate of Veterinary Antibiotics in the Terrestrial Environment," *Water, Air, and Soil*, vol. 214, no. 1-4, pp. 163-174, 2011.
- [34] G. R. Boyd, J. M. Palmeri, S. Zhang and D. A. Grimm, "Pharmaceuticals and personal care products (PPCPs) and endocrine disrupting chemicals (EDCs) in stormwater canals and Bayou St. John in New Orleans, Louisiana, USA," *Science of The Total Environment*, vol. 333, no. 1-3, pp. 137-148, 2004.
- [35] D. Ashton, M. Hilton and K. V. Thomas, "Investigating the environmental transport of human pharmaceuticals to streams in the United Kingdom," *Science of The Total Environment*, vol. 333, no. 1-3, pp. 167-184, 2004.
- [36] N. Lindqvist, T. Tuhkanen and L. Kronberg, "Occurrence of acidic pharmaceuticals in raw and treated sewages and in receiving waters," *Water Research*, vol. 38, no. 11, pp. 2219-2228, 2005.
- [37] N. Nakada, T. Tanishima, H. Shiohara, K. Kiri and H. Takada, "Pharmaceutical chemicals and endocrine disrupters in municipal wastewater in Tokyo and their removal during activated sludge treatment," *Water Research*, vol. 40, no. 17, pp. 3297-3303, 2006.
- [38] M. Carballa, F. Omil, T. Ternes and J. M. Lerna, "Fate of pharmaceutical and personal care products (PPCPs) during anaerobic digestion of sewage sludge," *Water Research*, vol. 41, no. 10, pp. 2139-2150, 2007.
- [39] R. Meffe and I. d. Bustamante, "Emerging organic contaminants in surface water and groundwater: A first overview of the situation in Italy," *Science of The Total Environment*, vol. 481, pp. 280-295, 2014.

- [40] T. P. Wood, C. S. J. Duvenage and E. Rohwer, "The occurrence of anti-retroviral compounds used for HIV treatment in South African surface water," *Environmental Pollution*, vol. 199, pp. 235-243, 2015.
- [41] S. Kumar, M. Nehra, N. Dilbaghi, G. Marrazza, A. A. Hassan and K.-H. Kim, "Nano-based smart pesticide formulations: Emerging opportunities for agriculture," *Journal of Controlled Release*, vol. 294, pp. 131-153, 2019.
- [42] H. A. Strydom, N. D. King, R. F. Fuggle and M. A. Rabie, "Pesticides," in *Environmental management in South Africa*, Juta, Cape Town, 2009, p. 746.
- [43] A. B. Vega, A. G. Frenich and J. M. Vidal, "Monitoring of pesticides in agricultural water and soil samples from Andalusia by liquid chromatography coupled to mass spectrometry," *Analytica Chimica Acta*, vol. 538, no. 1-2, pp. 117-127, 2005.
- [44] M. Köck-Schulmeyer, A. Ginebreda, C. Postigo, R. Lopez-Serna, S. Perez, R. Brix, M. Llorca, M. Lopez de Alda, M. Petrovic, A. Munne, L. Tirapu and D. Barcelo, "Wastewater reuse in Mediterranean semi-arid areas: The impact of discharges of tertiary treated sewage on the load of polar micro pollutants in the Llobregat river (NE Spain)," *Chemosphere*, vol. 82, no. 5, pp. 670-678, 2011.
- [45] Z. Vryzas, G. Vassiliou, C. Alexoudis and E. Papadopoulou-Mourkidou, "Spatial and temporal distribution of pesticide residues in surface waters in northeastern Greece," *Water Research*, vol. 43, no. 1, pp. 1-10, 2009.
- [46] D. Barcelo and M. Hennion, Trace determination of pesticides and their degradation products in water, Amsterdam: Elsevier, 1997.
- [47] W. Zhang, F. Jiang and J. Ou, "Global pesticide consumption and pollution: with China as a focus," *Proceedings of the International Academy of Ecology and Environmental Sciences*, vol. 1, no. 2, pp. 125-144, 2011.
- [48] D. Atwood and C. Paisley-Jones, "Pesticides Industry Sales and Usage," US EPA, Washington DC, 2017.
- [49] A. Ly, *Infographic: pesticide planet. Science*, 2013, p. 730–731..
- [50] S. Zou, W. Xu, R. Zhang, J. Tang, Y. Chen ve G. Zhang, «Occurrence and distribution of antibiotics in coastal water of the Bohai Bay, China: Impacts of river discharge and aquaculture activities,» *Environmental Pollution*, cilt 159, no. 10, pp. 2913-2920, 2011.

- [51] Y. Xu, H. Liu, C. Ren and Y. Sun, "Distributions of the triazine herbicides in the surface seawater of Laizhou Bay," *Progress in Fishery Sciences*, vol. 35, pp. 34-39, 2014.
- [52] H. Xie, X. Wang, J. Chen, X. Li, J. Gang, Y. Zou, Y. Zhang and Y. Cui, "Occurrence, distribution and ecological risks of antibiotics and pesticides in coastal waters around Liaodong Peninsula, China," *Science of the Total Environment*, vol. 656, pp. 946-951, 2019.
- [53] E. N. Papadakis, Z. Vryzas, A. Kotopoulou, K. Kintzikoglou, K. C. Makris and E. Papadopoulou-Mourkidou, "A pesticide monitoring survey in rivers and lakes of northern Greece and its human and ecotoxicological risk assessment," *Ecotoxicology and Environmental Safety*, vol. 116, pp. 1-9, 2015.
- [54] M. Köck-Schulmeyer, M. Villagrasa, M. Lopez de Alda, R. Céspedes-Sánchez, F. Ventura and D. Barcelo, "Occurrence and behavior of pesticides in wastewater treatment plants and their environmental impact," *Science of the Total Environment*, vol. 458, no. 460, pp. 466-476, 2013.
- [55] K. R. Ryberg and R. J. Gilliom, "Trends in pesticide concentrations and use formajor rivers of the United States," *Science of the Total Environment* , vol. 538, pp. 431-444, 2015.
- [56] A. J. Ebele, A.-E. Abdallah and S. Harrad, "Pharmaceuticals and personal care products (PPCPs) in the freshwater aquatic environment," *Emerging Contaminants*, vol. 3, pp. 1-16, 2017.
- [57] C. Purdom, P. Hardiman, V. Bye, N. Eno, C. Tyler and J. Sumpter, "Estrogenic effects of effluents from sewage treatment works," *J. Chem. Ecol.*, vol. 8, pp. 275-285, 1994.
- [58] R. Gomes and J. Lester, *Endocrine Disrupters in Receiving Waters*, Boca Raton: CRC Press, 2003.
- [59] K. Jones, M. Everard and A. Harding, "Investigation of gastrointestinal effects of organophosphate and carbamate pesticide residues on young children," *International Journal of Hygiene and Environmental Health*, vol. 217, no. 2-3, pp. 392-398, 2014.
- [60] L. Wang, H. M. Espinoza, J. MacDonald, T. K. Bammler, C. R. Williams, A. Yeh, K. W. Louie, D. J. Marcinek and E. P. Gallagher, "Olfactory Transcriptional Analysis of Salmon Exposed to Mixtures of Chlorpyrifos and Malathion Reveal Novel Molecular Pathways of Neurobehavioral Injury," *Toxicological Sciences*, vol. 149, no. 1, p. 145–157, 2016.

- [61] J. M. Hatcher, K. C. Delea, J. R. Richardson, K. D. Pennell and G. W. Miller, "Disruption of dopamine transport by DDT and its metabolites," *NeuroToxicology*, vol. 29, no. 4, pp. 682-690, 2008.
- [62] T. Colborn, "Clues from wildlife to create an assay for thyroid system disruption," *Endocrine Disruptors*, vol. 110, no. 3, pp. 363-367, 2002.
- [63] M. C. Kennedy, R. Glass, B. Bokkers, A. D. Hart, P. Y. Harney, J. Kruisselbrink, W. de Boer, H. van der Voet, D. G. Garthwaite and J. van Klaveren, "A European model and case studies for aggregate exposure assessment of pesticides," *Food and Chemical Toxicology*, vol. 79, pp. 32-44, 2015.
- [64] L. Cao, H. Zhang, F. Li, Z. Zhou, W. Wang, D. Ma, L. Yang, P. Zhou and Q. Huang, "Potential dermal and inhalation exposure to imidacloprid and risk assessment among applicators during treatment in cotton field in China," *Science of the Total Environment*, vol. 624, pp. 1195-1201, 2018.
- [65] A. E. Larsen, S. D. Gaines and O. Deschenes, "Agricultural pesticide use and adverse birth outcomes in the San Joaquin Valley of California," *Nature Communications*, vol. 8, pp. 1-9, 2017.
- [66] P. Jeschke and R. Nauen, "Neonicotinoid Insecticides," in *Comprehensive Molecular Insect Science*, L. I. Gilbert, K. Iatrou and S. S. Gill, Eds., Chapel Hill, North Carolina: Elsevier Pergamon, 2005, pp. 53-105.
- [67] M. Henry, M. Beguin, F. Requier, O. Rollin, J. Odoux, P. Aupinel, J. Aptel, S. Tchamitchian and A. Decourtye, "A Common Pesticide Decreases Foraging Success and Survival in Honey Bees," *Science*, vol. 336, pp. 348-350, 2012.
- [68] D. Stanley, M. Garratt, J. Wickens, V. Wickens, S. Potts and N. Raine, "Neonicotinoid pesticide exposure impairs crop pollination services provided by bumblebees," *Nature*, vol. 528, pp. 548-550, 2015.
- [69] S. Ghasemian, D. Nasuhoglu, S. Omanovic and V. Yargeau, "Photoelectrocatalytic degradation of pharmaceutical carbamazepine using Sb-doped Sn80%-W20%-oxide electrodes," *Separation and Purification Technology*, vol. 188, pp. 52-59, 2017.
- [70] J. Park, N. Yamashita, C. Park, T. Shimono, D. M. Takeuchi and T. Hiroaki, "Removal characteristics of pharmaceuticals and personal care products: Comparison between membrane bioreactor and various biological treatment processes," *Chemosphere*, vol. 179, pp. 347-358, 2017.

- [71] J. Tijana, O. Fatoba and L. Petrik, "Review of pharmaceuticals and endocrine-disrupting compounds: sources, effects, removal, and detections," *Water Air Soil Pollution*, vol. 224, no. 11, pp. 1-29, 2013.
- [72] M. Carballa, F. Omil, J. Lerna, M. Llombart, C. Garcia-Jares, I. Rodriguez, M. Gomez and T. Ternes, "Behavior of pharmaceuticals, cosmetics and hormones in a sewage treatment plant," *Water Research*, vol. 38, no. 12, pp. 2918-2926, 2004.
- [73] Y. Nie, Z. Qiang, H. Zhang and W. Ben, "Fate and seasonal variation of endocrine-disrupting chemicals in a sewage treatment plant with A/A/O process," *Separation and Purification Technology*, vol. 84, pp. 9-15, 2012.
- [74] A. Jelic, M. Gros, A. Ginebreda, R. Cespedes-Sanchez, F. Ventura, M. Petrovic and D. Barcelo, "Occurrence, partition and removal of pharmaceuticals in sewage water and sludge during wastewater treatment," *Water Research*, vol. 45, no. 3, pp. 1165-1176, 2011.
- [75] J. Radjenovic, M. Petrovic and D. Barcelo, "Fate and distribution of pharmaceuticals in wastewater and sewage sludge of the conventional activated sludge (CAS) and advanced membrane bioreactor (MBR) treatment," *Water Research*, vol. 43, no. 3, pp. 831-841, 2009.
- [76] R. Salgado, R. Marques, J. Noronha, G. Carvalho, A. Oehmen and M. Reis, "Assessing the removal of pharmaceuticals and personal care products in a full-scale activated sludge plant," *Environmental Science and Pollution Research*, vol. 19, no. 5, pp. 1818-1827, 2012.
- [77] T. Ternes, A. Joss and H. Siegrist, "Scrutinizing pharmaceuticals and personal care products in wastewater treatment," *Environ. Sci. Technol.*, vol. 38, p. 392A-399A, 2004.
- [78] N. Stamatis, D. Hela and I. Konstantinou, "Occurrence and removal of fungicides in municipal sewage treatment," *Journal of Hazardous Materials*, vol. 175, pp. 829-835, 2010.
- [79] R. Mailler, J. Gasperi, S. Gilbert-Pawlik, D. Geara-Matta, R. Moilleron and G. Chebbo, "Biofiltration vs conventional activated sludge plants: what about priority and emerging pollutants removal?," *Environmental Science and Pollution Research*, vol. 21, no. 8, pp. 5379-5390, 2014.
- [80] R. Mailler, J. Gasperi, Y. Coquet, S. Deshayes, S. Zedek, C. Cren-Olive, N. Cartiser, V. Eudes, A. Bressy, E. Caupos, R. Moilleron, G. Chebbo and V. Rocher, "Study of a large scale powdered activated carbon pilot: Removals of

a wide range of emerging and priority micropollutants from wastewater treatment plant effluent," *Water Research*, vol. 72, pp. 315-330, 2015.

- [81] A. R. Ribeiro, O. C. Nunes, M. F. Pereira and A. M. Silva, "An overview on the advanced oxidation processes applied for the treatment of water pollutants defined in the recently launched Directive 2013/39/EU," *Environment International journal*, vol. 75, pp. 33-51, 2015.
- [82] J. Margot, C. Kienle, A. Magnet, M. Weil, L. Rossi, L. Alencastro, C. Abegglen, D. Thonney, N. Chevre, M. Schärer and D. Barry, "Treatment of micropollutants in municipal wastewater: Ozone or powdered activated carbon?," *Science of the Total Environment*, Vols. 461-462, pp. 480-498, 2013.
- [83] C. Jung, J. Oh and Y. Yoon, "Removal of acetaminophen and naproxen by combined coagulation and adsorption using biochar: influence of combined sewer overflow components," *Environ Sci Pollut Res Int.*, vol. 22, no. 13, pp. 10058-69, 2015.
- [84] D. Huang, X. Wang, C. Zhang, G. Zeng, Z. Peng, J. Zhou, M. Cheng, R. Wang, Z. Hu and X. Qin, "Sorptive removal of ionizable antibiotic sulfamethazine from aqueous solution by graphene oxide-coated biochar nanocomposites: Influencing factors and mechanism," *Chemosphere*, vol. 186, pp. 414-421, 2017.
- [85] M. Dehghani, S. Kamalian, M. Shayeghi, M. Yousefi, Z. Heidarinejad, S. Agarwal and V. Gupta, "High-performance removal of diazinon pesticide from water using multi-walled carbon nanotubes," *Microchemical Journal*, vol. 145, pp. 486-491, 2019.
- [86] A. Cruz-Alcalde, C. Sans and S. Esplugas, "Priority pesticides abatement by advanced water technologies: The case of acetamiprid removal by ozonation," *Science of the Total Environment*, Vols. 599-600, pp. 1454-1461, 2017.
- [87] A. Cruz-Alcalde, C. Sans and S. Esplugas, "Priority pesticide dichlorvos removal from water by ozonation process: Reactivity, transformation products and associated toxicity," *Separation and Purification Technology*, vol. 192, pp. 123-129, 2018.
- [88] A. Cruz-Alcalde, Sans C. and S. Esplugas, "Exploring ozonation as treatment alternative for methiocarb and formed transformation products abatement," *Chemosphere*, vol. 186, pp. 725-732, 2017.
- [89] K. M. Hansen, A. Spiliotopoulou, R. K. Chhetri, M. E. Casas, K. Bester and H. K. Andersen, "Ozonation for source treatment of pharmaceuticals in hospital

wastewater – Ozone lifetime and required ozone dose," *Chemical Engineering Journal*, vol. 290, pp. 507-514, 2016.

- [90] K. B. Orhon, A. Koc Orhon, F. B. Dilek and U. Yetis, "Triclosan removal from surface water by ozonation - Kinetics and by-products formation," *Journal of Environmental Management*, vol. 204, pp. 327-336, 2017.
- [91] M. G. Antoniou, G. Hey, S. R. Vega, A. Spiliotopoulou, J. Fick, M. Tysklind, J. I. C. JanseN and H. R. Andersan, "Required ozone doses for removing pharmaceuticals from wastewater effluent," *Science of the Total Environment journal*, vol. 456, no. 457, pp. 42-49, 2013.
- [92] J. Gomes, R. Costa, R. M. Quinta-Ferreira and R. C. Martins, "Application of ozonation for pharmaceuticals and personal care products removal from water," *Science of the Total Environment*, vol. 586, pp. 265-283, 2017.
- [93] M. Bourgin, B. Beck, M. Boehler, E. Borowska, J. Fleiner, E. Salhi, R. Teichler, U. von Gunten, H. Siegrist and C. McArdell, "Evaluation of a full-scale wastewater treatment plant upgraded with ozonation and biological post-treatments: Abatement of micropollutants, formation of transformation products and oxidation by-products," *Water Research*, vol. 129, pp. 486-498, 2018.
- [94] F. Almomani, M. Shawaqfah, R. Bhosale and A. Kumar, "Removal of emerging pharmaceuticals from wastewater by ozone-based advanced oxidation processes," *Environmental Progress and Sustainable Energy*, vol. 35, pp. 982-995, 2016.
- [95] Z. Qiang, C. Liu, B. Dong and Y. Zhang, "Degradation mechanism of alachlor during direct ozonation and O<sub>3</sub>/H<sub>2</sub>O<sub>2</sub> advanced oxidation process," *Chemosphere*, vol. 78, no. 5, pp. 517-526, 2010.
- [96] K. Lekkerkerker-Teunissen, A. Knol, L. van Altena, C. Houtman, J. Verberk and J. van Dijk, "Serial ozone/peroxide/low pressure UV treatment for synergistic and effective organic micropollutant conversion," *Separation and Purification Technology*, vol. 100, pp. 22-29, 2012.
- [97] W. Yao, S. W. U. Rehman, H. Wang, H. Yang, G. Yu and Y. Wang, "Pilot-scale evaluation of micropollutant abatements by conventional ozonation, UV/O<sub>3</sub>, and an electro-peroxone process," *Water Research*, vol. 138, pp. 106-117, 2018.



- [98] G. Marquez, E. M. Rodriguez, F. J. Beltrán and P. M. Álvarez, "Solar photocatalytic ozonation of a mixture of pharmaceutical compounds in water," *Chemosphere*, vol. 113, pp. 71-78, 2014.
- [99] L. Prieto-Rodriguez, S. Miralles-Cuevas, I. Oller, A. Agüera, G. L. Puma and S. Malato, "Treatment of emerging contaminants in wastewater treatment plants (WWTP) effluents by solar photocatalysis using low TiO<sub>2</sub> concentrations," *Journal of Hazardous Materials*, Vols. 211-212, pp. 131-137, 2012.
- [100] S. Sanchis, A. Polo, M. Tobajas, J. Rodriguez and A. Modehano, "Coupling Fenton and biological oxidation for the removal of nitrochlorinated herbicides from water," *Water Research*, vol. 49, pp. 197-206, 2014.
- [101] C. Zaror, C. Segura, H. Mansilla, M. Mondaca and P. Gonzalez, "Effect of temperature on Imidacloprid oxidation by homogeneous photo-Fenton processes," *Water Science & Technology*, vol. 58, no. 1, pp. 259-265, 2008.
- [102] C. James, E. Germain and S. Judd, "Micropollutant removal by advanced oxidation of microfiltered secondary effluent for water reuse," *Separation and Purification Technology*, vol. 127, p. 77-83, 2014.
- [103] A. Mohammadi, M. Kazemipour, H. Ranjpar, R. Walker and M. Ansari, "Amoxicillin removal from aqueous media using multi-walled carbon nanotubes," *Fuller. Nanotub. Carbon Nanostruct.*, vol. 23, pp. 165-169, 2014.
- [104] S. Caranbineiro, T. Thavorn-Amornsri, M. Pereira, P. Serp and J. Figueiredo, "Comparison between activated carbon, carbon xerogel and carbon nanotubes for the adsorption of the antibiotic ciprofloxacin," *Catalysis Today*, vol. 186, pp. 29-34, 2012.
- [105] H. Peng, B. Pan, M. Wu, Y. Liu, D. Zhang and B. Xing, "Adsorption of ofloxacin and norfloxacin on carbon nanotubes: Hydrophobicity- and structure-controlled process," *Journal of Hazardous Materials*, Vols. 233-234, pp. 89-96, 2012.
- [106] H. Co, H. Huang and K. Schwab, "Effects of solution chemistry on the adsorption of ibuprofen and triclosan onto carbon nanotubes," *Langmuir* 27, vol. 27, no. 21, pp. 12960-12967, 2011.
- [107] M. S. Santos, A. Alves and M. Madeira, "Paraquat removal from water by oxidation with Fenton's reagent," *Chemical Engineering Journal*, vol. 175, pp. 279-290, 2011.

- [108] R. Andreozzi, V. Caprio, A. Insola and R. Marotta, "Advanced oxidation processes (AOP) for water purification and recovery," *Catalysis Today*, vol. 53, no. 1, pp. 51-59, 1999.
- [109] D. Miklos, C. Remy, M. Jekel, K. Linden, J. Drewes and U. Hübner, "Evaluation of advanced oxidation processes for water and wastewater treatment e A critical review David," *Water Research*, vol. 139, pp. 118-131, 2018.
- [110] Y. Luo, W. Guo, H. Ngo, L. Nghiem, F. Hai, J. Zhang, S. Liang and X. Wang, "A review on the occurrence of micropollutants in the aquatic environment and their fate and removal during wastewater treatment," *Science of the Total Environment journal*, Vols. 473-474, pp. 619-641, 2014.
- [111] E. C. Catalkaya and F. Kargi, "Degradation and Mineralization of Simazine in Aqueous Solution by Ozone/Hydrogen Peroxide Advanced Oxidation," *Journal of Environmental Engineering*, vol. 12, p. 135, 2009.
- [112] D. Kanakaraju, B. D. Glass and M. Oelgemöller, "Advanced oxidation process-mediated removal of pharmaceuticals from water: A review," *Journal of Environmental Management*, vol. 219, pp. 189-207, 2018.
- [113] N. De la Cruz, J. Gimenez, S. Esplugas, D. Grandjean, L. de Alencastro and C. Pulgarin, "Degradation of 32 emergent contaminants by UV and neutral photo-fenton in domestic wastewater effluent previously treated by activated sludge," *Water Research*, vol. 46, no. 6, pp. 1947-1957, 2012.
- [114] I. Yamamoto, M. Tomizawa, T. Saito, T. Miyamoto, E. C. Walcott and K. Sumikawa, "Structural factors contributing to insecticidal and selective actions of neonicotinoids," *Archives of Insect Biochemistry and Physiology*, vol. 37, no. 1, pp. 24-32, 1998.
- [115] B. Eskenazi, A. Bradman and R. Castorina, "Exposures of children to organophosphate pesticides and their potential adverse health effects," *Environ Health Perspect.*, vol. 107, pp. 409-419, 1999.
- [116] C. A. Morrissey, P. Mineau, J. H. Devries, F. Sanchez-Bayo, M. Liess, M. C. Cavallaro and K. Liber, "Neonicotinoid contamination of global surface waters and associated risk to aquatic invertebrates: A review," *Environmental International*, vol. 74, pp. 291-303, 2015.
- [117] W. Han, Y. Tian and X. Shen, "Human exposure to neonicotinoid insecticides and the evaluation of their potential toxicity: An overview," *Chemosphere*, vol. 192, pp. 59-65, 2018.

- [118] N. Simon-Delso, V. Amaral-Rogers, L. P. Belzunces, J. M. Bonmatin, M. Chagnon, C. Downs, L. Furlan, D. W. Gibbons, C. Giorio, V. Girolami, D. Goulson, D. P. Kreutzweiser, C. H. Krupke, M. Liess, E. Long, M. McField, P. Mineau, E. A. D. Mitchell, C. A. Morissey, D. A. Noome, L. Pisa, J. Settele, J. D. Stark, A. Tapparo, H. Van Dyck, J. Van Praagh, J. P. Van der Sluijs, P. R. Whitehorn and M. Wiemers, "Systemic insecticides (neonicotinoids and fipronil): trends, uses, mode of action and metabolites," *Environ Sci Pollut Res*, vol. 22, no. 5, pp. 5-34, 2015.
- [119] US Environmental Protection Agency (US EPA), "Rotam Imidacloprid 70WG Insecticide," Washington D.C., 2013.
- [120] R. Nauen, P. Jeschke and L. Copping, "In Focus: neonicotinoid insecticides," *Pest Management Science*, vol. 64, no. 11, p. 1081, 2008.
- [121] C. Bass, I. Denholm, M. S. Williamson and R. Nauen, "The global status of insect resistance to neonicotinoid insecticides," *Pesticide Biochemistry and Physiology*, vol. 121, pp. 78-87, 2015.
- [122] T. Iwasa, N. Motoyama, J. T. Ambrose and R. M. Roe, "Mechanism for the differential toxicity of neonicotinoid insecticides in the honey bee, *Apis mellifera*," *Crop Protection*, vol. 23, no. 5, p. 371–378, 2004.
- [123] L. W. Pisa, V. Amaral-Rogers, L. Belzunces, J. Bonmatin, C. Downs, D. Goulson, D. Kreutzweiser, C. Krupke, M. Liess, M. McField, C. Morissey, D. A. Noome, J. Settele, N. Simon-Delso, J. Stark, J. P. Van der Sluijs, H. Van Dyck and M. Wiemers, "Effects of neonicotinoids and fipronil on non-target invertebrates," *Environ Sci Pollut Res*, vol. 22, no. 1, p. 68–102, 2015.
- [124] T. Tisler, A. Jemec, B. Mozetic and P. Trebse, "Hazard identification of imidacloprid to aquatic environment," *Chemosphere*, vol. 76, pp. 907-914, 2009.
- [125] T. J. Wood and D. Goulson, "The environmental risks of neonicotinoid pesticides: a review of the evidence post 2013," *Environ Sci Pollut Res*, vol. 24, pp. 17285-17325, 2017.
- [126] P. Jeschke, R. Nauen, M. Schindler and A. Elbert, "Overview of the Status and Global Strategy for Neonicotinoids," *Journal of Agricultural and Food Chemistry*, no. 59, pp. 2897-2908, 2010.
- [127] S. Wagner, "Environmental Fate of Imidacloprid," Sacramento, CA, 2016.

- [128] C. Tomlin, *The Pesticide Manual, A World Compendium*, Surry, England: British Crop Protection Council, 2006, pp. 598-599.
- [129] J. M. Bonmatin, C. Giorio, V. Girolami, D. Goulson, D. P. Kreutzweiser, C. Krupke, M. Liess, E. Long, M. Marzaro, E. A. D. Mitchell, D. A. Noome, N. Simon-Delso and A. Tapparo, "Environmental fate and exposure; neonicotinoids and fipronil," *Environ Sci Pollut Res*, no. 22, pp. 35-67, 2015.
- [130] W. Zheng and W. Liu, "Kinetics and mechanism of the hydrolysis of imidacloprid," *Pesticide Science*, vol. 55, pp. 482-485, 1999.
- [131] J. Struger, J. Grabuski, S. Cagampan, E. Sverko, D. McGoldrick and C. H. Marvin, "Factors influencing the occurrence and distribution of neonicotinoid insecticides in surface waters of southern Ontario, Canada," *Chemosphere*, vol. 169, pp. 516-523, 2017.
- [132] F. Sanchez-Bayo and R. V. Hyne, "Detection and analysis of neonicotinoids in river waters – Development of a passive sampler for three commonly used insecticides," *Chemosphere*, vol. 99, pp. 143-151, 2014.
- [133] Canadian Council of Ministers of the Environment, "Canadian water quality guidelines for the protection of aquatic life: Imidacloprid. Scientific Supporting Document," Winnipeg, 2007.
- [134] M. Sarkar, S. Roy, R. Kole and A. Chowdhury, "Persistence and metabolism of imidacloprid in different soils of West Bengal," *Pest Management Science*, vol. 57, no. 7, pp. 598-602, 2001.
- [135] M. L. Hladik, D. W. Kolpin and K. M. Kuivila, "Widespread occurrence of neonicotinoid insecticides in streams in a high corn and soybean producing region, USA," *Environmental Pollution*, vol. 193, pp. 189-196, 2014.
- [136] V. Iancu and G. Radu, "Occurrence of neonicotinoids in waste water from the Bucharest treatment plant," *Royal Society of Chemistry*, vol. 10, p. 2691–2700, 2018.
- [137] A. Sadaria, S. Supowit and R. Halden, "Mass Balance Assessment for Six Neonicotinoid Insecticides during Conventional Wastewater and Wetland Treatment: Nationwide Reconnaissance in United States Wastewater," *Environmental Science and Technology*, vol. 50, no. 12, pp. 6199-6206, 2016.
- [138] A. Ccancapa, A. Masia, A. Navarro-Ortega and Y. Pico, "Pesticides in the Ebro River basin: Occurrence and risk assessment," *Environmental Pollution*, vol. 211, pp. 414-424, 2016.

- [139] A. Masia, J. Campo, P. Vazquez-Roig, C. Blasco and Y. Pico, "Screening of currently used pesticides in water, sediments and biota of the Guadalquivir River Basin (Spain)," *Journal of Hazardous Materials*, vol. 263, no. 1, pp. 95-104, 2013.
- [140] A. Ccancapa, A. Masia, V. Andreu and Y. Pico, "Spatio-temporal patterns of pesticide residues in the Turia and Júcar Rivers (Spain)," *Science of the Total Environment*, vol. 540, pp. 200-210, 2016.
- [141] A. Masia, J. Campo, A. Navarro-Ortega, D. Barcelo and Y. Pico, "Pesticide monitoring in the basin of Llobregat River (Catalonia, Spain) and comparison with historical data," *Science of the Total Environment*, Vols. 503-504, pp. 58-68, 2015.
- [142] C. D. Linde, "Physico-chemical properties and Environmental Fate of Pesticides," California, 1994.
- [143] V. Triantafyllidis, S. Manos, D. Hela, G. Manos and I. Konstantinou, "Persistence of trifluralin in soil of oilseed rape fields in Western Greece," *International Journal of Environmental and Analytical Chemistry*, vol. 90, no. 3-6, p. 344-356, 2010.
- [144] R. Calvet, "Adsorption of organic chemicals in soils," *Environmental Health Perspectives*, vol. 83, pp. 145-177, 1989.
- [145] L. Mamy and E. Barriuso, "Desorption and time-dependent sorption of herbicides in soils," *European Journal of Soil Science*, vol. 58, no. 1, p. 174-187, 2007.
- [146] S. K. Papiernik, W. C. Koskinen, L. Cox, P. J. Rice, S. A. Clay, N. R. Werdin-Pfisterer and K. A. Nonberg, "Sorption-Desorption of Imidacloprid and Its Metabolites in Soil and Vadose Zone Materials," *Journal of Agricultural and Food Chemistry*, no. 54, pp. 8163-8170, 2006.
- [147] L. Nemeth-Konda, G. Füleky, G. Morovjan and P. Csokan, "Sorption behaviour of acetochlor, atrazine, carbendazim, diazinon, imidacloprid and isoproturon on Hungarian agricultural soil," *Chemosphere*, no. 48, pp. 545-552, 2002.
- [148] M. Bajeer, S. Nizamani, S. Sherazi and M. Bhanger, "Adsorption and Leaching Potential of Imidacloprid Pesticide through Alluvial Soil," *American Journal of Analytical Chemistry*, vol. 3, pp. 604-611, 2012.

- [149] L. Cox, W. Koskinen and P. Yen, "Changes in Sorption of Imidacloprid with Incubation Time," *Soil Science Society of America Journal*, vol. 62, no. 2, pp. 342-247, 1998.
- [150] M. Oi, "Time-Dependent Sorption of Imidacloprid in Two Different Soils," *J. Agric. Food Chem*, vol. 47, no. 1, p. 327–332, 1999.
- [151] W. Liu, W. Zheng, Y. Ma and K. K. Liu, "Sorption and Degradation of Imidacloprid in Soil and Water," *Journal of Environmental Science and Health Part B*, vol. 41, p. 623–634, 2006.
- [152] D. Goulson, "An overview of the environmental risks posed by neonicotinoid insecticides," *Journal of Applied Ecology*, vol. 50, pp. 977-987, 2013.
- [153] K. Banerjee, S. Patil, S. Dasgupta, D. Oulkar and P. Adsule, "Sorption of thiamethoxamin three Indian soils," *J Environ Sci Health B*, vol. 43, pp. 151-156, 2008.
- [154] EFSA Scientific Report, "Conclusion regarding the peer review of the pesticide risk assessment of the active substance, Imidacloprid," European Food Safety Authority, 2009.
- [155] H. Selim, C. Jeong and T. Elbana, "Transport of Imidacloprid in Soils: Miscible Displacement Experiments," *Soil Science*, vol. 175, pp. 375-381, 2010.
- [156] J. Bonmatin, C. Giorio, V. Girolami, D. Goulson, D. Kreuzweiser, C. Krupke, M. Liess, E. Long, M. Marzaro, E. Mitchell, D. Noome, N. Simon-Delso and A. Tapparo, "Environmental fate and exposure; neonicotinoids and fipronil.," *Environ Sci Pollut Res Int*, vol. 22, pp. 35-67, 2015.
- [157] S. Hussain, C. Hartley, M. Shettigar and G. Pandey, "Bacterial biodegradation of neonicotinoid pesticides in soil and water systems," *FEMS Microbiology Letters*, vol. 363, pp. 1-13, 2016.
- [158] S. Phugare, D. Kalyani, Y. Gaikwad and J. Jadhav, "Microbial degradation of imidacloprid and toxicological analysis of its biodegradation metabolites in silkworm (*Bombyx mori*)," *Chemical Engineering Journal*, vol. 230, pp. 27-35, 2013.
- [159] K. Scholz and M. Spiteller, "Influence of groundcover on the degradation of <sup>14</sup>C-imidacloprid in soil," *Brighton Crop Prot. Conf. Pests Dis.*, vol. 2, pp. 883-888, 1992.

- [160] J. Anhalt, T. Moorman and W. Koskinen, "Biodegradation of imidacloprid by an isolated soil microorganism," *J Environ Sci Health B*, vol. 42, no. 5, pp. 509-514, 2007.
- [161] N. Sabourmoghaddam, M. Zakaria and D. Omar, "Evidence for the microbial degradation of imidacloprid in soils of Cameron Highlands," *ournal of the Saudi Society of Agricultural Sciences*, vol. 14, pp. 182-188, 2015.
- [162] R. Akoijam and B. Singh, "Biodegradation of imidacloprid in sandy loam soil by *Bacillus aerophilus*," *Int J Environ An Ch*, vol. 95, pp. 730-743, 2015.
- [163] A. Shetti and B. Kaliwal, "Biodegradation of imidacloprid by soil isolate *Brevunimonas* sp," *MJ15. Intern J Curr Res*, vol. 4, pp. 100-106, 2012.
- [164] M. Gopal, D. Dutta and S. Jha, "Biodegradation of imidacloprid and metribuzin by *Burkholderia cepacia* strain CH9," *Pesticide Res J*, vol. 23, p. 36-40., 2011.
- [165] M. Kandil, C. Trigo, W. Koskinen and M. Sadowsky, "Isolation and characterization of a novel imidacloprid-degrading *Mycobacterium* sp. strain MK6 from an Egyptian soil," *J Agr Food Chem*, vol. 63, no. 19, pp. 4721-4727, 2015.
- [166] P. Moza, K. Hustert, E. Feicht and A. Kettrup, "Photolysis of Imidacloprid in Aqueous Solution," *Chemosphere*, vol. 36, no. 3, pp. 497-502, 1998.
- [167] H. Wamhoff and V. Schneider, "Photodegradation of Imidacloprid," *J. Agric. Food Chem.*, vol. 47, p. 1730-1734, 1999.
- [168] T. Ding, D. Jacobs and B. K. Lavine, "Liquid chromatography-mass spectrometry identification of imidacloprid photolysis products," *Microchemical Journal*, vol. 99, pp. 535-541, 2011.
- [169] J. Bacey, "Environmental Fate of Imidacloprid," California.
- [170] M. A. Sarkar, P. K. Biswas, S. Roy, R. K. Kole and A. Chowdhury, "Effect of pH and Type of Formulation on the Persistence of Imidacloprid in Water," *Bulletin of Environmental Contamination and Toxicology*, vol. 63, pp. 604-609, 1999.
- [171] S. Malato, M. Caceres, A. Agüera, M. Mezcua, D. Hernando, J. Vial and A. R. Fernandez-Alba, "Degradation of imidacloprid in water by photo-Fenton and TiO<sub>2</sub> photocatalysis at a solar pilot plant: A comparative study," *Environmental Science and Technology*, vol. 35, pp. 4359-4366, 2001.
- [172] A. Mandal, N. Singh and T. Purakayastha, "Characterization of pesticide sorption behaviour of slow pyrolysis biochars as low cost adsorbent for atrazine

- and imidacloprid removal," *Science of Total Environment*, vol. 577, pp. 376-385, 2017.
- [173] U. Y. Kouakou, A. Dembele, A. Y. Yobouet and A. Trokourey, "Removal of Imidacloprid using Activated Carbon from Coconut Shells," *International Journal of Advanced Research in Science, Engineering and Technology*, vol. 3, no. 8, pp. 2573-2581, 2016.
- [174] E. Gonzalez-Pradas, M. Villafranca-Sanchez, M. Socias-Viciano, M. Fernandez-Perez and M. Urena-Amate, "Preliminary studies in removing atrazine, isoproturon and imidacloprid from water by natural sepiolite," *Journal of Chemical Technology and Biotechnology*, vol. 74, no. 5, pp. 417-422, 1999.
- [175] N. Daneshvar, S. Aber, A. Khani and A. Khataee, "Study of imidacloprid removal from aqueous solution by adsorption onto granular activated carbon using an on-line spectrophotometric analysis system," *Journal of Hazardous Materials*, vol. 144, pp. 47-51, 2007.
- [176] J. Lopez, A. Reina, E. Gomez, M. Martin, S. Malato and J. Perez, "Integration of Solar Photocatalysis and Membrane Bioreactor for Pesticides Degradation," *Separation Science and Technology*, vol. 45, no. 11, pp. 1571-1578, 2010.
- [177] R. Zabar, T. Komel, J. Fabjan, M. B. Kralj and P. Trebse, "Photocatalytic degradation with immobilised TiO<sub>2</sub> of three selected neonicotinoid insecticides: Imidacloprid, thiamethoxam and clothianidin," *Chemosphere*, vol. 89, no. 3, pp. 293-301, 2012.
- [178] V. Kitsiou, N. Filippidis, D. Mantzavinos and I. Poulios, "Heterogeneous and homogeneous photocatalytic degradation of the insecticide imidacloprid in aqueous solutions," *Applied Catalysis B: Environmental*, vol. 86, no. 1-2, pp. 27-35, 2009.
- [179] A. L. Patil, P. N. Patil and P. R. Gogate, "Degradation of imidacloprid containing wastewaters using ultrasound based treatment strategies," *Ultrasonics Sonochemistry*, vol. 21, p. 1778-1786, 2014.
- [180] A. Paitl, P. Patil and P. Gogate, "Degradation of imidacloprid containing wastewaters using ultrasound based treatment strategies," *Ultrasonics Sonochemistry*, vol. 21, pp. 1778-1786, 2014.
- [181] P. Patil and P. Gogate, "Degradation of methyl parathion using hydrodynamic cavitation: Effect of operating parameters and intensification using additives," *Separation and Purification Technology*, vol. 95, pp. 172-179, 2012.



- [182] M. Horvath, L. Bilitzky and J. Hüttner, *Ozone*, Amsterdam ; New York : Elsevier, 1985.
- [183] C. Gottschalk, J. Libra and A. Saupe, *Ozonation of Water and Waste Water*, Weinheim: WILEY, 2010.
- [184] D. Sabirov and I. Shepelevich, "Information entropy of oxygen allotropes. A still open discussion about the closed form of ozone," *Computational and Theoretical Chemistry*, vol. 1073, pp. 61-66, 2015.
- [185] B. Langlais, D. Reckhow and D. Brink, *Ozone in Water Treatment: Application and Engineering*, Chelsea, Michigan, USA: Lewis Publisher, 1991.
- [186] M. Eriksson, *Ozone chemistry in aqueous solution and stabilisation*, Stockholm: Department of Chemistry Royal Institute of Technology , 2004.
- [187] S. Parsons, *Advanced Oxidation Processes for Water and Wastewater Treatment*, London UK: IWA Publishing, 2004.
- [188] C. v. Sonntag and U. v. Gunten, *Chemistry of Ozone in Water and Wastewater Treatment-From Basic Principles to Applications*, London: IWA, 2012.
- [189] J. Staehelin and J. Hoigne, "Decomposition of ozone in water: rate of initiation by hydroxide ions and hydrogen peroxide," *Environ. Sci. Technol.*, vol. 16, pp. 676-681, 1982.
- [190] S. C. Iglesias, "Degradation and biodegradability enhancement of nitrobenzene and 2,4-dichlorophenol by means of Advanced Oxidation Processes based on ozone," Universidad de Barcelona, 2002.
- [191] R. Criegee, "Mechanism of Ozonolysis," *Angewandte Chemie International Edition in English*, vol. 14, no. 11, pp. 745-752, 1975.
- [192] J. Hollender, S. Zimmermann, S. Koepke, M. Krauss, C. Mcardell and C. Ort, "Elimination of organic micropollutants in a municipal wastewater treatment plant upgraded with a full scale post-ozonation followed by sand filtration," *Environ Sci Technol*, Vols. 7862-7869, p. 43, 2009.
- [193] V. Yargeau and C. Leclair, "Impact of operating conditions on decomposition of antibiotics during ozonation: a review," *Ozone: Sci. Eng.*, vol. 30, pp. 175-188, 2008.

- [194] Y. Wang, H. Zhang, J. Zhang, C. Lu, Q. Huang, J. Wu and F. Liu, "Degradation of tetracycline in aqueous media by ozonation in an internal loop-lift reactor," *Journal of Hazardous Materials*, vol. 192, pp. 35-43, 2011.
- [195] X. Jin, S. Peldszus and P. Huck, "Reaction kinetics of selected micropollutants in ozonation and advanced oxidation processes," *Water Research*, vol. 46, pp. 6519-6530, 2012.
- [196] Y. Jung, W. Kim, Y. Yoon, T. Hwang and J. Kang, "pH Effect on Ozonation of Ampicillin: Kinetic Study and," *Ozone: Science & Engineering*, vol. 34, p. 156-162, 2012.
- [197] Y. Lee and U. von Gunten, "Oxidative transformation of micropollutants during municipal wastewater treatment: Comparison of kinetic aspects of selective (chlorine, chlorine dioxide, ferrateVI, and ozone) and non-selective oxidants (hydroxyl radical)," *Water Research*, vol. 44, no. 2, pp. 555-566, 2012.
- [198] F. Benitez, J. Acero, F. Real and G. Roldan, "Ozonation of pharmaceutical compounds: Rate constants and elimination in various water matrices," *Chemosphere*, vol. 77, pp. 53-59, 2009.
- [199] J. Hoigne and H. Bader, "The role of hydroxyl radical reactions in ozonation processes in aqueous solutions," *Water Research*, vol. 10, no. 5, pp. 377-386, 1976.
- [200] W. Glaze, J. Kang and D. Chapin, "The chemistry of water treatment processes involving ozone, hydrogen peroxide and ultraviolet radiation," *Ozone Sci. Eng.*, vol. 9, pp. 335-352, 1987.
- [201] X. Wang, X. Huang, C. Zuo and H. Hu, "Kinetics of quinoline degradation by O<sub>3</sub>/UV in aqueous phase," *Chemosphere*, vol. 55, pp. 733-741, 2004.
- [202] J. Staehelin and J. Hoigne, "Decomposition of Ozone in Water in the Presence of Organic Solutes Acting as Promoters and Inhibitors of Radical Chain Reactions\*," *Environ. Sci. Technol.*, vol. 19, pp. 1206-1213, 1985.
- [203] S. Irmak, O. Erbatur and A. Akgerman, "Degradation of 17 $\beta$ -estradiol and bisphenol A in aqueous medium by using ozone and ozone/UV techniques," *Journal of Hazardous Materials B*, vol. 126, p. 54-62, 2005.
- [204] Z. Chen, J. Fang, C. Fan and C. Shang, "Oxidative degradation of N-Nitrosopyrrolidine by the ozone/UV process: Kinetics and pathways," *Chemosphere*, vol. 150, pp. 731-739, 2016.

- [205] T. Lau, W. Chu and N. Graham, "Degradation of the endocrine disruptor carbofuran by UV, O<sub>3</sub> and O<sub>3</sub>/UV," *Water Science & Technology*, vol. 55, no. 12, p. 275–280, 2007.
- [206] U. Yetis, "Tübitak Araştırma Projesi Gelişme Raporu," Ankara, 2017.
- [207] K. Kocaman, *Fate and Removal of Pesticides in Wastewater Treatment Plants- Case of Yeşilirmak Basin*, Ankara: METU, 2019.
- [208] K. Rackness, G. Gordon, B. Langlais, W. Masschelein, N. Matsumoto, Y. Richard, C. M. Robson and I. Somiya, "Guideline for Measurement of Ozone Concentration in the Process Gas From an Ozone Generator," *Ozone Science & Engineering*, vol. 18, pp. 209-229, 1996.
- [209] J. Hoigne and H. Bader, "Rate constants of reactions of ozone with organic and inorganic compounds in water," *Water Research*, vol. 17, no. 2, p. 173e183, 1983.
- [210] M. Elovitz and U. von Gunten, "Hydroxyl Radical/Ozone Ratios During Ozonation Processes. I. The Rct Concept," *Ozone: Science and Engineering*, vol. 21, pp. 239-260, 1999.
- [211] J. Peris-Vicente, J. Esteve-Romero and S. Carda-Broch, "Validation of Analytical Methods Based on Chromatographic," in *Analytical Separation Science*, vol. First edition, Wiley-VCH Verlag GmbH & Co., 2015, pp. 1-52.
- [212] J. Vial and A. Jarly, "Experimental Comparison of the Different Approaches To Estimate LOD and LOQ of an HPLC Method," *American Chemical Society*, vol. 71, no. 14, p. 2672–2677, 1999.
- [213] M. Franson, "DPDColormetric Method," in *Standard Methods for the Examination of Water and Wastewater*, Washington, DC, American Public Health Association, 1976, p. 332–334.
- [214] K. A. Buchan, D. J. Martin-Robichaud and T. J. Benfey, "Measurement of dissolved ozone in sea water: A comparison of methods," *Aquacultural Engineering*, no. 33, p. 225–231, 2005.
- [215] M. Metzger, "Ozone Applications and Measurements," *Water Conditioning & Purification*, August 2009.
- [216] J. R. Bolton, M. I. Stefan, P. S. Shaw and K. R. Lykke, "Determination of the quantum yields of the potassium ferrioxalate and potassium iodide–iodate actinometers and a method for the calibration of radiometer detectors," *Journal*

*of Photochemistry and Photobiology A: Chemistry*, vol. 222, pp. 166-169, 2011.

- [217] R. Rahn, "Potassium iodide as a chemical actinometer for 254 nm radiation: use of iodide as an electron scavenger," *Photochem. Photobiol*, vol. 66, no. 4, pp. 450-455, 1997.
- [218] A. E. Burgess and J. C. Davidson, "A Kinetic–Equilibrium Study of a Triiodide Concentration Maximum Formed by the Persulfate–Iodide Reaction," *J. Chem. Educ.*, vol. 89, no. 6, pp. 814-816, 2012.
- [219] X. Li, J. Ma, G. Liu, J. Fang, S. Yue, Y. Guan, L. Chen and X. Liu, "Effective reductive dechlorination of monochloroacetic acid by sulfite/ UV process," *Environ Sci Technol*, vol. 46, no. 13, pp. 7342-7349, 2012.
- [220] J. Restivo, J. Orfao, S. Armenise, E. Garcia-Bordeje and M. Pereira, "Catalytic ozonation of metolachlor under continuous operation using nanocarbon materials grown on a ceramic monolith," *Journal of Hazardous Materials jou*, vol. 239, no. 240, pp. 249-256, 2012.
- [221] M. S. Lucas, J. A. Peres and G. L. Puma, "Treatment of winery wastewater by ozone-based advanced oxidation processes (O<sub>3</sub>, O<sub>3</sub>/UV and O<sub>3</sub>/UV/H<sub>2</sub>O<sub>2</sub>) in a pilot-scale bubble column reactor and process economics," *Separation and Purification Technology*, vol. 72, pp. 235-241, 2010.
- [222] G. Boczkaj and A. Fernandes Gdansk, "Wastewater treatment by means of advanced oxidation processes at basic pH conditions: A review," *Chemical Engineering Journal journal*, vol. 320, pp. 608-633, 2017.
- [223] P. Chelme-Ayala, M. G. El-Din and D. W. Smith, "Kinetics and mechanism of the degradation of two pesticides in aqueous solutions by ozonation," *Chemosphere*, vol. 78, pp. 557-562, 2010.
- [224] Department of the Army, "Evaluation Criteria Guide for Water Pollution Prevention, Control and Abatement Programs," Washington DC, 1987.
- [225] M. Sui, S. Xing, L. Sheng, S. Huang and H. Guo, "Heterogeneous catalytic ozonation of ciprofloxacin in water with carbon nanotube supported manganese oxides as catalyst," *Journal of Hazardous Materials jou*, vol. 227–228, pp. 227-236, 2012.
- [226] B. Thalmann, U. von Gunten and R. Kaegi, "Ozonation of municipal wastewater effluent containing metal sulfides and metal complexes: Kinetics and mechanisms," *Water Research*, vol. 134, pp. 170-180, 2018.

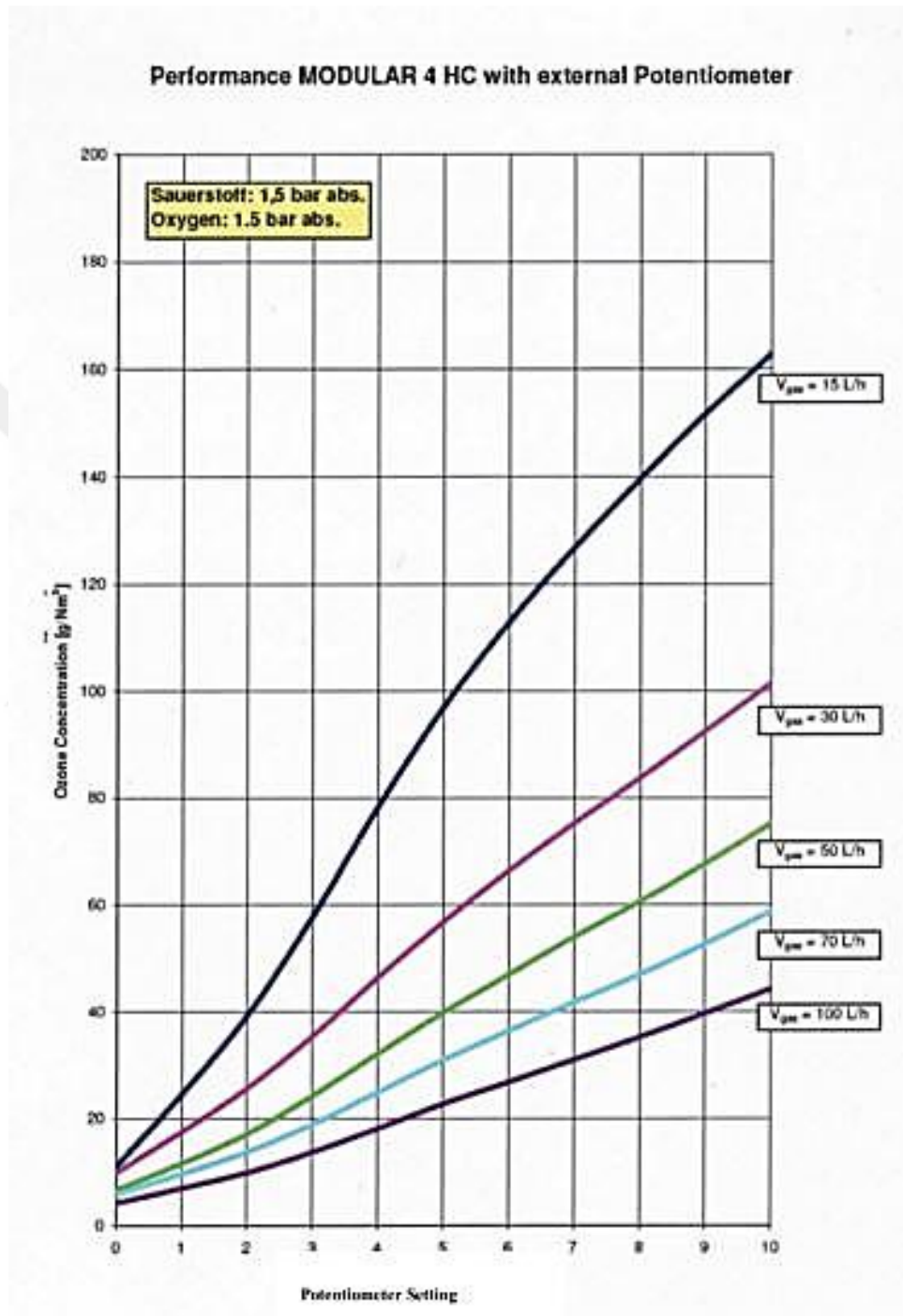
- [227] K. Ikehata and M. G. El-Din, "Aqueous Pesticide Degradation by Ozonation and Ozone-Based Advanced Oxidation Processes: A Review (Part I)," *Ozone: Science & Engineering*, vol. 27, pp. 83-114, 2005.
- [228] L. Rizzo, "Bioassays as a tool for evaluating advanced oxidation processes in water and wastewater treatment," *Water Research*, vol. 45, pp. 4311-4340, 2011.
- [229] A. Prasetyaningrum, D. A. Kusumaningtyas, P. Suseno, B. Jos and Ratnawati, "Effect of pH and Gas Flow Rate on Ozone Mass Transfer of K-Carrageenan Solution in Bubble Column Reactor," *Reaktor*, vol. 18, no. 4, pp. 177-182, 2018.
- [230] J. J. Wu and S. J. Masten, "Mass Transfer of Ozone in Semibatch Stirred Reactor," *Journal of Environmental Engineering*, vol. 127, no. 12, pp. 1089-1099, 2001.
- [231] E. Borowska, M. Bourgin, J. Hollender, C. Kienle, C. S. McArdell and U. v. Gunten, "Borowska, E., Bourgin, M., Hollender, J., Kienle, C., McArdell, C. S., & von Gunten, U. (2016). Oxidation of cetirizine, fexofenadine and hydrochlorothiazide during ozonation: Kinetics and formation of transformation products," *Water Research*, vol. 94, p. 350–362, 2016.
- [232] M. Sanchez-Polo, U. v. Gunten and J. Rivera-Utrilla, "Efficiency of activated carbon to transform ozone into d OH," *Water Research*, vol. 39, p. 3189–3198, 2005.
- [233] Y. Liu, J. Jiang, J. Ma, Y. Yang, C. Luo and X. Huangfu, "Role of the propagation reactions on the hydroxyl radical formation in ozonation and peroxone (ozone/hydrogen peroxide) processes," *Water Research*, vol. 68, pp. 750-758, 2015.
- [234] J. L. Acero, F. F. Real, F. J. Benitez and E. Matamoros, "Degradation of neonicotinoids by UV irradiation: Kinetics and effect of real water constituents," *Separation and Purification Technology*, vol. 211, pp. 218-226, 2019.
- [235] D. Gardoni, A. Vailati and R. Canziani, "Decay of Ozone in Water: A Review," *Ozone: Science & Engineering*, vol. 34, pp. 233-242, 2012.
- [236] J. L. Acero and U. Von Gunten, "Characterization of Oxidation Processes: ozonation and the AOP O<sub>3</sub>/H<sub>2</sub>O<sub>2</sub>," *Journal Awwa*, pp. 90-100, 2001.
- [237] S. Phattarapattamawong, Kaiser A. M., E. Saracevic, H. P. Schaar and J. Krampe, "Optimization of ozonation and peroxone process for simultaneous

control of micropollutants and bromate in wastewater," *Water Science and Technology*, vol. 2, pp. 404-411, 2017.

- [238] J. Grant, "UV-Advanced Oxidation Treatment Of Micropollutants In Secondary Wastewaters," 2015.
- [239] N. Nakada, H. Shinohara, A. Murata, K. Kiri, S. Managaki, N. Sato and H. Takada, "Removal of selected pharmaceuticals and personal care products (PPCPs) and endocrine-disrupting chemicals (EDCs) during sand filtration and ozonation at a municipal sewage treatment plant," *Water Research*, vol. 41, p. 4373–4382, 2007.
- [240] L. Kovalova, H. Siegrist, U. von Gunten, J. Eugster, M. Hagenbuch, A. Wittmer, R. Moser and C. McArdell, "Elimination of Micropollutants during Post-Treatment of Hospital Wastewater with Powdered Activated Carbon, Ozone, and UV," *Environ. Sci. Technol.*, vol. 47, p. 7899–7908, 2013.
- [241] M. Lucas, J. Peres and G. Puma, "Treatment of winery wastewater by ozone-based advanced oxidation processes (O<sub>3</sub>, O<sub>3</sub>/UV and O<sub>3</sub>/UV/H<sub>2</sub>O<sub>2</sub>) in a pilot-scale bubble column reactor and process economics," *Separation and Purification Technology*, vol. 72, p. 235–241, 2010.
- [242] C. Comninellis, A. Kapalka, S. Malato, S. A. Parsons, I. Poulios and D. Mantzavinos, "Advanced oxidation processes for water treatment: advances and trends for R&D," *Journal of Chemical Technology & Biotechnology*, vol. 83, no. 6, pp. 769-776, 2008.
- [243] P. Guittonneau, J. De Laat and M. Dore, "Kinetic study of the photodecomposition of aqueous ozone by UV irradiation at 253.7 nm," *Environmental Technology*, vol. 11, pp. 477-490, 1990.

## APPENDICES

### A. OZONE GENERATOR'S PERFORMANCE CURVE



## B. LC-MS/MS METHOD INFORMATION

Equipment	AGILENT 6460 LCMSMS					
Ionization source	ESI+Agilent Jet Stream					
Pump	AGILENT BinPump-SL (G1312B9)					
Autosampler	AGILENT h-ALS-SL+ (G1367D)					
Column Compartment	AGILENT G1316B 1200 Series Thermost. Col. Compart SL					
Micro degasser	AGILENT G1379B 1200 Series Micro Degasser					
Software	AGILENT G3793AA, MassHunter Optimizer software					
Nitrogen Gen.	Nitrogen generator UHPLCMS 30					
Scan Mode	MRM					
Gas Temp.	300 °C					
Gas Flow	9ml/min					
Nebulizer	45 psi					
Sheath Gas Temp.	300 °C					
Sheath Gas Flow	9ml/min					
Capillary	400V					
Nozzle Voltage	1500 V					
<b>LIQUID CHROMATOGRAPHY</b>						
Equipment	AGILENT 1200 HPLC Series					
Column	Poroshell 120 SB-C18 (3×100mm, 1.2 µm) (PN 685975-302)					
Mobile phase	Solvent A: 5% H <sub>2</sub> O (5 mM Ammonium Form. + 0,01 % Formic Acid) Solvent B: 95% ACN (5mM Ammonium Form. + 0.01% Formic Acid)					
Column Temp.	65 °C					
Flow	0,3 ml/min					
Run Time	15 min					
Flow Mode	Isocratic					
Injection Volume	1 µL					
<b>Scan Method (MS2 Scan)</b>						
Segment Name	Start Mass	End Mass	Scan Time	Fragmentor	Cell Accelerator Voltage	Polarity
Compound	50	1000	200	80	7	Negative
Compound	50	1000	200	80	7	Positive



## C. LC-MS/MS CHROMATOGRAMS

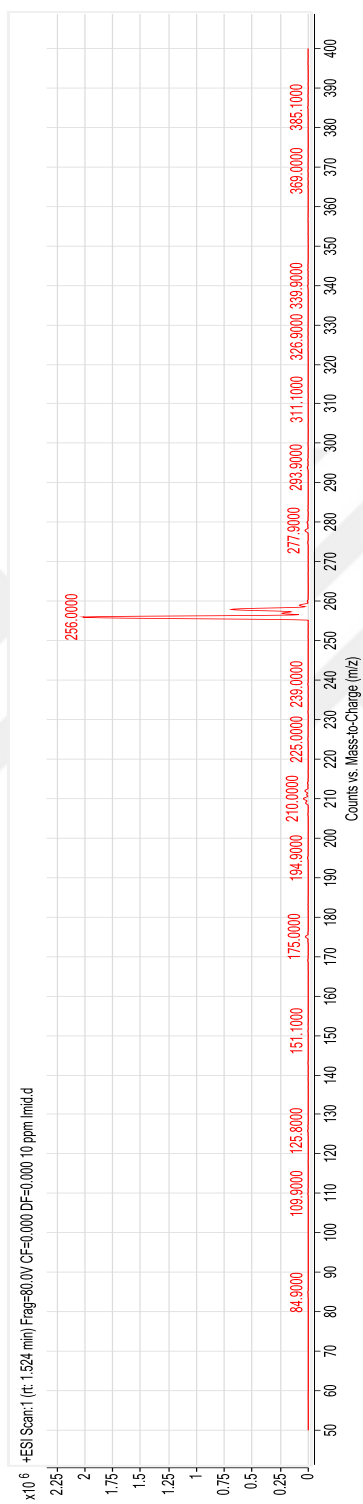


Figure C.1. LC-MS/MS chromatograms of 10 ppm IMI analytical standard (retention time: 1.524 min)

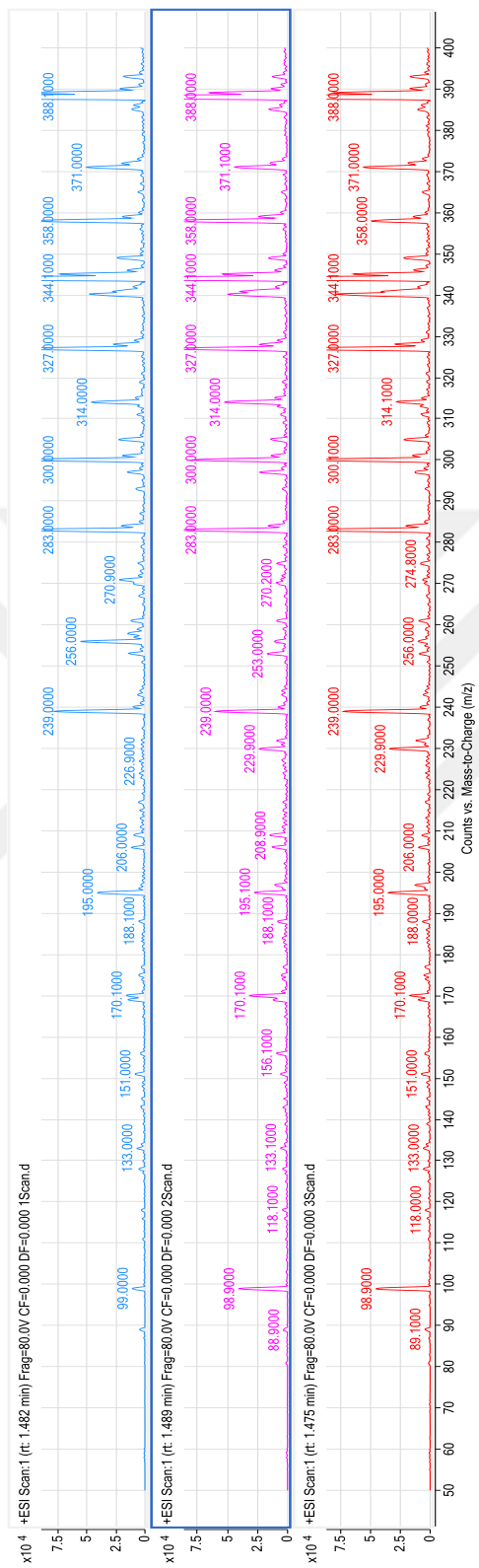


Figure C.2. LC-MS/MS chromatogram of ozonation in Mili-Q water (sampling times from top to bottom: 5, 70 and 180 min)

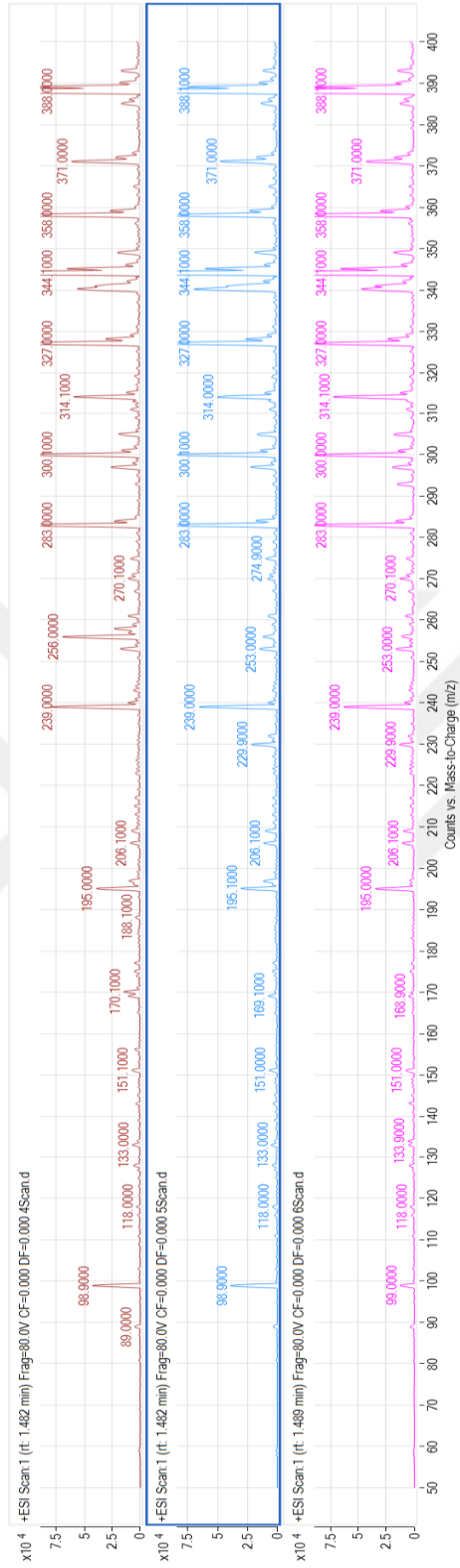


Figure C.3. LC-MS/MS chromatogram of ozonation in VRMBR WW (sampling times from top to bottom: 5, 90 and 180 min)

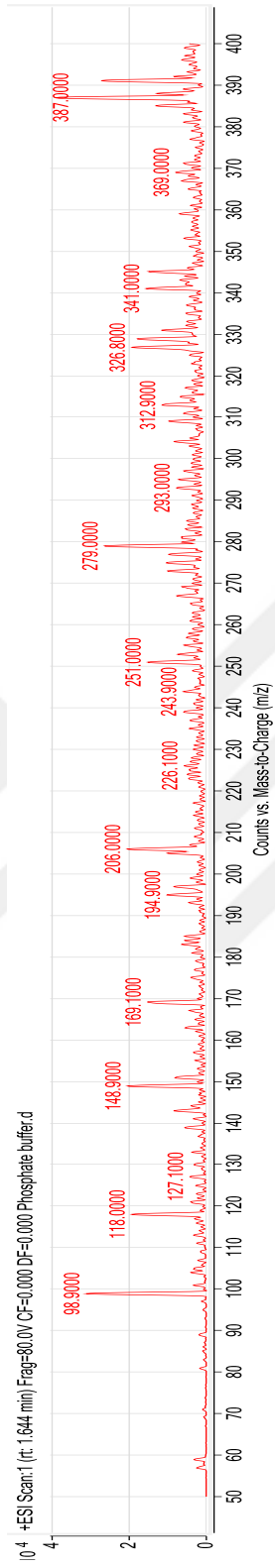


Figure C.4. LC-MS/MS chromatogram of phosphate buffer solution

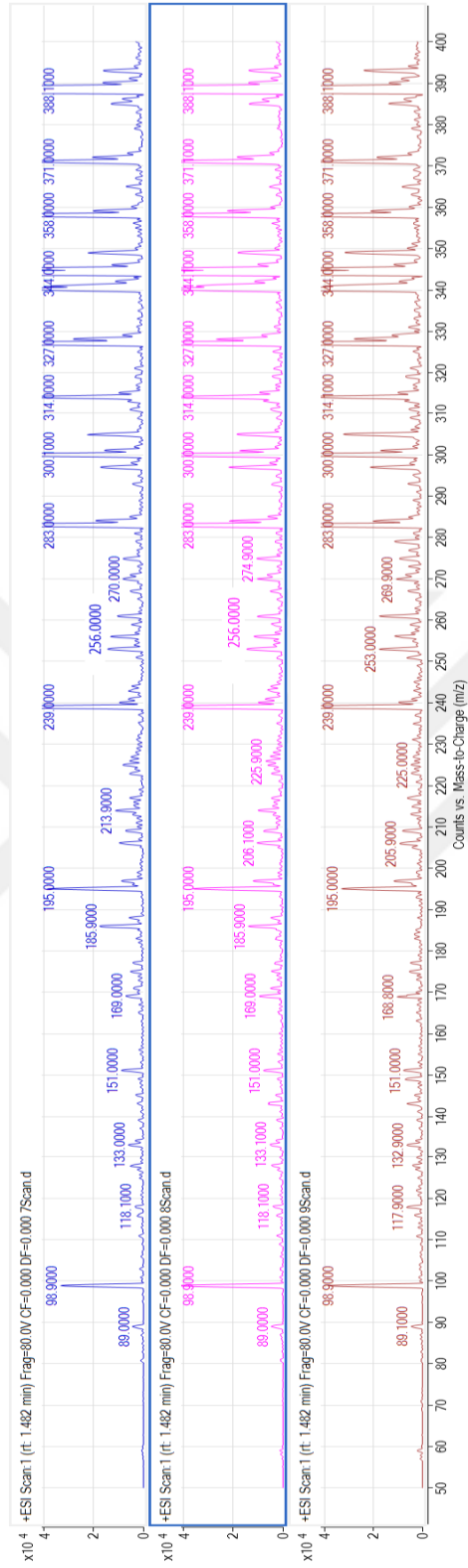


Figure C.5. LC-MS/MS chromatogram of O<sub>3</sub>/UV in Milli-Q water (sampling times from top to bottom: 5, 10 and 60 min)

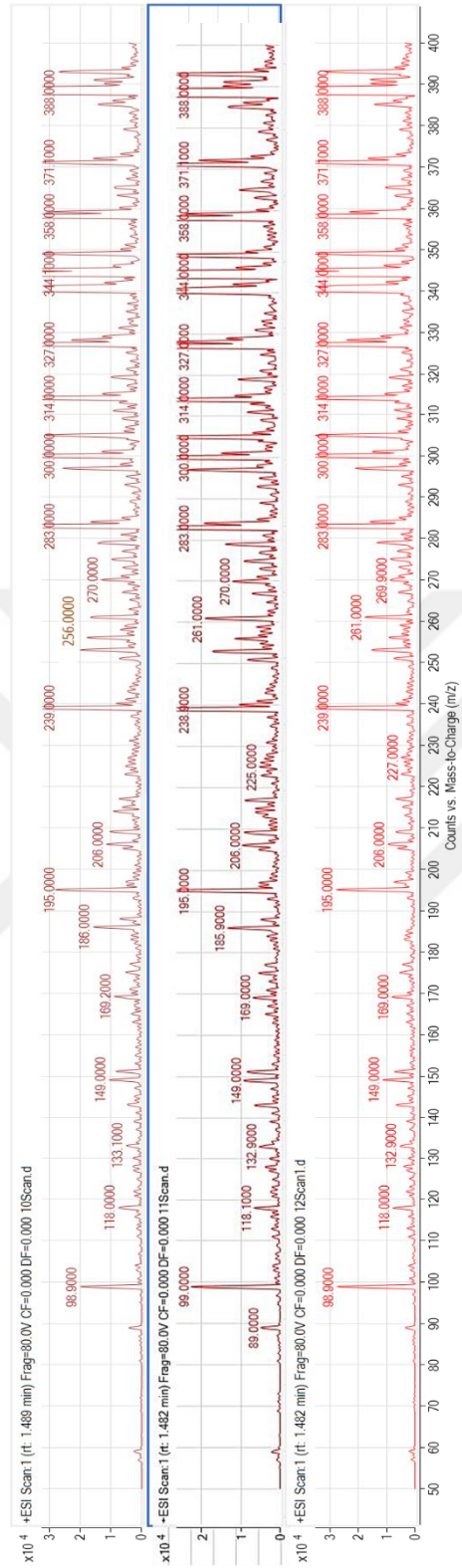


Figure C.6. LC-MS/MS chromatogram of O<sub>3</sub>/UV in VRMBR WW (sampling times from top to bottom: 5, 10 and 60 min)

Table C.1. By-products detected by LC-MS/MS in ozonation and photo-ozonation processes

<b>Ozonation</b>	<b>Photo-ozonation</b>	<b>Both</b>
<i>m/z</i> 148	<i>m/z</i> 186	<i>m/z</i> 186
<i>m/z</i> 175	<i>m/z</i> 209	<i>m/z</i> 209
<i>m/z</i> 186	<i>m/z</i> 253	<i>m/z</i> 253
<i>m/z</i> 188	<i>m/z</i> 270	<i>m/z</i> 270
<i>m/z</i> 209		
<i>m/z</i> 210		
<i>m/z</i> 230		
<i>m/z</i> 253		
<i>m/z</i> 270		
<i>m/z</i> 275		
<i>m/z</i> 314		